Evaluating Upstream-Downstream Linkages of Hydrological Dynamics in the Himalayan Region

Dissertation

for the obtainment of the academic degree doctor rerum naturalium

(Dr. rer. nat.)

submitted to the Faculty of Chemical and Earth Sciences of the
Friedrich-Schiller-University Jena
by MSc, MA, Santosh Nepal
born on 25. May 1980 in Nepal

Examination committee:

1. Prof. Dr. Wolfgang-Albert Flügel
2. Dr. Peter Krause
3. Prof. Dr. Volker Hochschild

Date of the public defense: 04. July 2012

This research was funded by the IPSWaT scholarship program,
an initiative of the German Federal Ministry of Education and Research (BMBF)

Acknowledgment

It's a great pleasure to acknowledge the contribution and generous support of a large number of people who helped me during the process of this PhD Study.

First of all, I would like to express my sincere gratitude to my supervisor Prof. Dr. Wolfgang-Albert Flügel, who provided this opportunity to carry out the PhD research at the Friedrich-Schiller-University Jena (FSU-Jena). The cooperation with him started in 2006 during the Integrated Watershed Management (INWAMA) project in Beijing where I expressed my interest to do a PhD in the field of Integrated Water Resources Management. In 2009, we were able to finalise the funding support through IPSWaT and I formally started the PhD. I am grateful to his support and guidance with his valuable inputs, motivation and criticism throughout the process of the research study. I would also like to express my gratitude to Dr. Peter Krause, my reviewer, for his continuous support and guidance in this period. He has always been supportive and available to discuss the J2000 hydrological model and related hydrological issues, and always enthusiastic to solve any problems encountered while running the model. I respectfully acknowledge Dr. Timothy Steel for his critical and valuable suggestions on the manuscript of the dissertation. He went through all the chapters and provided his valuable comments and suggestions which indeed were quite helpful.

I would like to appreciate the friendly and supportive behaviour of all the colleagues of the Department of Geoinformatics, Hydrology and Modelling of the FSU-Jena. Dr. Sven Kralisch and Dr. Manfred Fink were very friendly and were always available to discuss issues related to the research. I would like to thank Dr. Manfred for providing inputs on several chapters of the dissertation. Similarly, I am grateful to Franziska Zander, Christian Fischer, Björn Pfennig, Christian Schwartze, and Markus Wolf for their specific help concerning the tools they have developed. Thanks are also due to Dr. Jörg Helmschrot, Bettina Böhm, Sophie Biskop, Tanguang Gao, Miga Magenika Julian, Dr. Peter Selsam, Santiago Penedo, Annika Künne, Anita Bartosch, Markus Reinhold, and Dr. Houshang Beharwan. In addition, I also like to acknowledge the help of our system administrator, Rainer Hoffmann, and our secretary, Anita Martin for the administrative matters.

I would like to take this opportunity to express my admiration to the people who have been instrumental since my initial days in Jena. Mrs. Dorothee Flügel has always shown moral support and believed in me, which brought a positive energy and encouragement to continue my work. Corina Manusch and Reik Leitere were always there to support and help me to settle in Jena, both physically and emotionally. Special thanks also go to Dr. Klaus Bongartz for his help and assistance.

I appreciate the support of the Department of the Hydrology and Meteorology (DHM), Government of Nepal, which provided the hydro-meteorological data for the study area. Dr. K. P. Sharma and Bijay Pokharel were very supportive to discuss the issues related to hydro-meteorological data. Similarly

thanks go to Indian Institute of Tropical Meteorology (IITM), India for providing the data of the regional climate model. I am grateful to the colleagues of ICIMOD who have supported my PhD research from the very beginning and provided me the working space during my field trip in Nepal. Particularly, I would like to thank and remember the support of ICIMOD colleagues during this period: Prof. Dr. Hua Ouyang, Dr. Arun B. Shrestha and Dr. Mats Eriksson during this period.

I am grateful to the support of Ms. Verena Schaller for proofreading the manuscript. I would like to thank Mr. P. B. Adiga, Dr. Bhupendra Devkota and Dr. Nawa Raj Khatiwada for their encouragements and support from the very beginning. I am thankful to Dr. Maxime Souvignet for providing useful information about the statistical analysis.

I would like to acknowledge the IPSWaT programme of the German Federal Ministry of Education and Research (BMBF), for the financial support which enabled me to fully concentrate on the research. I would like to express my special thanks to Dr. Cornelia Parisius, Sara Sabzian, and Mrs. Gabrielle Al-Khinli for their friendly support.

Finally, I am forever indebted to my wife, Anita, and son, Amulya, for their loving support, endless patience, encouragement and understanding during this period. They have always supported my work even if I used to take 'family time' to research and used to be absent at times when they needed me most. I would also like to remember the encouragement provided by my parents without their support, I would not have been able to come a long way. My heartfelt thanks are also due to my brother, sisters, and other family members and friends for their support and encouragement.

Jena, May 2012 Santosh Nepal

Abstract

The glacierised mountain catchments of the Himalayan region serve lives and livelihoods for millions of people living downstream. When water (or streamflow) flows from headwaters to floodplains, the water resources are widely utilised for many activities such as agriculture, drinking water, and hydropower. The activities and processes (such as land-use change and snow and glacier melt) in upstream areas affect the spatial and temporal distribution of water resources to downstream regions. In the context of climate change, the hydrological regime of the Himalayan river systems is likely to be affected which might change the water availability for downstream people. The understanding of the hydrological dynamics is crucial for sustainable planning and management of water resources of the Himalayan region. However, the lack of hydro-meteorological data in the region, especially in high-altitude areas, hinders the process of understanding the system dynamics. In this context, the present study is intended to analyse the upstream-downstream linkages of hydrological dynamics in the Kosi river basin of the Himalayan region. The Kosi river basin is a transboundary river, dominated by glaciers in the high-altitude areas. It originates from the highlands of Tibet and the Nepal Himalaya and flows to the Indo-Gangetic Plain. The climate of the area is greatly influenced by the Indian monsoon system. The region receives high precipitation from June to September which brings floods and widespread damage to property and lives.

The primary focus of this study is to evaluate the upstream-downstream linkages of hydrological dynamics in the Kosi river basin. A special emphasis was given to the impact of land-use and climate change in upstream areas and their impacts on the quantity and timing of the distribution of water resources to downstream regions. For the purpose of this study, the western part of the river basin, located in the Nepal Himalaya, is selected, since it has a relatively a high station network density. In this context, the hydro-climatic conditions of the study area were analysed using the historic time series data available. The spatial distribution of precipitation in different mountain zones was analysed. In addition, a non-parametric trend analysis was used to analyse the past climatic trend in the region. In the next step, the process-oriented and distributed J2000 hydrological model was adapted and implemented to simulate the hydrological processes of the region. For this purpose, new modules such as, a glacier module, were implemented, and existing modules, such as the soil module, are modified to take into account the characteristic features of the region. The subdivision of the catchment was carried out by applying the concept of Hydrological Response Units (HRUs). The model was further adapted to understand the impact of land-use change on the hydrological regime. Similarly, the future precipitation and temperature in the context of climate change were analysed by using the climate projection data from a Regional Climate Model (RCM). Furthermore, climate projection data were used in the J2000 hydrological model and the impact of climate change on the distribution (quantity and timing) of water resources to downstream regions was also analysed.

The analysis of the hydro-meteorological data indicated that the region has experienced an increasing temperature trend in the recent decades. On the contrary, the precipitation data do not indicate a homogeneous significant trend. The adaptation of the J2000 hydrological model indicated that the model is able to simulate hydrological processes of the Kosi river basin fairly well, based upon the graphical and statistical evaluation of the model performance. The model results show uncertainty arising from different sources. The input data are the primary source of uncertainty. The input data, such as precipitation, are less representative due to the low station network density in the region. Similarly, the validation data, i.e. discharge, are another source of uncertainty as the measurement process of discharge during flood periods is less representative. Similarly, the model parameters are also a source of uncertainty in the model results. In spite of this, the modelling results improve the knowledge and understanding of the hydrological dynamics of the of the Himalayan rivers including evapotranspiration, discharge, and different forms of storage. Similarly, the model is able to quantify the role of different runoff components such as; snow and glacier melt, overland, interflow and baseflow. The modelling results suggested that the overland flow is the dominating component of the streamflow with a stake of about half of the total streamflow. Snow and glacier melt mostly occur from the pre-monsoon to post-monsoon period and nearly one third of the streamflow is contributed by the melt runoff.

The J2000 hydrological model was further adapted to understand the analysis of different scenarios. Two scenarios were formulated to quantify the impact of land-use change on the hydrological regime. The study showed that by changing the land-use pattern from one vegetation to another vegetation type (eg. from forest to shrubland), there is a minimum impact on downstream water availability. However, the scenario of complete deforestation indicated that evapotranspiration will be decreased due to the absence of vegetation. At the same time, due to reduced infiltration in the deforested land (eg. bare land), the overland flow will be increased and baseflow will be decreased. This will possibly increase flood-related events in the downstream region. However, there is a high uncertainty in the results as it primarily depends upon the infiltration capacity of soils after deforestation. The RCM data suggested that the temperature and precipitation of the Kosi river basin will be increased by 4^{o}C and 14 percent respectively by the end of the century. Based on RCM data, the impact of climate change on hydrology suggested that the streamflow will be increased primarily during the monsoon season. Similarly, due to a rise in temperature, on the one hand, more precipitation will occur as rain than snow, and on the other hand, the snowline will shift to high-altitude areas. This will overall decrease the snow storage capacity of the basin. The river is likely to shift from a 'melt-dominated river' to a 'rain-dominated river' in future, under the assumption of changes suggested by the RCM data.

This research study suggested that the tools from geoinformatics are supportive in addressing upstream-downstream linkages. The modelling approach of the model J2000, including other tools, is able to address the different processes in upstream areas and their effects on downstream areas with a focus on water availability. Similarly, the changes related to climate and land-use in upstream areas were realised and the effects to the downstream areas were quantified. Therefore, it is concluded that the methodology applied in this study is suitable for evaluating upstream-downstream linkages in the Himalayan region. In addition, it could be a basis for further assessment of other linkages to understand the broader picture of upstream-downstream linkages.

Kurzfassung

Die vergletscherten Einzugsgebiete in der Himalayaregion sind wesentlich für die Lebensgrundlagen der flussabwärtslebenden Bevölkerung. Das Wasser das von den Oberläufern in das Tiefland fließt, wird für viele Zwecke genutzt (Beispielsweise Bewässerung, Trinkwassergewinnung und Wasserkraft). Prozesse (wie Landnutzungsänderung und Schnee- /Gletscherschmelze) in flussaufwärts gelegenen Gebieten beeinflussen die räumliche und zeitliche Verteilung von Wasserressourcen in flussabwärts den gelegenen Gebieten. Der Klimawandel wird das hydrologische Regime des Flusssystems im Himalaya voraussichtlich beeinflussen, d.h. die Wasserverfügbarkeit für die flussabwärts lebende Bevölkerung könnte sich ändern. Das Verständnis der hydrologischen Dynamik der Himalaya-Region ist entscheidend für die nachhaltige Planung und das Management der Wasserressourcen. Jedoch behindert der Mangel an hydro-meteorologischer Daten in der Region, insbesondere in hochgelegenen Gebieten, das tiefere Verständnis der Systemdynamik. Im Zentrum der vorliegenden Studie steht vor diesem Hintergrund, die Analyse der hydrologischen Beziehungen der flussauf- und flussabwärts gelegenen Teilgebiete des Flusses Kosi. Das Flusseinzugsgebiet des Kosi ist grenzüberschreitend und wird in hochgelegenen Gebieten von Gletschern dominiert. Die Quellen des Kosi finden sich im tibetischen Hochland und dem nepalesischen Himalaya, der anschließend in die Gangesebene entwässert. Das Klima der Region wird stark von dem indischen Monsunsystem geprägt. Die Region weist von Juni bis September sehr hohe Niederschläge auf, was verbreitet Überflutungsschäden für Leben und Eigentum zur Folge hat.

Das Hauptaugenmerk dieser Studie liegt auf der Analyse und Bewertung der hydrologischer Dynamik zwischen den flussabwärts und flussaufwärts gelegenen Gebieten im Einzugsgebiet des Kosi. Im Fokus stand hierbei, der Einfluss von Landnutzungsänderungen und Klimawandel in den flussaufwärts gelegenen Gebieten, auf die zeitliche und räumliche Dynamik der Verfügbarkeit der Wasserressourcen der flussabwärts gelegenen Gebiete. Im Rahmen dieser Studie wurde der westliche Teil des Flussgebiets gewählt, da dieser sich im nepalesischen Himalaya befindet und daher die Verfügbarkeit von Zeitreihendaten deutlich besser war. Es wurden die hydro-meterologischen Eigenschaften des Testgebiets wurden mit hilfe der Zeitreihendaten analysiert die eine hinreichende Zeitspanne repräsentieren. Die räumliche Verteilung des Niederschlags wurde in verschiedenen Gebirgszonen analysiert. Des Weiteren wurde eine nichtparametrische Trendanalyse durchgeführt, um den Klimatrend der Vergangenheit der Region zu analysieren. Im nächsten Schritt wurde das prozessorientierte und distributive hydrologische Modell J2000 angepasst und eingesetzt, um die hydrologischen Prozesse im Gebiet zu simulieren. Hierfür wurden neue Module, wie das Gletschermodul implementiert und bestehende Module, wie das Bodenmodul, modifiziert, um die charakteristischen Merkmale der Region einzubeziehen. Die Unterteilung des Einzugsgebiets wurde unter Verwendung des Konzepts der Hydrological Response Units (HRUs) vorgenommen. Das Modell wurde weiterhin angepasst, um die

Auswirkung von Landnutzungsänderung auf das hydrologische Regime darstellen zu können. Auf ähnliche Weise wurden Daten zur zukünftigen Niederschlags- und Temperaturentwicklung mit Hilfe von Klimaprojektionsdaten aus einem Regional Climate Model (RCM) analysiert. Weiterhin wurden diese Klimaprojektionsdaten im hydrologischen Modell J2000 benutzt und die Auswirkungen des Klimawandels auf die Wasserressourcen in flussabwärts gelegenen Gebieten abzuschätzen.

Die Analyse der hydro-meteorologischen Daten zeigte, dass in der Region in den vergangenen Jahrzehnten die Temperaturen einen steigenden Trend zeigen. Beim Niederschlag konnte hingegen kein homogener signifikanter Trend der einzelnen Stationen festgestellt werden. Die graphischen und statistischen Auswertung der Modellergebnisse zeigt, dass mit Hilfe der vorgenommen Anpassungen, des hydrologischen Modells J2000 das Modell in der Lage ist die hydrologischen Prozesse des monsungeprägten des Kosi Einzugsgebiets gut wiederzugeben. Die Modellunsicherheiten setzten sich aus verschiedene Ursachen zusammen. So stellen die Eingabedaten dabei die Hauptquelle für die Unsicherheit dar. Diese wiesen, wie z.B. beim Niederschlag, eine geginge Messnetzdichte auf und sind daher nur bedingt repräsentativ für die Region. Ähnlich verhält es sich mit den Validierungsdaten, d.h. dass die Abflussmessungen wärend des Hochwasseres, aufgrund von Messproblemen, weniger repräsentativ sind. Gleichermaßen sind die Modellparameter eine Ursache für Unsicherheiten bei der Modellierung. Nichtsdestoweniger enthalten Ergebnisse der Modellierung wichtige Informationen über die Wasserbilanz des Testgebiets, einschließlich Evapotranspiration, Abfluss und Änderungen im Boden und Grundwasserspeicher. Außerdem ist das Modell in der Lage die verschiedenen Abflusskomponenten, Schnee- und Gletscherschmelze, Oberflächen-, Zwischen-, und Basisabfluss zu quantifizieren. Die Modellergebnisse weisen darauf hin, dass der Oberflächenabfluss die Hälfte des Gesamtabflusses einnimmt und somit das Abflussgeschehen domminiert. Schnee- und Gletscherschmelze findet hauptsächlich von der Vormonsun- bis zur Nachmonsunzeit und stellt fast ein Drittel der Abflussmenge dar.

Das hydrologische Modell J2000 wurde weiterhin angepasst, um die Analyse verschiedener Szenarien darstellen zu können. Zwei Szenarien wurden formuliert, um den Einfluss von Landnutzungsänderung auf das hydrologische Regime zu quantifizieren. Die Studie zeigte, dass der Wechsel von einer Landbedeckung zu einem anderen (z.B. Wald zu Strauchsteppe) eine minimale Auswirkung auf die Wasserverfügbarkeit der flussabwärts gelegenen Gebiete bewirkt. Deutlichere Auswirkungen zeigte das Szenario einer kompletten Abholzung. Hierbei nimmt die Evapotranspiration aufgrund nicht vorhandener Vegetation ab. Zugleich wird die Menge des Oberflächenabflusses durch die reduzierte Infiltration auf den abgeholzten Flächen steigen und der Basisabfluss abnehmen. Dies wird möglicherweise zu mehr Überschwemmungen in der flussabwärts gelegenen Region führen. Jedoch gibt es eine große Unsicherheit bei diesen Ergebnissen, da sie hauptsächlich von der Infiltrationskapazität der Böden nach der Abholzung abhängt. Die RCM-Daten ließen darauf schließen, dass sich bis zum Ende des Jahrhunderts im Einzugsgebiet des Kosi die Temperatur um 4^{o}C und der Niederschlag um 14% erhöht haben wird. Auf Grundlage der RCM-Daten lässt sich sagen, dass der Einfluss des Klimawandels bewirkt, dass sich die Abflussmengen insbesondere während der Monsunzeit erhöhen werden. Aufgrund des Anstiegs der Temperatur wird außerdem auf der einen Seite mehr Niederschlag in Form von Regen statt Schnee fallen und, auf der anderen Seite, wird die Schneegrenze sich in höher gelegene Gebiete verschieben. Dies wird insgesamt die Schneespeicherkapazität des Einzugsgebietes

verringern. Unter Annahme der Veränderungen, die die RCM-Daten aufzeigen, wird der Fluss voraussichtlich noch mehr von einem 'Schmelzfluss' zu einem 'Regenfluss' werden.

Diese Studie konnte aufzeigen, dass die Instrumente und Methoden der Geoninformatik hilfreich sind, um Beziehungen zwischen flussabwärts und Űaufwärts gelegenen Gebieten zu analysieren. Der Modellierungsansatz von J2000, einschließlich anderer Tools, kann die verschiedenen Aktivitäten und Prozesse in Gebieten flussaufwärts und ihre Auswirkungen auf Gebiete flussabwärts, insbesondere auf im Bezug die Wasserverfügbarkeit, darstellen. Des Weiteren konnten die Veränderungen in Bezug auf Klima und Landnutzung in den flussaufwärts gelegenen Gebieten und die Auswirkungen auf Gebiete flussabwärts dargestellt und quantifiziert werden. Daraus kann geschlossen werden, dass die in dieser Studien angewendete Methodik geeignet war, um die Beziehungen zwischen flussaufwärts und -abwärts gelegenen Gebieten in der Himalayaregion zu evaluieren. Dies bildet eine Grundlage zur Untersuchung anderer Zusammenhänge, um ein umfassenderes Verständnis von Beziehungen zwischen flussaufwärts und -abwärts gelegenen Gebieten zu gewinnen.

Contents

List of Figures

List of Tables

Acronyms, symbols and units

^{o}C	Degree Celsius
AET	Actual Evapotranspiration
AAP	Average Annual Precipiation
ahum	Absolute humidity
AIDIS	Adaptive Integrated Data Information System
AOGCM	Atmosphere-Ocean General Circulation Models
CBS	Central Bureau of Statistics
cm	Centimeter
DEM	Digital Elevation Model
DHM	Department of Hydrology and Meteorology
DoS	Department of Survey
DPR	Detailed Project Report
E_{NS}	Nash-Sutcliffe
EDA	Exploratory Data Analysis
FAO	Food and Agriculture Organisation
GCC	Global Climate Change
GCM	General Circulation Model
GIS	Geographical Information System
GLUE	General Likelihood Uncertainty Estimation
GOI	Government of India
GON	Government of Nepal
GWP	Global Water Partnership
HadCM3	Hadley Centre Coupled Model
HD	Human Dimention
HRU	Hydrological Response Unit
IDW	Inverse Distance Weighting
IITM	Indian Institute of Tropical Meteorology
IPCC	Intergovernmental Panel on Climate Change
IWRM	Integrated Water Resources Management
JAMS	Jena Adaptable Modelling System
KosiRBIS	Kosi River Basin Information
KRBMSP	Kosi River Basin Management Strategic Plan
LAI	Leaf Area Index
LNS	Log Nash-Sutcliffe
LPS	Large Pore Storages

m	Meter (or above mean sea level)
m/s	Meter per second
m^2	Meter square
m^3/sec	Cubic meter per second
MBT	MainBoundaryThrust
MCA	Monte Carlo Analysis
MCT	MainCentralThrust
MFT	Main Frontal Thrust
mhum	Maximum humidity
MK	Mann-Kendall
mm	Millimeter
MoFSC	Ministry of Forest and Soil Conservation
MPS	Middle Pore Storages
NE	Natural Environment
NMI	Normalised Melt Index
OGCM	Oceanic General Circulation Model
OSS	Open-source software
PES	Payment for Environmental Services
PET	Potential Evapotranspiration
PRECIS	Providing REgional Climates for Impact Studies
PRMS/MMS	Precipitation Runoff Modelling System/Modular Modelling System
PWP	Permanent wilting point
QUM	Quantifying the Uncertainty in the Model Predictions
r^2	Co-efficient of determination
RBIS	River Basin Information
RCM	Regional Climate Model
RD1	Overland Flow
RD2	Interflow 1
RG1	Interflow 2
RG2	Baseflow
rhum	Relative humidity
RUPES	Rewarding Upland Poor for Environmental Services
satLPS	Saturated Large Pore Storages
satMPS	Saturated Middle Pore Storages
SOTER	Soil and Terrain
SRES	Special report on emission scenarios
SRTM	Shuttle Rader Topographical Mission
SWAT	Soil and Water Assessment Tool
SWE	Snow Water Equivalent
t/ha	Tonne per hectare
Tavg	Average Temperature
THED	Theory of Himalayan Environmental Degradation

Tmax	Maximum Temperature
Tmin	Minimum Temperature
TWI	Topographic Wetness Index
UNEP	United Nation Environment Programme
UNESCO	United Nations Educational, Scientific and Cultural Organization

1 Introduction

This study addresses upstream-downstream linkages in the Kosi river basin of the Himalayan region. Special emphasis is given to the impact of land-use and climate change in upstream areas and their impacts on downstream region. To address this issue, the J2000 hydrological model has been adapted and implemented in the monsoon dominated Himalayan river system. After the successful implementation of the model in two sub-catchments of the Kosi river basin by using a proxy-basin approach, the model is further adapted to analyse the impact of land-use and climate change on hydrological regime. This study primarily focuses upon the hydrological dynamics of the upstream-downstream linkages. This introduction chapter begins with the background of and motivation for the study. The scope and brief outline of the dissertation are presented at the end.

1.1 Background and motivation

In a mountainous region, an action taken in upstream has influence on downstream areas. With regard to hydrology, as surface waters flow from headwaters (upstream) to lower-elevation floodplains (downstream), it creates linkages between upstream and downstream areas. The linkages are relative to the physical hydrologic system in nature. A point in a mountain (e.g. irrigation land) is considered as downstream from the upstream catchment area which provides water to the irrigation land. However, both catchment and irrigation land could be upstream relative to the region below which receives water after irrigation. Therefore, upstream and downstream relationships can be seen throughout a river basin at different scales. As the scale of the watershed changes (from small plots to an entire river basin), the nature of the linkages and related effects varies. The effect which occurs at one scale (micro catchment) might have a different magnitude and impacts on another level (river basins).

The activities in upstream areas have both beneficial and adverse effects on downstream communities. Good watershed management practices provide better opportunities to downstream communities, for example, a clean and sustainable water supply for irrigation. However, bad watershed management practices do not only degrade upstream environmental conditions, but also limit the opportunities in downstream areas. Hence, as the 'opportunities' and 'threats' flow from upstream to downstream areas, the users in downstream areas often have great 'concerns' about upstream land-use and water management practices. A better understanding of the linkages provides an opportunity to transform the 'concerns' of the downstream users into 'cooperation' so that both communities can work together for the benefits of a larger group.

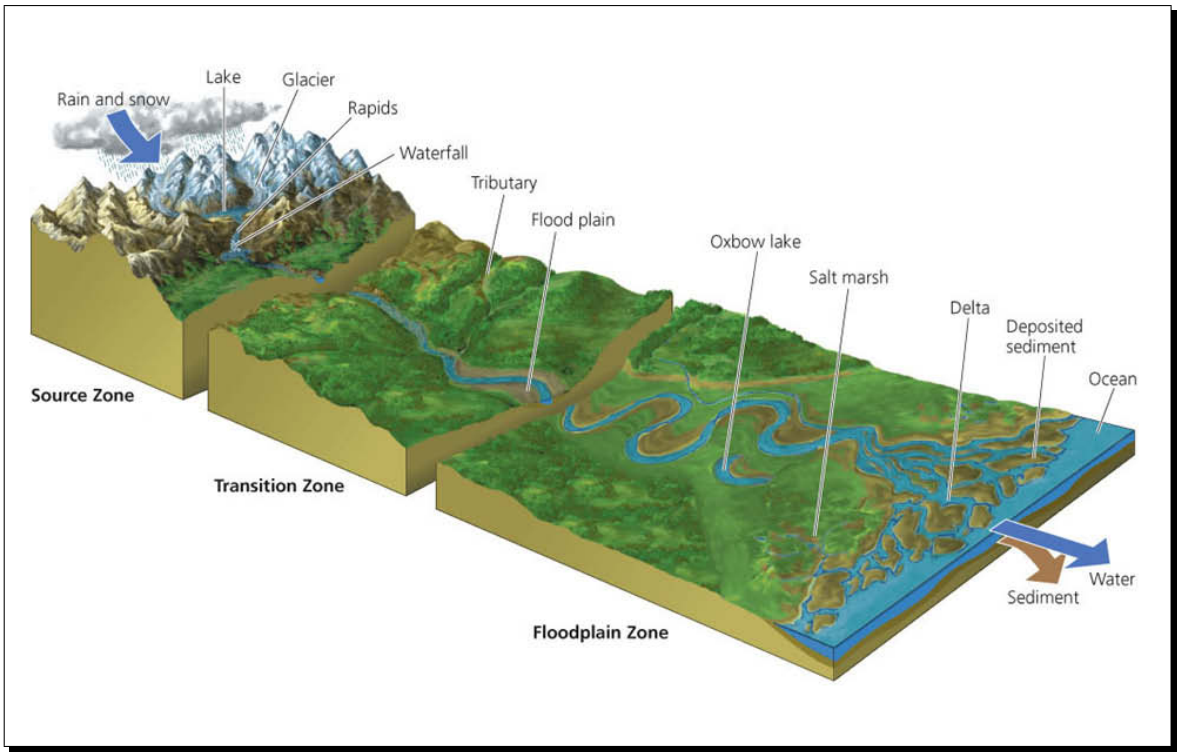

Figure 1.1: Three zones of a river system while flowing from headwaters to downhill. Source: (Miller and Spoolman 2009)

.

Figure 1.1 shows a conceptual longitudinal profile of an alpine region similar to the Himalaya, depicting the three important zones in the profile: Source zone (or headwaters), transition zone, and floodplain (or depositional) zone (Miller and Spoolman 2009). In the context of this study, the first two zones can be considered as an upstream area. **The source zone (headwaters)** has the steepest gradient with mountains and ridges. Most of the glaciers and snow storage are also located in these areas. The headwaters area might have little or no vegetation due to high elevation. For example, the headwaters of the Himalayan river systems are full of permanent snow and glaciers. Due to the high degree of slope, soil erosion occurs and resultant sediment moves downstream. **The transition zone** also shows a high degree of slope, along with mixed vegetation as it is located in the lower elevation areas. It is usually characterized by wide flood plains and meandering channel patterns (FISRG 1998). In the Himalayan region, human activities are found in this region with livelihood activities such as agriculture. **The floodplain zone** begins when the river starts flowing to the plain areas where the gradient flattens. At lower elevation, a river wanders and meanders. At its mouth, a river may divide into many separate channels as it flows across a delta built up of river- borne sediments and into the seas (Miller and Spoolman 2009). The Indo-Gangetic Plain of the Himalayan region represents this zone. As suggested by FISRG (1998), causes and effects (for example, soil erosion and sedimentation) occur in all zones, but the zone concept, presented here, focuses on the most dominant processes. However, some unique processes such as glacier melting always occur in the headwaters. Different processes occur in different zones such as, land-use change and glacier melting which

indicate upstream-downstream significance.

The Himalayan region is one of the most dynamic and young mountain system in the world. The headwaters of the major rivers of the region; Indus, Ganges, Brahmaputra are located in the high altitude areas of the Himalayan region. The basins of these rivers are inhabited by nearly 700 million people (Eriksson et al. 2009). The water resources of the region have been utilised for livelihood related activities such as irrigation, hydropower and drinking water. Therefore, water is an integral part of the livelihoods in the region. IPCC (2007) suggested that the glaciers in the Himalaya are receding faster than in any other part of the world. The growing water demands and a warming temperature trend all over the region are likely to result in water shortage. In such scenarios, the water supply in areas fed by glacier and snow melt will be adversely affected (Barnett et al. 2005).

In spite of the great significance of the region, the hydrological dynamics of the Himalayan rivers are still less known. The hydrology of the basin is quite complex, because of having too much water during the monsoon season and having too little water during the rest of the year. Floods bring havoc to the region every year. The understanding of the role of snow and glacier melt to streamflow is still not clear. The rainy periods and melting seasons occurring in the same period bring complexities to the region. As suggested by Alford (1992), Armstrong (2011), understanding the existing hydrological regime of these river systems is essential. Therefore, it is important that the river systems are better understood and the relationships among the different watershed components (such as soil, groundwater, snow and glaciers) and streamflow are quantitatively assessed.

In the context of global climate change, the water resources of the Himalayan region are vulnerable which might influence the water supply of the downstream areas (Immerzeel et al. 2010, Nepal et al. 2011, Eriksson et al. 2009, Barnett et al. 2005). The effect of climate change is already visible in the Himalayan region. The maximum temperature of Nepal is increasing at a rate of 0.6 ^{o}C/decade (Shrestha et al. 2000) and glaciers are shrinking and developing many potentially unstable glacial lakes (Kattelmann 2003, Bajracharya et al. 2007, Mool et al. 2001b). The shrinking glaciers might impact the seasonal discharge of the rivers originating from high altitude areas. In such cases, the livelihood patterns of the downstream areas might be affected.

The deforestation of the mountains in the upstream areas of the Himalayan river basins has been blamed for increased flooding of the Gangetic Plain in India and Bangladesh (Ives and Misserli 1989, Ives 1989). To what extent the hydrology and floods of the monsoon-dominated areas are affected by the land-use changes in the upstream areas is still unclear. Such knowledge of activities and processes which occur in upstream areas and cause direct impacts to downstream regions provides better understanding of the linkages between upstream and downstream areas. In assessing this aspect, risk (such as floods,) can be reduced and benefits (less soil erosion) can be augmented.

Against this background, it is of utmost importance to understand the different watershed components of upstream areas and their subsequent impacts to downstream areas in relation to hydrology. In addition, it is also important to understand how the dynamic process of different components might be affected within the context of global climate change. The better understanding among the different components of the watershed provides an opportunity for the improved and sustainable management of water resources. The contribution of melt water to streamflow and the change in distribution of

these components in future is vital information for future water availability in the region. Hydrological models have been considered as a useful tool to apply for better understanding of watershed behaviors and processes. However, due to limited availability of hydro-climatic data in the region, research studies related to hydrology present a challenging task (Alford 1992, Ives and Misserli 1989). In addition, uncertainties due to practical difficulties in maintaining data quality make the hydrological studies more difficult (Kattelmann 1987). The role of different watershed components is not fully understood in the Himalayan river systems. Few studies have attempted to understand the hydrological dynamics in a segregated approach. There is still insufficient information about the relative roles of the different watershed components (overland flow, baseflow, snow and glacier melt) to streamflow. Similarly, the way in which variation in activities and processes in upstream areas (such as land-use and climate changes) impacts the water availability in the downstream areas is still unclear. Therefore, the focus of this study is to understand the impact of land-use and climate changes in upstream areas and subsequent impact to downstream areas with focus on water availability.

The Kosi river basin is one of the major river tributaries of the Ganges river system in the Himalayan region. In Nepal, more than five million people are living in the Kosi river basin (WECS 2011). This river system faces floods annually during the monsoon season. Huge amounts of sediment are transported every year to downstream areas which has resulted in shifts in the stream channels. The basin is dominated by glaciers in the upstream areas and glacier and snowmelt contributes to streamflow. In recent years, the impact of climate change on the distribution of glaciers has been visible in the form of rapidly retreating glaciers. It is of utmost importance to understand how the climate change will impact the hydrological regime of the basin. Therefore, the Kosi river basin has been selected for this study.

1.2 Limitations and assumptions

The study is focused on the hydrological dynamics of the upstream-downstream linkages in the Himalayan region. Soil erosion and sedimentation are important factors impacting the upstream-downstream linkages. The land-use and land-cover changes have direct influence on the amount of soil erosion and sedimentation. However, due to the lack of available data for this region, soil erosion and sedimentation aspects are beyond the scope of this study. Rather, a theoretical review of soil erosion and sedimentation with a specific focus on the Himalayan region was done. Similarly, the socio-economic linkages are also not included in the scope of this study. The Chinese part of the Kosi river basin is not included in this study due to limited and restricted data availability of those areas.

1.3 Overview of the dissertation

This dissertation is organised into eight chapters. A detailed state-of-the-art review of upstream-downstream linkages is presented in Chapter 2. This will include the theoretical linkages and what has been observed in the Himalayan river systems with focus on the Kosi river basin. The objectives and methodological approach are briefly described in Chapter 3. In Chapter 4, a brief discussion of

the Kosi river basin is presented. The chapter deals with the general overview of the basin particularly regarding hydrology. In Chapter 5, the hydro-meteorological time series analysis is described. First, the spatial distribution of precipitation in the Kosi river basin is presented. In addition, the time-trend analysis of historical precipitation, temperature and discharge data is also discussed in this chapter.

Chapter 6 begins with the introductory overview of the J2000 hydrological model. The different modules of this model used in this study are described. In addition, the new modules and the changes in the existing modules are also discussed. Afterwards, the J2000 model is calibrated and validated using data from two different river sub-basins within the Kosi river basin. The chapter describes different components of hydrological dynamics (runoff components, glacial and ice melt, evapotranspiration) based on the output results of the model.

Chapter 7 describes the upstream-downstream linkages of the river system using the J2000 hydrological model as a tool. First, the impact of land-use and land-cover changes on the hydrology and downstream water availability is discussed. Second, the impact of climate change on hydrology is presented. In this section, the future scenario of precipitation and temperature is presented based upon the output from the regional climate model. Next, results of the impact of climate change on the hydrological regime are discussed on the basis of available climate-model data. A brief discussion on possible water management scenarios (using as an example of the proposed Sapta Kosi high dam project) and their upstream-downstream linkages are discussed. Finally, Chapter 8 provides the summary and conclusions of the main results. The final discussion concludes with suggestions for future research.

2 Literature review

This chapter provides an extensive review of upstream-downstream linkages with a focus on the Himalayan region. First, a theoretical review of upstream-downstream linkages is presented. Next, the methodological approach to assess the linkages will be discussed, followed by an identification of deficiencies and future research needs. This study focuses on hydrological dynamics of upstream-downstream linkages. Although soil erosion and sedimentation impacts are not included in this study, a review of literature related to this critical topic in the context of upstream-downstream linkages are included in this section.

2.1 Review of upstream-downstream linkages

Upstream-downstream linkages in mountainous regions are widely discussed from various aspects in the literature. The linkages are mainly categorized into physical, related to land-use change (Ives 1989, Tiwari 2000, Thanapakpawin et al. 2007, Sangjun et al. 2009, Chang 2004, Wasson et al. 2008, Chang and Franczyk 2008) socio-economic linkages (Ives and Misserli 1989, Ives 2004, Blaikie and Muldavin 2004, Jodha 2002) and institutional linkages (Bandyopadhyay and Gyawali 1994, Gyawali and Dixit 1999, Nepal and Adiga 2006). A general understanding of these aspects of upstream-downstream interactions can be derived from a group of natural and social science disciplines. In the recent decades, the effects of global climate change and its impact on hydrological dynamics also have been discussed. The major concern is how climate change and associated variability will influence water availability to downstream regions (Eriksson et al. 2009, Akhtar et al. 2008, Singh and Kumar 1997, Barnett et al. 2005). Therefore, the upstream-downstream relations have multiple aspects which comprise the complex relationships of natural environment (NE) and human dimension (HD). The degree of such complexities is even high in the mountains and especially in the Himalayan region because of inaccessibility, fragility, marginality and heterogeneity in the environment (Jodha 2002). The complexity of these issues needs to be recognized so that inevitable trade-offs can be identified and evaluated in order to ensure maximum benefits and to avoid unnecessary losses (Ives 2004).

In this section, upstream-downstream linkages are discussed with regard to the physical environment considering hydrology in the middle of the discussion. Other linkages are discussed briefly. This research study focuses on the upstream-downstream linkages of the hydrological dynamics of a river system. Hence, other linkages though they may have effects on the region's hydrology, are not considered in this study.

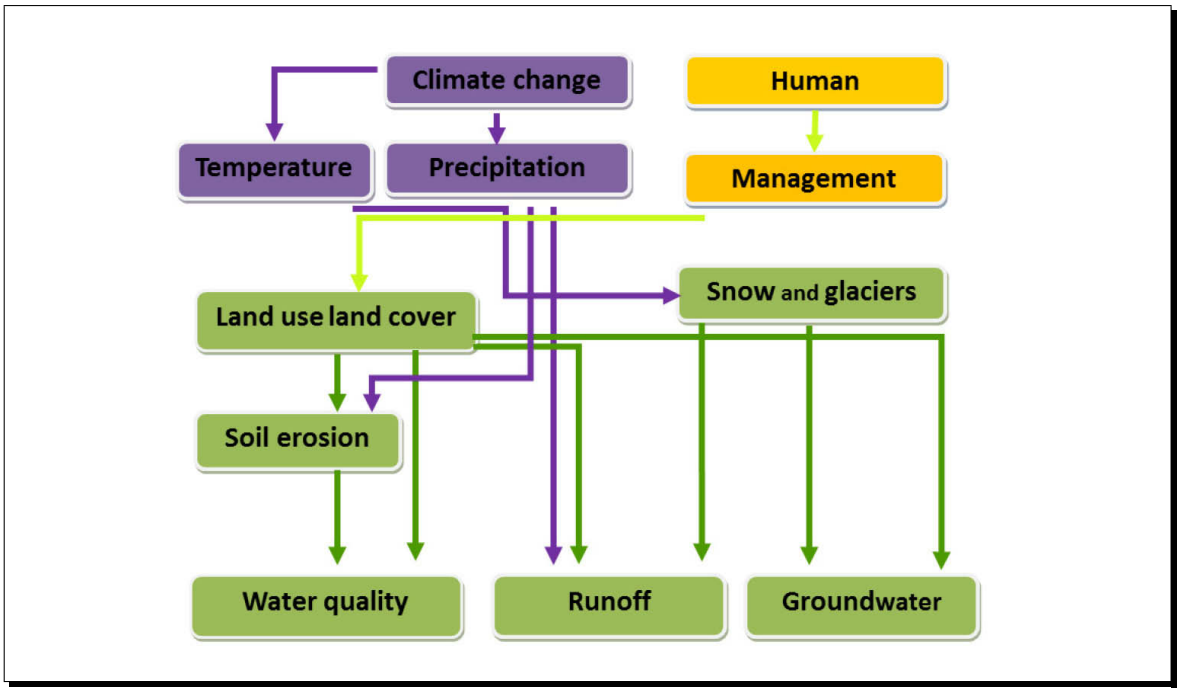

Figure 2.1: Upstream-downstream linkages considering the natural (hydrologic) environment and associated human systems

2.2 Physical linkages

Physical linkages consist of any activities and processes that occur in upstream areas in connection with the physical environmental components (such as land-use change, rainfall-runoff, snow and glacier melting) and their impacts to the downstream environment. There are many processes which occur simultaneously at different spatial and temporal scales which are complex in their relationships. As shown in Figure 2.1, the changes in the status of natural environment (such as climatic conditions) and human systems (such as resource-management practices) may impact the water resources- both qualitatively and quantitatively. The physical linkage of mountain environment can be broadly classified into the following categories, however, they are controlled and influenced by human activities and resource-management practices:

- Impact of land-use changes on water quantity (annual and seasonal streamflow) and water quality (soil erosion, temperature, sedimentation and nutrients)
- Impact of climate change on hydrology

2.2.1 Impact of land-use change on hydrological regime

Land-use change and its impact on different aspects of the environment have been studied, considering global (Watson and Verardo 2000) and local issues (Calder et al. 1995, Awasthi et al. 2002). The impacts of land-use changes can have both positive and negative aspects. Land-use management

Table 2.1: Potential impacts of land-use changes on surface and near-surface hydrological processes and relevance for components of the hydrological cycle. Source: Bronstert et al. (2002)

Processes	Potential impact of land-use change
Interception storage	Greatly affected by vegetation changes (e.g. crop harvest, forest cutting); relevant for evapotranspiration/energy balance
Litter storage	Affected by vegetation changes, in particular forest cutting; relevant for evapotranspiration/energy balance
Root zone storage	Affected by management practices like tilling method, etc.; relevant for evapotranspiration and storm runoff generation
Infiltration-excess overland flow	Affected by crop cultivation and management practices; relevant for storm runoff generation in the case of high rainfall intensities and low soil conductivity; may be enhanced by soil siltation and crusting
Saturation-excess overland flow	Only slightly affected by land-use changes (process is controlled by topography and subsurface conditions)
Subsurface stormflow	Only slightly affected by land-use changes (process is controlled by topography and subsurface conditions)
Runoff from urbanized areas	Highly affected by sewer system and sewage retention measures; relevant for storm runoff from urban areas
Decentralized retention in the landscape	Affected by landscape structuring and agricultural rationalization of arable land; relevant for storm runoff concentration from arable land

practices have impacts on both water quantity (water availability, groundwater recharge and runoff), and water quality (soil erosion, sedimentation, pollution) (DeFries and Eshleman 2004). These processes and associated attributes have important relationships between upstream and downstream areas. Therefore, a better understanding of the interaction between land-use change and hydrological processes is a major concern (DeFries and Eshleman 2004) in the context of sustainable water-resources management.

The potential impact of land-use changes on different hydrological processes is summarised by Bronstert et al. (2002) and provided in Table 2.1. Forests generally influence local hydrology through transpiration. Forests also enhance relatively-high infiltration into underlying soil and ground cover due to organic/nutrient rich litter and humus layers, the presence of macro pores and high interception from canopy coverage. However, different climates influence the processes by which trees affect the hydrological cycle in different manners (Wilk 2002). Studies on the impact of land-use change on hydrological regimes indicate that such impacts differ from place to place depending on the site-specific factors such as; vegetation cover and local topography (Hibbert 1967, Legesse et al. 2003, Loerup and Refsgaard 1998, Zhang et al. 1999, Siriwardena et al. 2006). In nearly all cases, these studies indicated increases in water yield with reduction of forest cover (Hibbert 1967, Bosch and Hewlett 1982, Zhang et al. 1999, Herron et al. 2002, Andreaassian 2004). There is a critical need to improve the understanding of large-scale interactions and the influence of forests on dry season flows, flood mitigation and groundwater recharge as suggested by Shiga Declaration on Forests and Water, 2002 (Shiga Declaration 2002).

2.2.1.1 Average runoff

Contrary to popular wisdom, most research on forest removal in catchments has resulted in greater streamflow (Douglass and Swank 1975, Gilmour 1977, Hamilton and King 1983, Ives and Misserli 1989). Hibbert (1967) experimented the effect of altering forest cover on water yield in 39 catchments worldwide. The results collectively suggested that i) forest reduction increases water yield, ii) reforestation decreases water yield, and iii) response to individual treatment is highly variable and, for the most part, unpredictable. Bosch and Hewlett (1982) further extended Hibbert's work and reviewed land-use changes in an additional 55 catchments i.e. altogether 94. The results of the 94 catchments in general suggested that none of the experiments to deliberately reduce cover-caused reductions in yield, nor have any deliberate increases in cover-caused increases in water yield from a given catchment.

It is very difficult to make experimental alterations of the vegetation cover of large river basins. Equally, seldom can one find studies dealing with observations made in small catchments applying hydrologic models to predict the impact of vegetation changes in large catchments (cited in (Siriwardena et al. 2006)).

Only a few studies (examples include (Eschner and Satterlund 1966, Costa et al. 2003, Siriwardena et al. 2006, Ring and Fisher 1985, Wilk et al. 2001) reported on the impact of forest cover and streamflow in large river basins. The latter two studies could not establish similar results that are found to exist for small catchments. The different results of the two studies are attributed to non-uniform variations in land-uses in the catchment, regeneration with various stages of vegetation, and spatial and temporal variation in rainfall.

A study by Siriwardena et al. (2006) of the large Comet river basin (16,400 km^2) in Australia which used a conceptual daily rainfall-runoff model (SIMHYD) suggested that the impact of clearing forest vegetation (from 83 percent forest vegetation to 38 percent) increased the runoff (approximately 40%). This outcome was reported to be consistent with the increase in runoff that results for this degree of clearing vegetation in small catchments. The study suggests that models developed to estimate the impact of land-cover changes derived largely from small catchment experiments may be applicable at this large scale. Similarly, Helmschrot (2006) studied the impact of afforestation on catchment hydrology in the Weatherly catchment of South Africa using modelling application. The results showed that the runoff will be significantly reduced by forest plantations by amounts ranging from 13 to 21 percent .

The simulated results of hypothetical land-use change and streamflow derived by using hydrological models also suggest similar results from the small-scale catchments (Wilk 2002, Herron et al. 2002). Wilk (2002) simulated the impact of land-use change on the availability of water resources for a large tropical catchment in the south Indian, Upper Bhavani basin (4,100 km^2). Various land-use change scenarios were tested to assess their effects on mean annual runoff. The largest increase in runoff of about 19% was the result of conversion of forest and savanna into agriculture. Mean annual runoff decreased by 35% after the conversion to commercial forest and decreased by 6% after partial conversion to tea plantations. Similarly, Herron et al. (2002) modeling results suggested that large-scale tree planting will substantially reduce river flows and impose costs on downstream water users (for example, causing a reduction in the security of water supply to irrigation areas downstream).

2.2.1.2 Peak flows and flooding

Peak flows can be changed due to change in land-use and land cover when the infiltration capacity of the soil is reduced. For example, this can occur through soil compaction or erosion, or increase in drainage capacity. Peak flows may increase due to the removal of trees (Bruijnzeel 1990). Relative increases in streamflow after tree removal is smallest for large events and largest for small events. As the amount of precipitation increases, the influence of soil and plant cover on streamflow diminishes (Brooks et al. 1991, Bruijnzeel 1990). Contrary to popular belief, forests have only a limited influence on major downstream flooding, especially large-scale events (FAO and CIFOR 2005). The impact of land-use on peak flow is less visible in the case of a large basin because of the time-lag difference between various tributaries, spatial and temporal variations in rainfall and land-use. This phenomenon may reduce the effect of land-use change on peak discharge; however, a sub-watershed (or micro-catchment) may experience overall increases in stream-flows (Bruijnzeel 1990, Brooks et al. 1991, FAO and CIFOR 2005).

Hydrological processes and relationships between forests and floods are often used to make generalizations that are frequently inappropriate or misleading. Much of the confusion arose from the sponge theory, according to which, the complex of forest soil, roots and litter acts as a giant sponge, soaking up water during rainy spells and releasing it evenly during dry periods, when the water is most needed. Although the theory came under criticism as early as in the 1920s, it continues to appeal to many people (foresters and non-foresters alike). In many countries, it is firmly embedded in national forest policies and programs (FAO and CIFOR 2005) including Nepal and the surrounding Himalayan countries (Ives and Misserli 1989). In fact, much of the water that does soak into the soil is used by the trees themselves for transpiration. Chang and Franczyk (2008) reviewed studies to identify primary causes of floods and suggested that changes in precipitation intensity or amount are responsible for increasing floods in coastal cities. Extensive and long-lasting floods in plain areas occur in macro-catchments which are generally caused by rainfall lasting for several days and often associated with melting of snow and ice with high antecedent soil saturation, a similar situation like the one which prevails in the Himalayan region during the monsoon season. Moreover, flash floods which occur in micro- to meso-scale catchments are mainly caused by intense localized precipitation (eg. thunderstorms, glacial lake outburst floods and lake burst) and common in hilly or mountainous areas (Bronstert et al. 2002).

Studies in Nepal indicated that the increases in surface infiltration rate which can accompany forestation are not likely to have a significant effect on the occurrence of downstream flooding (Gilmour et al. 1987). Hamilton and Pearce (1987) concluded that reforestation will not prevent floodings or sedimentation in the lower reaches of major rivers or significantly reduce flooding during major storm events. The main cause of the flooding commonly involves too much and intense rainfall over a too-short period. Similarly in case of very good forest cover also, those flood events are likely. Carson (1985) indicated that flooding and sedimentation problems in India and Bangladesh are a result of the geomorphological character of streams and human's attempts to contain the rivers. Deforestation is likely to play a minor, if any role in the major monsoon flood events on the lower Ganges. When major floods occur, it most often occurs towards the end of the rainy season, when heavy rainfalls si-

multaneously occur in a number of sub-basins and soils are already saturated and therefore incapable of soaking up additional water (FAO and CIFOR 2005).

2.2.1.3 Dry-season flows

The impact of land-use change on dry-season flows depends on the infiltration capacity of land cover and evapotranspiration by plants. Most experimental evidence in rainfall-dominated regimes suggest that forest removal (or change from high-water-use plants to low-water-use plants) increases dry-season flows (Brooks et al. 1991). In contrast, dry-season flows from deforested land may decrease if the soil infiltration capacity is reduced during the rainy season to the extent that groundwater reserves are replenished insufficiently (e.g. through use of heavy machines, during forest harvesting or subsequent agriculture, or due to an increase in impervious areas such as roads and villages/building rooftops) (Bruijnzeel and Bremmer 1989, Beven 2001a, Bruijnzeel 1990). If, on the other hand, soil-surface characteristics are maintained sufficiently after clearing to allow the continued infiltration of the rainfall, then the reduced evapotranspiration associated with forest removal will appear as increased dry-season flow (Bruijnzeel 2004). The continuous exposure of bare soil after the forest clearance (compaction of top soil, overgrazing, machinery) also contributes to gradual reduction of rainfall infiltration opportunities in cleared areas.

Significant reduction in low-flow rates was observed in the Mid-Mahaweli basin, Sri Lanka from 1955 to 1980 because of the impacts caused by large-scale conversion of tea estates into smaller area homesteads and other crops without proper soil-conservation measures (Bandara and Kuruppuarachchi 1988). Large-scale pine afforestation in 60,000 ha of watershed previously covered by grassland resulted in a reduction in dry-season flows of between 50-60% in the Fiji Islands (FAO and CIFOR 2005). Similarly, in the humid tropics of Australia, a stream that formerly ceased to flow in many dry periods flowed throughout the year after logging (Gilmour 1977). Helmschrot (2006) showed that after afforestation, low flow during dry season was decreased by 48 percent in the Weatherley catchment of South Africa. Loerup and Refsgaard (1998) suggested various factors should be taken into account for assessing the impacts of land-use changes on hydrology. One should focus not only on the percentage of various land-use categories, but also on the changes in crops and other management practices.

Bruijnzeel and Bremmer (1989) suggested that an important issue is whether reforestation of severely degraded soils in the Himalayas would eventually lead to such improved infiltration conditions. Bruijnzeel (1990) cautioned that more rigorous work is required to obtain firm answers on the relationship between reforestation and dry-season flows. However, reforestation leads to a decrease in water flow downstream should not be accepted as a sound, technical rationale for the reduction of reforestation programs. Reforestation has many benefits: reduction of soil erosion, maintenance of soil fertility, better environment for infiltration which are more important on a local level (upstream people), rather than downstream water yield (Bruijnzeel and Bremmer 1989).

In general, the studies related to the role of vegetation indicated that a greater impact is visible in small basins compared to large river basins. Only on a local scale, forest soil is capable of reducing runoff. The forest has very limited influence in major flooding events. In the monsoon-dominated

Himalayan region, too much water during a short period of time reduces the infiltration capacity of the soil and thus the vegetation (deforestation/afforestation) is likely to play a relatively minor role in flood events.

Studies related to Nepal

No regular land-use and land-cover information is available for the entire Kosi river basin. The Ministry of Forest and Soil Conservation, Department of Forest Research and Survey (DFRS), Government of Nepal, has conducted a number of forest resources assessments since the 1960s throughout Nepal (Acharya and Dangi 2009). According to the inventory by DFRS (1999), the total area of forest is about 29 percent and shrubland is 10.6 percent in Nepal. The forest area has decreased at an annual rate of 1.7 percent from 1978/79 to 1994 whereas forest and shrubland together have decreased at an annual rate of 0.5 percent. During this period, although the forest is decreased from 37 to 29 percent, the shrubland is increased from 5 to 11 percent (Acharya and Dangi 2009). Sharma et al. (2000a) compared the land-use data for the period from 1960-1965 through late 1978-1979 in the Nepalese part of the Kosi river basin: they reported that there is not much noticeable difference in land use and land cover during these periods. Forest cover increased from 54.7 to 56.2 percent during this period. The shrub and grassland later in the period was reported to be 6 and 4 percent respectively. Similarly, Virgo and Subba (1994) made a comparison of land-use change between 1978 and 1990 in middle mountains of Dhankuta district in the Kosi river basin in a pilot area of 200 km^2 based upon aerial photographs and a field survey. The results indicated that there is no statistically significant changes in land-use although the population was increased by 19 percent during the period. The total forest cover has increased from 36.5 percent to 38.8 percent during the period. Although the land-use has been stable, shifting has occurred in land-use patterns, with exchanges between different vegetation categories. A similar study by Gautam et al. (2003) in a small area (153 km^2) in the Kosi river basin using satellite images from 1976, 1989 and 2000 also indicated that there is an increase in broad-leaved forest, conifer-forest and lowland-agriculture areas and a decrease in shurblands, grasslands and upland agricultural areas. In total, nearly 5 percent forest area has increased between 1976 and 2000. The increases in forest cover is attributed to the implementation of a community forestry program where the local forests are handed over to and managed by local communities for its resource management.

In the context of the Himalayan region, very few studies have reported the impact of land-use change on hydrology. Sharma et al. (2000b) completed an impact assessment using a conceptual hydrological model. The study suggested that the transformation of all agricultural land into forest reduced the runoff by 1.3 percent compared to the baseline. The study by Rai and Sharma (1998) shows that the land-use change from forest and agroforestry to open agriculture has increased the streamflow by 11 percent.

The impact of land-use change on hydrology is observed from experiments in small-scale catchments (Hibbert 1967, Bosch and Hewlett 1982). For large-scale catchments, most of the results are based upon observational records (Costa et al. (2003), Ring and Fisher (1985), Wilk et al. (2001) and hydrological modelling (Siriwardena et al. 2006, Krause 2002). Hydrological models are widely used to assess the scenarios of land-use and land-cover change (Pauleit et al. 2005, Krause 2002, Niehoff et al. 2002, Siriwardena et al. 2006). These studies suggested that spatially distributed and process-oriented

hydrological models can simulate the response of land-use change on streamflow fairly well. The hypothetical scenarios (e.g. deforestation) can be easily adapted in a distributed hydrological model by considering the major impacts of deforestation.

2.2.2 Soil erosion and sedimentation

Vegetation cover is acknowledged to be the principal determinant of specific erosion rates. The lack of vegetation cover accelerates high erosion (Stocking 1984). Walling (1999) suggested that the change in surface condition from natural undisturbed land to cultivation in general will result in increases in the soil-erosion rate. The impact of land-use change on rates of soil loss and particularly the impact of land clearance and cultivation on increasing erosion rates have been extensively documented. However, the evidence of major changes in the sediment loads of larger rivers is less clear (Walling 1999). Results obtained from erosion plots and catchment experiments provide clear evidence of the sensitivity of erosion rates with regard to land-use change and related human activity (Walling 1999).

More importantly, ground-surface protection is largely ensured by under-story vegetation and litter, and by the stabilizing effect of the root network of vegetation. It is widely perceived that forests can control erosion and sediment processes. Although forest cover does not tend to eliminate erosion, it is not the tree canopy that is directly responsible for this, rather it is the undergrowth and forest litter. Experiments indicate that the erosive power of raindrops under trees actually tends to be relatively great because the raindrops merge before dripping off of the leaves and therefore hit the ground with greater force (FAO and CIFOR 2005). In steep slopes, the net stabilizing effect of trees is usually positive (e.g. beneficial in reducing erosion and/or soil loss). Vegetation cover can prevent the occurrence of shallow landslides (Bruijnzeel 1990). The actual soil loss, however, depends largely on the use to which the land is put after the trees have been cleared. Surface erosion from well-kept grassland, moderately grazed forests and soil-conserving agriculture are judged to be low to moderate (Bruijnzeel 1990).

Gardner and Gerrard (2003) studied the runoff and soil erosion on cultivated rainfed terraces in the Middle Hills of Nepal named Likhu Khola. The soil loss was reported to be from 2.7 to 12.9 t/ha. The study by Shrestha (1997) in the Middle Hills of Nepal estimated annual soil loss rates based upon a soil-erosion assessment model (Morgan et al. 1984). The rate is the highest (up to 56 t/ha) in areas with rain-fed cultivation, which is directly related to the sloping nature of the terraces. Soil losses are comparatively lower (less than 10 t/ha) among land-use types, such as forest, grazing land and rice cultivation. The lowest soil losses (less than 1 t/ha) are recorded in dense forest. Ramsay (1987), Impat (1981) summarized the literature based on the measured rates of surface erosion in Nepal. The high rates of surface erosion under different circumstances and the relative differences between varying land-use types, eg. overgrazed pasture (9.85 t/ha), protected pasture (1.01 t/ha) and forest (0.43 t/ha) were reported.

Soil erosion is one of the most serious problems in Nepal which has affected adversely the country's economy as well (Carson 1985). The rates of soil erosion in Nepal vary depending upon the method, location and the nature of the study. Ives (2004) indicated that there is little precise information on rates of erosion and mass movement processes in the Higher Himalaya. It is assumed that the erosion

rates might be very high because of the steepest mountain system, very high-angle glaciated slopes and influenced by tectonic instability.

Effects of soil erosion are likely to be apparent on-site. An inverse ratio occurs between sediment delivery and basin size. In big river basins, effects of erosion may only be noticeable after a considerable time lag (decades) due to storage effects (Kiersch 2000, Bruijnzeel 1990). Effects of erosion-control measures on sediment yield will be most readily recognized on site. Ives and Misserli (1989) suggested that human intervention probably changes the landscape at micro-watershed level or on individual mountain slopes. However, impacts of intense rainfall tends to exceed (or mask) the effects of human activity (accelerated erosion) with regard to the overall natural process. At the macro-scale, however, natural processes will reduce the role of human intervention to insignificant proportions. Walling (1999) suggested that the impact of land-use change and related human activities on sediment yields should consider the overall sediment budget of a catchment rather than simply the sediment output.

Downstream sediment yields are not always the result of upstream land-use practices. Human impacts on sediment yield may be substantial in regions with stable geological conditions and low natural erosion rates. In regions with high rainfall rates, steep terrain, and high natural erosion rates (similar to the Himalayan region), the relative impact of land-use may be negligible (Kiersch 2000). According to Bruijnzeel (1990), in a Himalayan river basin, a combination of several factors is likely, including intense rainfall and resulting high streamflow rates, steep and unstable terrain with relatively few opportunities to store sediment and a resultant high rate of sediment transport (e.g. output from a basin).

Wasson (2003) suggested that the relationship between land-use and sedimentation is not clear despite many decades of research in the Himalayan region. The only substantial progress made since the 1980s is the identification of the Higher Himalaya as the most likely dominant source of sediment. The study suggested that the Higher Himalaya contributes about 80 percent of total suspended sediment budget to the Ganga-Brahmaputra catchment. Wasson et al. (2008) suggested that it is difficult to identify the role of human activities in the erosion and sediment transport system of the Himalaya. However, both deforestation and its effects on erosion and sediment transport are far from uniform throughout the Himalayas. The impact of erosion caused by natural events and land-cover change on the Gangetic Plain remains uncertain. Natural erosion in the Himalayas has been shown to be an important phenomenon and is probably higher than in most other mountain systems in the world (Ives and Misserli 1989). This is also partly due to the monsoon climate which includes high annual precipitation concentrated within in a short period of time associated with steep slope and a young and fragile mountain system.

2.2.3 Impact of climate change on hydrology

Much of the literature has discussed the impact of climate change on water resources in the context of existing global warming and growing atmospheric concentration of carbon dioxide (Gleick 1989, Arnell 1999a, Nijssen et al. 2001, Bates et al. 2008). This literature is mostly related to specific regions, although not limited to them: this includes part of **Europe** (Arnell 1999b, Middelkoop et al.

2001, Bergstroem et al. 2001), **North America** (Christensen et al. 2004, Hauer et al. 1997, Schindler 1997, Hamlet and Lettenmaier 1999), **Australia** (Whetton et al. 1993, Chiew et al. 1995, Chiew and McMahon 2002), **Asia** (Sharma et al. 2000b,a, Cruz et al. 2007, Eriksson et al. 2009, Bajracharya et al. 2007, Gosain et al. 2006). IPCC (2007), Bates et al. (2008) suggested that both observational records and climate projections provide abundant evidence that water resources are vulnerable and have the potential to be strongly impacted by climate change with widespread consequences for human societies and ecosystems.

Hydrological models driven by output from a General Circulation Model (GCM) by using different SRES (Special report on emission scenarios) alternatives have been used recently. Recent hydrological research strongly suggests that global climate change will alter the water balance of river basins, soil moisture and water quality. Eventually such changes will bring challenges for sustainable water-resources management (Gleick 1989, IPCC 1996, Bates et al. 2008, IPCC 2007). In the background of such alteration, changes in hydrological resources have the potential to impact on the socio-economic and livelihoods on global (Alcamo 1994) as well as regional scales (Eriksson et al. 2009).

In Asia, especially in the Himalayan region, the impact of climate change on snow and glaciers and associated hydrological response are well discussed in the literature (Singh and Kumar 1997, Barnett et al. 2005, Singh and Bengtsson 2004, Mool et al. 2001b,a, Paul et al. 2004, Bajracharya et al. 2007, Eriksson et al. 2009, Dyurgerov and Meier 2000, 2005, Sharma et al. 2000b,a). All these studies suggested that the global warming and a rise in temperature has impacted the spatial distribution of glaciers and related flows. In Nepal, the maximum temperature was reported to be increasing at the rate of 0.06^{o}C/year between 1971-1994 (Shrestha et al. 1999). Similarly, in the Tibetan Plateau also, the temperature was found to be increasing at the rate of 0.16^{o}C/decade (Liu and Chen 2000).

Himalayan glaciers cover about three million hectares or 17 percent of the mountain area as compared to 2.2 percent in the Swiss Alps. They form the largest body of ice outside the polar caps and are the source of water for the numerous streams that flow across the Indo-Gangetic plains. These glaciers are receding faster than in any other part of the world (IPCC 2007). Rapid glacier shrinkage and the formation of glacial lakes are widespread in many parts of the Himalayan region (Mool et al. 2001b, Bajracharya and Mool 2009). IPCC (2007) suggested that mountain glaciers and snow cover have declined on the average in both hemispheres. In the coming decades, many glaciers in the Himalayan region will retreat while smaller glaciers may disappear altogether. According to the study based on remote-sensing images in the Dudh Kosi river basin (where the hydrological model is run, Chapter 6) the glacier areas have decreased by nearly 12 percent (in the range of 2 to 39 percent) between 1976 and 2000 (Bajracharya and Mool 2009). Dyurgerov and Meier (2005) indicated that most of the glaciers indicated negative cumulative mass balance between 1960 and 2003 as shown in Figure 2.2. The figure indicates that glaciers of the Himalayan region are receding at a relatively high rate compared to glaciers of the other region of the world.

Mountain glaciers play an important role in the water budget of many regions in the world. Many rivers originating from glacier-dominated area are sustained by snow and glacier melt. For the planning of many water resources development projects (such as hydropower, irrigation and dams), the understanding of the role of glaciers is vital (Schneeberger et al. 2003). Kundzewicz et al. (2007)

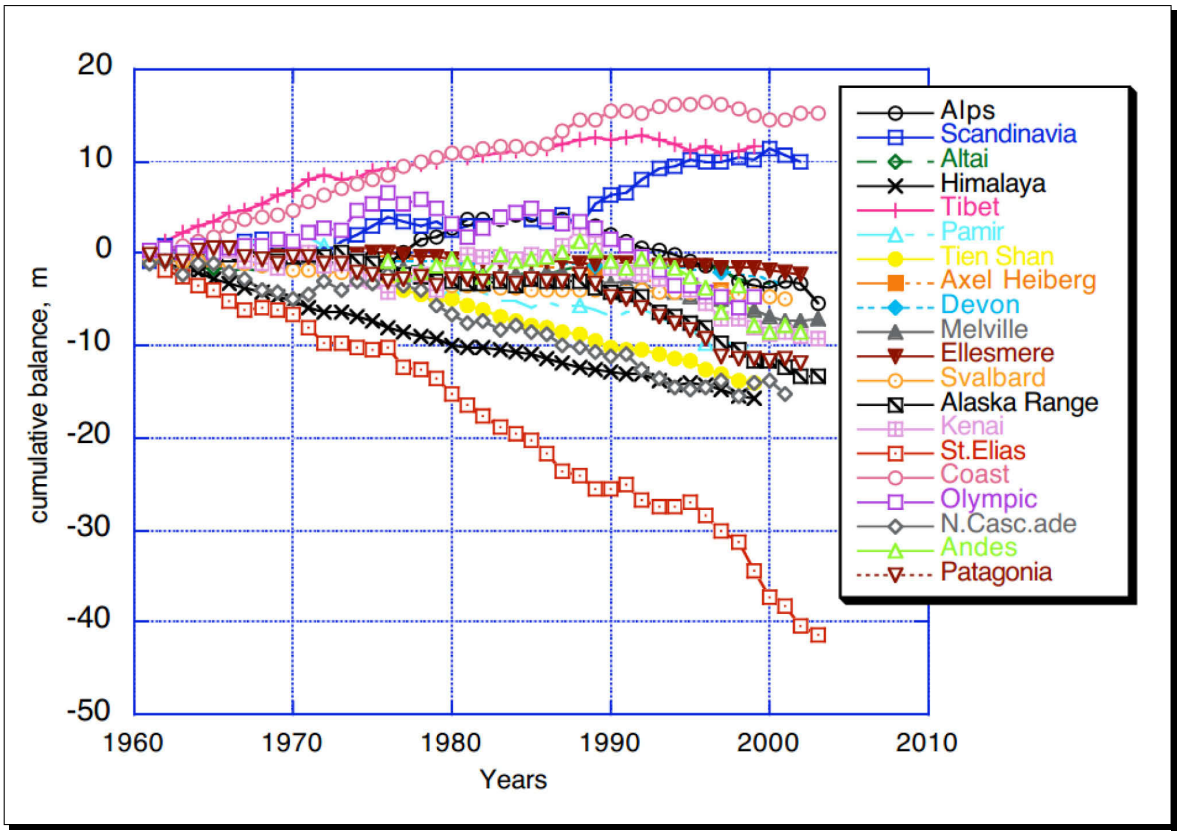

Figure 2.2: Cumulative mass balances of selected glacier systems. Source: Dyurgerov and Meier (2005)

indicated that as the glaciers retreat, river flows are increased over the short term, but the contribution of glacier melt is expected to gradually decrease over the next few decades. The melting of glaciers may change the hydrological discharge of a river basin. Eriksson et al. (2009) suggested that with the current rate of glacier melting in the Himalayan region, the amount of water that flows downstream will increase, which may appear as normal over the short term. However, when the water shortages occur due to the high rate of melting, water systems may go from abundance to scarce within a very short period of time. This will severely affect downstream water availability, agricultural production and hydropower generation. Excessive melt waters, in combination with precipitation may also trigger flash floods and debris flows (Hewitt 2005).

The melt contributions from snow and glacier melt vary across the Himalayan region. Immerzeel et al. (2010) suggested that the snow and glacier melt components (or contributions) in the region are important in sustaining seasonal water availability and are likely to be affected substantially by climate change. However, the extent of the potential impact is still unclear. The author further suggested that meltwater is very important to the western Himalayan region (such as the Indus basin) and plays only a modest role in the eastern Himalaya (such as the Ganges river basin).

A very few studies have attempted to quantify the role of snow and glacier melt in the region. Alford and Armstrong (2010) estimated the role of glaciers in streamflow from the Nepal Himalaya using

orographic runoff model (based on the relationship between mean specific runoff and mean elevation of a basin). Glacier melt is estimated using the ablation-gradient. Immerzeel et al. (2010) quantified the meltwater using the Normalized Melt Index (NMI) method. NMI is defined as the volumetric snow and glacier upstream discharge divided by the downstream natural discharge where the upstream discharge is calculated using a snowmelt runoff model. Similarly, (Sharma 1993) made an assessment of snow and glacier melt by comparing the hydrograph of snowfed and rainfed rivers in Nepal. Singh and Jain (2006) estimated the snow and glacier melt in the Satluj river of the western Himalayan region using a simple water balance approach and by subtracting from the total streamflow that part of streamflow estimated from rain contribution. Most of these studies do not take into account the physical interaction involved in snow and glacier melting processes affecting streamflows. In addition, these studies do not differentiate the contribution from glacial icemelt from snow and glacier melt. Few other studies included hydrological modelling in the Nepal Himalaya such as Sharma et al. (2000b). The study used a conceptual distributed hydrological model in the Tamor river sub-basin (one of the catchments in the Kosi river basin) for a monthly time interval, however, the results do not provide information regarding the several runoff components.

Immerzeel et al. (2012) made a study about the impact of climate change on hydrology of a glacierized catchment in central Nepal using the PCRaster environment for numerical modelling (Karssenberg and Burrough 2002). The study simulated the glacier evolution (including location and permanent snow) using a historic dataset and estimated the impact of future climate change on glacier hydrology. The study results suggested that both glacial area and glacial ice volume will substantially decrease in the future, due to increasing temperature scenarios. The glacial area will be decreased by 32 percent in 2035 and by 50 percent in 2055 in this study catchment.

2.3 Other linkages

The assessment of the socio-economic and institutional dimensions of upstream-downstream linkages are beyond the scope of this study. Nonetheless, they are an integral part of assessing the water resources and subsequent livelihood related activities. A short review is included herein in order to provide a broader picture of upstream downstream linkages within the framework of integrated systems analysis.

Upstream-downstream communities share socio-economic and cultural linkages (for example, migration, customs and rituals). Migration is perhaps the most significant part of the upstream-downstream linkages, because human migration is a means of commodity transfers (Ives 2004). The fundamental basis of upstream-downstream economic linkages arises from differences in the availability of natural resources and the potential opportunities of production and exchange they generate. Equally important are human interventions, ranging from infrastructure and institutions to technological and human capabilities that shape the pace and pattern in implementation of development opportunities. Due to constraints imposed by relatively high degrees of inaccessibility, fragility, marginality and even diversity, the means and mechanisms of 'capturing' niche opportunities and engaging in external exchange transactions are quite limited in this region. Because of these circumstances, mountain areas and com-

munities acquire the status of marginal entities, given their economic state and other interactions in comparison with mainstream, more urban, economies that tend to be located in the lower-elevation plains (Jodha 1997).

In a definite manner, economic linkages are manifested by the flow of products (such as agriculture), services and resources from upstream to downstream. An understanding of these flow of goods, i.e., their nature and magnitudes as well as their processes and impacts, can help us develop approaches to make them more equitable and sustainable. This can strengthen the complementarity of upstream-downstream economic linkages (Jodha 1997) in a broader framework of Integrated Water Resources Management (IWRM). The flows of resources, products and services between the two are characterized by terms of trade that tend to commonly be unfavorable to those living in highlands (Jodha 2000). The land and water management in upstream has effects to downstream which are of significant relevance, not only from a physical point of view, but also from a socio-economic perspective.

2.4 Upstream-downstream linkages in the Himalayan region

The existing upstream-downstream linkages in the Himalayan region in general and in the Kosi river basin in particular are discussed here. The different aspects of upstream-downstream relationships in the region are discussed in the literature. Eckholm (1976) addressed the environmental crisis in the Himalayan region and mainly claimed, among other things, that the environmental degradation in the Himalayan region is a major cause of flooding in the Gangetic plain in India and Bangladesh. Similar conclusions regarding "eco-crisis" were named the ‘Theory of Himalayan Environmental Degradation’ (THED) by Ives and Misserli (1989). The other highlights of the THED include that accelerated erosion, sedimentation and increasingly severe downstream flooding in the Himalayan region was driven by population growth, forest clearance, ineffective agricultural technologies, cultivation of steep slopes, over-grazing, and unsustainable use of forests, fodder and fuel wood (Ives and Misserli 1989).

Ives and Misserli (1989) reported that the theory pulled into the assumptions, emotions and widespread generalizations of deforestation, changes in hydrologic conditions, soil erosion and sediment transfer linkages. They argued that the theory, in general, was unacceptable on the grounds that it lacks scientific substantiation. More focused and rigorous empirical research is required in order to confirm many issues that have been raised as a part of the THED. Furthermore, such impacts may not be significant when compared to the natural erosion and mass wasting (e.g. landslides) which generate large amounts of sediment to river systems (Bandyopadhyay and Gyawali 1994). Experts believe that there are more complex basic causes (Jodha 1995, Kasperson et al. 1995).

Thomson and Warburton (1985), Thomson et al. (2006) contributed to the critical assessment of the shortcomings of this constructed approach. They argued that the scale of scientific uncertainty in the Himalayan region is so great that it is difficult to get objective information from existing research for use in public policy and decision making. The authors further suggested that difficulties are due to interconnected natural and human forces. Describing the nature and the extent of the problem is a complex process full of uncertainty. There are many levels of interdependent cause-and-effect

relationships to consider in the context of extremely complicated ecological and social systems. Uncertainty has become just as important a feature of the problem as any of its other attributes.

> *"The Himalaya, all the experts agree, face serious environmental problems; they are caught in a downward spiral. The rate of fuel wood consumption, for instance, is asserted to be far in excess of the rate at which the forest grows. However, the expert estimates of these two rates vary by such immense factors that we simply cannot say whether the spiral, if it exists, is upward or downward. There is something severely wrong with the Himalaya but we cannot tell what it is. The traditional response - a call for more research - has not worked and the perceived urgency of the situation calls for action now, before it is too late. The challenge is to furnish a non-arbitrary strategic framework for the action."* Source: (Thomson et al. 2006)

The upstream-downstream linkages in the Kosi river basin are discussed primarily regarding: **i)** upstream land-use changes and associated soil erosion and sedimentation **ii)** watershed degradation and impact on downstream water flow, and **iii)** snow and glacier melting in high-altitude areas and water availability in downstream areas. However, no attempt has been made to look at the activities within the framework of integrated systems analysis. Natural Environment (NE) and Human Dimension (HD) of the Himalaya in general and the Kosi river basin in particular are closely interlinked suggesting strong cause-and-effect relationships of activities and processes with the system.

2.5 Need for integrated hydrological modelling

The review of linkages between upstream-downstream clearly indicated that the linkages are interactive and interlinked among natural environment and human system components. From the hydrological point of view, precipitation is a major driving factor and the flow of water in a river connects the upstream areas with the downstream areas. A traditional sector approach considers water management as a separate entity from other natural resources such as forests and agriculture. The mountain hydrology across the landscape has complex and interlinked linkages between the different components of upstream and downstream areas. In this context, the research area of integrated modelling is rapidly gaining interest for application within the context of climate and environmental change (such as land-use change) (Krol et al. 2006) and its cumulative impact on water resources and society in general. Therefore, it is vital to understand the hydrological system dynamics of a catchment to assess upstream-downstream linkages. Once the role of different watershed components (such as land-use, soil, geology, snow, glaciers and climate) to streamflow are understood, it provides a basis to understand the linkages. Hydrological models are an important tool to understand the different watershed components and their respective roles in hydrology. In recent decades, with the invention of powerful computer technologies and geographical information system, the hydrological models have become more robust to incorporate other aspects of a natural environment which influence the hydrology such as global climate change. However, the output from the model depends upon the nature of the model and its structure which takes into account the different components of watershed. Flügel (2009) suggested that geoinformatics offers a wide range of concepts, methods and software tools, i.e.

models, GIS, remote sensing which account for scale related issues of interactive process dynamics in river basins. An example is the Jena Environment System Analysis Toolset (JESAT) which has been successfully applied in integrated systems analysis (Flügel 2009) .

The 'what-if'-scenario analysis is another important aspect of upstream-downstream linkages and has the critical role of applying hydrological models. This can be done when the system dynamics are better understood by using hydrological models as suggested in the previous paragraph. This will help to understand the behavior of a catchment under different scenarios (such as land-use and climate change). Such information is very useful for planning and management of water resources (such as hydropower development, irrigation systems etc.) in the context of adaptive IWRM options (Flügel 2011). Eventually, this information will provide a basis for strengthening linkages between upstream and downstream communities in the context of sustainable IWRM.

> Integrated Water Resources Management (IWRM) is 'a process, which promotes the co-ordinated development and management of water, land and related resources, in order to maximize the resultant economic and social welfare in an equitable manner without compromising the sustainability of vital ecosystems' (GWP 2000).

Within the framework of IWRM in a river basin, the land and water management in upstream areas has an effect to downstream communities. On the one hand, there are 'opportunities' of good watershed management and on the other hand, there could be 'threats' due to bad watershed management practices (such as unsustainable and forest and land management). These activities can influence the river flow, seasonality and quality of the water flowing to downstream areas (Nepal and Adiga 2006, Falkenmark and Lundqvist 1999). Balancing these opportunities and threats constitutes a major challenge within IWRM. On the regional level, upstream-downstream dependencies within river basins involve major challenges related to conflicts of interest on the national or regional level between several countries (Falkenmark and Lundqvist 1999). Nepal and Adiga (2006) suggested that at local level, it is necessary to bring both user groups of upstream and downstream areas so that the synergy of land and water management will benefit the communities of an entire river basin and beneficial aspects are augmented and adverse effects mitigated. GWP and IBNO (2009) suggested that 'whole basin approach' (considering implementation of policies and actions at basin scales) may resolve upstream-downstream (for a river) and region-to-region (for a lake or groundwater resource) controversies. The whole basin approach allows the assessment of impact at a system level under the framework of IWRM. Flügel (2009, 2011) suggested that the development of adaptive IWRM options must apply a holistic system's approach to account for impacts from climate change.

While assessing and analysing upstream-downstream linkages, it is important to choose the indicators which are measurable and objectively verifiable for the assessment of the linkages. Some of the socio-economic issues need a detailed dataset to establish the linkages. For example, to assess the benefits of upstream watershed conservation to downstream agricultural productivity, a comprehensive dataset is required. Therefore, the following priorities are set for the assessment of upstream-downstream linkages in this study: rainfall-runoff processes, land-use and land-cover change and climate change. The linkages are evaluated and discussed primarily with regard to these priorities.

2.5.1 Snow and glacier melt modelling

There are different approaches for snow and glacier melt modelling. In general, they can be classified into energy balance, temperature index and combined approaches (Hock 2005, Braun 1986, Morris 1985, Fox 2003). The energy-balance approach considers energy input into the snowpack by considering surface-energy balance. Physically-based models compute melt runoff using this approach by taking energy balance into account. This approach requires a greater amount of physical data such as net radiation, albedo, latent heat flux, turbulent heat flux and ground heat flux. (Hock 2005) which are not readily available. The temperature-index approach assume an empirical relationship between air temperature and snow and ice melt based on a strong and frequently observed correlation between these quantities. This approach "lumps" all of the components of energy balance into a degree-day factor (Hock 2003). It requires only air temperature to estimate the melt runoff. The hybrid approach combines the importance of energy balance (such as solar radiation, albedo) with a degree-day factor (Fox 2003) and also known as the "enhanced degree-day factor". The available energy-balance information can be integrated into temperature index approach to replicate physical processes of snow and ice melt. Hock (2005) compared the snowmelt pattern based on different modelling approaches. The results indicated that the model based on a degree-day factor (temperature-index model) adequately represents the observed seasonal discharge pattern but results are poor for representing daily discharge fluctuations. However, model performance is considerably improved by incorporating potential direct solar radiation as an index of local and daily variability in the energy available for melt.

In the context of the Himalayan region, snow and glacier melt are estimated by using an empirical approach. For example, snowmelt based on ablation gradient (Alford and Armstrong 2010), threshold air temperature (Sharma et al. 2000b), degree-day factor (Immerzeel et al. 2010). Immerzeel et al. (2012) recently used an enhanced degree-day factor considering aspect and debris covered glaciers and this also replicates the glacial icemelt process in an improved way.

Modelling glaciers require very detailed information about different components of glacial regime (such as energy balance, physiographic properties and debris cover). In most glaciers, water is stored inside either englacially (within voids in the body of glaciers) or subglacially (at the interface between glaciers and substrate). During spring and early summer, net water storage increases whereas during late summer and autumn, net water storage decreases (Walder and Fountain 1997). Large volumes of stored water may be rapidly released and generate so-called outburst floods (Walder and Costa 1996, Walder and Fountain 1997). When the glacial lakes are formed, the liquid water can be stored under the frozen lake, which can supply water to streamflow, even when the surface is frozen and temperature is below zero. It is very difficult to estimate such dynamic processes inside the glaciers especially in the case of the Himalayan region where the data are lacking, especially in the high altitude areas.

2.5.2 Challenges of hydrological modelling in the Himalayan region

It is very important to understand the hydrological system of alpine mountains of the Himalayan region to better understand the impact of environmental and climate change on water resources and subsequently on future water availability. Such information is useful for the implementation of sus-

tainable IWRM and for the plan of adaptation strategies critical to minimize the effects of climate change. Understanding the hydrological dynamics of Himalayan river systems using a hydrological model is challenging for the following reasons:

- Lack of representative data (Alford 1992, Sharma et al. 2000b, Kattelmann 1987) due to a low density station network and a particular location (low altitude and valleys) which is unable to capture the dynamics of precipitation in the mountains for the entire catchment (spatial factors),
- Uncertainties due to the absence of long term records (temporal factor) and due to practical difficulties in maintaining data quality (e.g. remoteness and lack of accessibility) (Kattelmann 1987) which results in inaccuracy in decisions concerning water resources management (Alford 1992),

The hydrological model should be able to capture the important hydrological processes of Himalayan rivers which comprises high floods (during the monsoon season) and low flow (during the winter season). Besides, the streamflow is contributed by glacier and snow melt. Therefore, there is a need of a robust and dynamic hydrological model which can deal with the limitations as much as possible as described above in a meso- and macro-scale catchment where the heterogeneity of the catchment parameters increases with a decrease in data accuracy (Krause 2002, Alford 1992).

The glacier and snowmelt is particularly significance for the Himalayan region. In recent years, the importance of glacier melt is discussed widely. However, the role of snow and glacier melt (including glacier ice) has been mostly discussed from general observation, empirical and conceptual approaches as discussed above. In addition, the role of different runoff components has not been conducted in detail, which questions the reliability of the output from empirical approaches. Very few studies have attempted to differentiate the various runoff components, more critically in this case, including the effects of snow and glacier melt.

2.5.3 Classification of hydrological models

Hydrological models are simplified representation of the real world (Refsgaard 1996). Hydrological modelling systems can be grouped into many categories based on the modelling approaches used. The basic distinction among models involves underlying stochastic and deterministic approaches. Stochastic models are statistical characteristics and therefore results in a certain amount of randomness in simulated results. In contrast, deterministic models are based on mathematical relations in which outcomes are obtained through known relationships among state and events. Most hydrological models are deterministic in nature. Depending on the hydrological processes and modelling approach, the hydrological models can be categorized as follows: physically based, conceptual and black-box (Daniel et al. 2011, Singh and Frevert 2002, Cunderlik and Simonovic 2003).

Physically-based models, also known as "white"-box models, are fully based on laws of physics. They consist of a complex set of mathematical equations to represent the hydrological processes in a catchment. Examples of such models are: the MIKE-SHE model (Jayatilaka et al. 1998), the PRMS/MMS model (Leavesley et al. 1983), the J2000 model (Krause 2002, 2001), and the HSPF (Bicknell et al. 1997).

Conceptual models, also known as "gray"-box models, are a combination of an empirical approach and simple functions of physical processes. Generally, this category of models considers physical laws but in a simplified form. The requirements of input data are less extensive than that of physically-based models. Due to this nature, conceptual models are often preferred over physically-based models. Examples of conceptual models are SWAT (Arnold et al. 1993) , HBV (Bergstroem 1976), QUAL-2K (Chapra and Pelletier 2003) and J2000g (Krause et al. 2009).

Empirical models, also known as black-box models, do not take into account any physical processes. They consist of functions used to approximate or fit available data. Examples include simple regression models or water-balance/water-quality spreadsheet models.

Another classification is based on the spatial variability of system variables and parameters. Under this classification, the models are categorized into: distributed, semi-distributed and lumped models. Most of the physically-based hydrological models rely on either spatially distributed or lumped characterizations of topography and other spatial variables (Singh and Frevert 2002, Cunderlik and Simonovic 2003, Daniel et al. 2011).

Lumped models simplify physical characteristics of the hydrological system by lumping processes and treat catchments as a single entity. This approach considers a watershed as a single unit for computations where the watershed parameters and variables are averaged over this unit. The lumped approach is often implemented in conceptual models.

Semi-distributed models have a more physically-based structure than lumped models have. They are a composition between the lumped and distributed model and demand less input data than distributed models do. Generally, the small sub-catchments are lumped so that the whole catchment has more than one lumped basins. An example of semi-distributed models is the SWAT (Arnold et al. 1993).

Distributed models comprise the spatial variation of watershed characteristics with state variables (such as precipitation, temperature, soil, geology and land-use) by discrediting the system into a large number of elements or grid squares (Beven 2001b). These models need a large amount of data for parameterization in each modelling unit. Because the physical process of a catchment is simulated in detail, they provide the highest degree of accuracy. They have become more common in recent years. Examples of distributed models are the PRMS/MMS (Leavesley et al. 1983) and the J2000 (Krause 2002, 2001).

Flügel (1995), Bongartz (2003) recommended that the distributed concept of a catchment is useful for hydrological systems analysis. The distributed approach comprises a specific assembly of components characterizing the catchment's natural and human environment which are essential for integrated systems analysis. In addition, Anderson and Burt (1985) emphasized the role of physical-based models which offer the ability to predict a complete (e.g. multi-component) runoff regime with multiple outputs being provided. Similarly, they are able to predict the effect of catchment changes, which is particularly important where resources management is involved.

2.6 Role of hydrological modelling in the planning and management

Challenges in water resources management exist both on a global and a local level. Hydrological models related to water quantity and quality are being developed and used in increasing numbers and varieties to support water management decisions (Refsgaard 2007). The role of hydrological modelling in different phases of the planning and implementation of water resources development are well recognized. Within the approach of IWRM, which emphasizes the integrated management of land and water resources on a river basin scale, the role of hydrological modelling is ever increasing (Flügel 2009, Refsgaard 2007).

For many years, there has been a major gap of information about the baseline condition of different watershed components and how they influence the hydrological regime when planning water management. In order to bridge these gaps, hydrological models are among the available tools used to acquire an adequate understanding of the characteristics of the river basin (Tessema 2011). The main purpose of a hydrological model is two fold:

1. To better understand the system dynamics of a physical system (such as a watershed in this case) and the interaction of the different system components (soil, groundwater, snow, and glacier); and
2. Based on that understanding, to forecast (referring to certain periods in real-time) or predict (independent of a specific time reference) the behavior of this real-world system (DeCoursey et al. 1982, Anderson and Burt 1985) based upon one or more sets of underlying resource-development or physical-setting (such as climate change) assumptions.

Beven (2001a) emphasized that the ultimate aim of hydrological simulations is to improve decision-making concerning a hydrological problem for different sectors such as planning, flood protection etc. Due to an increasing demand on water resources throughout the world, improved decision making, within the context of global climate change, should benefit from application of improved models. Hence, the role of hydrological modelling in understanding the hydrological behavior of the system and thereby assessing the impact of climate change is increasing in various sectors. In fact, hydrological simulation models are one of the robust tools to assess the impact of climate change on hydrology. Among those studies, only a few (Akhtar et al. 2008, Singh and Kumar 1997, Barnett et al. 2005, Singh and Bengtsson 2004, Krause and Hanisch 2004) have applied different models to assess the impact of climate change on hydrology. Similarly, hydrological models are also instrumental in quantifying the potential impacts of land-use change on water resources. This can provide a prognostic scenario of what will be the impact on hydrology if the land-use and land-cover conditions are changed.

2.6.1 Application of the J2000 hydrological model

For the purpose of this study, the J2000 hydrological model (Krause 2001, 2002) has been chosen. The primary rationale for selecting the J2000 hydrological model for this study involve its process-

oriented and distributed nature to replicate the hydrological dynamics in meso-scale river basins. A meso-scale catchment in a mountainous region comprises heterogeneity in terms of topography, land-use and other conditions complemented by decreasing data accuracy and availability on the larger scales. In general, the mountain topography leads to the formation of unique climatic conditions in different elevation zones, due to change in temperature with elevation. The distributed concept of J2000 takes into account such heterogeneity by using an Hydrological Response Unit (HRU) approach (Flügel 1995) which is an advantage over lumped or semi-distributed models. Moreover, the model has high flexibility and adaptability to integrate different components within the model framework without much change in the other existing modules. With such flexibility, a glacier module is integrated into the existing J2000 model in this study. Due to limited access to model code and implementation process, such flexibility is difficult to achieve in other models. The glacier module takes into account the enhanced degree-day factor including radiation, slope, aspect and debris covered factor into account. In addition, snow module calculate different phases of snow accumulation, metamorphosis and snowmelt processes take into account the different components of energy balance (such as snow density, snow depth, slope, aspect and sublimation).

In addition, the distributed process-oriented modelling of the runoff generation makes the J2000 a suitable tool for the quantification of the impact of land-use changes on the water balance of large catchments. The specific conditions of the catchment environment can be altered to understand 'what if' scenarios. For example, to study the land-use change scenarios, the distributed land-use and land-cover information can be changed to hypothetical land-cover (example: deforestation) to understand the impact of land-use on hydrology. Moreover, there is a flexibility to choose the different sets of algorithms to calculate the environmental conditions (such as evapotranspiration) depending upon the availability of hydro-climatic data sets. The model has already been applied in micro to meso-scale catchment in different parts of the world to understand different aspects of hydrology such as water balance and impact of land-use and climate change. Originally developed for large river basins to reproduce hydrological dynamics in Germany, the main idea for the J2000 model was to bridge the gaps between the models developed for small catchment vs. those those for large scale basins (Krause 2002). In this study, the J2000 model was applied to and adapted for the specific context of the monsoon-dominated Himalayan river basins dominated by glaciers in high altitude areas. Moreover, it intended to use the model as a tool to understand the upstream-downstream linkages in the region with focus on changes in upstream state of the environment and the water availability to downstream.

Many efforts have been put in the study of the upstream-downstream linkages using a segregated approach in the region. This study presents a unique approach to understand the different components of upstream-downstream linkages by using a hydrological model . It emphasizes that the linkages should be assessed within the framework of integrated systems analysis. Therefore, the J2000 hydrological model is adapted and implemented in the region and used as a tool to assess the different components of the upstream-downstream linkages.

3 Research objectives and methodological approach

The literature review in Chapter 2 provides the detailed information about the upstream-downstream linkages, including the research deficits in this area. Therefore, the following objectives, research questions and methodological approach have been proposed:

3.1 Research objectives

The primary objective of this study is to evaluate the upstream-downstream linkages of hydrological dynamics in the Himalayan region and their influence on water availability to downstream areas. The specific objectives are:

1. Analysis of spatial distribution of precipitation in relation to topography and elevation in different river corridors of the Kosi river basin,
2. Analysis of the hydro-meteorological dataset (precipitation, temperature and discharge) and the estimation of past climatic time trends,
3. The application (adaption and implementation) of the J2000 hydrological model to assess the hydrological system of the monsoon-dominated Himalayan river systems characterized by glaciers in the high altitude areas, and
4. Assessment of the impact of land-use and climate change on hydrology and water availability to downstream regions.

3.2 Research questions

By elaborating on these objectives, the following major research questions will be investigated.

1. How is the precipitation distribution affected by the mountains of the Himalayan region?
2. What are the seasonal dynamics and long-term trends in hydro-meteorological time series in the region?
3. Is the distributed and process oriented nature of the J2000 hydrological model able to reproduce the hydrological system dynamics of the monsoon dominated Himalayan river basins with glaciers in the high altitude areas?

4. What are the roles of different runoff components (overland, baseflow, snow and glacial melt) reflected in the streamflow from sub-basins in the Kosi river region?
5. How do land-use and climate change impact the hydrological processes and water availability to downstream areas?
6. Can the hydrological model serve as a basis for an integrated system analysis to understand the upstream-downstream linkages of the mountainous region and support for the implementation of Integrated Water Resources Management (IWRM)?

3.3 Methodological approach

The assessment and evaluation of linkages between upstream and downstream areas requires an integrated system analysis approach. This study involves methods combining hydro-meteorological analysis with a strong focus on hydrological modelling and system assessment. The following scientific and technical methods are proposed to achieve the overall objectives. The methodological approach can be categorised into three main parts.

i) Assessment of time series data analysis

The analysis of existing datasets provides an important opportunity to assess spatial and temporal process characteristics between upstream and downstream dimensions. Therefore, a prototype of KosiRBIS was developed (Section 5.2) in the study area by means of the Adaptive Integrated Data Information System (AIDIS) system (Flügel 2007, Kralisch et al. 2009). The RBIS is a web-based data and information management system primarily focused on hydro-meteorological time series dataset. After setting up the KosiRBIS (Chapter 5), the data quality assessment was conducted by using a double-mass analysis. Precipitation, temperature and discharge data were checked thoroughly and some stations were excluded as they failed the double-mass analysis test (Chapter 5.3).

The spatial distribution of precipitation in different elevation zones of the mountains in the study area was carried out using the annual average precipitation of certain periods (Section 5.4). The precipitation amount was used to understand the spatial distribution of precipitation in the mountains and underlying geology. The trend analysis (precipitation, temperature and discharge) was carried out by using a non-parametric Mann-Kendall (MK) test (Mann 1945, Kendall 1975). Similarly, the existing trend (as change per year) was conducted by using Sen's slope estimation (Section 5.6). The analysis provided the hydro-climatic trend of the available time series data to understand the past climate change situation in the study area.

ii) Hydrological system assessment and analysis

To understand the precipitation-runoff processes in the upstream areas, the process-oriented distributed hydrological model J2000 (Krause 2001, 2002) was adapted and implemented in the two sub-basins of the Kosi river basin (Chapter 6). During the process, some of the existing modules were changed and new modules were developed to adapt the process characteristics and input data scarcity of the Himalayan river basins. A glacier module was integrated to take into account the snow and

glacial melt processes in the headwaters of the basin. The climate input data required for the model was used after the assessment of quality control as explained earlier.

Hydrological Response Units (HRUs) were delineated as model entities (Flügel 1995) for the J2000 hydrological model (Section 6.7). HRUs are distributed, heterogeneously structured spatial model entities having common climate, land-use, soil and geology controlling their hydrological dynamics. A tool developed by (Pfennig and Wolf 2007) was used in the ArcInfo program to delineate the HRUs.

The process-oriented distributed J2000 hydrological model was calibrated and validated in the Dudh Kosi river basin. The calibration was conducted by using the hybrid approach of automatic and manual calibration. In addition, the model parameters were transferred to the Tamor river basin (a sub-catchment of the Kosi river basin) to examine the model performance and credibility using a proxy-basin validation approach. The output of the model was used to analyse the different hydrological system components (such as runoff components, snow and glacier melt etc.) (Section 6.9). The model was instrumental in understanding precipitation-runoff processes in upstream areas and related consequences to downstream areas.

iii) Analysis of upstream-downstream linkages

After understanding the processes characteristics of precipitation and runoff generation, upstream-downstream linkages of hydrological dynamics were further analysed. The hydrological model was used as a tool to analyse the impact of land-use change on hydrology and downstream water availability (Chapter 7). The distributions of land-use and land cover in the HRU parameter file were changed to two different scenarios. Particular focus was given on how the land-use change in upstream areas might affect the spatial and temporal distribution of water (or streamflow) to the downstream communities (such as floods and baseflow).

To understand the impact of climate change, climate projected data based on Providing REgional Climates for Impact Studies (PRECIS) regional climate model were analysed. Future temperatures and precipitation distribution were analysed to understand to which extend these two climate variables are likely to change. The calibrated and validated model was applied to run the future scenarios with input from PRECIS data for the Dudh Kosi river basin. Finally, two future scenarios were analysed to understand how the projected climate change is likely to impact the hydrological regime of the basin. Special focus was given to the understanding of how downstream communities might be affected by the climate change in terms of the distribution of water resources (such as flooding).

4 Study area

This chapter describes the characteristic features of the Kosi river basin and its relevancies with this study.

4.1 Location and landscape

The Kosi river is one of the major tributaries of the Ganges river basin located in the Himalayan region. The Himalayan region is generally referred to the mountain range immediately at the north of the Indian subcontinent. The region extends 2,500 km from the Indus river (Pakistan) in the west to the Brahmaputra river (China) in the east. Sometimes, the mountain systems of the entire region is referred as the 'Greater Himalayan region' which extends 3,500 km from Afghanistan in the west to Myanmar in the east and is the source of ten of the largest river systems in Asia (Sharma 1997, Eriksson et al. 2009, Singh et al. 2000). Figure 4.1 shows the geographical location of the Kosi river basin in reference to the Ganges and Brahmaputra river basins in the Himalayan region. The Kosi river is the largest river system in Nepal. It starts from Tibet and continues to the Nepalese Himalayas before reaching the foreland and the Gangetic Plain of India. In India, the Kosi flows into the river Ganges at Kursela. Originating in the Mount Everest region, 8,848 m, the highest mountain peak in the world (Figure 4.2), the river drains from highest and steepest mountain system of the world. The average elevation of the Kosi river basin is 3,800 m, ranging from below 100 m the Gangetic plains to the more than 8,000 m in the great Himalayan alpine mountain system.

The Kosi river basin is composed of seven rivers: the Indrawati, Bhote Kosi, Tama Kosi, Likhu Khola, Dudh Kosi, Arun and Tamor. These tributaries encircles Mount Everest from all sides. The tributaries of the Kosi river basin is provided in Figure 4.2. The Bhote Kosi river meets the Sun Kosi to downstream and sometimes also referred as Sun Kosi as a whole (Figure 4.2). All the major tributaries (Sun Kosi and Tamor from west and east respectively, and Arun from north) meet at Tribeni from where the river flows through a narrow gorge passing the gauging station at Chatara. After this confluence, the river is called **'Sapta Kosi'** or Kosi (literally meaning Seven Rivers) (Table 4.1). Before spreading over the Gangetic plains, the flow of the Kosi is controlled by Kosi barrage (or Bhimnagar barrage) in Nepal. This was built in 1963 for the purpose of irrigation, flood control and generation of hydro-electric power under a bilateral agreement between the Government of Nepal and the Government of India. The major part of the Arun river is located in Tibet. All of the tributaries of the river systems in the high altitude areas are fed by glaciers and permafrost which contribute a fair amount of streamflow during dry season. The total area of the basin, upstream of Chatara, is about 57,700 km^2. Nearly 46% of the basin lies in Nepal while the remainder area is located in Tibet. The

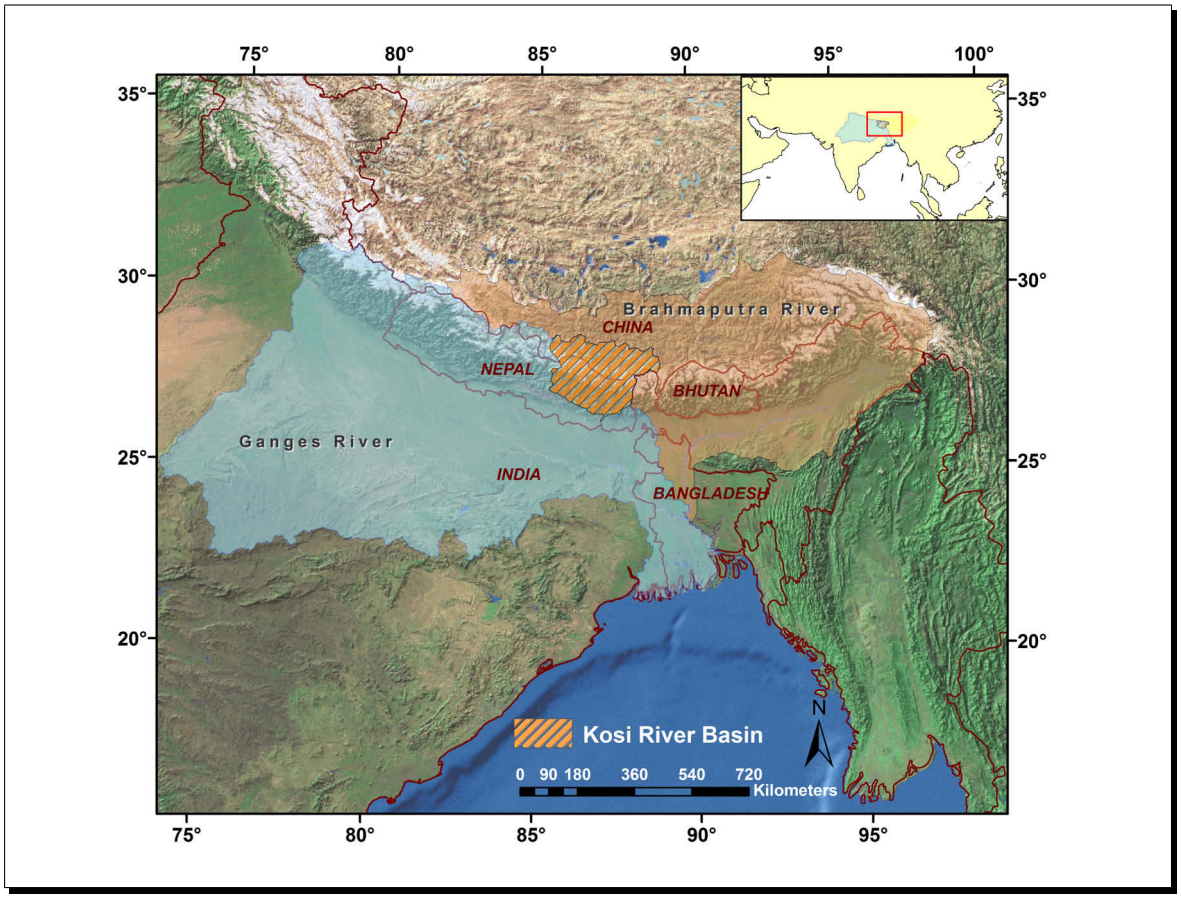

Figure 4.1: Geographical location of the Kosi river basin

area lies within the latitudes $26°51'0''$ $29°79'0''$ and longitudes $85°24'0''$ $88°57'0''$. The two major tributaries, coming down to Nepal are known by different names in Tibet. The Bhote Kosi and Arun are known as Poiqu and Pumqu respectively in Tibet.

The research study is mainly focused on the Nepalese part of the Kosi basin, upstream of Chatara (Figure 4.2). The northern part of the Kosi river basin located in the Tibetan Plateau has very few stations (Sharma et al. 2000a) and is therefore not included in this study. Furthermore, the hydro-meteorological dynamics (Chapter 5, page 45) are carried out in the southern side of the Nepalese Himalaya. Hydrological modelling (Chapter 6, page 81) is carried out in the Dudh Kosi and Tamor river basins. Most of the information referred to the study is from the Nepalese part of the southern Himalayan region. The Kosi river drains in the foreland of the Gangetic Plain in India after flowing from Nepal. This study does not include the Indian part of the Kosi river basin.

4.2 Geological framework of the Nepal Himalaya

As a result of the emergence from the tectonic uplift of sedimentary deposits, the rock mass in the Himalaya has a high degree of fragility and a greater tendency to undergo accelerated decomposition

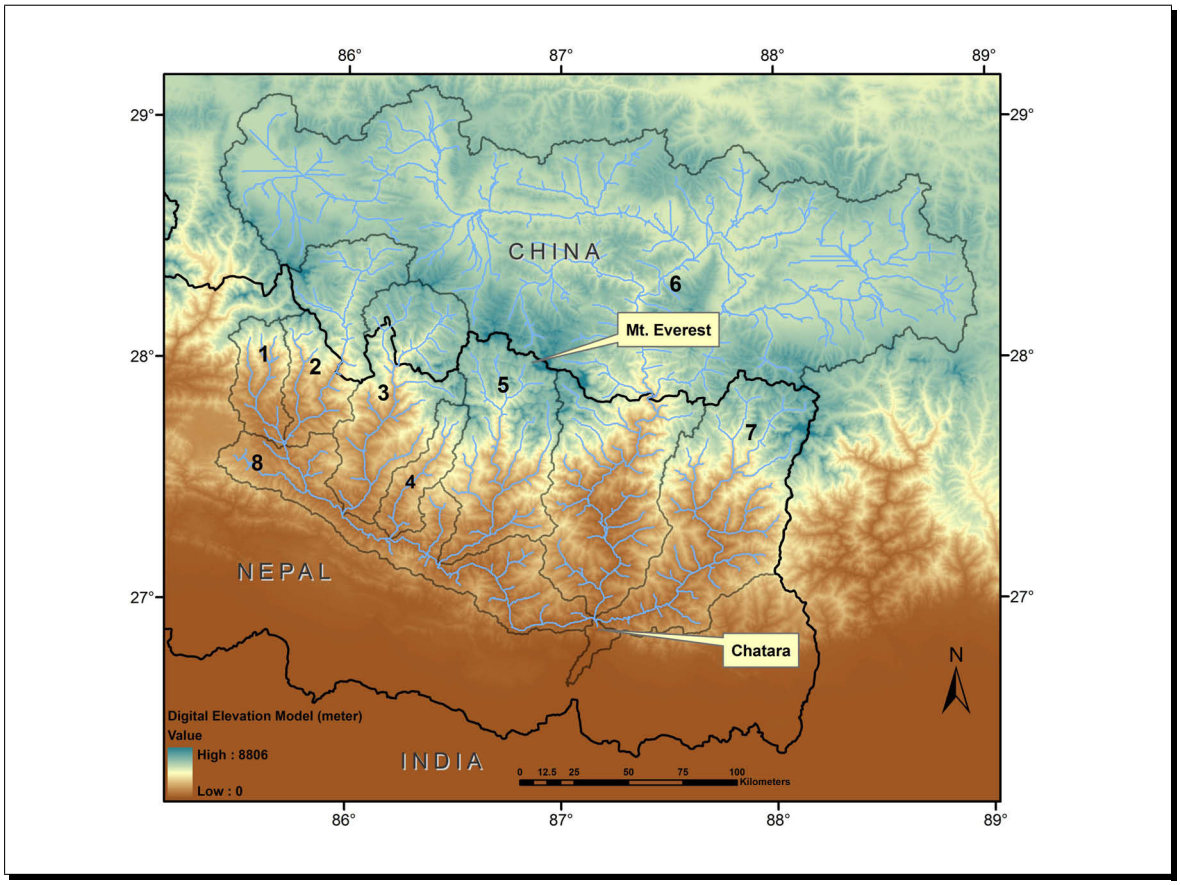

Figure 4.2: The Kosi river basin and its tributaries (**1:** Indrawati, **2:** Bhote Kosi **3:** Tama Kosi **4:** Likhu Khola, **5:** Dudh Kosi, **6:** Arun, **7:** Tamor **8:** Sun Kosi)

Table 4.1: Tributaries of the Kosi river basin

S.N.	**Name**	**Area** (km^2)	**Location**
1	Indrawati	1,229	Nepal
2	Bhote Kosi	3,398	Tibet, Nepal
3	Tama Kosi	4,123	Tibet, Nepal
4	Likhu Khola	1,050	Nepal
5	Dudh Kosi	4,064	Nepal
6	Arun	33,500	Tibet, Nepal
7	Tamor	6,053	Nepal
8	Sun Kosi	4,285	Nepal

under the influence of climatic factors (Dahal and Hasegawa 2008). In general, the physiography of Nepal is divided into the following zones: Terai, Siwalik (Sub-Himalaya), Lesser Himalaya (Middle mountains), Higher Himalaya and Trans Himalaya (Upreti 1999, Shrestha et al. 1999). Figure 4.3 shows the physiographic division of Nepal. The physiography of the Kosi river basin is similar to the Nepal Himalaya. Therefore, in this section, the general physiography of Nepal Himalaya is present which is applicable also for the Kosi river basin. Each of these zones has unique altitudinal variation, slope and relief characteristics which control the local climatic condition.

The structural framework of the Himalaya is characterized by three northerly inclined major breaks in the upper crust of the Indian Plate, namely, the Main Central Thrust (MCT), the Main Boundary Thrust (MBT) and the Main Frontal Thrust (MFT). These thrust faults distinctly separate the tectonic zones in the Nepal Himalaya, which include the Higher Himalaya zone, Lesser Himalaya Zone, Siwalik Zone and Terai region (Dahal and Hasegawa 2008). The generalised cross section of the Himalayan region showing different mountain system is provided in Figure 4.4. The MFT in the south separates the sedimentary sequence of the Siwalik Zone and the alluvial deposits of the Gangetic Plains (Terai). The MBT separates the low grade metamorphic rocks of the Lesser Himalayan Zone and the Siwalik Zone. Likewise, the MCT is a boundary between the high grade metamorphic rocks of the Higher Himalayan Zone and the Lesser Himalayan Zone (Schelling 1992).

About 80 percent of the land is covered by rugged hills and mountains. Nepal stretches 885 km from east to west and has a non-uniform width of 193 km north to south. The total area of the country is 147,181 km^2. It lies within the sub-tropical to the mountainous region at $26°22'0''$ to $30°27'0''$ latitudes and $80°4'0''$ to $88°12'0''$ E longitudes, with an altitude that ranges from 90 m to 8,848 m (HMG 2000).

The detailed description of the physiographic division of Nepal is provided below:

Terai region

The Terai region is the lowest elevation zone (60-330 m) of Nepal which is located along the southern edge of the country. This narrow strip of flat alluvial terrain is a fertile land and an extension of the Gangetic Plain. Its general slope towards the south is less than one percent and constitutes about 14 percent of the country. In the north, it is bounded by the Main Frontal Thrust (MFT) the outcrops of which are exposed at many places along the southern front of the Siwalik range (CBS 2001, Upreti 1999).

Siwalik region

The first elevation next to the Terai region in the north is the Siwalik zone. The elevation varies from 200 to 1,500 m. The region is the youngest member of the Himalaya family and has dry and unconsolidated soil materials including sandstone, mudstone, shale and conglomerate mollasse deposits of the Himalaya (Upreti 1999, HMG 2000). The region is bounded to the south by the MFT and to the north by the MBT. Within the Siwalik range, many valleys (also known as Dun valleys) can be observed which are filled by coarse to fine alluvial sediments.

Lesser Himalaya

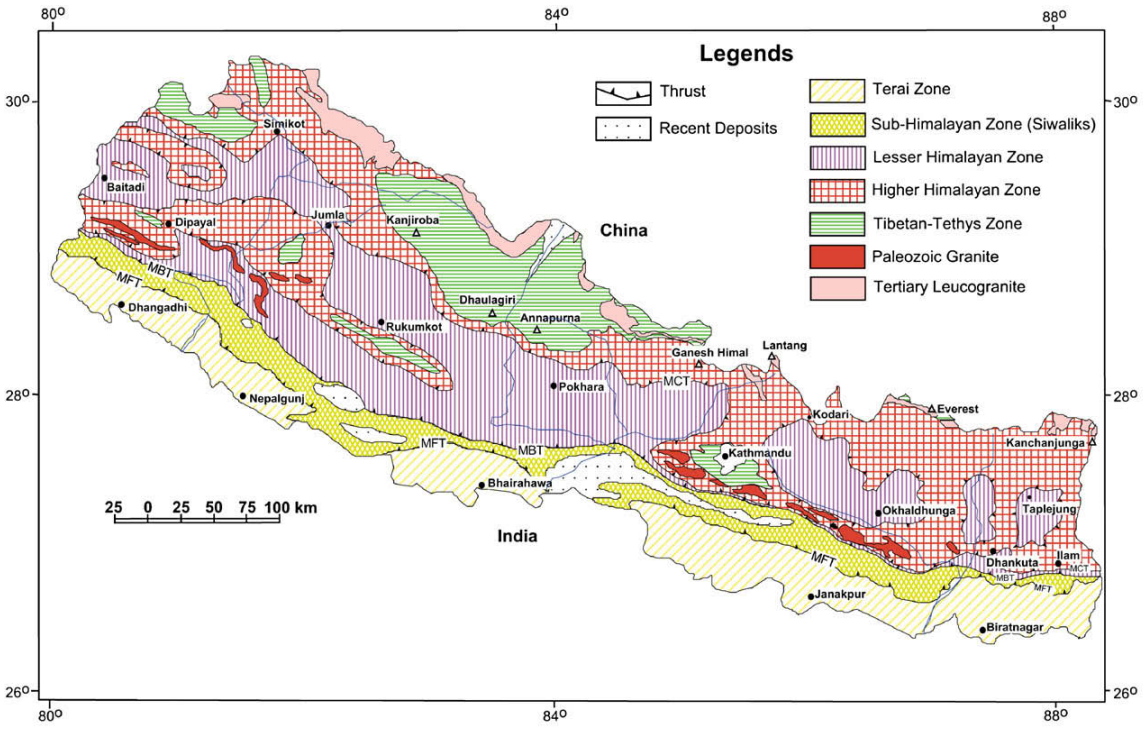

Figure 4.3: Physiographic division of Nepal. Source: Dahal and Hasegawa (2008)

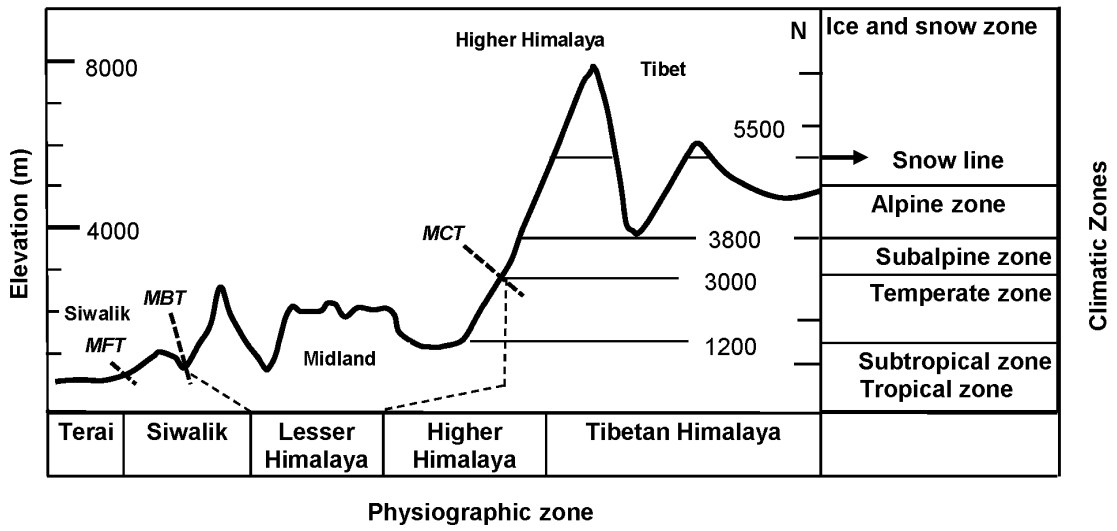

Figure 4.4: Generalized cross section of the Himalayan region: Source: modified after Regmee (2004)

To the north of the Siwalik range, the Lesser Himalaya (Middle mountains or Mahabharat range) is located. The Lesser Himalaya lies between the MBT to the south and the MCT to the north. The altitude ranges from 500 m the low lying valleys to 3,000 m. The region comprises many valleys and river valleys (Upreti 1999, HMG 2000, Dahal and Hasegawa 2008).

Higher Himalaya

The Higher Himalaya region is located to the north of the Lesser Himalaya and is characterized by an abrupt rise of topography forming steep Himalayan peaks. The MCT is located to the south and the South Tibetan Detachment System (STDS) marks the boundary between the Higher Himalayan Zone and the overlying sedimentary sequence of the Tibetan - Tethys Himalayan Zone. This zone is an area of rocky, ice-covered massifs, snow fields and valley glaciers. The highest peak of the world, Mt. Everest (8,848 m) is located in the region, including several other peaks exceeding 8,000 m. The Tibetan Tethys Himalaya (Trans Himalaya) is located to the north of the Higher Himalaya. It begins at the top of the STDS and extends to the north in Tibet (Upreti 1999, HMG 2000, Dahal and Hasegawa 2008).

4.3 Land use and land cover

In general, the lower-elevation basin area, the Terai and Siwalik region, is covered by tropical evergreen and deciduous riverine forest with mixed vegetation such as grassland and shrubland. The tree species are dominated by *Shorea Robusta* and *Acacia catechu*. In the middle mountain areas, the natural vegetation includes broadleaved forests dominated by *Schima-Castanopsis* species as shown in Figure 4.5(b). The plain areas in the Terai region have systematic irrigation practices whereas middle mountain farmers practices rainfed agriculture supported by irrigation in some places. In these areas, human activities are dominated by subsistence agriculture and farming. The community forestry, where the local forests are handed over to and managed by local communities for its management and resource utilization, is a very successful program in the area. The management of the many accessible forests in these areas is conducted under the community forestry program (Awasthi et al. 2002, Nepal and Adiga 2006, Gautam et al. 2003). Between 2,000-4,000 m, the vegetation type in the basin area is dominated by coniferous forest along with grass land. Figures 4.5(a) 4.5(c), 4.5(d) show the coniferous forests in the Dudh Kosi river basin. Higher than 4,000 m, the area is dominated by essentially bareland with few patches of grasslands and shrubland. Figure 4.5(d) shows the mountain peaks and bare land in the elevation higher than 4,000 m. Higher than 5,500 m, there are rocky mountain peaks covered by glaciers and permanent snow cover (MoFSC 2002, Sharma et al. 2000a). The photographs of land use and land cover of the study area are provided in Figure 4.5

The northern side of Tibet has alpine climate and is mostly dominated by baren land. Because the elevation in general of these areas is higher than 4,000 m, only seasonal vegetation, such as grassland and rangelands, can be expected. No systematic study of the land use and land cover in this area has been conducted. The land use and land cover derived from the GlobCover data of two sub-basins within the Kosi river basin are described in Chapter 6.

(a) Coniferous forest at 3,000 m

(b) Deciduous forest with mixed vegetation at 500 m

(c) Coniferous forest at about 4,000 m

(d) The geographical setting and mountains in the high-altitude areas

(e) Higher Himalaya with barelands and mountain peaks

(f) Frozen Lake at the elevation of 4,800 m

Figure 4.5: Photographs of the geographical settings and land-cover in the Kosi river basin

4.4 Soil

A significant variation of soil is found in the Himalaya region in terms of texture, mineral, content, depth and other characteristics. The soil texture in the Higher Himalaya mountains is relatively thin due to the influence of rocky landscape and steep slope. Soil in these areas area mostly shallow and loose soil with sandy gavel and cobbles in valleys. Areas higher than 5,500 m mostly contains rocks. In the middle mountain regions, soil is dominated by dark brown color and silt loam in texture (Sharma et al. 2000b, Sharma 1997, Narayana 1987).

The soil database from SOTER (Soil and Terrain) database (Section 6.5.4) indicates that the soil types in the Higher Himalaya are dominated by a Regosol which are weakly developed mineral soils with unconsolidated materials. Similarly, the lower altitude soil is dominated by the mixture of Cambisol, Umbrisol and Regosol which characterize medium to fine texture materials.

4.5 Climatic conditions

The climate of the Himalayan region in general is greatly influenced by the Indian monsoon system. The summer monsoon dominates the climate from May to September and westerly circulation dominates from November to March (winter monsoon). Within Nepal, the onset of summer monsoon starts from the eastern part (and the Kosi river basin) from mid June to September (Ueno et al. 2008). During the summer season, the Tibetan Plateau warms rapidly relative to the Indian ocean. The resulting low pressure over Asia/Himalaya and higher pressure over the Indian Ocean gives rise to the strong low-level atmospheric pressure gradient that in turn generates the southwest monsoon (Overpeck et al. 1996) which brings moist air currents flow from the Bay of Bengal to the Indian subcontinent. When the moist flow approaches the land, maximum precipitation occurs upstream and over the lower windward slopes of the west-and south-facing mountain barriers (Medina et al. 2010).

There are primarily four seasons in the region. They are: the winter (December - February), the pre-monsoon period (March - May), the monsoon period (June - September) and the post-monsoon period (October - November) (Shrestha et al. 1999). The temperature starts to rise after February and reaches its maximum level during the monsoon season. The rainy season coincides with the summer monsoon. The basin has tropical to sub-tropical climate at the lower altitude (Terai and Siwalik) characterised by a hot and wet summers and mild and dry winters. The Middle Mountain (the Lesser Himalaya) exhibits a warm temperate monsoon climate. The higher altitude area has sub-alpine to alpine climate up to 4,800 m associated with low temperatures. Higher than snowline exhibit very cold climatic conditions where the temperature remains below zero degree Celsius throughout the year which provides conditions for the development of glaciers in the region (MoFSC 2002, Mool et al. 2001b).

About 80% of the total annual precipitation occurs during the months of June through September, however, this varies annually (Ueno et al. 2008). During this period, the region receives intense rainfall which brings floods and widespread damage to property and lives. The Kosi river basin experiences floods every year which impact eastern Nepal and the plain areas of India.

Figure 4.6: Ngozumpa glaciers with debris cover surface

4.6 Glaciers and glacial lakes

Mool et al. (2001b) probably was the most comprehensive study regarding the glaciers and glacial lakes in Nepal. According to this study, about 3,252 glaciers and 2,323 glacial lakes were identified in Nepal of which 20 were considered potentially dangerous. There are about 779 glaciers on the Nepalese side of the Kosi river basin which covers an area of about 1,410 km^2 with an estimated ice reserve of 152 km^3. Regarding glacial lakes, there are 1,062 lakes in the Kosi river basin covering an area of 25 km^2 of which the largest number is of erosion lakes and supraglacial lakes. Generally, erosion lakes are isolated and are located some distance from the glaciers, and the supraglacial lakes are situated in groups within the ice mass.

In the recent decade, the glaciers have been retreating at a higher rate leading to the formation of many glacial lakes in the Himalaya region (Kattelmann 2003, Mool et al. 2001b). The outburst from these unstable lakes is a major concern because the resultant flash floods would cause significant damage to properties, lives and livelihoods (Shrestha et al. 2010). In the Dudh Kosi river basin, a glacial lake outburst flood occurred from Dig Tsho lake on 4 August 1985 which damaged the nearly completed Namche hydropower plant and 14 bridges and cultivated land etc. The most recent GLOF event is that of Tam Pokhari (Sabai-Tsho) on 3 September 1998 in the Dudh Kosi river basin (Mool et al. 2001b). According to the study based on remote sensing images in the Dudh Kosi basin, nearly 12% of the total glacier area is retreated between 1976 to 2000. In the recent decade, Himalayan glaciers have generally been shrinking and retreating at a faster rate (Bajracharya and Mool 2009).

4.7 Water uses and conservation significance

The water from the basin has been utilised for many purposes. The Chatara canal supplied irrigation water from the Kosi river to the Sunsari Morang Irrigation Project (SMIP) in Eastern Nepal . The project is the largest irrigation system in Nepal and was designed to irrigate 66,000 hectares (Fish et al. 1986). In India, the total command area which receives water for irrigation from the Kosi barrage is about 969,110 hectares (Dhungel 2009). About 130 MW of electricity have been generated from the Kosi river system and the full hydropower potential of the basin is estimated to be about 3,000 MW. The Government of Nepal and the Government of India have agreed to conduct a joint investigation for the preparation of a detailed project report on the Sapta Kosi High Dam Multipurpose Project for the development of hydropower generation, flood control, irrigation and navigation.

The basin has high significance from the standpoint of nature conservation because important protected areas are located within the basin. The **Sagarmatha (Mt. Everest) National Park** is located in the Dudh Kosi region which comprises an area of 1,148 km^2 of the Himalayan ecological zone. The **Makalu Barun National Park and Buffer Zone** covers 2,330 km^2 in the Arun river basin. The **Kosi Tappu Wild Life Reserve** lies on the flood plain of the Kosi river covering an area of 176 km^2 . The Koshi Tappu was also declared as a Ramsar site, a wetland of international significance in 1978. The **Kanchenjunga Conservation Area** is located in the Tamor river basin which covers an area of 2,035 km^2. More detailed information and significance of these protected areas are provided on the website[1] of the Department of National Park and Wildlife Conservation of the Government of Nepal.

4.8 Sedimentation and hydrology

The amount of sediment transported by the Ganga-Brahmaputra river system is the highest among the rivers of the world. It is estimated to be about 2.4 billion tonnes (15 t/ha) annually, to which the Ganges alone contributed about two thirds (cited in (Bruijnzeel and Bremmer 1989)). A more modest estimation was provided by Milliman and Meade (1983) with a value of 1.67 billion tonnes (11.3 t/ha). Although sediment load transported by such very large rivers can never be estimated with great precision, it is clear that the amounts of sediment carried by the two rivers must be enormous (Bruijnzeel and Bremmer 1989). Figure 4.7(a) shows the comparison of sediment load and drainage basin area of major sediment discharge rivers (greater than 10 million t /year). Open circles represent low-yield rivers draining Africa and the Eurasian arctic. Smaller basins have larger yield, although the largest rivers (Yangtze, Ganges-Brahmaputra and Yellow) all have greater loads than their basin areas would predict (Milliman and Meade 1983).

The Kosi river basin represents about 5 percent of the Ganges river system, however, it contributes nearly 25% of total sediment load transported through the Ganges. Nearly 135 million tonnes per year of sediment load is transported from the Kosi river basin (Sharma 1997). In another study, the sediment load is reported to be about 119 million tonnes per year which is equivalent to 2 mm topsoil depth over its entire catchment (Cited in Tiwari (2000)). As suggested by Bruijnzeel and Bremmer

[1] http://www.dnpwc.gov.np/protected-areas.asp

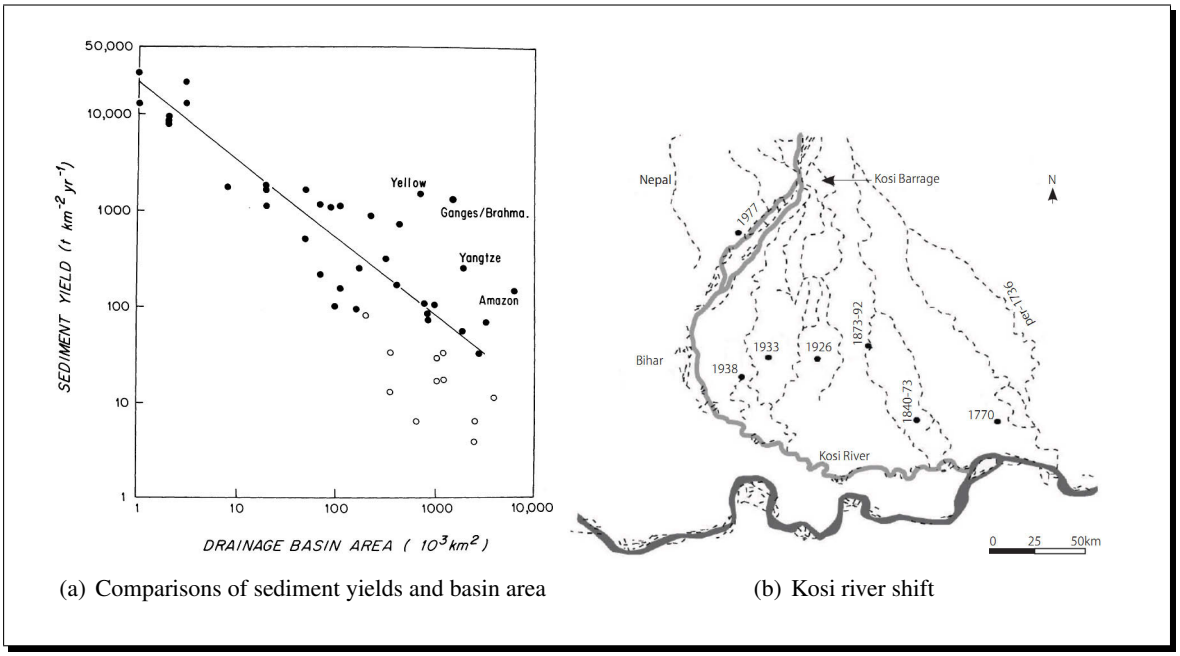

(a) Comparisons of sediment yields and basin area

(b) Kosi river shift

Figure 4.7: a) Comparisons of sediment yields and drainage basin areas for major sediment-discharging rivers. Source: Milliman and Meade (1983) **b)** Westward shift of the Kosi river stream channel. Source: Gole and Chitale (1966)

(1989), the sediment loads from large river basins cannot be estimated accurately because of the wide range of erodible materials contributing sediment and different methods used for estimation in different studies. However, in both of these studies, the sediment load of the Kosi river is estimated to be very high. The specific sediment yield is reported to be around 2,500 tonnes/km^2/year (equivalent to 25 t/ha) which is very high compared to the other river systems in the world (For example: Ganges: 491, Brahmaputra: 578, Amazon: 207 and Nile 40 tonnes/km^2/year) (Sharma 1997, Mool et al. 2001b, Alford 1992).

The Kosi river is also known for exceptionally high sediment carrying capacity and channel shifting which has formed a broad alluvial fan into the Indo-Gangatic Plain. Sediments eroded from mountains of the upstream region are transported to the lowland areas and deposited on plain areas and valleys. Much of the sediment from the upstream areas is brought down to Chatara in the Terai and is deposited on the river bed as the slope decreases. Over time, its main channel has aggraded and thereby the Kosi river has shifted its course. The Kosi alluvial fan indicates the dynamic nature of the river's channel shifting over the past 220 years where the river has shifted westward by about 115 km across the northern Bihar State in India as shown in Figure 4.7(b) (Gole and Chitale 1966) and (Thakur and Tamrakar 2001). As the sediment load is transported by the Kosi river from the mountains to the plains, extensive river cutting and bank erosion occur. The resulting sediment load forces the river to shift laterally and meander. This natural process can create problems when rivers erode lands, wash away crops and results in serious implications to local livelihoods.

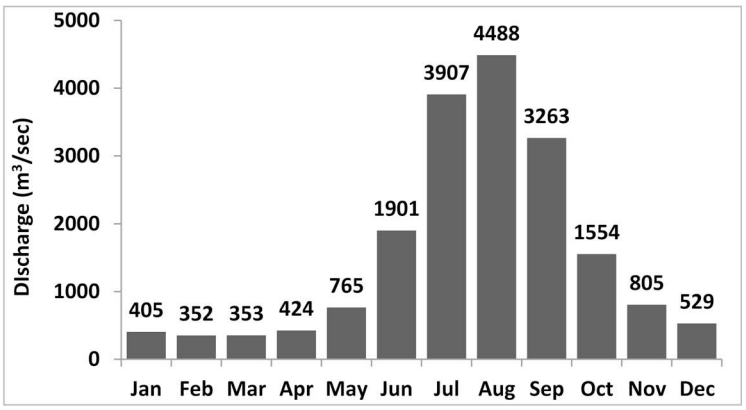

(a) Monthly average discharge (1985-2006)

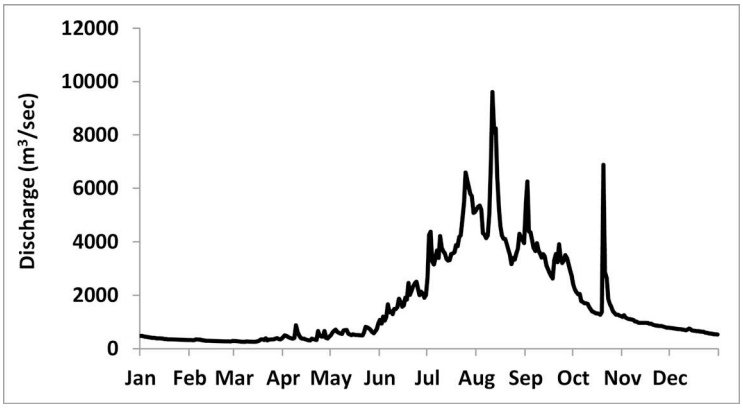

(b) Daily discharge in 1987

Figure 4.8: Discharge of the Kosi river at Chatara

The streams in the Kosi basin are predominately fed by snow and glacier melt, runoff and rainfall. The Kosi river basin has a notorious reputation in the region for causing widespread destruction through floods, especially in lowland areas of Nepal and India during the monsoon season. During the period, the floods create havoc to downstream areas by causing loss of life and damage to property. The Kosi river decreases in elevation by nearly 9 km over a distance of just 200 km along its channel reach from the area of Mt. Everest to Bihar in India.

The average monthly discharge of this river was found to vary from 343 m^3/sec in February to a maximum of 4,488 m^3/sec in August with an annual average of 1,562 m^3/sec between 1985-2006 (Figure 4.8(a)). Between this period, the maximum discharge of 9,610 m^3/sec was recorded on 11 August 1987 which is nearly doubled in magnitude compared to the long-term average of August. In general, the volume of discharge starts increasing during June and reaches its maximum flow in August. The maximum flood peak recorded till date was about 25,878 m^3/sec in August 1968. The Kosi river exhibits seasonal variations in both flow and sediment load. The fluctuation in its flow in

Table 4.2: Long-term water balance of the Kosi river basin. Source: Sharma et al. (2000b)

Area	Precipitation (mm) P	Runoff (mm) R	Evapotranspiration (mm) ET = P - R
Kosi basin (All)	1,288	919	369
North Himalaya (Tibet)	536	358	178
South Himalaya (Nepal)	1,931	1,424	507

the gorge area can occur suddenly and be high; a rise of 20 to 30 ft in streamflow depth in 24 hours is common (Dixit 2009).

Sharma et al. (2000b) analysed the annual water balance based on the long-term observed precipitation and actual stream discharge of the entire Kosi river basin. The northern area represents the dry climate associated with low precipitation and the southern area represents humid climate with relatively high precipitation. As shown in Table 4.2, the southern half of the basin is four times wetter than the northern half of the basin in Tibet. Similarly, evaporation loss in the south is about three times higher than the loss in the north. This is because of the climatic condition in the north (Tibetan Plateau) which is arid climate associated with low temperature and low rainfall.

On August 18, 2008, the Kosi river breached its eastern embankment at Kushah in Nepal (about 12 km upstream of the barrage) which displaced about 60,000 people in Nepal and nearly three and half million in India including losses of lives (Moench 2010). The river's channel took a new course after the incident which was believed to be follow the channel course of 80 years ago. When the river breached, its flow was below average, considering the same time period in different years. The embankment failure was not caused by an extreme event. Instead the breach represented a failure of interlinked physical and institutional infrastructure systems in an area characterized by complex social, political, and environmental relationships (Moench 2010).

5 Hydro-meteorological data analysis

An analysis of the hydro-meteorological conditions of an area provides the opportunity to understand system dynamics in a better way. Moreover, the analysis provides historic trends which can be a basis for potential indicators for future climate change patterns. Many studies have emphasized the importance of hydro-climatic system analysis and future climate change patterns and their impacts on water resources so that appropriate adaptation strategies can be developed (Krause et al. 2010, Aziz and Burn 2006, Souvignet 2011, Sharma et al. 2000a). This chapter has three sections which deals with the hydro-meteorological data analysis of the Kosi river basin.

- The first part describes the Kosi River Basin Information System (KosiRBIS) which is an online data-and-information management system and its uses in the data analysis for the study;
- The second part describes the precipitation dynamics in four different river corridors of the Kosi river basin; and
- The third part describes the hydro-meteorological trend analysis of the Kosi river basin which includes precipitation, temperature and discharge information derived from available data.

5.1 Data and information management

The understanding of hydro-climatic conditions in meso- to macro-scale river basins mostly comprises huge amount of dataset which needs to be throughly investigated. Such data set mostly include: geo referenced and distributed data components, measured and simulated time series and socio-economic information. The analysis and assessment of issues related to sustainable and adaptive Integrated Water Resources Management (IWRM) requires an efficient data and information management system (Flügel 2007).

To address this challenge and cope with data organization and management, a River Basin Information System (RBIS) has been developed by means of the Adaptive Integrated Data Information System (AIDIS) at the Department of Geoinformatics at the Friedrich Schiller University of Jena. RBIS is a web-based data-and-information management and data sharing system with a focus on time series and geospatial data (Flügel 2007, Kralisch et al. 2009). It provides user-friendly interfaces for data input and output, a powerful visualization component and an adaptable set of functions for data analysis, management and enrichment. The RBIS is especially suitable for managing time-series data and provides various functions for analyzing data and filling data gaps, which is a vital pre-possessing step for environmental data analysis (Kralisch et al. 2009). The detailed technical description of the

RBIS, its functions and usability have been described in (Kralisch et al. 2009). The flexible and user-friendly approach of the RBIS makes the handling of datasets quite easy and productive. It is based on an open-source software (OSS) program and uses multi-tier class hierarchy structure. The web-based nature of the RBIS makes it possible to access the data from anywhere using an internet connection. The general layout of the RBIS is shown in Figure 5.1(a).

5.2 Kosi RBIS

A prototype of RBIS has been developed and adapted for this study in the Kosi river basin and named as 'KosiRBIS'[1]. All the available hydro-meteorological data (precipitation, temperature, discharge, wind speed, sunshine hour and evaporation) from the study area were populated in the RBIS as time series data and geo-data together with their corresponding meta data. All these data sets can be accessed using a web browser. The operational part of the RBIS will be discussed now with focus on how the RBIS can be instrumental to large-scale data processing and analysis. The following functionalities and analysis are provided by the RBIS.

1) Exploratory data analysis

The KosiRBIS provides an Exploratory Data Analysis (EDA) through visual examination of data sets. In statistical analysis, the EDA is an essential component to examine the raw data in order to identify issues related to data problems (outliers, gaps in the record, etc.), temporal patterns (eg. time-trends or step-change, seasonality) and regional and spatial patterns (Kundewicz and Robson 2004). The visual graph of data in the KosiRBIS was instrumental to delineate any abnormal behavior of the data sets such as outliers.

An example of EDA and data quality problems is presented in Figure 5.1(b) with precipitation data from the Jiri station. In 1966 August 25, the precipitation of the station is extremely high (nearly 400 mm) which is clearly visible in the plot (Figure 5.1(b)). In a detailed analysis, it was found that there is very low precipitation in nearby stations located around the Jiri station with values ranging from 1-5 mm. Furthermore, the discharge data of the downstream station was checked and it was found that there was no increase in discharge values on that particular day. This clearly indicates a data error.

2) Missing values

Missing data are common in stations located in mountainous regions for various reasons. Gaps during a maintenance period, damage of stations by events like floods and landslides, and failure of instruments are some of the prominent causes for missing data.

The KosiRBIS provides detail information about the missing values in the dataset. As shown in Figure 5.2 (Top), the length of the missing values and the period are also provided in the table. Filling the missing data is an important prerequisite for data analysis and management. The KosiRBIS comprises many sets of algorithms which can be used to fill the data gaps as provided in Figure 5.2 (middle). The methods and equations describing the process of filling the missing data gaps are provided in Section

[1] KosiRBIS can be accessed at http://leutra.geogr.uni-jena.de/kosiRBIS

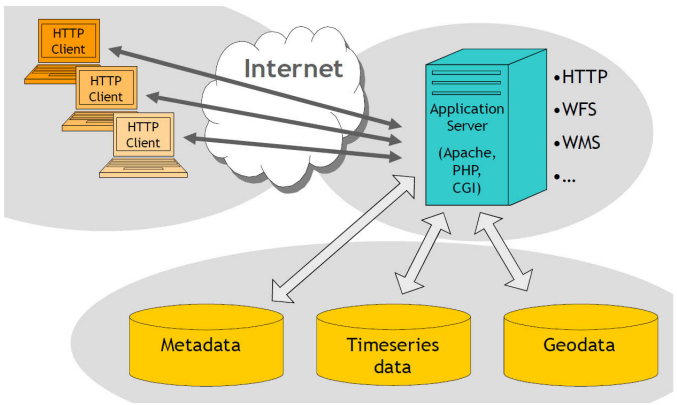

(a) Technical layout of the RBIS (Kralisch et al. 2009)

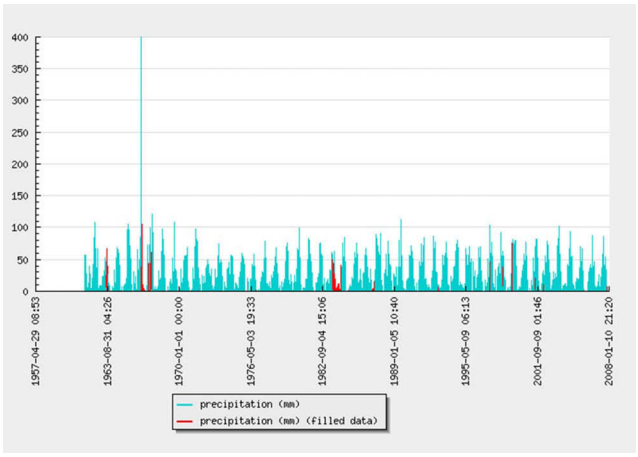

(b) Exploratory data analysis (EDA) of precipitation data

Figure 5.1: River basin information system

6.4. The users can also upload their own method to fill the gaps as shown on the right side (external Interpolation method) of Figure 5.2 (middle).

3) Aggregation of data

Once the missing data are filled, the data can be downloaded in different temporal resolution and statistics (such as daily, monthly, annual, as sum or average together with maximum and minimum values) as shown in Figure 5.2 (bottom). Such aggregated data are easy to use in any statistical software such as Excel.

The KosiRBIS is found to be very instrumental in the analysis of time series data in this study. Specially, the different algorithms of filing missing data and getting the data in different temporal resolution is very handy and useful for the further analysis. In addition, the web based nature of the RBIS makes it easy to access the data by using internet. For this study, the data were processed inside

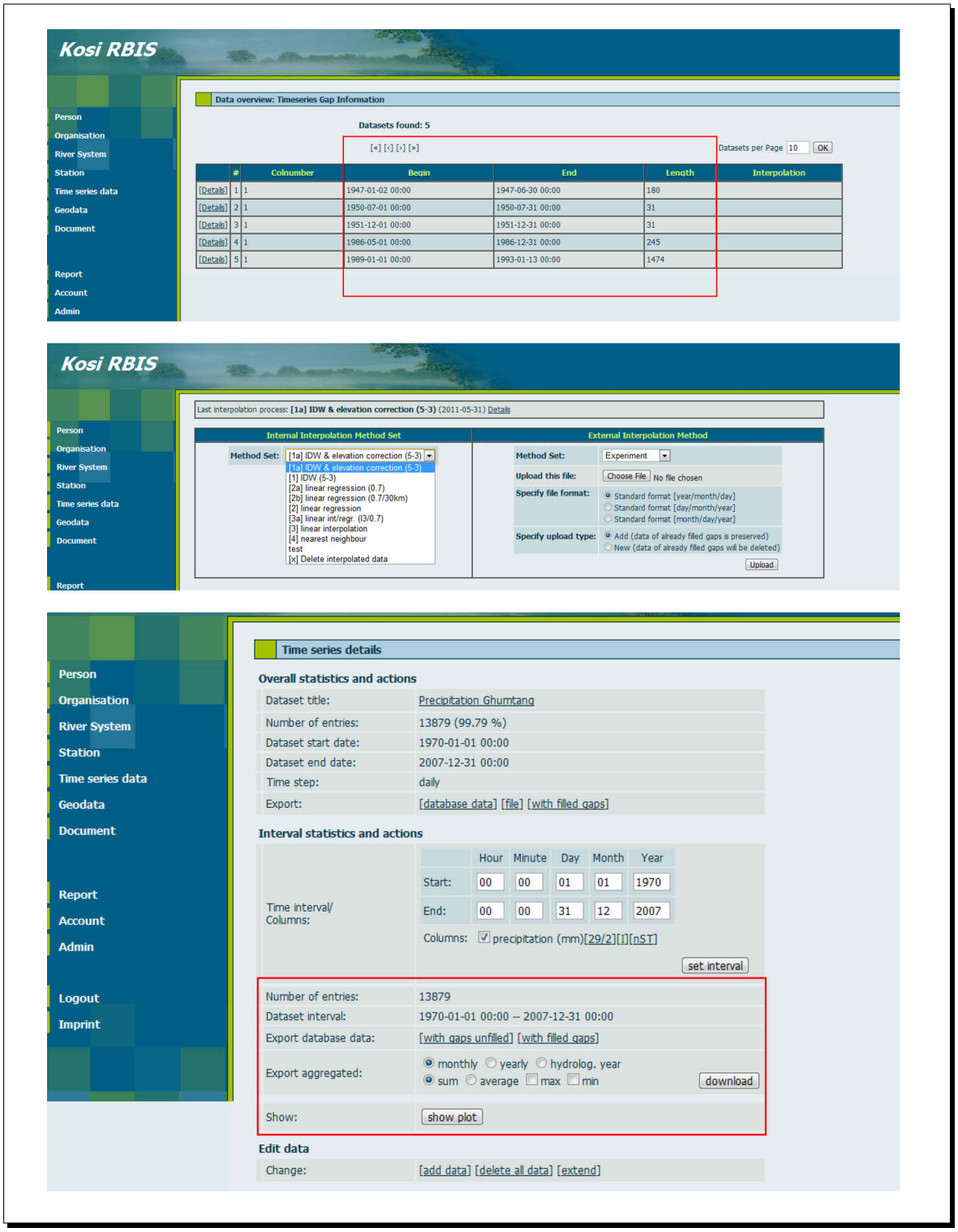

Figure 5.2: Top: Details of missing precipitation values as shown in the KosiRBIS **Middle:** Different algorithms to fill the missing data values in the KosiRBIS **Bottom:** Option for aggregation of datasets for download from the KosiRBIS (red box)

.

the KosiRBIS. After completing the pre-processing (EDA, filling missing values), the datasets were downloaded in different temporal resolution (daily, monthly, yearly etc) and used for further analysis.

5.3 Data quality control

The time-series data are considered to be accepted if they satisfy some level of quality control (WMO 1988). For trend analysis (Section 5.6), the annual value was calculated from daily data. If the dataset had gaps in the monsoon period, the year was left blank because the Sen's slope estimation (Section 5.6.1) can estimate the trend with missing values.

The double-mass analysis (or sometimes called double-sum analysis) is useful for assessing homogeneity in a weather parameter (Allen et al. 1998, Raghunath 2006, Silveira 1997). It is a useful tool for checking the consistency of climatic variable where the error is caused due to various reasons, such as change in environment (or exposure) of a station such as planting of trees or cutting of forest nearby, which affect the catch of the gauge due to change in the wind pattern or exposure. The replacement of instruments with new methods also might bring such deviation (Raghunath 2006). This procedure requires data sets from two weather stations, where Xi (i = 1, 2,..., n) in a chronological data set for a given variable observed for a certain time length at a "reference" station, and which is considered to be homogeneous. Similarly, Yi is a dataset of the same variable, with the same time duration, observed at another station and for which homogeneity needs to be analysed. In this technique, starting with the first observed pair of values X1 and Y1, cumulative data sets are created by progressively summing values of Xi and Yi to verify whether the long-term trends in variation of Xi and Yi are the same. This procedure is typically applied as a graphical procedure. The graphical application of the double-mass analysis is done by plotting all the coordinate points from cumulative values (xi and yi). The plot is then visually analysed to determine whether successive points of two stations follow an unique straight line, indicating the homogeneity of the data set Yi relative to data set Xi. If there appears to be a break line or deviation (or more than one deviations or break lines) in the plot of xi and yi, then there is a visual indication that the data series Yi (or perhaps Xi) is not homogeneous (Allen et al. 1998). An example of double-mass analysis is provided in Figure 5.3 between the precipitation and discharge data of the Dudh Kosi river basin.

The double-mass analysis for precipitation data is carried out among stations within the same corridor. For this, two or three reference stations with relatively long time period and less or no data gaps were chosen which indicate a good quality of the data. Figure 5.4provides the stations located in four different river corridors in the Kosi river basin. One precipitation station in the Arun river corridor (Machuwaghat) and one in the Dudh Kosi river (Udayapur Gadhi) failed the test. Similarly, another station from the Indrawati Corridor (Sarmanthag) indicated some deviation in the test after 1986. This station therefore was omitted from the long-term trend analysis. However, to get the idea of spatial distribution of precipitation, instead of 1985 to 1997, data from the 1973-1986 period were selected to provide the needed information about the annual precipitation. In discharge data, one station in Tamor river corridor failed the homogeneity test. Similarly, in temperature data, one station (Chainpur East) also failed the homogeneity test and therefore excluded from the analysis.

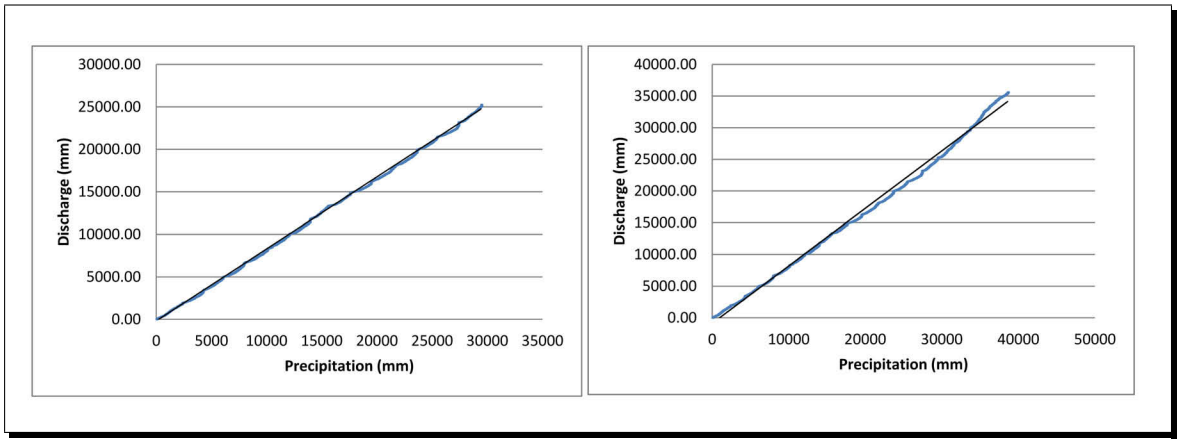

Figure 5.3: Double-mass analysis between precipitation and discharge in the Dudh Kosi river basin. Left: 1985-1997, Right: 1985-2006

Between 1985 to1997, no abnormal behavior of data was found except in the case of one station in the Indrawati corridor as explained in the previous paragraph. This time period was used to calculate the precipitation dynamics, spatial distribution of the precipitation and subsequent input into a hydrological model. The trend analysis was carried out relatively longer period depending upon the availability of time series data.

Double-mass analysis was also conducted between precipitation stations and discharge data for the Dudh Kosi and Tamor river basin. In the Dudh Kosi river basin, some outliers in the trend line were observed after 1998 as shown in Figure 5.3. The outliers can be seen in the right hand plot with a slight deviation towards higher values. The rainfall-runoff ratio after 1998 also indicated that that the discharge is higher than precipitation. It subsequently was revealed that there was a big glacial lake outburst flood that occurred in 1998 in the river basin and which damaged the gauging station at Rabuwabazaar and probably this might be the cause of deviation in the discharge data. Hence, the modelling period was selected from 1985 to 1997.

Some of the stations had data gaps ranging from a number of days to several years. These data gaps were filled inside KosiRBIS by using the methods described in Section 6.4. No significant long-term data gap was found in the model run period in these two river basins. For the trend analysis of the longer period, data gaps were analysed carefully. If the data gap was higher than one month during the monsoon season, the year was kept empty. It is because the trend analysis was not affected by missing years. During the non-monsoon season, gaps up to 3 months were filled. To fill the missing gaps, extra care was given to choose the nearby stations because the precipitation pattern was found to vary substantially in some cases within a short distance. This is well described in Section 5.4.1.1 especially between the stations located in river valleys and the windward side of mountains. For temperature data, gaps lesser than 4 days were filled by linear interpolation by taking average from days before and after the gaps. Gaps lesser than 2 months were filled by using linear regression from nearby stations. The co-efficient of determination (r^2) of nearby stations to fill the missing gaps were in the range of 0.8 to 0.95. Relatively, temperature data had very few gaps compared to precipitation data.

5.4 Precipitation dynamics in river corridors

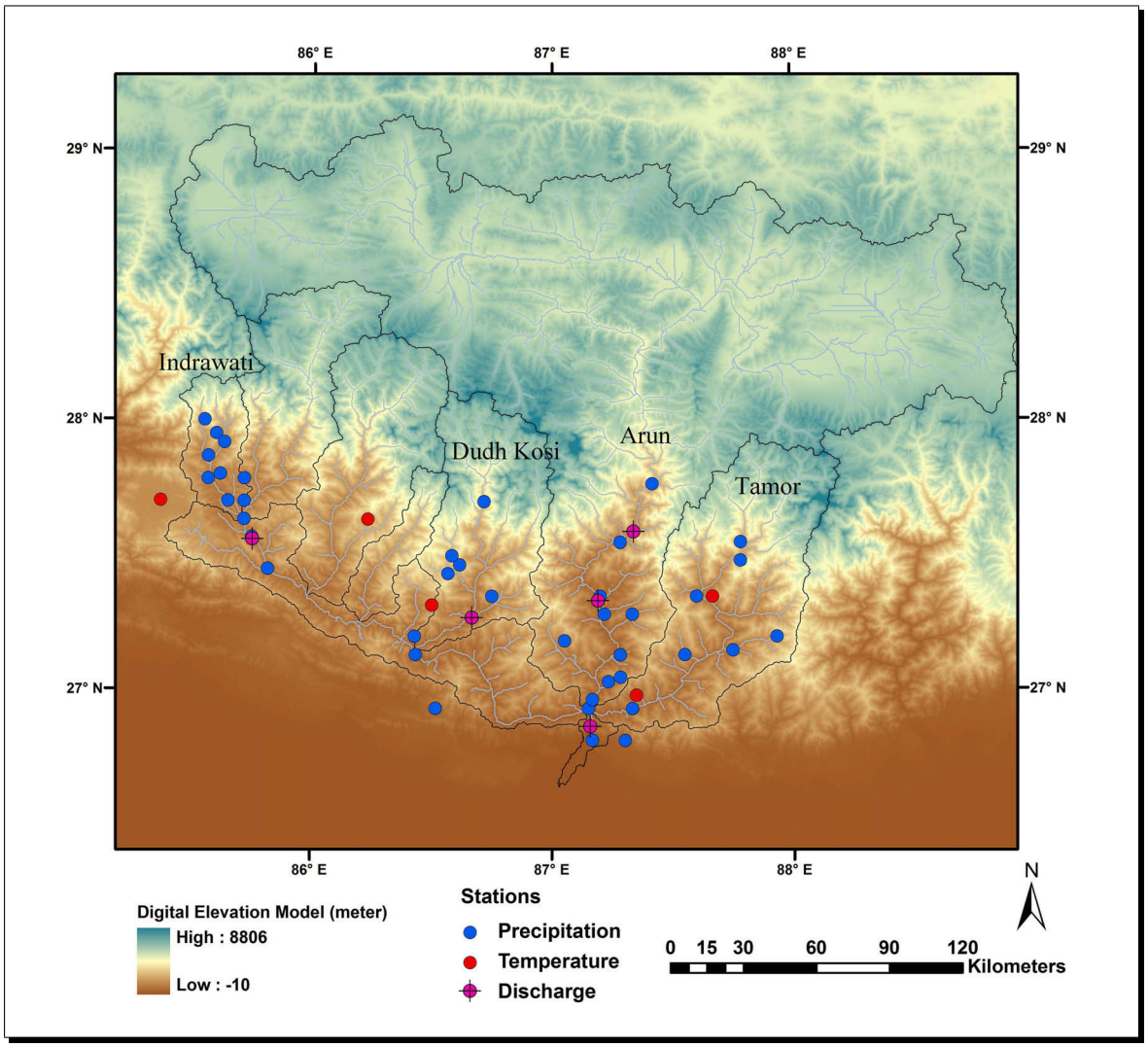

Figure 5.4: Precipitation, temperature and discharge stations in the Kosi river basins

This section comprises the analysis of monthly precipitation dynamics and topographical influence on precipitation between 1985-1997. The 13 years time period was chosen because the hydrological modelling was also carried out on the same time period. A longer time period for this analysis was avoided because of possible gaps in the data period. Based on the availability of the data set, four river corridors, i.e. Indrawati, Dudh Kosi, Arun and Tamor, as indicated in Figure 5.4, were selected. The pre-processed data inside the KosiRBIS was downloaded and the daily data were converted to monthly and yearly values for further analysis. Detailed information about different elevation zones and topography in the mountain ranges in the Nepalese Himalaya were described previously in Section 4.2

The description of each corridor is provided below:

Table 5.1: Precipitation stations in the Indrawati river corridor.

Station Number	Station Name	Elevation (m)	AAP (mm)	Remarks (data gaps)
S-1	Nepalthok	1,098	890	- -
S-2	Pachuwarghat	633	991	- -
S-3	Dolalghat	710	1,146	- -
S-4	Sangachok	1,327	1,574	1992 and 1997
S-5	Mandan	1,365	913	1986 and 1992-1993
S-6	Chautara	1,660	2,021	- -
S-7	Baunepati	845	1,865	- -
S-8	Nawalpur	1,592	2,536	- -
S-9	Dubachuar	1,550	2,435	- -
S-10	Dhap 1025	1,240	1,698	1986 and 1989-1992
S-11	Sarmanthang	2,625	4,074	- -
S-12	Tarke Ghyang	2,480	3,759	1991 and 1992

5.4.1 Indrawati river corridor

The Indrawati river basin is located in the western boundary of the Kosi river basin. The total drainage area of the basin is 1,229 km^2. The corridor has 12 precipitation stations. The detailed information of the stations, their respective elevations and average annual precipitation (AAP) are provided in Table 5.1. In the station Sarmanthang, a deviation in data after 1986 in double-mass analysis was found and therefore this station is only considered for the spatial distribution of precipitation (Section 5.4.1.1) by taking the average data from 1973-1986 in stead of 1985-1997. Although the precipitation in those years might be different from the period selected for other stations, the differences in long-term average can be considered minimal. The catchment profile of the river basin is shown in Figure 5.6(a).

The annual average precipitation from 1985-1997 for the Indrawati river corridor is 1,939 mm with a standard deviation of 954 mm. In this river corridor, 83 percent of the precipitation occurred during the months of June-September. July is the wettest month followed by August. More than 50 percent of the precipitation fell in July and August. November is the driest month which receives an average of nearly 11 mm of precipitation. The precipitation remains low during the winter season and gradually increases from March. Among the monsoon months, September receives the lowest precipitation. The station Tarke Gyang received the highest precipitation of 3,759 mm and the lowest precipitation was recorded in the station Nepalthok with a value of 890 mm. The average monthly precipitation is shown in detail in Figure 5.5(a) and the monthly precipitation of each station is shown in Figure 5.5(b).

5.4.1.1 Spatial distribution of precipitation

This basin has the highest precipitation station density network and stations are located in different topographical positions. Therefore, further analysis of the role of topography for precipitation was also carried out. This was mainly based on the location of the stations in the river valley and on the

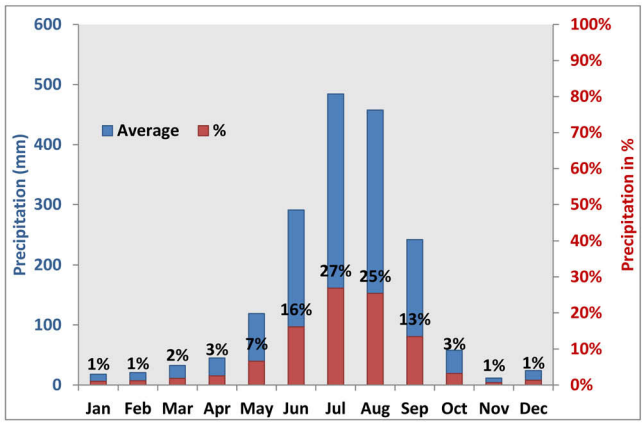

(a) Average monthly precipitation

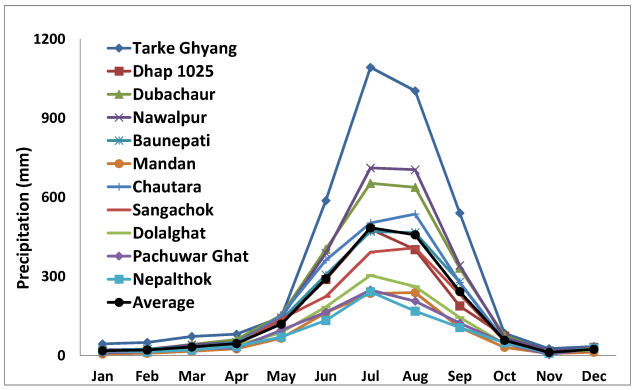

(b) Average monthly precipitation of each station

Figure 5.5: Monthly precipitation dynamics in the Indrawati river corridor (1985-1997)

windward sides of mountains and hills. The position of the station was plotted in Google Earth based on the latitude and longitude provided by the Department of Hydrology and Meteorology (DHM). The latitude and longitude was provided in degree decimal with a precision of two decimal places (eg. 26.89 N and 87.17). In mountainous regions, degree decimal when plotted in Google Earth does not locate at the exact station point. Even a slight difference in degree decimal (two digit precision) might change the position of a station in different elevation and spatial locations (windward or leeward). This issue occurred in two stations was resolved by taking the elevation and the name of the place as a reference.

The average annual precipitation (mm) of stations in this corridor is provided in Table 5.1. The spatial distribution of annual precipitation in this corridor is shown in Figure 5.6. The stations (1, 2, 3, 5 7, and 10) have been considered as stations located in river valleys and the rest are located on the windward side of the mountain for station numbers. The first four leeward stations (Stations 1, 2, 3, and 5) clearly showed much lower precipitation. Station 7 received the highest precipitation (1985

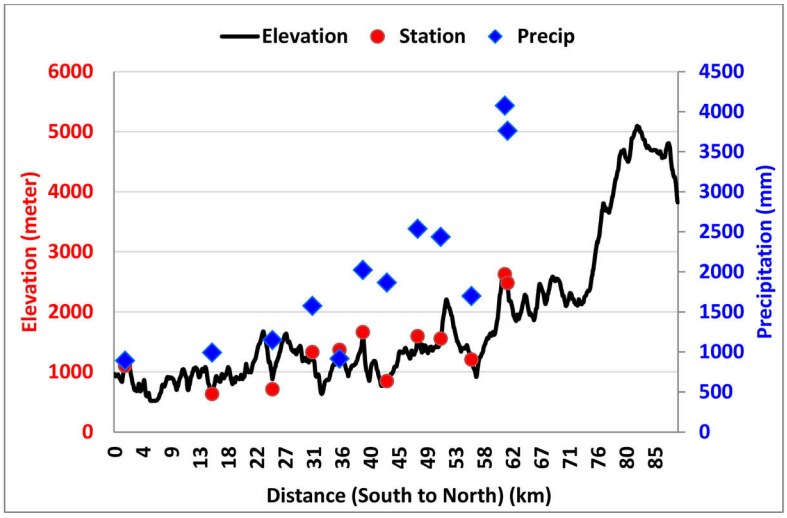

(a) Distribution of precipitation in different elevation zones

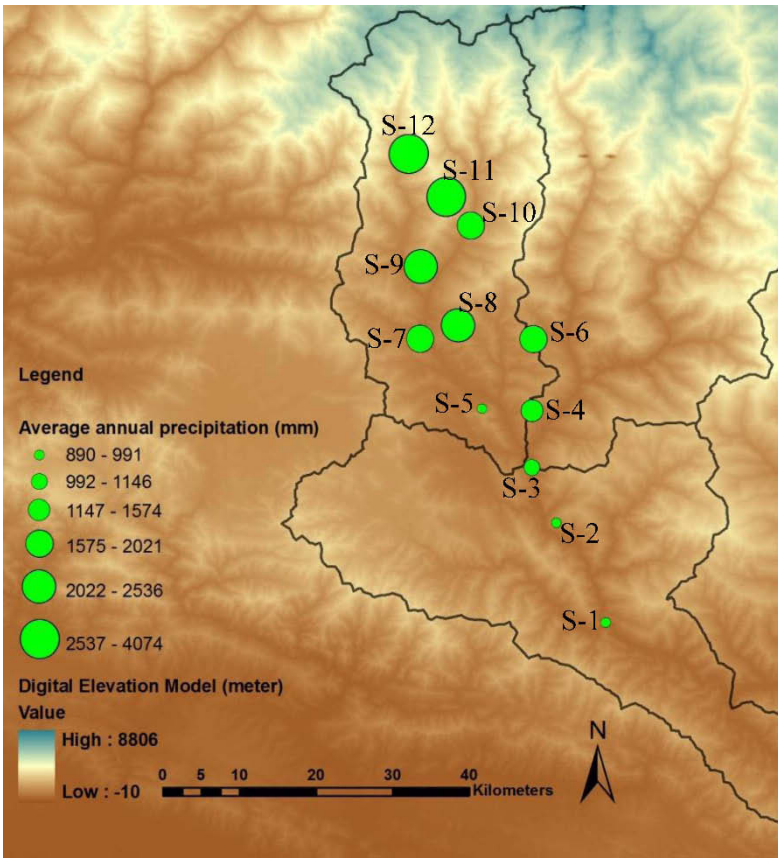

(b) Average annual precipitation

Figure 5.6: Spatial distribution of precipitation in the Indrawati river corridor (1985-1997)

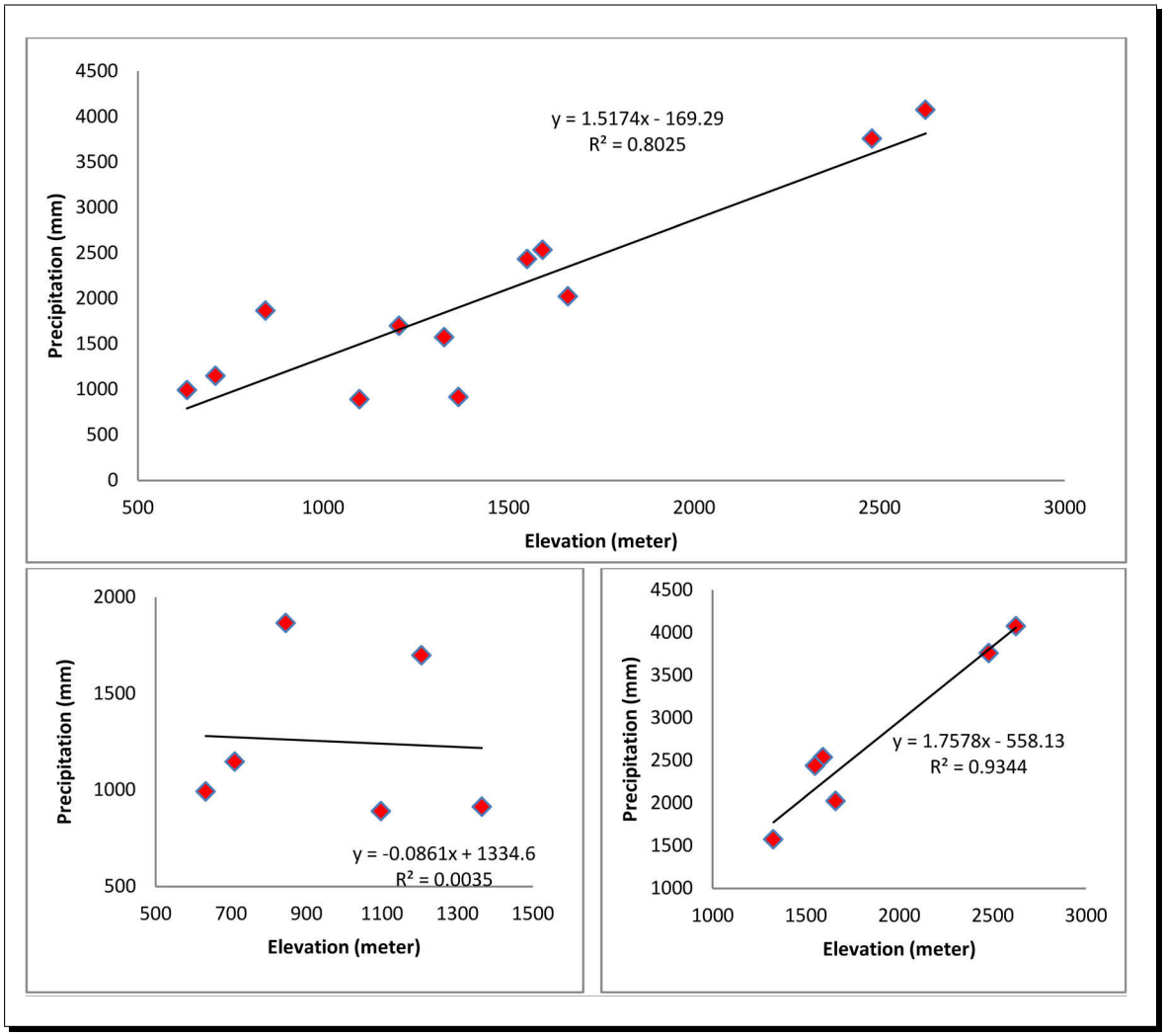

Figure 5.7: Top: Variation of rainfall with elevation in the Indrawati corridor (all stations), **bottom left:** leeward station, **bottom right:** windward station

mm) among the leeward stations. Similarly, the station 10 received the second highest precipitation (1698 mm) among the leeward stations. Though these stations are located in river valleys, the increase in precipitation with elevation in general in the corridor (as indicated in Figure 5.7: Top) may have caused higher precipitation in the river valleys located in higher elevation to the north as shown in Figure 5.6(a). In addition, the foothill of the Higher Himalaya in general receives higher precipitation (stations 11 and 12) as indicated in Figure fig:indrawatiprecip. As indicated in Figure 5.7 (bottom left), there is no correlation between elevation and precipitation amongst stations located on leeward side. However, the windward stations clearly showed a pattern of increasing precipitation with increase in elevation (Figure 5.7: bottom right). The coefficient of determination (r^2) in this case is 0.87.

Station 11 (windward side) received nearly 1,600 mm more precipitation than station 10 (river valley) which is located about 6 km to the south. Similarly, station 7 (river valley) received nearly 700 mm less precipitation than station 8 (mountains) which is about 5 km to the north-east. This indicates relatively

high variation in precipitation amounts in river valleys and mountains within a short distance of each other.

The spatial distribution of precipitation in the Indrawati river corridor indicates that in general the higher elevation towards the foothills of the Higher Himalaya received higher precipitation. Similarly, the river valleys and leewards side received less precipitation compared to nearby ridges and mountains. In addition, the amount of precipitation is increasing towards north in general as shown in Figure 5.6.

5.4.2 Dudh Kosi river corridor

The Dudh Kosi river corridor is located to the south of the Indrawati river basin. The total area of the basin is 4,123 km^2 at the confluence of the Sun Kosi river. This corridor has 9 precipitation stations extending from the Siwalik to the foothill of the Higher Himalaya. The detailed information of the stations, their respective elevations and average annual precipitation (AAP) are provided in Table 5.2. The catchment profile is shown in Figure 5.9(a).

Station 1 (Udayapur Gadhi) has failed the test of double-mass analysis specially showing deviation after 1990. Hence, this station is only included for the analysis of the spatial distribution of precipitation by taking the average annual precipitation of 1985-1989.

The average annual precipitation (APP) from 1985-1997 is 1,699 mm with a standard deviation of 466 mm. About 82 percent of the total precipitation occurred in the month of June to September. The details of the monthly precipitation of each station are shown in Figure 5.8(b) and average monthly precipitation of the basin is shown in Figure 5.8(a). July is the wettest month followed by August. More than 50 percent of the precipitation fell in July and August. January is the driest month which receives nearly 14 mm of precipitation. The precipitation remains low during the winter season and gradually increases from March. Among the monsoon months, September receives the lowest precipitation. Station 5 (Aisealukhark) has the highest precipitation of 2,417 mm and the lowest precipitation is recorded in station 2 (Kuruleghat) with a value of 969 mm.

Table 5.2: Precipitation stations in the Dudh Kosi river corridor.

Station Number	Station Name	Elevation (m)	AAP (mm)
S-1	Udayapur Gadhi	1,175	1,970
S-2	Kuruleghat	497	969
S-3	Mane Bhanjyang	1,576	1,016
S-4	Okhaldhunga	1,720	1,805
S-5	Aisealukhark	2,143	2,417
S-6	Pakarnas	1,982	1,885
S-7	Chialsa	2,770	1,806
S-8	Sallery	2,378	1,587
S-9	Chaurikhark	2,660	2,096

5.4.2.1 Spatial distribution of precipitation

The spatial distribution of average annual precipitation of station referred in Table 5.2 is shown in Figure 5.9. The stations located behind the Siwalik range (station 2 and 3) received the lowest precipitation of around 1,000 mm. It may be because the station is located in the river valley and the Siwalik mountains located in the southern part produces the leeward effect (rain shadow) to the river valley. Station 1 which is located in Siwalik region receives nearly 1,000 mm higher precipitation than stations 2 and 3.

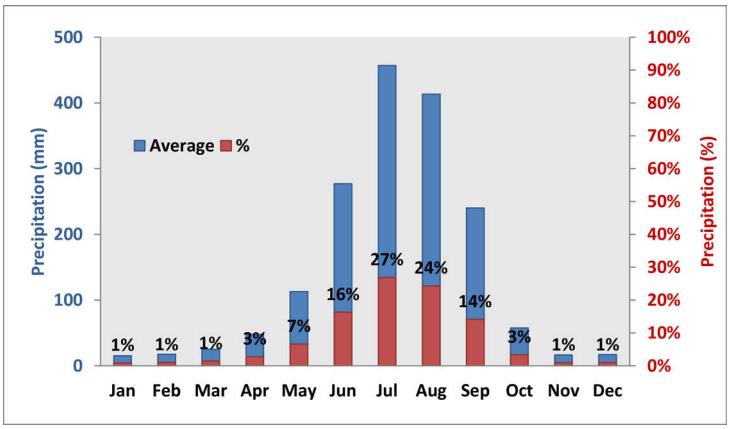

(a) Average monthly precipitation

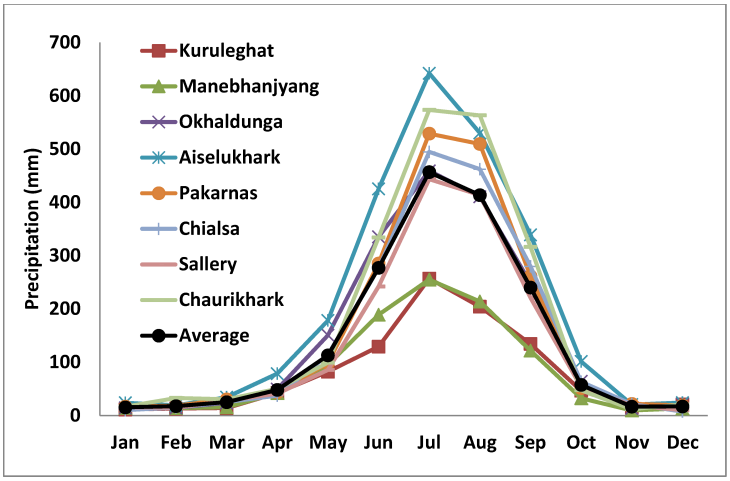

(b) Average monthly precipitation of each stations

Figure 5.8: Precipitation dynamics in the Dudh Kosi river corridor (1985-1997)

Station 5 (Aisealukhark), located in the Middle mountains, received the highest amount of precipitation. This station is located on the windward side (towards the top of the hills) and this may have caused higher precipitation. Another high precipitation zone is the station 9 (Chaurikhark) located

to the foothill of the Higher Himalaya (Figure 5.9(a) and 5.9(b)). This station although positioned in the river valleys, received high precipitation probably due to located in the foothill of the Higher Himalaya.

Station 8 (Sallery) is located close to the stations 6 and 7 (Pakarnas and Chialsa). However, the annual precipitation varies a lot. This may be because station 8 is located in the river valley which caused less precipitation due to rain shadow effect. Station 6 is also located in leeward side, but the precipitation is slightly higher than that of station 8.

In this corridor, the highest precipitation zone is found to be in the Middle Mountains and the foot hills of the Higher Himalayas between 2,000-3,000 m. The highest precipitation zone indicates that the windward (or stations in hills/mountains) receives higher precipitation. Similarly, stations located in river valleys (and on the leeward side) receive a lower amount of precipitation. In general, the precipitation rises with increasing elevation towards northern part with some variation, except for station 1 (Udayapur Gadhi) which is located in the Siwalik range as indicated in Figures 5.9(b) and 5.9(a).

5.4.2.2 Precipitation pattern in the high altitude areas of the Dudh Kosi river basin

The hydrological modelling (Chapter 6) is applied in the Dudh Kosi river basin. There is little information about the precipitation pattern in the upstream areas of the basin, which has been discussed in this section to provide a general overview of the precipitation pattern in those areas. There are few studies conducted to understand the relationship between precipitation and topography in the Himalayan region (Singh et al. 1995, Yasunari and Inoue 1978, Dhar and Rakhecha 1981, Ageta 1976, Higuchi et al. 1982, Kochanowski 2009).

Topography has a profound effect on spatial distribution of precipitation – both globally and regionally (Smith 1979). Mountains influence the flow of air, and cloud formation, and they disturb the vertical stratification of the atmosphere by acting as physical barriers and as sources or sinks of heat (Barros and Lettenmaier 1994). There are many valleys in the high altitude areas of the Himalayas including the Kosi river basin, each with distinctive local circulation and climatic conditions, depending upon factors such as altitude, area, aspects and presence of glaciers etc (Yasunari 1976). Therefore, some occasional measured data at these high altitude areas are influenced both by large-scale disturbances and by local cumulus convection which depends on solar energy and altitude. (Tartari et al. 1998).

A team of Japanese scientists made a study and formed an expedition in the high-altitude areas of the Dudh Kosi river basin and, among other things, investigated the precipitation patterns in different altitudes ranges. The study results were published in a series of publications, which are summarised below:

Higuchi et al. (1982) and Yasunari and Inoue (1978) suggest that precipitation along the main valley of the Dudh Kosi river decreases with altitude in the range from 2,800 m to 4,500 m. They compared the precipitation pattern between the valleys and mountains. The valley station (Lhajung) is located at 4,420 m elevation and nearly 25 km upstream of the Chaurikhark (Station 9). The location of these stations in reference to the Station Chaurikhark is provided in Figure 5.10. One station (EB050) in a

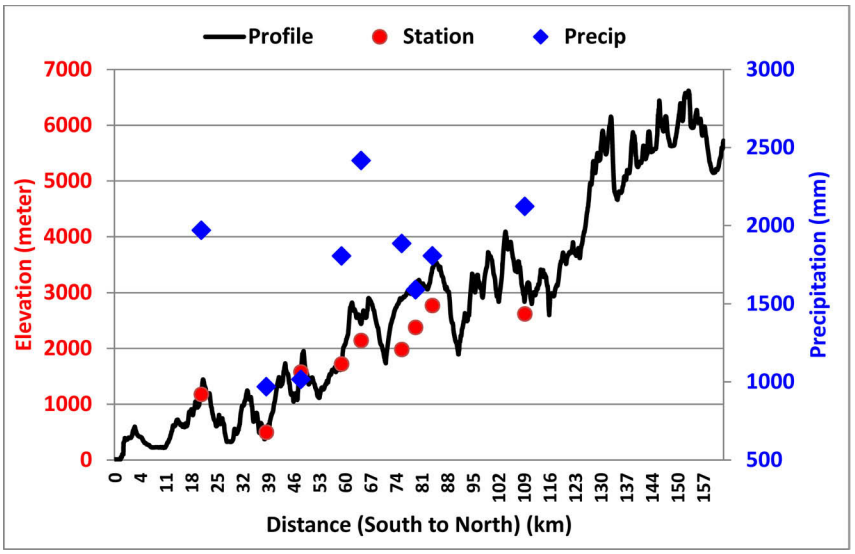

(a) Spatial distribution of precipitation in different elevation zones

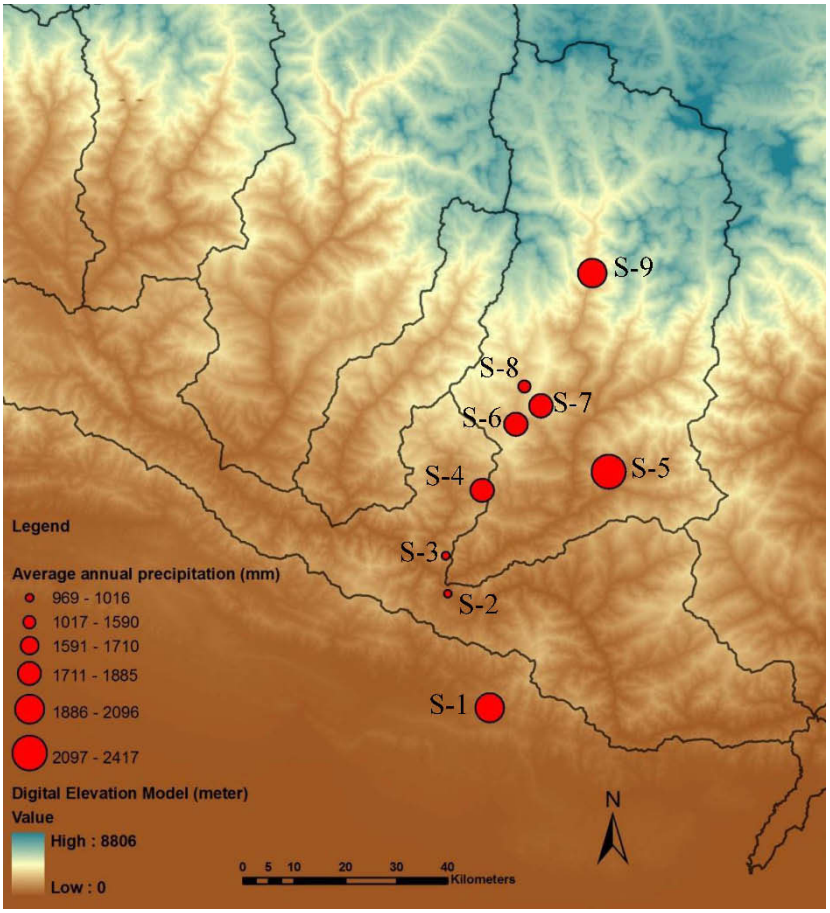

(b) Average annual precipitation

Figure 5.9: Spatial distribution of precipitation in the Dudh Kosi river corridor (1985-1997)

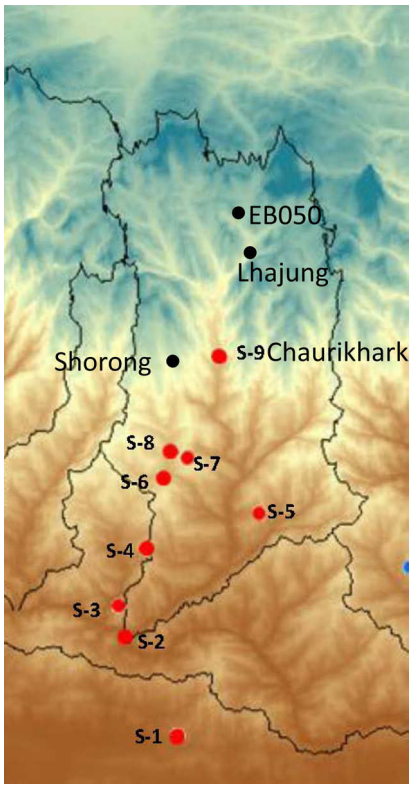

Figure 5.10: The location of the three stations (EB050, Lhajung and Shorong) in reference to Chaurikhark station. The position of these stations were taken from Yasunari and Inoue (1978)

mountain is located 5 km further upstream of Lhajung and is situated at the elevation of 5,160 m in a glacier slope. Another one (Shorong: 4,850 m) is located about 15 km to the west of Chaurikhark, along the slope of the glaciers. The stations in red dots are regular stations for precipitation measurements from DHM (Figure 5.9. Yasunari and Inoue (1978) suggested that ratio of the total precipitation during the measured period at the two mountains slopes is 4.2 and 4.8 times higher than the valley precipitation. During this period, the amount of precipitation of Chaurikhark station (14.6 mm/day) is slightly higher than that of Glacier EB050 (12.5 mm/day) whereas at Shorong station, the amount is 11.3 mm/day. The precipitation in the river valley at that period is nearly 3 mm/day. The precipitation at the mountain slopes was concentrated mainly during the daytime due to orographically and thermally induced convection and local cumulus convection. On the other hand, precipitation in the river valleys mainly occurred at night due to large scale disturbances. Yasunari and Inoue (1978) suggested that the precipitation phenomenon around these peaks and ridges are probably due to local cumulus convection .

The high altitude station (4,355 m) operated by DHM near Lhajhung indicates that the precipitation is in the range of 500-1,000 mm/year. However, the station data are quite erratic with frequent gaps over time. These datasets are not provided by DHM for public use because of the data-quality is-

sues (B. Pokharel, DHM, personal communication, April 2011). Recently, the Ev-K2-CNR project (www.evk2cnr.org) has established four high-altitude stations in the Dudh Kosi river basin areas. The data from 2002-2007 are publicly available upon request. The highest station named, Pyramid, is located at 5,050 m elevation about 3 km upstream of station EB050 (Figure 5.10). This station in general shows precipitation of 500 mm/year based on the average of a few years. However, due to practical difficulties of maintaining the station in the high-altitude areas, only 40-50 percent of the dataset are reported to be in "good" quality. The remaining data are tagged as dubious and bad in quality. It was reported in the documentation of the project that the field measurements frequently are hindered by problems, such as sensor freezing and snow measurement (0 precipitation being recorded during snowfall if the air temperature is below 0 degree Celsius).

Shiraiwa et al. (1992) studied the precipitation pattern in the Langtang valley of the Central Himalaya in Nepal in order to study the mass balance of glaciers. This study has indicated that the station located at the bottom of the valley (about 4,000 m) receives nearly two thirds of the precipitation compared to the stations located in mountains and ridges (5,000 m). In the stations located at the bottom of the valley, less precipitation from cumulus cloud occurs in comparison with precipitation for the stations along mountain slopes. Similarly, stations located further north (the upper part of the valley) receive precipitation amounts similar to those recorded at the river valley station. This is because less moist air is conveyed to the upper part of the valley by monsoonal circulations prevailing from the south.

In the Higher Himalayan region, the precipitation in general is lower than in the middle mountain ranges, because the moist air resulting from the monsoon are consumed in the middle mountains and foothills of the Higher Himalayas in the form of precipitation. By the time the clouds reach the Higher Himalaya, less moisture is available in the cloud, a condition which is also suggested by (Singh et al. 1995) based on the study in the western Himalayas.

There are a few possible explanations why precipitation in the high-altitude areas might be underestimated. First, the location of these stations is in valley areas which, in general, receives less precipitation. However, the mountain and ridges receive high amounts of precipitation as suggested by Ageta (1976), Yasunari and Inoue (1978). Second, the precipitation in general may be measured lower than actual values in the rain gauge, due to measurement errors such as wind-induced error and evaporation loss. The wind error is very high during the measurement process in the case of windy areas (such as the higher Himalayan region) and with snow measurement. Allamano and Claps (2010) reported that the underestimation of precipitation in the presence of snow can be up to 60-70 percent of the total volume in the Italian Alps. Similarly, Sevruk (1986) suggested that the wind-induced error is much larger (10-50 percent) for snowfall measurement. This in general suggested that, although the occasional data measurement on these high-altitude areas are lower, they should be higher when considering the different measurement errors.

5.4.3 Arun river corridor

The centrally located Arun river basin is the biggest sub-catchment of the Kosi river basin, which is extended from Tibet to Nepal. The total area of the basin is 33,500 km^2 of which nearly 80 percent is located in Tibet. The corridor has 11 precipitation stations. The detailed information of the stations,

their respective elevations and average annual precipitation (AAP) are provided in Table 5.3. The catchment profile is shown in Figure 5.12(a)

Table 5.3: Precipitation stations in the Arun river corridor.

Station Number	Station Name	Elevation (m)	AAP (mm)
S-1	Chatara	183	1,991
S-2	Tribeni	143	1,622
S-3	Munga	1,317	1,132
S-4	Pakhribas	1,680	1,567
S-5	Laguwa Ghat	410	821
S-6	Bhojpur	1,595	1,320
S-7	Tumlingtar	303	1,195
S-8	Chainpur East	1,329	1,468
S-9	Dingla	1,190	2,029
S-10	Num	1,497	4,542
S-11	Chepuwa	2,590	2,815

In this corridor, the average annual precipitation from the 1985-1997 period is 1,809 mm with a standard deviation of 1,008 mm. The monthly average precipitation is provided in Figure 5.11(a). About 73 percent of the total precipitation occurred in the months of June-September. July is the wettest month followed by August. About 41 percent of the precipitation occurs on the average in July and August. December is the driest month which received nearly 18 mm of precipitation. Among the monsoon months, September received the lowest amount of precipitation. About 11 percent of the total precipitation occurs during the month of May, which is high compared to the Indrawati and Dudh Kosi river corridors which are only 6 and 7 percent respectively. The precipitation remains low during the winter season and gradually increases from March. The station Num has the highest precipitation of 4,542 mm and the lowest precipitation is recorded at Laguwa Ghat station with a value of 821 mm. The Num station received nearly 16 percent precipitation (531 mm) during the month of May. As indicated in Figure 5.11(b), this amount of precipitation is higher than the single month precipitation of other stations. Similarly, second highest precipitation of the station Chepuwa also receives 14 percent precipitation in the month of May. This indicates that the precipitation during the pre-monsoon period is higher in this corridor compared to the others. In this period, precipitation is mostly caused by convective rainfall which is due to the higher temperature and associated heating of the surrounding lands which produce moisture-laden air (Singh and Singh 2001). The detail of the monthly precipitation of each station is shown in Figure 5.11(b) and the average monthly precipitation is provided in Figure 5.11(a).

5.4.3.1 Spatial distribution of precipitation

The spatial distribution of average annual precipitation of stations referred in Table 5.3 is shown in Figure 5.12. Station 1 is located in the Terai region which records nearly 2,000 mm of precipitation. Station 2 is located in the river valley where the seven rivers of the Kosi meet. This station recorded

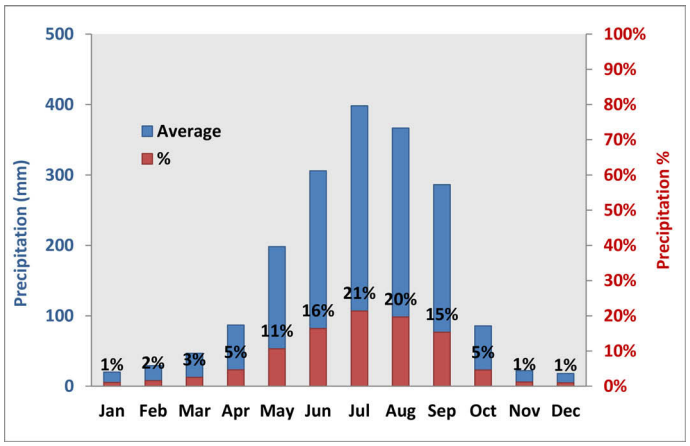

(a) Monthly average precipitation

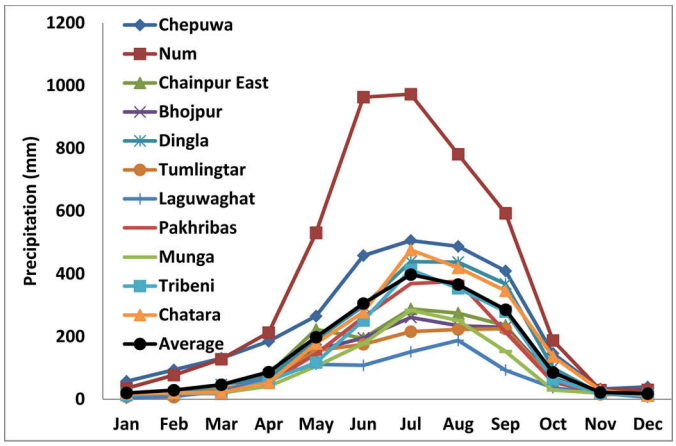

(b) Monthly average precipitation of each stations

Figure 5.11: Precipitation dynamics in the Arun river corridor (1985-1997)

about 400 mm less precipitation than station 1. Hence, within the distance of just 5 km between station 1 and 2, the precipitation decreased heavily. This may be because when one proceeds from the south along the stations towards the north, more rain-shadow effects are created by the Siwalik mountain range as in the similar case in the Dudh Kosi river basin.

In this corridor, the stations (5 and 7) which are located in the river valleys, received lower amount of precipitation. On the contrary, stations located in mountains and leeward sides (3, 4 and 8) received higher amount of precipitation. For example, the higher elevation of the station 8 than station 7 may have caused higher precipitation which indicates the orographic effect on precipitation. However, there is variation in amount of precipitation among the river valley stations as well. For example, station 7 received nearly 400 mm higher precipitation than station 5, although both are located in the valleys. The local climatic conditions and topography of the stations might have influence on the precipitation pattern. The most northern stations Num and Chepuwa (10 and 11) received the highest

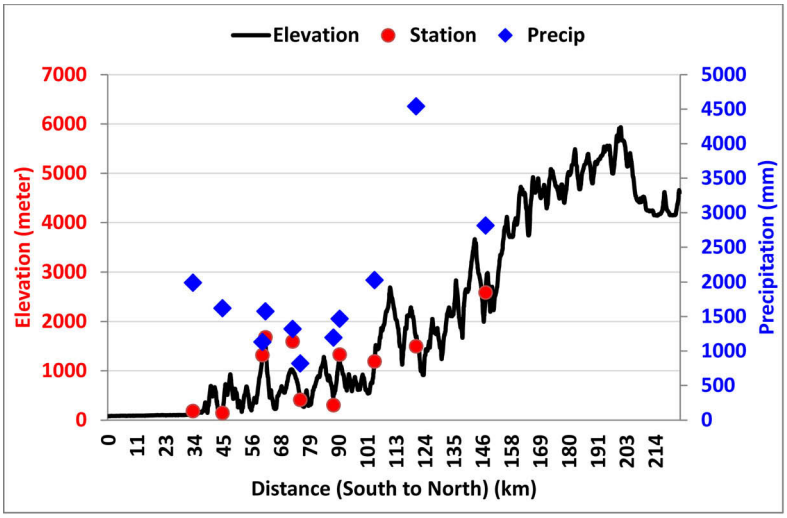

(a) Distribution of precipitation in different elevation zones

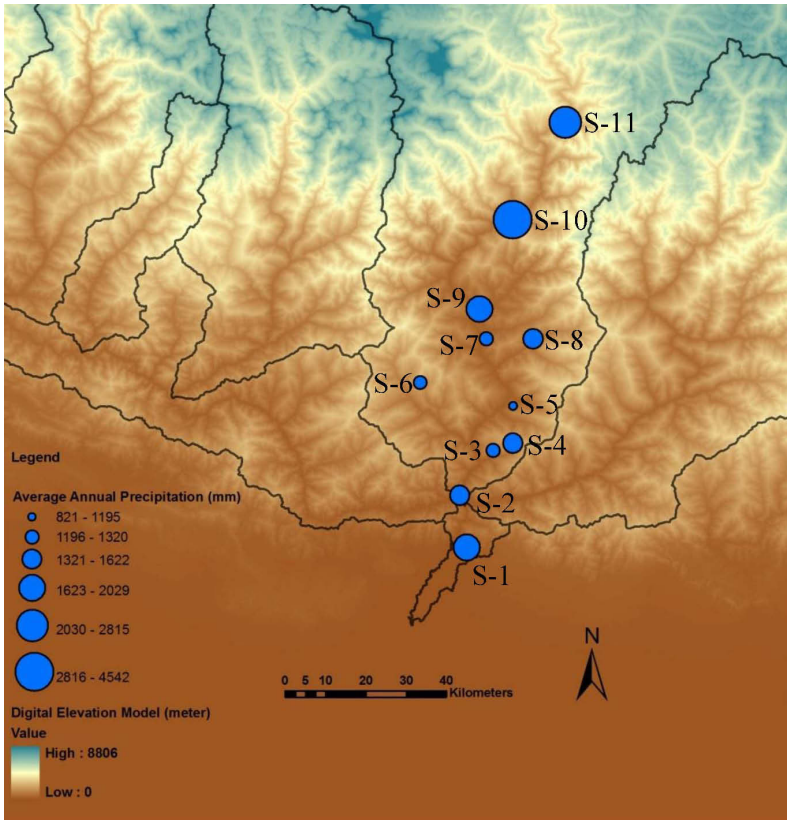

(b) Average annual precipitation

Figure 5.12: Spatial distribution of precipitation in the Arun river corridor (1985-1997)

amount of precipitation. The Num station received precipitation with a value of 4,541 mm which is among the highest in the whole Nepal. At times, it received about 5,500 mm of precipitation.

Kattelmann (1990) suggested that the Arun valley should enhance the flow of air and water vapor from the Bay of Bengal to the Tibetan Plateau by providing a route through the river valley rather than over the Himalaya. This provides an opportunity for the unobstructed flow of air and water vapor from south to north as indicated in Figure 5.12(b). In the case of Indrawati and Dudh Kosi, the Siwalik mountains provide barriers to the south. Shrestha (1989) suggested that the occurrence of tropical monsoon forests, with tree ferns at lower altitude and big-leaved species of Rhododendron at higher elevations may have caused the area to receive higher precipitation. A similar environmental condition was also reported in the northern Pokhara Valley in central Nepal, which is also a pocket of high rainfall area of about 5,000 mm (cited in (Shrestha 1989)). The Arun Valley further allows the monsoon rain to penetrate far towards the north, creating a corridor of humid climate even across the main range of the Himalaya (Shrestha 1989).

In summary, in this corridor, the station in the Terai region indicated average annual precipitation of about 2,000 mm. The middle mountain ranges received precipitation in the range of 1000-2000 mm; however, the river valleys and the leeward side receive less precipitation than stations located in mountains and on the windward side as indicated in Figures 5.12(a) and 5.12(b)). The stations located to the north towards the foothills of the Himalaya are the wettest regions which received average annual precipitation of about 4,500 mm.

5.4.4 Tamor river corridor

The Tamor river basin is located in the eastern part of the Kosi river basin. The total area of the basin is 6,053 km^2. The river corridor has 10 precipitation stations, including one in the Terai region. The detailed information of the stations, their respective elevations and average annual precipitation (AAP) are provided in Table 5.4. The catchment profile is shown in Figure 5.14(a).

Table 5.4: Precipitation stations in the Tamor river corridor

Station Number	Station Name	Elevation (m)	AAP (mm)
S-1	Dharan	444	2,284
S-2	Mulghat	365	1,069
S-3	Dhankuta	1,210	1,020
S-4	Terhathum	1,633	1,131
S-5	Phidim (Panchther)	1,205	1,397
S-6	Memen Jagat	1,830	2,330
S-7	Dovan	763	1,643
S-8	Taplejung	1,732	2,041
S-9	Taplethok	1,383	2,848
S-10	Lungthung	1,780	2,102

The annual precipitation from 1985 to 1997 for this corridor is 1,787 mm with a standard deviation

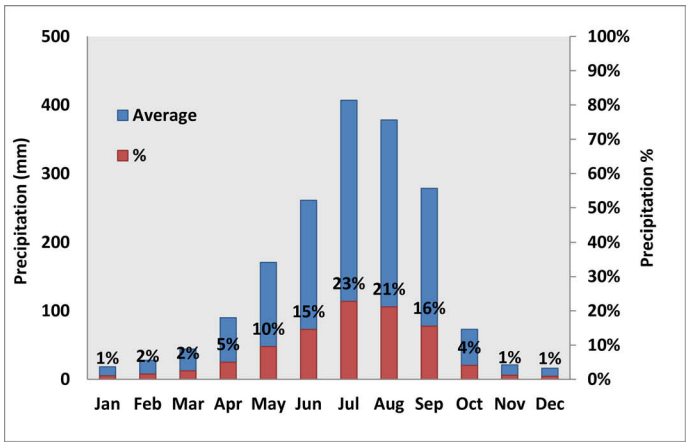

(a) Monthly average precipitation

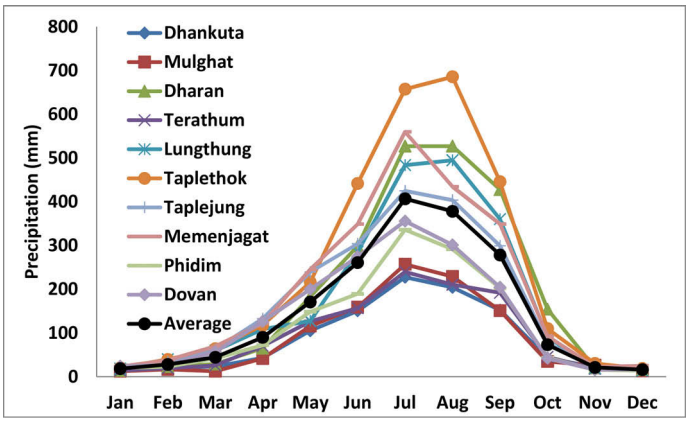

(b) Monthly average precipitation of each stations

Figure 5.13: Precipitation dynamics in the Tamor river corridor (1985-1997)

of 627 mm. About 74 percent of the total precipitation occurred during the months of June through September. July is the wettest month followed by August. About 44 percent of the precipitation on the average occurs during July and August. December is the driest month which received nearly 16 mm of precipitation. Among the monsoon months, June received the lowest precipitation. 10 percent of the total precipitation occurred in May. The precipitation remains low during the winter season and gradually increases from March. Details of the monthly precipitation of each station is shown in Figure 5.13(b) and the average monthly precipitation values are shown in Figure 5.13(a). The Taplethok station recorded the highest precipitation of 2,848 mm and the lowest precipitation was recorded at Dhankuta station (1,020 mm).

5.4.4.1 Spatial distribution of precipitation

The spatial distribution of average annual precipitation of stations referred in Table 5.4 is shown in Figure 5.14. Station 1 located in the Terai region (towards the foothills of the Siwalik) received about 2,284 mm of precipitation. To the north of the Siwalik range, the two stations received nearly 1,000 mm of precipitation. Station 2 is located in the river valley (behind Siwalik mountains) and received low precipitation, however, the Dhankuta station located in higher elevation (1,210 m) in a hilly region, did not show higher precipitation than a river valley station. The spatial distribution of the precipitation is provided in Figure 5.14(b)

The stations in the middle mountains ranges (4, 5, 7 and 8) recorded between 1,000-2,000 mm of annual average precipitation, whereas the station 6 (Memen Jagat) is wetter (2,300 mm) than other stations. In this corridor also, the stations in river valleys in middle mountains ranges received lower precipitation as well. The station 7 (Dovan) is located in the river valley and the nearby station 8 (Taplejung) is located at 1,732 m about 5 km to the east. The Taplejung station receives about 400 mm higher precipitation than Dovan which shows that the large orographic differences over short distance cause high precipitation in mountains. The two stations (9 and 10) located towards the foothills of the Higher Himalaya received higher amount of precipitation with a value of 2,848 mm and 2,102 mm respectively. Similar to other river corridors, the stations located towards the foothills of the Higher Himalaya received higher precipitation and stations located in the river valleys receive low precipitation.

5.4.5 Inter-comparison of precipitation patterns in corridors

The analysis of the precipitation data in the Kosi river basin corridor suggests that there is no linear trend between precipitation and elevation. The precipitation pattern is controlled by underlying geology and associated elevation zones. Figure 5.15 shows the spatial distribution of precipitation in the study area. In general, the following observations can be made resulting from the analysis above:

1. Precipitation stations located in the Terai region and on the windward side of the Siwalik range receive precipitation in the range of about 2,000-2,300 mm. The only station located on the Siwalik range showed a precipitation of nearly 2,000 mm. The higher amount of precipitation in the Terai region is possibly caused by higher effects of convective phenomenon due to lower elevation associated with temperate climate.

2. The precipitation pattern in the Middle Mountains range (Lesser Himalaya) is not uniform. In general, the region receives precipitation between 800-2,500 mm. The stations located in river valleys and on leeward sides receive less precipitation in the range of 1,000 to 1,500 mm. Some of the leeward stations receive only around 900 mm. Among the stations located in river valleys or on the leeward side, stations located towards north (foothills of the Higher Himalaya) receive higher precipitation than stations to the south of the Middle Mountains ranges. The stations located in high elevation between 2,000-3,000 m in Middle Mountain range receive higher precipitation. In many cases, large orographic differences over a short distance has

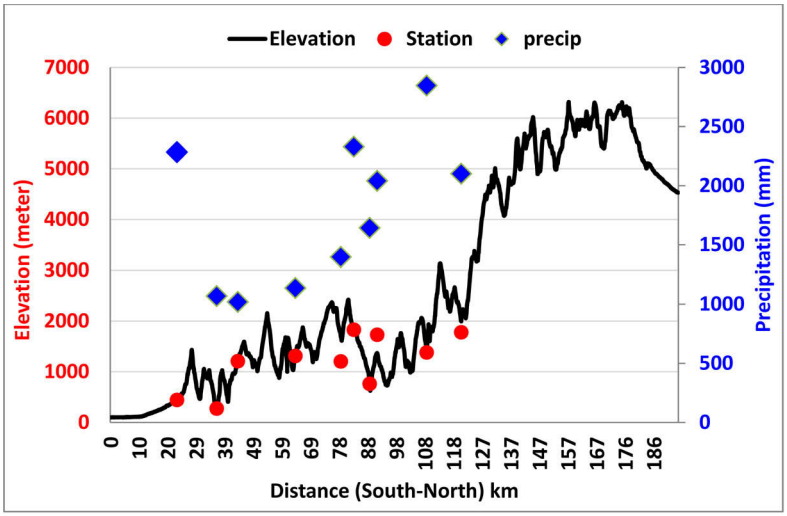

(a) Distribution of precipitation in different elevation zones

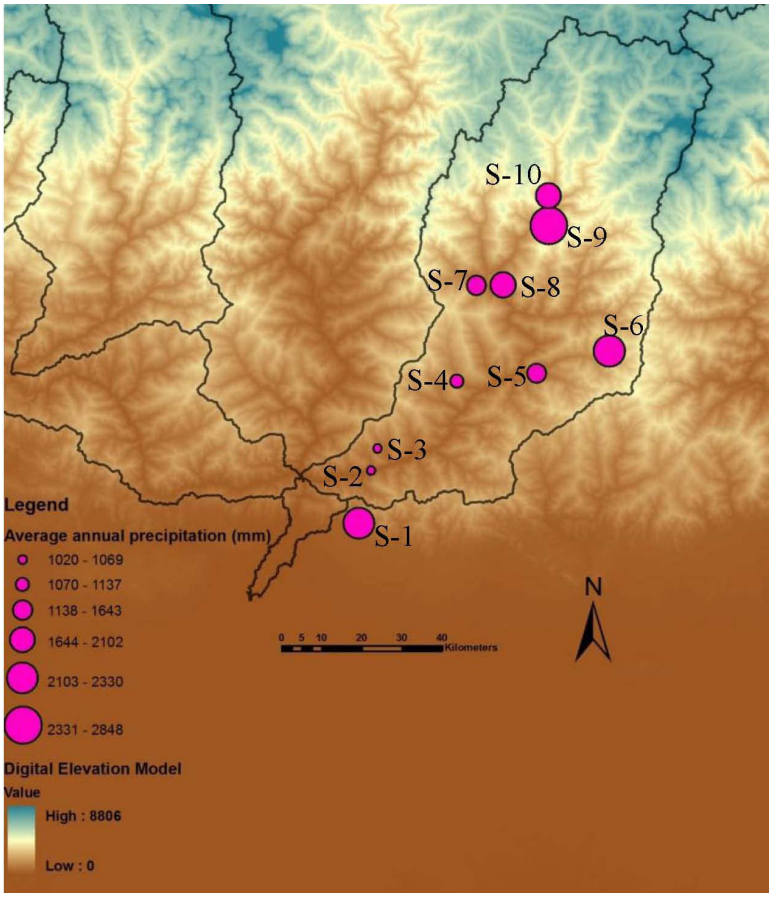

(b) Average annual precipitation

Figure 5.14: Spatial distribution of precipitation in the Tamor river corridor (1985-1997)

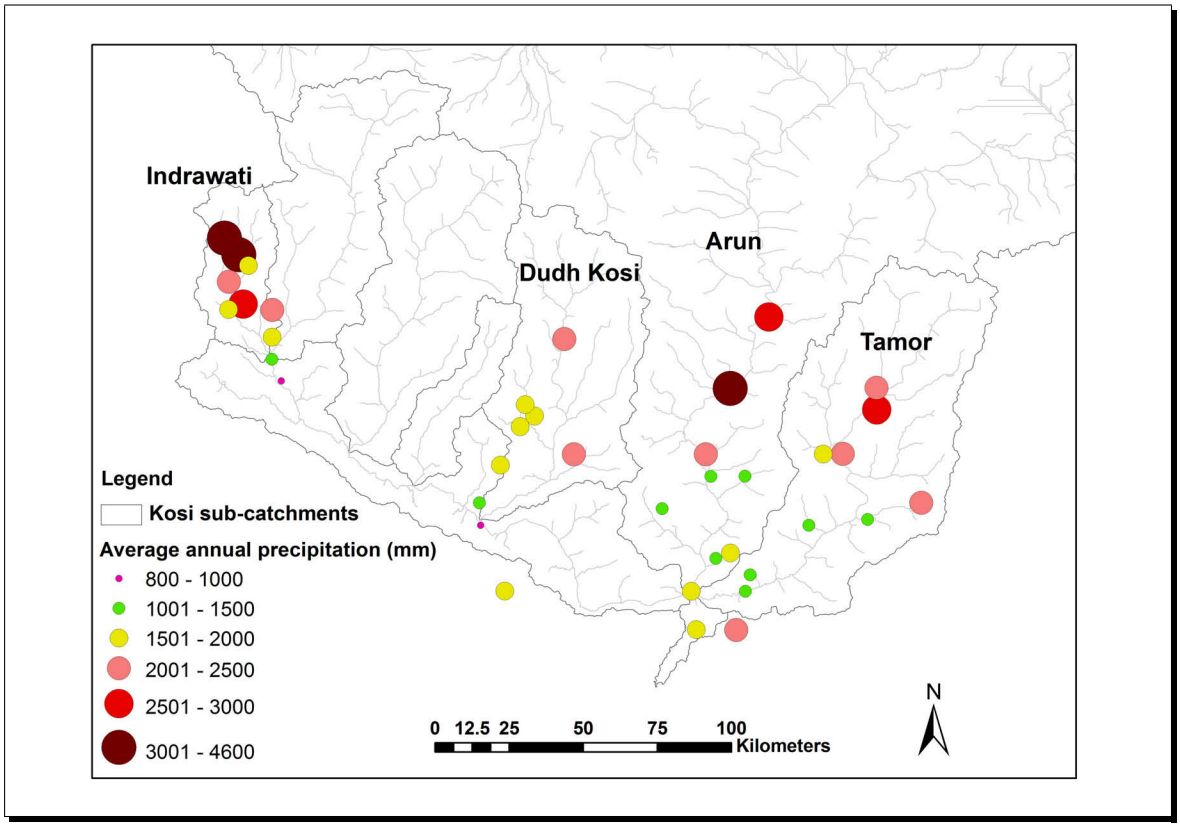

Figure 5.15: Spatial distribution of average annual precipitation (1985-1997) in the Kosi river basin in Nepalese Himalaya

caused higher precipitation. This has shown the strong orographic effects on precipitation in this region.

3. Similarly, the stations located behind the Siwalik range showed a lower amount of precipitation because of the leeward (rain shadow) effect created by the Siwalik mountains to those stations.

4. Stations located in the foothills of the Higher Himalaya (to the north) are the wettest part of the region. Among the four corridors studied, stations in this region indicated the highest amount of precipitation.

The schematic representation of the spatial distribution of a precipitation pattern in the Kosi river are provided in Figure 5.16. The blue dot represents the average annual precipitation of the stations located in the corresponding mountain system as shown in the right axis of the figure. The mountain systems have the following number of stations from which the average value is determined: Terai (two stations), Siwalik (one station), Lesser Himalaya (33 stations) and Foothills of the Higher Himalaya (six stations). The figure indicates that the Terai region has slightly higher precipitation than the Siwalik region. The Lesser Himalaya region has the average annual precipitation of about 1,620 mm. However, the range of precipitation in this region is from about 821 mm to 4,542 mm which represents the variation in the amount caused by the location of the stations. The precipitation increases to the north and the stations located in the foothills of the Higher Himalaya receives in average about 3,000

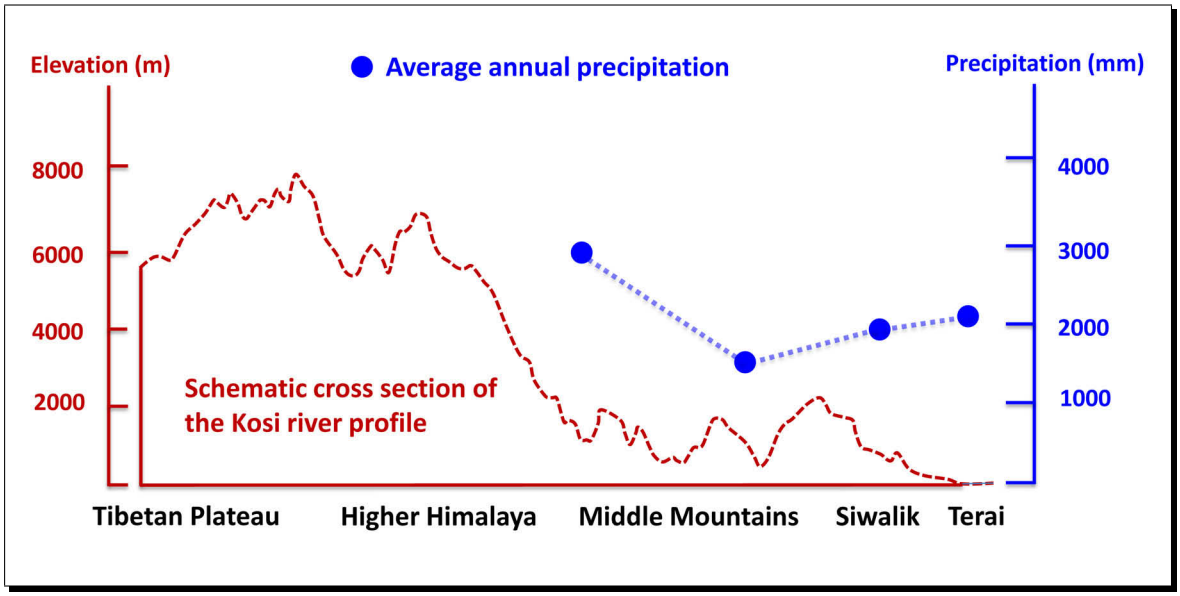

Figure 5.16: Distribution of precipitation patterns in different elevation zones. The blue dots represents the average precipitation of stations located on the underlying mountain systems.

mm of precipitation. In general, it can be concluded that the mountains in the Higher Himalaya region are the greatest barrier for the movement of air and water vapor to the north. These mountain barriers acts as orographic barriers which results in large amounts of precipitation especially in the foothills of the Higher Himalaya. The entire precipitation pattern of the Kosi river basin and its corridor are shown in Figure 5.15 and Table 5.5.

Table 5.5: Precipitation dynamics in the Kosi river basin

Variables	Indrawati	Dudh Kosi	Arun	Tamor
Average annual precipitation (mm)	1,939	1,728	1,809	1,787
Standard deviation	954	475	1,008	627
Monsoon (%)	83	82	73	74
Non-monsoon (%)	17	18	27	26
Maximum precipitation (mm)	3,759	2,417	4,542	2,848
Minimum precipitation (mm)	890	969	821	1,020

5.5 Discharge dynamics

Although, river discharge (or streamflow) is believed to be one of the most accurately measured components of the hydrological cycle, the accuracy of discharge data depends upon many factors. The error of any river discharge time series originates from a number of sources such as measurement instruments and techniques, human errors etc (Shiklomanov et al. 2006). The daily discharge is com-

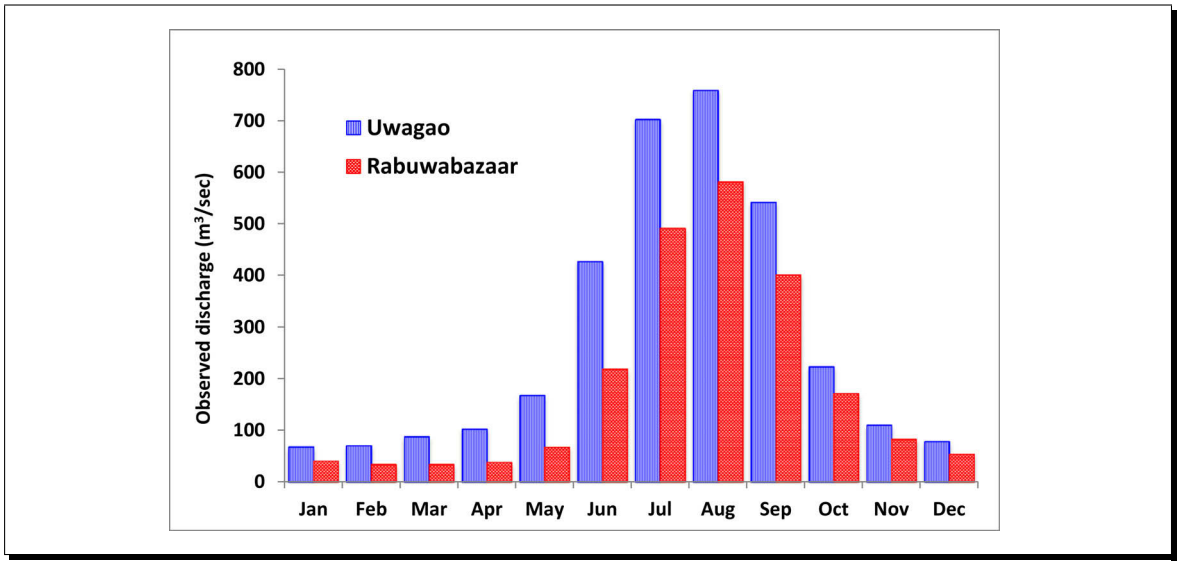

Figure 5.17: Average monthly discharge of two gauging stations in the Kosi river basin

puted from the estimation of mean daily stage from the observation records at a gauging station and the application of the stage data to a rating curve to obtain mean daily discharge. For any given gauging station, the rating curve is developed from a few measurements of stage values (water level) in a river. While doing so, many factors such as cross section of a river and flow velocity etc. specially during low flow periods are taken into account to define the relationship between stage and flow volume. This relationship is further extrapolated by using regression equation to define a continuous value of discharge. The high streamflow values are mainly defined from that extrapolation assuming that the uncertainty associated with discharge measurement is significantly higher than that for stage measurement (Shiklomanov et al. 2006). The measurement of high floods are subject to higher uncertainty in the Himalaya region because the stage-rating-curve may be based on an inadequate number of measurements (Kattelmann 1987). The analysis of the stage-rating curve values of the Dudh Kosi river basin indicates that the higher values during flood times remain unchanged whereas the river profile is continuously changing due to bank erosion associated with the force of the water during the flood period which affects the rating curve.

The streamflow dynamics of the Kosi river basin have strong seasonal components. The discharge is driven by seasonal monsoon precipitation complemented by snow and glacier melt. Figure 5.17 shows the monthly discharge patterns of two stations, Rabuwabazaar (Dudh Kosi river) and Uwagao (Arun river) between 1986-1997. The name of the stations and their geographical locations are provided in Figure 5.21(b)). The maximum discharge normally occurs during the monsoon season from June to September. In these two stations, about 76 and 73 percent of the annual flow volume occurs during the monsoon season. The flooding period of higher streamflow during the monsoon season is followed by low flows during winter and dry season (October till May). During the months of April and May, the low flow is supplemented by contribution from snow and glacier melt. The average monthly discharge of the entire Kosi river basin at the gauging station Chatara is provided in Figure 4.8(a), page 42. The discharge graph of the Uwagao indicates that the annual streamflow pattern is slightly higher than

that of the Rabuwabazaar, although the proportion of area contributing streamflow to the outlet is far larger than that of the Rabuwabazaar. This is mainly because most of the Arun river basin is located in the Tibetan part of the Kosi which represents arid climate with low precipitation. Because of this, the discharge is less in spite of having larger area. On the contrary, the Dudh Kosi river basin is entirely located in the southern part of the Kosi river basin which represents humid climate associated with high precipitation.

5.5.1 Flow-duration curve

The flow-duration curve is a cumulative curve that shows the percent of time that flow in a stream is likely to equal or exceed during a given period (Searcy 2002). It combines in one curve the flow characteristics of a stream throughout the range of discharge, without regard to the sequence of occurrence. In addition, it shows the percentage of time river flow can be expected to exceed a design flow of some specified values and to show the discharge of the stream that occurs or is exceeded some percent of time (eg. 70 percent of the time). Flow-duration analysis can be used for many purposes in the field of water resources engineering and have been used to solve problems in water management, flood control, hydropower and scientific comparison of streamflow (Vogel and Fennessey 1995, Searcy 2002). The flow-duration curve of five gauging stations in the Kosi river basin is provided in Figure 5.18. The period of the analysis is from 1982 to 2006, however, a few stations have data gaps between this period. The gap information of the five stations can be seen in Figure 5.21(a). The figure shows that the Chatara gauging station has the highest magnitude of discharge. The discharge of higher than 500 m^3/sec occurs more than 50 percent of the time and the lowest flow is higher than 200 m^3/sec. The discharge of the Uwagaon gauging station is slightly higher than Pachuwarghat and Rabuwabazaar, although the size of the basin contributing to the former is far larger. This is mainly because the streamflow contribution to the Uwagaon station is from the Tibet region, as described in the previous section also.

5.6 Hydro-meteorological trend analysis

This section describes the hydro-meteorological trend in the Kosi river basin which includes precipitation, temperature and discharge.

5.6.1 Trend analysis

To test the hypothesis of whether or not a long-term trend in time series data exists, the trend analysis is broadly divided into parametric and non-parametric. There are several methods available in both these categories which are well described in (Helsel and Hirsch 1992). The parametric method is a simple linear trend which can be computed using a linear equation and assumes that the data follows normal distribution. In this study, the non-parametric rank-based Mann-Kendall (MK) test (Mann 1945, Kendall 1975) has been chosen. The non-parametric test for trend makes no assumption about

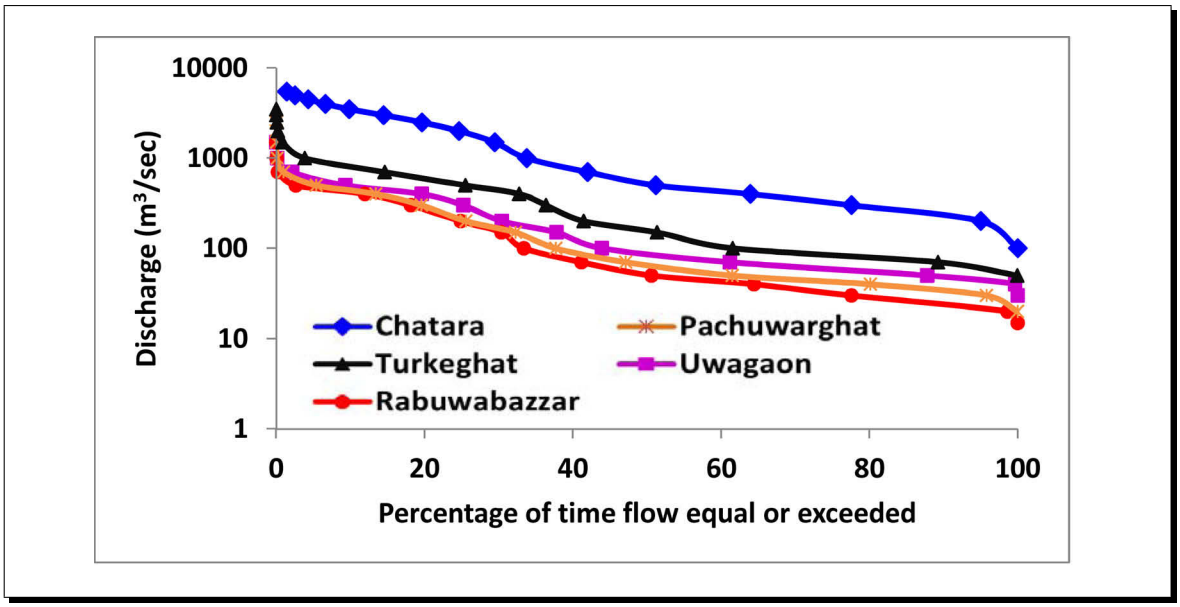

Figure 5.18: Flow duration curve of gauging stations within the Kosi river basin (1982-2006)

the distribution of the data. Therefore, distribution free test is useful for monotonic trend detection. MK test is based on sign differences rather than value, it is robust to the effect of extreme values and outliers (Helsel and Hirsch 2002). Many researchers have found the MK test as an excellent tool in similar applications (Gemmer et al. 2004, Hamed 2008, Sharma et al. 2000b).

MK test is based on the difference (xi - xj) between successive years of data for a given period. A test statistic (S) is estimated as the summation of signs:

$$S = \sum_{i=1}^{n-1} \sum_{j=i+1}^{n} sign(x_i - -x_j) \tag{5.6.1}$$

A Z value is then computed to estimate the significance level of the trend. The significance level will increase with number of identical successive signs. Three different significance levels are used to test the annual trends of precipitation, temperature and discharge. They are: α = 0.001 or 99.9 percent confidence level (***), α = 0.01 or 99 percent confidence level (**), and α = 0.05 or 95 percent confidence level (*). The significance level 0.001 means that there is a 0.1 percent probability that the values xi are from a random distribution and with that probability we make mistake when rejecting H_0 of no trend. Thus the significance level 0.001 means that the existence of a monotonic trend is very likely (Helsel and Hirsch 1992).

To estimate the true slope of an existing trend (as change per year), the non-parametric Sen's method (Sen 1968) was used. This method calculates the median of all possible pairwise slopes. This procedure is particularly useful since missing values are allowed during the analysis. The Sen's method can be used in cases where the trend can be assumed to be linear. A positive value of the Sen's slope indicates an upward trend (i.e. increasing with time), whereas a negative value indicates a downward

trend (i.e decreasing trend).

5.6.2 Precipitation trend analysis

Precipitation trend analysis was conducted using the corridor approach (i.e. applied to individual river corridors). Because the datasets are not uniform in time series, different corridors have different time span based on the available time series. The trend was measured at higher than 0.05 level of significance (95 percent confidence level). The trend of each station is carried out and plotted in Figure 5.19.

Indrawati river corridor

In this corridor, the trend analysis was conducted using data from 1973 to 2007 (35 years). None of the stations showed a statistically significant trend in precipitation. However, station 12 (Tarke Ghyang) and 10 (Dhap 1025) showed -14 and +14 mm/year time-trends respectively.

Dudh Kosi corridor

In this corridor, the trend analysis was conducted using data from 1952-2007 (56 years). None of the stations indicated a statistically significant trend. Only one station (Aisealukhark) showed a decreasing trend, while others showed an increasing trend in the range of 0 - 5 mm/year. The Sallery station has a gap of about 10 years from 1962-1974 and therefore it is not included in the long trend analysis.

Arun river corridor

In this corridor, the trend analysis was conducted using data from 1974 to 2007 (34 years). Only one station (Laguwa Ghat) indicated a significant decreasing trend with a value of -9 mm/year. The other stations indicated both increasing and decreasing trend in the range of -5 to +5 mm/year.

Tamor river corridor

In this corridor, the trend analysis was conducted using data from 1952 to 1997 (56 years). Two stations indicated a significant increasing trend. Those were: Taplethok (+12 mm/year) and Mulghat (+5 mm/year). Except for the station Dharan, every station indicated an increasing trend.

Both increasing and decreasing trends are observed in the Kosi river basin. Out of 36 stations, 24 stations showed increasing and 12 stations showed decreasing trends. However, only two stations showed an increasing and one station showed an decreasing trend which are statistically significant at 0.05 level of significance. Hence, it is observed that in the long run at the regional level, the basin does not exhibit any significant trend however, trends at a few localized stations were observed. Shrestha et al. (2000) analysed the precipitation trend in the Nepal Himalaya and found no distinct long-term trend. The study by Sharma et al. (2000a) also analysed the precipitation trend in the Kosi river basin using a parametric test and indicated the trends are of more localized in nature lacking a distinct basin-wide significance. Both the studies indicated a similar pattern of precipitation trend which is statistically insignificant.

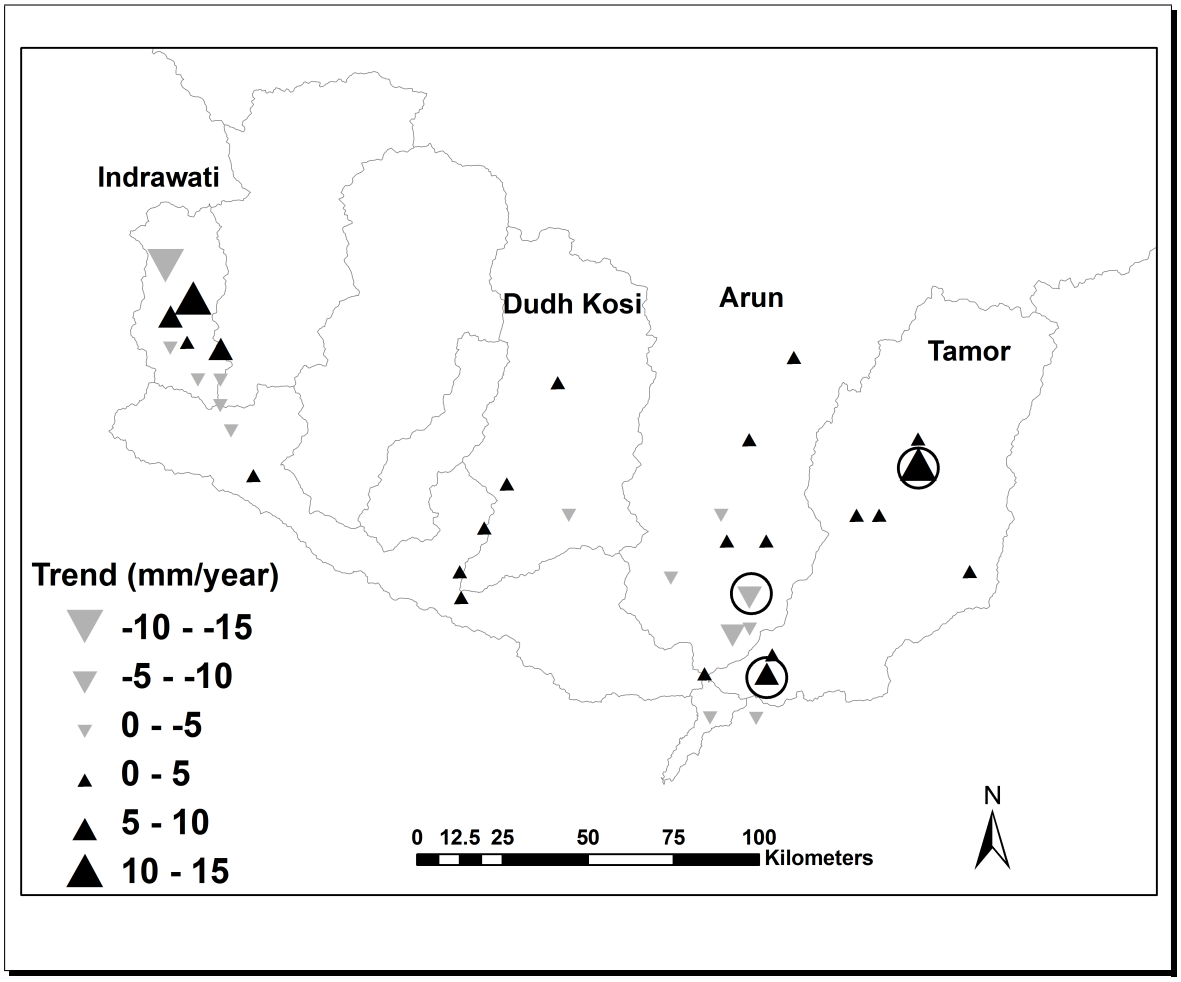

Figure 5.19: Annual precipitation trend in the Kosi river basin. The upward and downward pointing triangles indicate increasing and decreasing trends. The magnitude of the trend is proportional to the size of the triangles. The circles indicate the significance of the trends at 0.05 level of significance

5.6.3 Temperature trend analysis

Five stations are included in the temperature trend analysis from the Kosi river basin. One station from Kathmandu, the capital city of Nepal, is also included mainly because of two reasons: First this station is located just 15 km east from the basin boundary and secondly, it comprises long time series data. The other stations are not included because of missing values which are as long as 4-5 years in some cases and a very short duration of time series. The temperature stations selected for the trend analysis are provided in Figure 5.20(b).

Table 5.6 indicates that there is a high confidence in recent warming which is also statistically significant. The majority of the stations indicated a rising temperature trend (both maximum and minimum) although the magnitude of the trend is higher in the maximum temperature than in the minimum temperature. The only exception is the station Jiri which showed a decreasing trend for minimum

temperature. The two stations (Dhankuta and Taplejung) which have data for a short period of time of 20 years (starting 1987) showed a higher rate of increasing trend. This is mainly because after the 1980s, there has been monotonic rise in temperature in the area.

Table 5.6: Temperature trend in the Kosi river basin (^{o}C/year)

Station ID	Name	Elevation	Data period	SS: MT ‖ NT	Trend (^{o}C): MT ‖ NT
1103	Jiri	2003	1967 - 2009	*** ‖	+ 0.044 ‖ - 0.013
1206	Okhaldhunga	1720	1963 - 2009	*** ‖ ***	+ 0.053 ‖ + 0.023
1307	Dhankuta	1210	1987 - 2009	*** ‖ *	+ 0.219 ‖ + 0.029
1330	Kathmandu airport	1336	1968 - 2009	*** ‖ ***	+ 0.073 ‖ + 0.032
1405	Taplejung	1732	1987 - 2009	*** ‖	+ 0.077 ‖ + 0.024

Notes on variables in Table 5.6: SS : Statistically significant; MT : Maximum Temperature, NT: Minimum Temperature

Figure 5.20(a) and 5.20(b) show the trend of maximum and minimum temperature. Most of the stations indicated a monotonic rise in temperature after the 1980s. Among the three stations (Kathmandu, Jiri and Okhaldhunga) which have data of a longer time series indicated the general rise in temperature for which the level of significance is 0.001 (99.9 percent level of significance). For example, a sudden drop in temperature in the year 1997 was observed in both maximum and minimum temperature in all stations. Similar behavior was observed in the year 1971 except for the station Kathmandu in the case of minimum temperature. The temperature trend analysis carried out by Shrestha et al. (1999) suggested that the recent warming trends after the 1980s were preceded by similar widespread cooling trends. On average, the maximum temperature trend of the Kosi river basin (based on the three stations with long-term data) was 0.057^{o}C/year and the minimum is 0.014^{o}C/year.

The maximum temperature trend analysis in Nepal between 1971-1994 showed an average warming trend of 0.06^{o}C/year (Shrestha et al. 1999). The middle mountains and the Higher Himalaya were reported to be warming at the rate of 0.075 and 0.057^{o}C/year in average. Similarly, the rate of rise in temperature in the Tibetan Plateau was reported to be 0.16^{o}C/decade (Liu and Chen 2000).

The study by Sharma et al. (2000a) in the Kosi river basin indicated that the basin-wide increasing trend of average temperature was homogeneous with respect to seasons but heterogeneous with respect to sites. However, the results from this study showed higher confidence in a increasing temperature trend in the basin. This is possibly because the study by Sharma et al. (2000a) was carried out with dataset till 1993. The more recent dataset shows that there is monotonic rising temperature especially after 1980s as shown in Figure 5.20(a), which may have caused more homogeneous rising temperature trends.

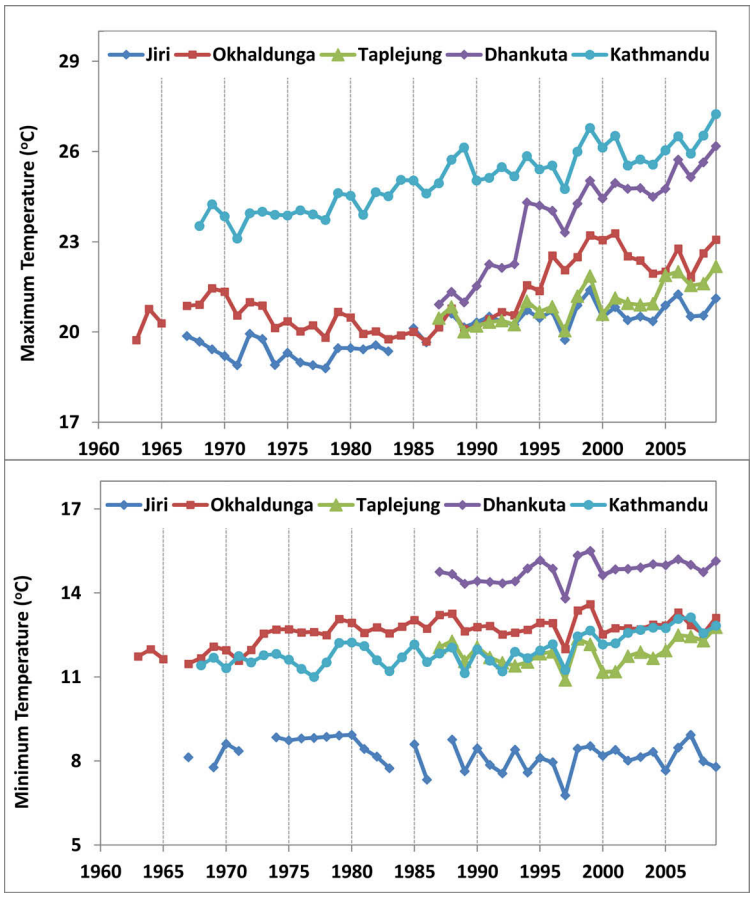

(a) Temperature trends in the Kosi river basin. (Above: maximum temperature, Below: minimum temperature

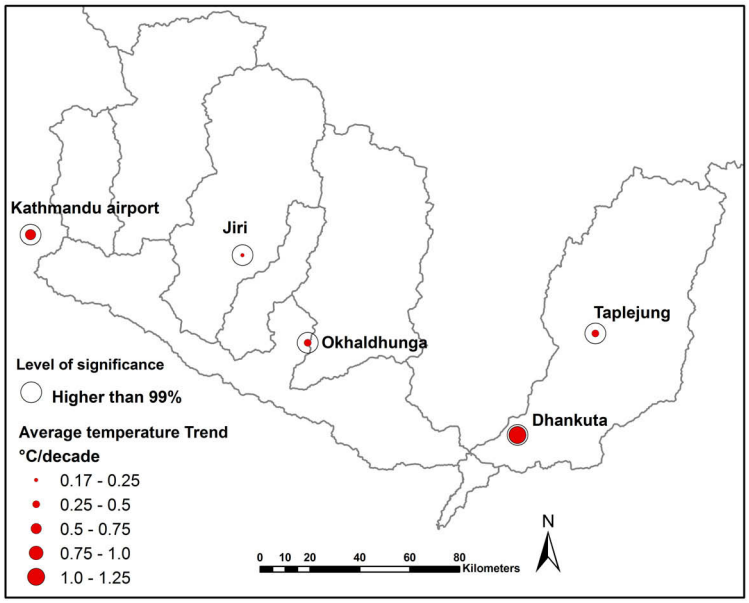

(b) Average temperature trend in the Kosi river basin. The magnitude of the trend is proportional to the size of the red circles. The open circles indicate statistically significance trend higher than 99 percent confidence level.

Figure 5.20: Temperature trend in the Kosi river basin

5.6.4 Discharge trend analysis

Altogether, there are 21 discharge stations in the Kosi river basin. However, only five stations as shown in Figure 5.21(b) are selected for the discharge trend analysis because some stations have only few years of data and in some cases, relatively long data gaps.

The trend analysis of the discharge data indicated the inter annual variability as shown in Figure 5.21(a). The rising and falling trends have similar behavior among the stations, except for some years. The most notable behavior was found during the years 1992-1995. Another decrease in 1997 is also indicated by data at most stations. A similar drop in temperature data in 1997 was also observed .

Table 5.7: Trends in the discharge data of the selected stations in the Kosi river basin (m^3/sec/year)

Station ID	Name	Elevation	Trend (m^3/sec/year)	AD (m^3/sec)	SS
1	Rabuwabazaar	460	1.8	190	
2	Pachuwarghat	602	-2.6	209	* *
3	Uwagaon	1,294	-5.3	263	* *
4	Turkeghat	414	3.0	449	*
5	Chatara	140	-6.3	1,544	

Notes on variables in Table 5.7: SS : Statistically significant; AD : Average discharge

Figure 5.21(b) and Table 5.7 summarizes the statistically significant long-term time trends of the stations data. Both increasing and decreasing trends can be observed. Only three stations showed a statistically significant trend higher than 95 percent confidence level. The Uwagaon and Turkeghat stations are located in the Arun river and the distance between them is only 40 km. However, the Uwagaon is showing a decreasing trend and Turkeghat is showing a increasing trend. This is possibly because the catchment area contributing to the Uwagaon gauging station (in the upstream area) is located in the the Tibetan part of the Kosi river basin associated with semi-arid climate and low precipitation. On contrary, Turkeghat station is located in the downstream region where additional streamflow is contributed by the area where more precipitation occurs. However, the gauging station at Chatara (which is the combination of all the tributaries) shows a statistically insignificant decreasing trend. It has to be noted that most of the discharge occurred during the monsoon season when the water level is high. The uncertainty in measuring discharge during the flood season is very high as discussed in Section 5.5.

5.7 Summary of this chapter

The following are the summary of the chapter:

1. The analysis of precipitation dynamics in the different river corridors within the Kosi river basin reiterated the fact that most of the precipitation occurs during the months of the monsoon sea-

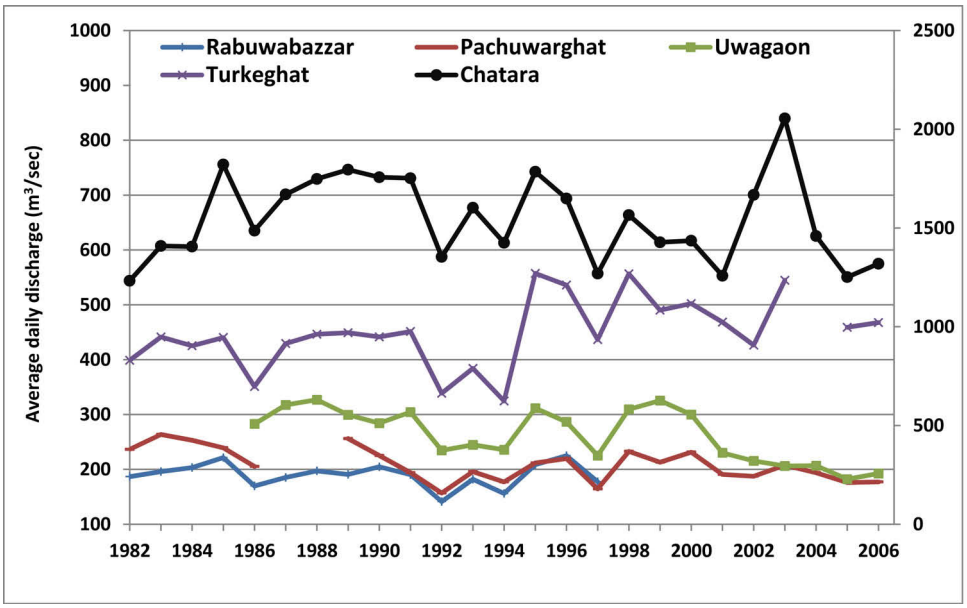

(a) Discharge trend in the selected gauging stations in the Kosi river basin (The right axis is for Chatara station)

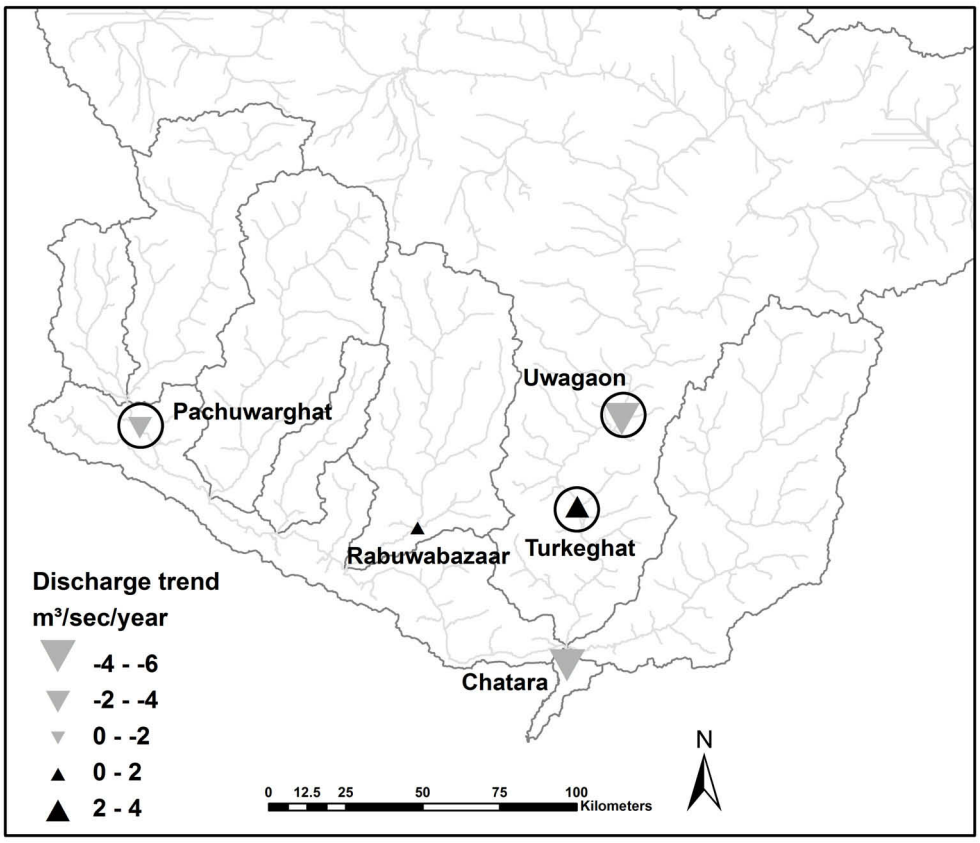

(b) Discharge trend in the selected gauging stations in the Kosi river basin. The magnitude of the trend is proportional to the size of the triangles. The open circles indicate statistically significance trend higher than 95 percent confidence level.

Figure 5.21: Trend in the discharge data of the Kosi river basin

son with an average value of 77 percent. Some stations which have higher annual precipitation (such as Num in the Arun river Corridor) also indicate that the pre-monsoon precipitation (especially during the month of May) is higher, which suggest that the convective precipitation phenomenon might be the cause of a higher amount of annual precipitation.

2. The spatial distribution of precipitation is not uniform in the mountains of the river basin. Precipitation is influenced by topography and underlying geology suggesting that different elevation zones have different rates of precipitation due to windward and leeward effects. The higher precipitation zones are the foothills of the Higher Himalaya followed by the windward side of the Middle Mountain region. The amount of precipitation is found to be increasing with elevation from the middle mountains (lesser Himalaya) up to the foot hills of the Higher Himalaya. The river valleys in general receives less precipitation. However, river valleys located to the North (towards the foothills of the Higher Himalaya) usually receive higher precipitation than others.

3. There is no regional trend in precipitation. Only three stations showed statistically significant trend in precipitation suggesting a localized trend, if any.

4. There is higher confidence in increasing temperature trend in the river basin. Both increasing trends for maximum temperature (0.057^{o}C/year) and minimum temperature (0.014^{o}C/year) have been observed suggesting the higher magnitude of the former. The results are based on the three temperature stations which have relatively data available for last 40-50 years.

5. Both increasing and decreasing trends in streamflow have been observed, suggesting a localized trend, if any. However, the trend of the gauging station Chatara (after merging all tributaries) showed a decreasing trend.

6 Hydrological modelling

This Chapter addresses the third study objective and describes the results of the hydrological modelling of the two sub-basins **(Dudh Kosi and Tamor)** of the Kosi river basin using the J2000 hydrological model. The calibrated parameters of the Dudh Kosi river basin are transferred to the Tamor river basin (proxy-basin test) to understand the robustness of the model parameters to represent the hydrological conditions of these two monsoon dominated Himalayas river systems. In addition, results from the hydrological system analysis and water balance of the river basins will also be discussed. The model, after successful calibration and validation, has been considered as an important tool to assess the upstream-downstream linkages (land-use and climate change) in the later sections.

6.1 The J2000 modelling system

To address the issues of upstream-downstream linkages, the J2000 hydrological model (Krause 2001, 2002) was used in this study. The J2000 is a distributed, process oriented hydrological model for hydrological simulation of meso- and macro-scale catchment (Krause 2001). It is implemented in the Jena Adaptable Modelling System (JAMS) framework (Kralisch and Krause 2006, Kralisch et al. 2007) which is a software framework for component based development and application of environmental models. The model describes the hydrological processes as encapsulated process modules. The JAMS is a modular structured environmental modelling framework which has been developed to meet current challenges in sustainable management of water resources. JAMS can simulate environmental processes at discrete points in time and/or space. This approach is widely-used by many distributed hydrological models which are applied in current practice (Kralisch et al. 2007).

Modular model framework systems provide an object-oriented model development environment for the researcher and a user-friendly runtime environment for the practitioner and IWRM researcher. The traditional modelling systems use monolithic[1] software packages which do not provide sufficient flexibility for component exchanges, but instead encapsulate their know-how within the model's code, making it unusable for other model developments. A modular approach overcomes this methodological shortcomings and permits the assembly of different process modules into an adaptable model, hence accounting for individual data availability and process know-how (Flügel 2009). Due to its flexibility and adaptability, the JAMS framework has been used to build different models: that is the process-oriented hydrological model **J2000**, the simplified water balance model **J2000g**, and the distributed, process-oriented nutrient-transport model **J2000s**, which includes modules for the simulation of land-use management (Krause 2001, Krause et al. 2006, Bende-Michl et al. 2006, Fink et al. 2007).

[1] unstructured system which is difficult to distinguish in different parts

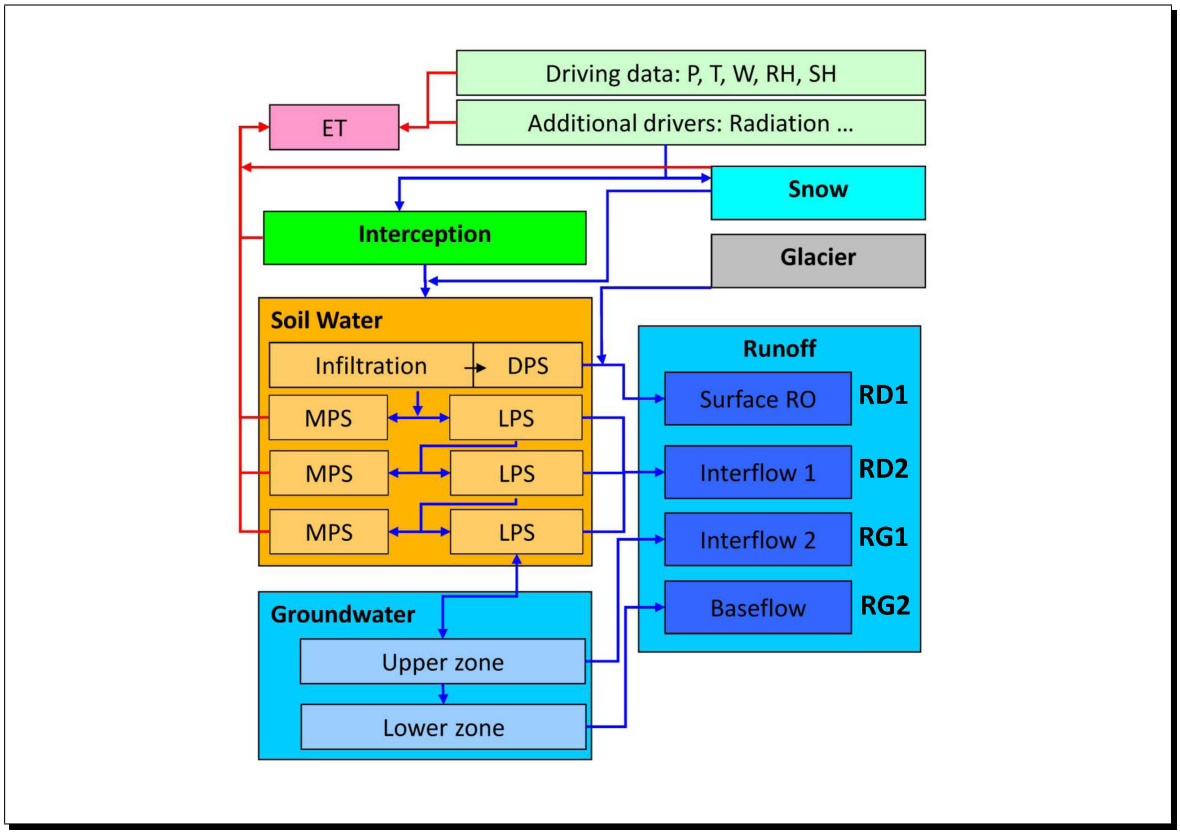

Figure 6.1: Principal layout of the J2000 model concept. Source: adapted from Krause et al. (2009)

The J2000 model produces four different runoff components according to their specific origin (Krause 2001). The principal configuration of these model components is shown in Figure 6.1 shown in Figure 6.1. The component with the highest temporal dynamics is the fast direct runoff (**RD1**). It consists of runoff from sealed areas, saturation or infiltration access runoff and snow and ice melt from glacier areas which drain directly to a stream. The slow direct runoff (**RD2**), (also known as Interflow 1) which can be regarded as similar to the lateral subsurface flow within the soil zone, reacts slightly more slowly. Two further base flow runoff components can be distinguished. The relatively 'fast' baseflow-runoff component (**RG1**), (also known as Interflow 2) simulates the runoff from the upper part of an aquifer, which is more permeable due to weathering, compared to the lower zone of the aquifer. The slow baseflow runoff component (**RG2**), which can be seen as flow within fractures of solid rocks or matrix flow in homogeneous loose rock aquifers.

A glacier module is integrated into the modeling system to understand the glacier melt runoff in the basin. The glacier module calculates melt water from snow and ice. The ice melt is calculated using an enhanced degree day factor (Hock 1999) and has been further modified by taking into consideration the radiation, slope aspect and debris covered factors. It is important that the process of glacier melt (snow and ice) are included in the modelling for this study. Many process models do not achieve this aspect to an acceptable degree to reflect the specific characteristics of the Himalayan region.

6.2 Modules within the J2000 modelling system

The J2000 is a modular process-oriented hydrological system, which implements single hydrological processes as encapsulated process modules. Different modules can be used depending upon the availability of the data for the simulation of runoff generations and upon the objectives of the modeling application. In this study, the following modules were used:

- Distribution of precipitation
- Interception module
- Snow module
- Glacier module
- Soil module
- Groundwater module
- Routing module

The important processes within the modules are described below in the respective section of the module.

6.2.1 Distribution of precipitation

In the J2000 modelling system, the precipitation is first distributed between rain and snow depending upon the air temperature. In order to determine the amount snow and rain, it is assumed that coming below a certain threshold temperatures results in total snow precipitation and exceeding a second threshold results in total rainfall as precipitation. In the range between those threshold temperatures, mixed precipitation occurs. Two calibration parameters (*Trans*, and *Trs*) are used where *Trs* is base temperature and Trans is a temperature range (upper and lower boundary) above and below the base temperature. Between those thresholds, rain-snow mixtures with variable percentages for each component are calculated. The acutal amount of snow (P(s)) of daily precipitation subject to air temperature is calculated according to:

$$P_s = \frac{Trs + Trans - Temperature}{2 \cdot Trs} \tag{6.2.1}$$

The daily amount of snow (P_s) or amount of rain (P_r) is calculated according to :

$$P_s = Precipitation \cdot P_s \quad [mm] \tag{6.2.2}$$

$$P_r = Precipitation \cdot (1 - P_s) \quad [mm] \tag{6.2.3}$$

6.2.2 Interception module

Interception is a process during which the precipitation is stored in leaves, and other open surfaces of vegetation. During precipitation, interception by crop canopy and residue layer occurs. This process is identified as important components of a hydrological cycle that can affect the water balance components. Canopy and residue interception are considered losses to the system, as any rainfall intercepted by either of these components will subsequently be evaporated (Kozak et al. 2007).

The interception module in the J2000 modelling system serves the calculation of the net precipitation from the observed precipitation against the particular vegetation covers and its development in the annual cycle. The observed precipitation is reduced by the interception part to calculate the net precipitation. Thus net precipitation only occurs when the maximum interception storage capacity of the vegetation is reached. The surplus is then passed on as throughfall precipitation to the next module. The interception module uses a simple storage approach according to Dickinson (1984), which calculates a maximum interception storage capacity based on the Leaf Area Index (*LAI*) of the particular type of land cover. The emptying of the interception storage is done exclusively by evaporation. The maximum interception capacity (Int_{max}) is calculated according to the following formula:

$$Int_{max} = \alpha \cdot LAI \quad [mm] \tag{6.2.4}$$

The parameter α has a different value, depending on the type of the intercepted precipitation (rain or snow), because the maximum interception capacity of snow is noticeably higher than of liquid precipitation. The *LAI* for individual vegetation types is provided in the land-use parameter file throughout the year. Because the *LAI* changes according to the seasons, four different *LAI* types for four different seasons for each vegetation type are proposed in land-use parameter file. The value of LAI for the study area is determined by literature (MoFSC 2002), expert knowledge, and field visit.

6.2.3 Snow module

The snow module calculates the different phases of snow accumulation, metamorphosis and snowmelt. The more complex module is adapted in the model from Knauf (1980). The snow module takes into account the changes of state of snow pack during its existence, especially changes of snow density due to melting and subsidence. This process is important because snow pack can store free water, like a sponge, until reaching a certain threshold density and only then a sudden discharge of water occurs. For the model different water capacities of the snow pack are considered: the actual snow water equivalent (SWE_{dry}) which corresponds to the amount of water which has actually frozen and the total snow water equivalent (SWE_{tot}) which in addition considers liquid water stored in the snow pack. The subsidence of the snow pack, which results from the liquid water through the snowmelt to the surface or from precipitation as rainfall, is calculated according to the empirical subsidence (snow-compaction scheme) by Bertle (1966).

The snow pack and its conditions are described in the modell according to the following parameters: snow depth *(SD)*[in mm], dry snow density *(dryDens)* [in g/cm^3] as the quotient from total water

content and snow depth.

If there is minimum, mean or maximum air temperature for a certain time (daily data for this study period), the module calculates separate accumulation or melt temperatures. In this way, accumulation and melting can occur within a time step. The accumulation and melt temperatures can be calculated according to:

$$T_{acc} = \frac{T_{min} + T_{avg}}{2} \quad [^oC] \tag{6.2.5}$$

$$T_{melt} = \frac{T_{max} + T_{avg}}{2} \quad [^oC] \tag{6.2.6}$$

Accumulation phase:

The snow module simulates accumulation and compaction of the snow pack caused by snowmelt or rain on snow precipitation.

The thermal circumstances under the snow cover are taken into account with the cold content in the snow cover in connection with the snowmelt. At the temperature below the freezing point, the snow pack cools down significantly. Because melted water freezes immediately due to negative isothermal circumstances under the snow cover, no runoff occurs. The cold content needs to reach the value zero so that the process of snowmelt begins again. Consequently, negative temperatures raise the cold content whereas the positive temperature reduces it. The calculation of storage of cold content results from the product of air temperature by a calibration parameter (*coldContFact*).

$$CC = coldContFact \cdot T \quad [mm] \tag{6.2.7}$$

In doing so, negative air temperatures are accumulated and decreased only by positive temperature and resulting potential rates of melting. Only when the cold content has reached a value of 0, snowmelt occurs.

Snow accumulation occurs in the model if precipitation falls in solid form (*newSnow* > 0). Therefore the density of new snow is determined subject to air temperature. The calculation is carried out according to Kuchment et al. (1983) and Vehvilaeinen (1992), if the air temperature is higher than -15 ^{o}C.

$$newSnowDens = 0.13 + 0.0135 \cdot T_{acc} + 0.000045 \cdot T_{acc}^2 \quad [g/cm^3] \tag{6.2.8}$$

If the air temperature is below -15 ^{o} C, the density of the new snow is assumed to be 0.02875.

The **change of snow depth** (δ SD) resulting from snow precipitation is calculated according to :

$$deltaSD = \frac{netSnow}{newSnowDens} \quad [mm] \tag{6.2.9}$$

The snow water equivalent of the previous day (*SWEdry*) increases by the value of snow precipitation according to:

$$SWEdry_t = SWEdry_{t-1} + netSnow \quad [mm] \tag{6.2.10}$$

The dry snow water equivalent and the total snow water equivalent are increased by the same value. If the precipitation event involved mixed (rain/snow) precipitation, the rain amount is allocated to the total snow water equivalent.

If rain is part of the precipitation event, it results in subsidence of the snow pack. The calculation of the subsidence amount is discussed below. In the model, the snow pack remains in the accumulation phase until the temperature value (T_{melt}) for the snowmelt exceeds a threshold value (*(baseTemp)* which has to be determined during the parameterisation phase of the modeling application. Then it enters the metamorphosis phase which simulates melting and subsidence processes. However, it can go back to the accumulation phase if temperatures are correspondingly low. Due to different temperature values, accumulation and melting processes can be modeled during one time step.

Melting and subsidence phase:

If the melt temperature value (T_{melt}) exceeds the temperature limit value (*baseTemp*), the snow pack goes from the accumulation phase to the metamorphosis. The amount of energy which is required for snowmelt is available in three different ways. First, by input of sensible heat by air temperature (*t_factor*), second, by energy input from precipitation as rain (*r_factor*) and third, by input due to soil heat flow (*g_factor*). The sum of all energy inputs gives the potential snowmelt rate (Mp). The calculation of Mp is carried out according to:

$$Mp = t\_factor \cdot T_{melt} + r\_factor \cdot netRain \cdot T_{melt} + g\_factor \quad [mm] \tag{6.2.11}$$

The variable Mp is then also modified according to the slope and the exposition of the spatial model entity:

$$Mp = \ Mp \cdot actSlAsCf \quad [mm] \tag{6.2.12}$$

Mp is initially used to balance out the cold content of the snow cover and is then also used to generate snowmelt. The potential snowmelt rate then is taken to calculate the resulting maximum change of snow depth (δ SD):

$$\delta SD = \frac{M_P}{dryDens} \quad [mm] \tag{6.2.13}$$

If δ SD is greater than the entire snow depth, it defrosts completely and the entire snow water equivalent contributes to runoff generation in the form of snowmelt. If this is not the case, the snow depth is

reduced correspondingly, which does not change the snow water equivalent at first. Rather the result is an increase in the total density of the snow cover.

In addition to this change in density, additional changes in subsidence and density according to the **snow compaction-scheme** (Bertle 1966) are taken into account. This method is based on the fact that water, no matter whether it results from temperature-induced snowmelt or from precipitation, seeps into the snow pack which leads to subsidence by recrystallization of snow and by structural changes and concentration in the storage (Knauf 1980). The resulting subsidence rate is calculated using the snow-subsidence method described in Bertle (1966). This method is based on the observation of an empirical relation between inflowing free water and the resulting change in elevation by subsidence which was derived from laboratory experiments of the US Bureau of Reclamation. For the calculation the increase of accumulated water content in percentage is seen in relation to the snow water equivalent using this formula:

$$P_w = \frac{totSWE}{drySWE} \cdot 100 \ \ [\%] \tag{6.2.14}$$

This equation shows that the more liquid water there is as input, the greater is the snow pack subsidence (P_w) (Knauf 1980). An input of the exact the amount of water corresponding to the snow water equivalent of the snow pack leads to halving the snow depth by subsidence. The percentage of snow depth change (P_H) is calculated subject to the input of free water:

$$P_H = 147.4 - 0.474 \cdot P_W \ \ [\%] \tag{6.2.15}$$

The new snow depth (*SD*) is:

$$SD = SD \cdot \frac{P_H}{100} \ \ [mm] \tag{6.2.16}$$

Together with the snow depth which has been calculated the total density *(totDens)* and the dry snow density *(dryDens)* are calculated according to the following formulas:

$$dryDens = \frac{SWE_{dry}}{SH} \ \ [g/cm^3] \tag{6.2.17}$$

$$totDens = \frac{SWE_{tot}}{SH} \ \ [g/cm^3] \tag{6.2.18}$$

Melt runoff

The snow pack can store liquid water in its pores up to a certain critical density (*snowCritDens*). This storage capacity is lost nearly completely and irreversibly when a certain amount of liquid water in relation to the total SWE (between 40 and 45 percent) is reached according to (Bertle 1966, Herrmann 1976, Lang 2005). In this threshold limit, the retention capacity of a naturally developing snow pack is also suddenly decreased without rain impact. In such a case, a sudden water release from the

snow pack can be observed (Herrmann 1976). In the model, this process is simulated by using the calculation of a maximum water content of the snow pack (SWE_max) according to :

$$WS_{max} = snowCritDens \cdot SD \quad [mm] \tag{6.2.19}$$

The critical density (*snowCritDens*) needs to be provided by the model user. The water stored in the snow pack which exceeds this limit is conveyed as runoff.

$$Q_{snow} = SWE_{tot} - SWE_{max} \quad [mm] \tag{6.2.20}$$

In the following time steps, the density of the snow pack keeps the critical threshold density until it is either defrosted or starts the accumulation due to recurring snowfall.

6.2.4 Glacier module

The glacier module is integrated into the standard J2000 hydrological model, as a part of this study. The glacier module is treated as a separate module within J2000 in which snow- and ice- melt (SIM) runoff is estimated and the output is directly provided to a stream as overland flow (RD1). The approach suggested by Hock (1999) is implemented in the J2000 model and further adapted for ice-melt estimation. This approach considers ice melt by using a day-degree-factor. From this study, slope, aspect and debris-covered factors are further included in the model for ice-melt runoff. The melting of snow in the glacier area is calculated in the same way as described earlier. The same soil heat flux (calibration parameter: g_factor) is proposed for the snowmelt in glacier areas as most of the glaciers are debris-covered and behave similar to soil.

The glacier area is provided as a GIS layer which provides a unique land-use ID for glaciers during HRU delineation. All the processes which occur in the glacier are separately treated based on the unique ID. First the seasonal snow occurs on top of the glacier (or glacier HRU). The model first treats the snow as described earlier and produces snow runoff. In order to make sure that ice melt occurs, two conditions have to be met. First, the entire snow cover of a glacier HRU has to be melted (i.e.storage is zero), and second, the base temperature *(tbase)*, as defined by users, has to be less than *meltTemp*. Only under these circumstances, does the ice melt occur as a model process.

$$meltTemp = \frac{Tmax + Tmean}{2} \quad [^oC] \tag{6.2.21}$$

The melt rate (iceMelt) (mm/day) is obtained by the following equation:

$$iceMelt = \frac{1}{n} \cdot meltFactorIce + alphaIce \cdot radiation \cdot (meltTemp - tbase) \quad [mm] \tag{6.2.22}$$

where:

radiation = actual global radiation

meltFactIce = generalized melt factor for ice as a calibration parameter

alphaIce = melt coefficient for ice

n = time step (i.e. for daily model, n=1)

The ice melt is further adapted by the debris cover factor. Because the glaciers in the study area are in general debris cover, a simple segregation method is applied to identify debris-covered glaciers based on slope. If the slope is higher than 30 degrees, the gravels, stones and pebbles are rolled down and the glacier is regarded as a clean glacier. The slope lower than this threshold is suitable for the accumulation of debris on top of glaciers. By using this approach, about 77 percent of the glaciers are estimated as debris-covered glaciers. According to Mool et al. (2001b), about 70 percent of the glaciers in the Dudh Kosi river basin are valley types. One of the most common characteristics of glaciers located in the Himalayan region is the presence of debris material. In general, valley glaciers are debris-covered in the Himalayan region (Fujji and Higuchu 1977, Sakai et al. 2000). It can be assumed that the debris-covered glacier areas estimated by this approach are fairly representative and adequate for purposes of this modelling application.

The presence of debris affects the ablation process. Supra-glacial debris cover, with thickness exceeding a few centimeters, leads to considerable reduction in melt rates (Oestrem 1959, Mattson et al. 1993). According to Oestrem (1959) the melt rate decreased when the thickness of the debris cover was more than about 0.5 cm thick. The report further mentioned that not only the melting will be slower under the moraine cover, but also the ablation period will be shorter for the covered ice. The clean glaciers as reported on the Tibetan Plateau have higher retreat rates. Kayastha et al. (2000) studied the ice-melt pattern in the Khumbu glaciers (Dudh Kosi river basin where the J2000 model is being applied) and found that the debris ranging thickness from 0 to 5 cm indicates that ice ablation is enhanced by a maximum at 0.3 cm. Therefore, when a glacier is covered by debris, the ice melt is reduced. Using the calibration parameter, the effects of debris cover on melt is controlled as follows.

$$iceMelt' = icemelt - \left(icemelt \cdot \frac{debrisFactor}{10} \right) \tag{6.2.23}$$

The melt from glaciers, which is the product of snowmelt, ice melt and rain on top of glaciers, is considered as glacier runoff. The glacier runoff directly contributes to streamflow and is regarded as a overland flow (RD1) component. However, for the long-term estimation of glacier runoff in the context of climate change, the module is less suitable because it does not account for the changing spatial extent of glacier areas.

Routing of glacier melt is made separately for snowmelt, ice melt and rain runoff using the following formula:

$$Snow_{runoff} = meltRes_{t-1} \cdot e^{-} \left(\frac{1}{kSnow} \right) \cdot Snow_{melt} \cdot e^{-} \left(\frac{1}{kSnow} \right) \tag{6.2.24}$$

where:

snow_{melt} = total snowmelt during the time step (mm/day)

meltRes_{t-1} = outflow of reservoir during the last time step

kSnow = storage coefficient (recession constant) for reservoir

A similar routing procedure is applied for ice melt and rain runoff with a different recession constant (*kIce* and *kRain*). It is assumed that the routing of rain runoff is faster than that of ice and snow.

In reality, snow is stored in the accumulation zone of high-altitude areas. The snow is transported to low-altitude by wind, avalanches and gravity. As snow gets buried under new snow, it is gradually converted into firn and eventually into glacier ice. This ice flows by gravity downstream towards the ablation zone as glaciers (Jansson et al. 2003). However, such dynamic processes of snow transformation and transportation are not included in the glacier module of the J2000 model. Therefore, some part of the precipitation is always stored as snow in the accumulation zone of high-altitude areas. To compensate for this long-term storage process, a constant glacier layer is used as a surrogate which provides melting from glacier ice.

6.2.5 Soil module

The central and most complex part of the J2000 model is its soil module, which controls the regulation and distribution of water movement and interacts with most of the other modules, except the glacier module. The Figure 6.2 indicates the important process within the soil module. The abstraction of the soil water is accomplished by two parallel and connected storages MPS and LPS (Figure 6.2). The input for the soil module comes from snowmelt and rain through infiltration. The infiltrated water is distributed to both soil storage components (MPS and LPS). Any surplus water, if it exceeds the maximum infiltration capacity of the corresponding soil or saturation of the LPS, is stored as depression storage. Emptying the depression storage component is done through evaporation, and the generation of overland flow and/or seepage at a later point in time. Emptying the MPS is done by evapotranspiration whereas the LPS is emptied by generating interflow and recharging groundwater. In addition, at the end of any given time step a certain amount of water stored in the LPS can be transferred to the MPS. The MPS can receive water, in addition to infiltration, from the saturated zone due to capillary rise. These processes are explained in detail below.

Infiltration

The first process which contains the water from snowmelt and net precipitation is infiltration. The infiltration capacity is an important process which determines whether water can seep downward in the soil horizon entirely or whether it is stored for a short time at the surface; and whether it generates depression storage at this location or results in surface runoff. The infiltration capacity is calculated using a simplified method which is suitable for a daily time interval (as used in this model's application). First, it is based on the assumption that infiltration capacity is subject to water saturation of the soil. Two values are proposed for the summer months and for the rest of the time period. The threshold value for the summer period takes into account thundershowers (or convective precipitation)

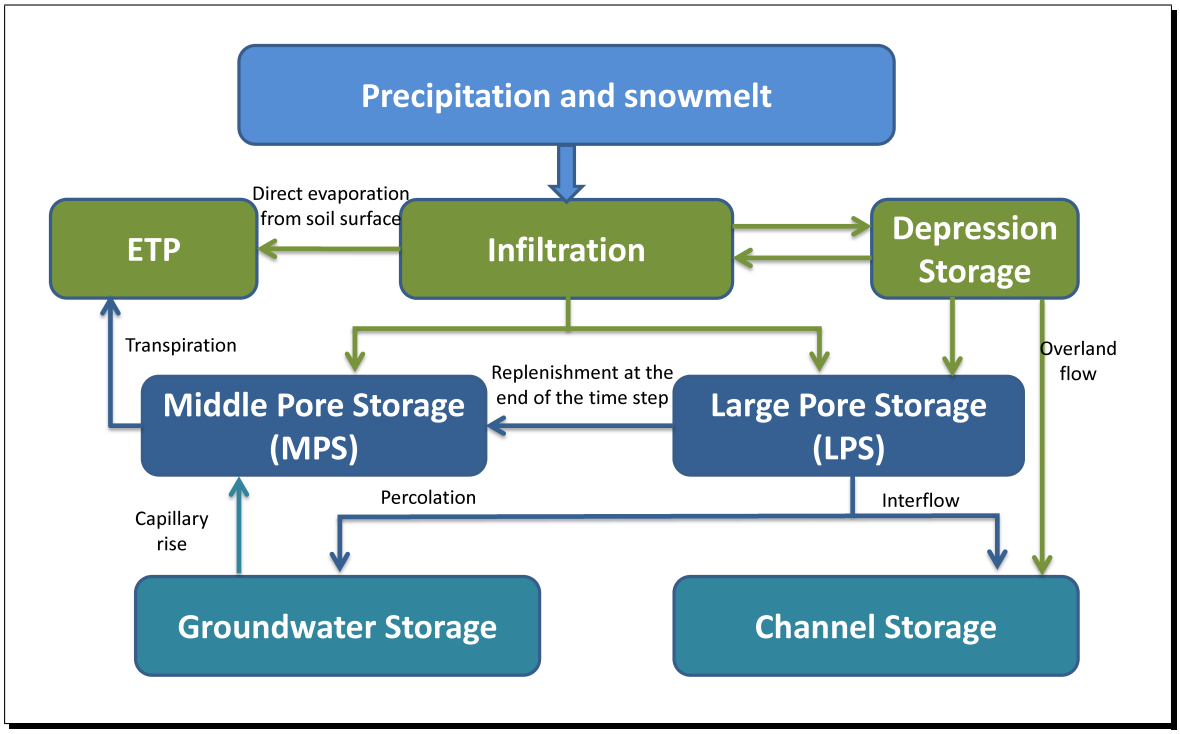

Figure 6.2: Principal layout of the J2000 soil module. Source: (Krause 2002)

with high intensities within a short period of time which occurs mainly during summer months. The monsoon season is provided by conditions during the months of July to September. Although the monsoon period extends from June, the month of June is excluded for summer infiltration period. It is because the monsoon starts generally from the middle of the June, and any initial precipitation is used to fill the MPS and LPS storages. The second threshold value is applied for October to June period when there is low intensity of rainfall. Secondly, a maximum infiltration rate for snowmelt is applied. Using this value, the reduced infiltration capacity of the soil with a partly or completely frozen surface is considered. This value can be used to take into consideration the runoff of melt and precipitation water within the snow cover. Therefore three threshold values have to be determined by the user (*soilMaxInfSummer, soilMaxInfWinter, soilMaxInfSnow* referred below as $soilMaxInf_1, 2, 3$ respectively). These values are weighted in the model with the relative saturation deficit of the soil δ_{sat}

$$Inf_{max} = soilMaxInf_{1,2,3} \cdot (1 - satSoil) \ \ [mm/d] \tag{6.2.25}$$

The relative water saturation of the soil can be calculated using the following equation:

$$soilSat = \frac{actMPS + actLPS}{maxMPS + maxLPS} \ \ [mm/d] \tag{6.2.26}$$

The amount of water which exceeds the maximum infiltration rate is transferred to the depression

storage and remains there. The actual infiltration (Inf$_act$) is distributed between the MPS and LPS storages. The amount of water which is in every soil storage is subject to the saturation deficit of the MPS and is calculated using the calibration parameter *soilDistMPSLPS* as follows:

$$MPS_{in} = Inf_{act} \cdot \frac{1 \cdot soilDistMPSLPS}{satMPS} \ [mm] \tag{6.2.27}$$

The LPS receives the remaining water according to:

$$LPS_{in} = Inf_{act} - MPS_{in} \ [mm] \tag{6.2.28}$$

Due to the water distribution according to these equations used in the model, the MPSs operate similar to a sponge and its potentiality for taking water increases with decreasing moisture condition. However, a certain amount always remains in the MPS storage. The weighted distribution has the advantage that even in dry soils, especially during the summer months, part of the infiltrated water can runoff relatively quickly.

Other special cases of infiltration occur in sealed areas where only a certain amount of water on the surface seeps into the ground subject to the degree of sealing (e.g. 25 percent with degree of sealing > 80 percent and 60 percent with degree of sealing < 80 percent according to Wessolek (1993)). The remaining part contributes to the total runoff in the form of surface runoff. This is considered in the model by using the corresponding coefficient (*soilImpGT80 and soilImpLT80*) which has to be adjusted by the user. As there are no sealed areas (similar to urbanization) in the study area, only the *soilImplT80* has been used in the case of bare land.

Depression storage

As was mentioned earlier, the water amount which exceeds the maximum infiltration rate and saturation excess flow is transferred to depression storage. Part of the depression storage thereby is used to produce surface runoff. The maximum depression storage (in mm per m^2) has to be defined during model parameterisation. As the depression storage is only important in lower slope areas, the maximum depression storage is weighted using the slope of the specific area. As indicated by Maniak (1997), the maximum depression storage decreases by 50 percent in slope higher than 5 degrees, the volume of the depression storage is halved for areas exceeding this slope. If the maximum limit of depression storage is reached for an area, the surplus water is released as surface runoff.

Middle Pore Storage (MPS)

The water stored in the MPS of the soil is held against gravity due to adsorption powers. An active soil water suction is required to extract water from the MPS. The potential for such soil water suction is made available by the process of evapotranspiration. Two different cases have to be defined: 1) the direct evaporation from the soil surface and 2) the evaporation caused by the transpiration by the vegetation cover. The direct evaporation of the soil surface is comparably low because only a few mm of dry soil can cause an effective isolation of the underlying layers for evaporation. The vegetation roots consume the water stored in the MPS through transpiration. With increasing dehydration of the

soil, the actual evaporation decreases significantly over time in relation to potential evaporation.

For simulating this reduction, an established linear approach by (Gurtz et al. 1999, Schulla 1997, Uhlenbrook 1999) is used in the model. In this approach, it is assumed that the real evaporation is equal to potential evaporation until a specific water saturation limit is achieved. When the value goes below this water saturation level, the real evaporation decreases consistently in relation to potential evaporation until it is zero representing the permanent wilting point (= complete emptying of nFK). As threshold value *(siolLinRed)* for this specific water saturation values between 0.8 to 0.6 are reported in the technical literature (Gurtz et al. 1999, Menzel 1996). This threshold value and the actual water saturation of the MPS *(satMPS)* is used in the model to calculate a reduction factor *(RF)*:

$$\text{RF = 1 for satMPS} \geq \text{soilLinRed}$$

$$RF = \frac{satMPS}{soilLinRed} \tag{6.2.29}$$

Large Pore Storage (LPS)

The water which is available in the LPS component of the J2000 model is subject to gravitation and is therefore considered as the source of actual flow processes and runoff generation in the soil. This storage is filled by an infiltration process and any remaining amount of water is added after subtracting the inflow to the MPS.

The special runoff behavior of different soils is reflected very well by the pore volumes which have been described earlier. Clay soil has a relatively large proportion of fine and middle-sized pores, whereas sandy soil has a comparably greater amount of large pores. The generation of lateral and vertical runoff and the amount of precipitation is correspondingly different. Under the same conditions (e.g. vegetation cover, slope, etc), the water which is stored in rather clayey soil contributes less to lateral and vertical runoff than by sandy soil. In contrast, the water amount available for evaporation is significantly greater in clay soils than in sandy soils. Clayey or silty soil has the largest potential water storage capacities because it has the highest amount of middle pores.

The water amount which generates runoff from the LPS in the time interval is subject to the relative water saturation of the entire soil zone (LPS_{soil}) and is calculated according to:

$$Q_{LPS} = {Sat^{\alpha}}_{soil} \cdot LPS_{act} \ \ [mm] \tag{6.2.30}$$

where: Q_{LPS} : Outflow from LPS

LPS_{act} : Actual storage amount of the LPS (mm)

Sat_{soil} : Relative water saturation of the soil at location (percent).

α : calibration coefficient

The advantage of this non-linear outflow function in the model is that much less water runs off during low humidity area than if it was a linear-outflow function. The common behavior of catchment

areas which generate much more and faster runoff when there is high soil moisture (Baumgartner and Liebscher 1990, Dyck and Peschke 1995) than when there is low soil moisture (assuming the same precipitation amount) can be better displayed using an outfall function.

The gravitational water flowing out from the LPS (Q_{LPS}) is distributed among three different storages. A certain amount goes to the MPS and is stored there for a longer period of time. A second part percolates into the groundwater storage (vertical component) and the remaining amount provides a source for interflow (lateral component). The size of the components is subject to soil-physical parameters (especially kf values) Therefore, it is assumed in the model that the slope area generates much interflow, whereas in flat areas percolation into the groundwater is the primary source. The amount which goes from large pores into middle pores is, however, subject to the degree of saturation in the MPS. In order to determine the runoff amounts, the slope and the two kf values have to be specified for each HRU. This includes: the kf value of the soil horizon with the lowest permeability and the kf value of the overlying horizon.

Diffusion

At the end of the time step, a deficit of the MPS resulting from evaporation can be balanced out by water from the LPS. The diffusion *(diff)* component is estimated in the model using the calibration coefficient *soilDiffMPSLPS* according to:

$$diff = actLPS \cdot (1 - e\frac{-1 \cdot diff}{satMPS}) \ [mm] \tag{6.2.31}$$

Percolation and interflow generation

The vertical (percolation) and lateral (interflow) water movement occurs in the LPS and is therefore dependent on the amount of the large pores. At first, the runoff from the LPS (LPS_{out}) is calculated which is later divided into the two mention runoff components. It is calculated against the relative saturation of the soil (Sat_{soil}), the actual storage amount in LPS (LPS_{act}) and a calibration parameter *soilOutLPS* and described in Equation 6.2.30.

The following Q_{LPS} is distributed between vertical and laterflow (interflow). First the $slope_{weight}$ is calculated using slope and a user specific calibration factor (*LatVertDist*).

$$slope_{weight} = (1 - tan(slope \cdot \frac{\pi}{180})) \cdot soilLatVertDist \tag{6.2.32}$$

with:

α : slope of the corresponding HRU (degree)

soilLatVertDist : calibration coefficient

Using this equation, the relation between vertical and lateral runoff is determined. The water amount which is available for percolation is calculated in the model according to:

$$Percolation = (1 - slope_{weight}) \cdot LPS_{out} \tag{6.2.33}$$

This percolation rate is then set against the calibration coefficient *(soilMaxPerc)* which describes the maximum percolation rate (*soilMaxPerc*) per time step.

The interflow 1 (RD2) is calculated according to:

$$Interflow = slope_{weight} \cdot LPS_{out} \tag{6.2.34}$$

Runoff detention

Both runoff components, direct runoff (RD1) and Interflow (RD2) are delayed in time in order to take into account the areal expansion of the spatial model entity. The detention occurs in the model by using the corresponding retention coefficient *(soilConRD1, soilConcRD2)*. The detention is calculated according to:

$$RD1 = \frac{1}{soilConcRD1} \cdot RD1gen \ \ [mm] \tag{6.2.35}$$

$$RD2 = \frac{1}{soilConcRD2} \cdot RD2gen \ \ [mm] \tag{6.2.36}$$

However, in the case of RD1, the delayed time may be different during high-flow periods due to non-linear behavior of a catchment. Beven (2001a) highlighted that the non-linear responses primarily exist due to two causes. The first reason is the antecedent condition when the relationship between rainfall and runoff is generally considered to be nonlinear because the wetter the catchment prior to a unit input of rainfall, the greater the runoff that will be generated. Second, a non-linearity exists also due to change of velocity with discharge. Average flow velocities increase with the flow with both surface and subsurface flow processes. Faster flow velocities mean that the runoff will reach a measurement point in the stream-channel flow system more quickly. In case of high precipitation events (such as during the monsoon season in the study area) which are responsible for high flood peaks, a high degree of non-linearity is noted. During those events, the soil becomes saturated by the initial rainfall events and a higher rainfall-runoff coefficient is likely after some periods of rainfall. These typical conditions have been taken into account by introducing a new parameter into the J2000 modelling system. The new parameter *(concRD1Flood)* is used by the model when the $RD1_{gen}$ crosses a threshold value (*RD1FloodThreshold*) provided by a user. The value of *concRD1Flood* should be lower than concRD1 because it produces higher RD1 output flow.

$$RD1_{flood} = \frac{1}{soilConcRD1Flood} \cdot RD1gen \ \ [mm] \tag{6.2.37}$$

6.2.6 Groundwater module

The groundwater module in the J2000 modelling system takes into account the groundwater runoff from all geological formations existing in the catchment area by considering their respective storage and runoff attributes. Those formations have to be parameterised in the hydrogeology parameter file (Table 6.3). The geological units are subdivided into two units. The upper groundwater storage (RG1) represents in the weathered loose materials on top of the bedrock with high permeability and short retention time. The lower groundwater storage (RG2) represents matrix, fissures, and aquifers (saturated areas for long time) with low permeability and long retention time. Correspondingly, two basic runoff components are generated, a fast one from the upper groundwater storage (RG1) and a slow one from the lower groundwater storage (RG2) similar to baseflow. Filling the groundwater storage results from the vertical runoff component of the soil module (percolation). Similarly, emptying can be done by the lateral underground runoff component and the capillary rise on the unsaturated zone. The parameterisation of the groundwater storage is done using the maximum storage capacity of the upper (maxRG1) and the lower groundwater storage (maxRG2) as well as the retention coefficient for both storages, (kRG1) and (kRG2). The maximum storage capacity can be estimated by multiplying the part of the underground chamber by the thickness of the individual storages per m^2 standard area. However, such detail geological information is not available in the study area and therefore a simple conceptual approach used. Three types of storage is realised in the study area based on the geological information of the Nepal Himalaya (Section 4.2 and Section 6.5.5). The glacier area does not have any infiltration and groundwater storage. The upstream areas with high-mountain slope and low elevation with relatively flat areas distinguished . The former has less groundwater storage compared to the latter one as the flat areas can have higher groundwater storage.

For the adaptation of water storage between two groundwater reservoirs, a calibration parameter *gwRG1RG2dist* has to be set up. It influences the allocation of the percolated water from the soil module (percolation) to both groundwater reservoirs (RG1 and RG2) for each HRU in consideration of the slope. First, the weight of the slope (slope_{weight}) is determined

$$slope\_weight = tan(slope \cdot \frac{\pi}{180}) \tag{6.2.38}$$

$$gradh = (1 - slope\_weight) \cdot gwRG1RG2dist \tag{6.2.39}$$

Then the percolation rate is allocated:

$$potRG1 = (1 - gradh) \cdot percolation \tag{6.2.40}$$

$$potRG2 = gradh \cdot percolation \tag{6.2.41}$$

The calculation of water discharge from the two different storages is made according to the current

storage amount (in the form of a linear-outflow function. The storage retention coefficients *(kRG1, kRG2)*, which are considered as the time water rests in the specific storage, are factors of the current storage volume (actRG1, actRG2) used for the calculation of the groundwater outflow (outRG1 and outRG2) as follows:

$$outRG1 = \frac{1}{gwRG1Fact \cdot kRG1} \cdot actRG1 \ \ [mm] \tag{6.2.42}$$

$$outRG2 = \frac{1}{gwRG2Fact \cdot kRG2} \cdot actRG2 \ \ [mm] \tag{6.2.43}$$

In order to take the groundwater reservoirs' runoff dynamics into account, the groundwater runoffs outRG1 and outRG2 are multiplied by the calibration parameter *gwRG1Fact* and *gwRG2Fact* for the particular upper and lower groundwater reservoir. Generally, the runoff from the groundwater reservoirs is carried out faster when a small factor is given and slower when a big factor is given. The value remains in between 0 to 1.

In addition to the mentioned parameters, the capilary rise of the groundwater has an important influence on the filling of the soil storage (in soilwater module) in plain areas with very high groundwater level. In order to take this effect, the free MPS (deltaSoilStor), and relative saturation of MPS (satSoilStor) in the upper soil zone and the calibration parameter (*gwCapRise*) are taken into account.

$$inSoilStor = deltaSoilStor \cdot \left(1 - exp\frac{-1 \cdot gwCapRise}{satSoilStor}\right) \tag{6.2.44}$$

Capillary rise is calculated in the model if the current storage amount of the groundwater storage is higher than the deltaSoilStor and if the calibration parameter *gwCapRise* is above zero. By putting it to zero, the capillary rise can be prevented.

6.2.7 Routing

The J2000 modelling system has two routing components. The first **HRU Routing** is implemented for the simulation of lateral water transport from one HRU to the next HRU until the water finally reaches a stream network. In order to do so, the individual runoff components (RD1, RD2, RG1 and RG2) which are generated in the model entities are transferred to the corresponding recipient.

The second and most important routing is named **Process Reach Routing**. This component is used for modelling flow processes in the reach (or stream) network. The information required in the reach parameter file is provided in Table 6.6. The individual reaches receive water from neighboring spatial model entities and upstream reaches. In a given stream reach, a velocity for water amount is calculated and then a certain amount is given to the next downstream reach based on the velocity and the length of the reach network. Although the entire amount of water allocated by the model is routed, the relative amounts of the individual runoff components are maintained, so they can be considered separately anytime in every reach.

This module describes flow processes in the stream channel by using the commonly applied kinematic wave approach and the calculation of velocity according to Manning and Strickler as described in (Krause 2001). The only model parameter that has to be estimated by the user is a routing coefficient *(TA)*. It represents the runtime of the runoff wave which moves in the channel until it reaches the catchment outlet after a precipitation event. Its value is required for the calculation of the restraint coefficient *(Rk)* together with the velocity of the river *(v)* and flow length *(fl)*:

$$Rk = \frac{v}{fl} \cdot TA \cdot 3600 \tag{6.2.45}$$

Prior to this, however, the velocity (v_{new}) has to be determined using the roughness factor by Manning (*M*), the slope of the river bed (*l*) and the hydraulic radius (Rh). The hydraulic radius is calculated using the drained cross section (*A*) of the reach resulting from the flow rate (*q*), velocity (*v*) and river bed width (*b*). For this procedure, an initial starting velocity (v_{init}) is assumed which is then iteratively adjusted with regard to the new calculated velocity (v_{new}) until both velocities differ by a value smaller than 0.001 m^{-1}.

$$Rh = \frac{A}{b + 2\frac{A}{B}} \quad [m] \tag{6.2.46}$$

with:

$$A = \frac{q}{v_{init}} \quad [m^2] \tag{6.2.47}$$

$$v_{new} = M \cdot Rh^{\frac{2}{3}} \cdot l^{\frac{1}{3}} \quad [m^3/sec] \tag{6.2.48}$$

Finally, the amount of water of the corresponding reach *(q_{act})* is calculated in the model which is allocated to runoff *(q)* using the runoff restraint coefficient *(Rk)* which has been generated.

$$q = q_{act} \cdot e^{\frac{-1}{Rk}} \quad [m^3/sec] \tag{6.2.49}$$

The higher the assumed value of *TA*, the faster does the runoff wave move within a certain time span and the less water remains in the channel.

6.3 Requirements of the dataset

6.3.1 Hydro-meteorological data

The modelling system requires few datasets as a prerequisite to start the model. Input files are the temporal static parameters as well as temporal variables as input data (climate, precipitation and runoff)

(Table 6.1).

Table 6.1: Input dataset requirements for the J2000 hydrological model

S.N.	Name	description	unit
1	orun.dat	observed runoff	m^3/sec
2	rain.dat	measured amount of precipitation	mm
3	rhum.dat	relative humidty	%
4	sunh.dat	sunshine hour	h
5	tmax.dat	maximum temperature	^oC
6	tmean.dat	mean temperature	^oC
7	tmin.dat	minimum temperature	^oC
8	wind.dat	wind speed	m/s

The specific requirements of the dataset for a given model application can vary depending upon modules selected and used in the model. For example, to calculate evapotranspiration, the Hargreaves method needs only temperature and solar radiation whereas the Penman-Monteith method requires temperature, wind speed, sunshine hour and relative humidity. The observed discharge data are required for the validation of the model results. All these datasets have to be provided in the specific data formats as inputs to the model system.

6.3.2 Model parameter files

Another set of required model inputs is known as a parameter file. The model parameters of J2000 describing a catchment and its hydrological response can be divided into two categories: **i)** The spatially distributed but temporally static descriptors (spatial attributes), which describe the spatial heterogeneity and variability of the river basin and **ii)** the spatial and temporal static calibration parameters are used for the adaptation of the model response. To limit the degrees of freedom during model calibration, only the second group is changed to obtain a good and acceptable modelling result; whereas the first group is quantified inside the GIS based on the input data layers (Krause et al. 2006). The J2000 hydrological model requires the following parameter files for the model initialization:

- landuse.par – landuse
- hgeo.par – hydrogeology
- soils.par – soil types
- hrus.par – parameter of the derived Hydrological Response Units (HRUs)
- reach.par – network of river channels

Hydrological Response Units (HRUs) were applied as model entities which were derived from spatially distributed information about topography, landuse, soil and geology. Detailed information about HRUs is presented in a subsequent Section 6.7. Each input parameter file contains specific information about the characteristics of the catchment controlling the hydrological dynamics.

1) Land-use parameter file

Table 6.2: Land-use parameter information

S.N.	Parameter (Unit)	Description
1	LID	land-use ID
2	albedo (%)	albedo of land surface
3	RSCO_1	minimum surface resistance for water-saturated soil in January
4	...	.....for water-saturated soil in February to November
5	RSCO_12	minimum surface resistance for water-saturated soil in December
6	LAI_d1	leaf area index (LAI) at the beginning of the vegetation period
7	...	second and third quarter
8	LAI_d2	leaf area index (LAI) at the end of the vegetation period
9	effHeight_d1 (m)	effective vegetation height at the beginning of the vegetation period
10	...	second and third quarter
11	effHeight_d4 (m)	effective vegetation height at the end of the vegetation period
12	rootDepth_d4 (m)	root depth
13	sealedGrade	sealed grade to check infiltration

The detailed information required in the land-use parameter file is provided in Table 6.2. The values for each land-use type are derived from various sources. First, the template from the J2000 hydrological model from the Gelberg catchment in Germany (http://jams.uni-jena.de) was taken and further adapted in the ecological context of Nepal using different literature (MoFSC 2002), expert knowledge and a field visit. For example, the seasonal pattern and magnitude of leaves regenerating/falling from tress vary in ecological zone which was considered for defining LAI in this case.

2) Hydro-geology parameter file

Table 6.3: Hydro-geology parameter information

S.N.	Parameter	Description
1	RG1_max	maximum storage capacity of the upper ground-water (RG1) reservoir
2	RG2_max	maximum storage capacity of the lower ground-water (RG2) reservoir
3	RG1_k	storage coefficient of the upper ground-water (RG1) reservoir
4	RG2_k	storage coefficient of the lower ground-water (RG2) reservoir

The detailed information required in the hydro-geology parameter file is provided in Table 6.3. The storage capacities of RG1 and RG2 can be estimated by analyzing the geological information of the area. This value indicates only the maximum water storage capacity (RG1_max and RG2_max) of each of the two storages. The storage coefficient values (RG1_k and RG2_k) are used as a general recession co-efficient of two storages. The recession is further controlled by a flexible calibration parameter within the model.

3) Soil parameter file

The detailed information required in the soil parameter file is provided in Table 6.4. The soil parameter file is one of the important parameter files which needs a range of information to produce a compre-

Table 6.4: Soil parameter information

S.N.	Parameter	Description
1	SID	soil type ID
2	depth	thickness of soil
3	kf_min	minimum permeability coefficient
4	depth_min	depth of the horizon above the horizon with the smallest permeability coefficient
5	kf_max	maximum permeability coefficient
6	cap_rise	capillary ascension
7	aircap	air capacity representing excess water in a Large Pore Storage Storgae (LPS)
8	fc_sum	useable field capacity representing a Middle Pore Storage (MPS)
9	fc_1...22	useable field capacity per decimeter of profile depth

hensive characterization regarding the soil properties inherent in controlling the model's hydrological dynamics. First the different soil horizons and the texture of the soil (combination of sand, silt and clay) in percentage are required. This information is generally available in the soil dataset. The texture information is useful to describe the characteristics of the soil water retention curve. The soil texture information (generally in percentage) is provided as input data to the software component Rosetta inside **'HYDRUS 1D[2]'** to understand the pedotransfer functions of soils in three different hypothetical pressure scenarios (0 mbar, 60 mbar and 15,000 mbar). The soil zone of each response unit is classified according to the specific pore volumes of the soil (Scheffer and Schachtschabel 1984).

- The water stored in shallow-soil horizon's fine pores (< 0.2 μm diameter), soil moisture tension (pF) > 4.2; (pressure equivalent to 15,000 mbar) which corresponds to the permanent wilting point (PWP). It is so strongly bound due to its adsorption powers that it is not at all available for water balance. The water stored in the fine pores can be neglected during the modelling as it is not available for transpiration or flow processes due to constant binding due to the fine pore size.

- The Middle Pore Storage (MPS) represents the pores with a diameter of 0.2-50 μm, pF 1.8 to 4.2 (pressure equivalent between 60 to 15,000 mbar), corresponding to the usable field capacity (nFK) (Scheffer and Schachtschabel 1984). The water is stored in middle pores and narrow coarse pores in which water is held against gravity but can be subtracted by an active tension e.g. plant transpiration during the calculation of evapotranspiration.

- The water stored in Large Pore Storage (LPS) (coarse and macro pores) with a diameter of >50 μm, pF > 1.8 (pressure equivalent to less than 60 mbar) cannot hold water against gravity. The water in LPS can be kept for only a short period of time (1 to 2 days) according to (Scheffer and Schachtschabel 1984). Therefore, in the J2000 model, the LPS is considered as the source of part of overland and subsurface flow processes.

Subsequently these three state conditions of water holding capacities in different storages provide information about the volume of the LPS and MPS. The air capacity in Table 6.4 represents the

[2]http://www.pc-progress.com/en/Default.aspx?hydrus-1d

Table 6.5: HRU parameter information

S.N.	Parameter	Description
1	ID	HRU ID (numbers)
1	x	easting of the centroid point (Longitude in UTM)
2	y	northing of the centroid point (Latitude in UTM)
3	elevation	mean elevation (meter)
4	area	area (m^2)
5	type	drainage type: HRU drains in HRU (2), HRU drains in channel part (3)
6	to_poly	ID of the underlying HRU
7	to_reach	ID of the adjacent channel part
8	slope	slope
9	aspect	aspect
10	flowlength	flow length
11	soilID	ID soil class
12	landuseID	ID land-use class
13	hgeoID	ID hydrogeologic class

volume of the LPS and the useable field capacity represents the volume of MPS. The latter is divided into different soil depths (fc_1...22) through soil horizons.

4) HRU parameter file

The detailed information required in the HRU parameter file is provided in Table 6.5. The HRU parameter file stores the spatial attributes of the catchment area where information about elevation, area, aspect, coordinates, land-use type, hydrogeology and soil is stored for each HRU. The interactions among the various parameter files involve relations between the soil, land-use and hydrogeological descriptors in the HRU parameter file and corresponding descriptors in the other files. The detailed description of the development of the HRU parameter file is described in Section 6.7.

5) Reach parameter file

The detailed information required in the reach parameter file is provided in Table 6.6. The reach parameter file describes the stream characteristics as well as the relationship between stream networks to accomplish an accurate depiction of reach routing. The individual parameters which have to be assigned, are length (m), slope (percent), mean width (m) and reach roughness according to Manning-Strickler. Those are stored in a reach parameter file. In addition, the reach parameter file contains information on the structure of the flow topology by noting the ID for every reach into which it transfers. The detailed description of the development of the reach parameter along with the HRU parameter file is described in Section 6.7. The relationship between HRU and reach parameters while transferring water from upstream to downstream areas are provided in Figure 6.8, page 120.

Table 6.6: Reach parameter information

S.N.	parameter (unit)	description
1	ID	Reach ID
2	Length (m)	length of a stream network
3	to-reach	the next reach ID where the water is supplied
4	slope (percentage)	mean slope of reach
5	rough	roughness of reach surface
6	width (meter)	width of a reach channel

6.4 Regionalisation of the input dataset

The regionalisation of the input dataset is conducted within the J2000 modelling system. The regionalisation process has been well-described by (Krause 2001): in German) and in the technical documentation of the J2000 modelling system (Krause 2010). The descriptions of the regionalisation approach and the different modules of the J2000 were taken from these two sources. The changes (or adaptations) of the module structure as a part of this research study are also described below (such as temperature regionalisation, glacier module, adaptation to floods etc). In the regionalisation approach, a new approach was introduced for temperature regionalisation. Due to only a few number of temperature stations in the study area, a constant lapse rate for the regionalisation of temperature was implemented, which is described in Section 6.4.1.

Initial process of climate data regionalisation

First, the linear regression between the daily station values and the elevation of the station is made. In doing this, the coefficient of determination (r^2) and the slope of the regression line (b_H) of this relation is calculated. It is assumed that the measurement value (MW) depends linearly on the terrain elevation (H) according to:

$$MW = a_H + b_H \cdot H \tag{6.4.1}$$

The unknown values of a_H and b_H are defined according to the Gaussian method of least squares:

$$b_H = \frac{\sum_{i=1}^{n}(H_i - \overline{H})(MW_i - \overline{MW})}{\sum_{i=1}^{n}(H_i - \overline{H})^2} \tag{6.4.2}$$

$$b_H = \overline{MW} - b_H * \overline{H} \tag{6.4.3}$$

The correlation coefficient of the regression is calculated according to the following equation:

$$r = \frac{\sum_{i=1}^{n}(H_i - \overline{H})(MW_i - \overline{MW})}{\sqrt{\sum_{i=1}^{n}(H_i - \overline{H})^2 * \sum i = 1^n (MW_i - \overline{MW})^2}} \tag{6.4.4}$$

The number of stations (n) which are nearest to the particular HRU for the consideration of regionalisation has to be defined in advance by the user as a calibration parameter. The station number depends upon the density of the station network as well as on the relative positions of the individual stations.

The distance **Dist(i)** of each station is calculated in the area of interest. The n stations with the shortest distance to the particular HRU are used for further calculations. The distances of these stations are then converted to weighted distance wDist (i) via potentialization with the weighting factor pIDW. With the help of this pIDW, the influence of nearby stations can be increased and the influence of further distanced stations can be decreased. Good results can be achieved with values used of 2 or 3 for pIDW.

Via Inverse-Distance-Weighted (IDW), the weightings of the n stations are defined with regard to their distances for every HRU in a diferent module. upon their distances for each HRU. By using the IDW method, the horizontal variability of the station data is taken into account according to its spatial position. The calculation is made according to the following equation:

$$W(i) = \frac{\left(\frac{\sum_{i=1}^{n} \omega Dist(i)}{\omega Dist(i)}\right)}{\left(\sum_{i=1}^{n} \frac{\sum_{i=1}^{n} \omega Dist(i)}{\omega Dist(i)}\right)} \tag{6.4.5}$$

Calculation of data value for each HRU

The calculation of data for each HRU is made using the weightings from the equation 6.4.5 and an optional elevation correction for the consideration of vertical variability. The elevation correction is done only when the coefficient of determination (r^2) goes beyond the threshold value provided by the user. There is also an option to make a calculation without considering elevation correction using the following equation (6.4.6). In the model, a user has the option to choose an elevation correction factor.

$$DW_{DF} = \sum_{i=1}^{n} MW(i) \cdot W(i) \tag{6.4.6}$$

For data values that are affected by elevation, an elevation correction for the measured values is done in addition when the values have a high regression relation (r^2) which is greater than the threshold entered by the user. The following equation is applied for the calculation:

$$DW_{DF} = \sum_{i=1}^{n} ((\triangle H(i) * b_H + MW(i)) * W(i)) \tag{6.4.7}$$

The climate dataset, except temperature, used in this study was regionalised by using the IDW method.

To fill the missing values in the dataset required to run the model, the IDW method with elevation correction factor, was applied in the KosiRBIS (Section 5.2). Instead of calculating the data value for each HRU as mentioned here, the missing data for each station are estimated. The distance between the stations is calculated and converted to weighted distance (Equation 6.4.5). A maximum of 5 and a minimum of 3 stations were used to fill the missing gaps. At the same time, the linear regression

between daily stations values and elevation is calculated within RBIS. If the regression's correlation between the daily values and elevation is higher than 0.7, the elevation factor was used to calculate missing values for the particular day along with the IDW. Otherwise, only the IDW method is applied. During the model-run phase of the study, there were no gaps in the precipitation data especially during the more-critical monsoon season. The gaps of a few weeks outside the monsoon period were filled using the procedure described here. The temperature data gaps of fewer than 4 days were filled by using linear interpolation within the RBIS by taking the average from days before and after the gaps.

6.4.1 Regionalisation of temperature data

A temperature lapse-rate method is integrated into the model because of the lack of adequate temperature data as required by the IDW method. The problem with the IDW approach regarding the low density of temperature stations is the following: when there is a higher lapse rate on some given day (less temperature difference between stations at higher and lower altitudes), the regionalisation approach estimates higher temperatures in higher altitude areas. This might cause higher snowmelt in some particular days. This issue was realised while using the IDW method with elevation correction while using data from 3 stations.

In the temperature lapse approach, first the distance between the particular HRU and temperature station is calculated. If there is more than one temperature station, the model recognizes the station which is closest to the HRU (ELEV_station(closest)). In the next step, the elevation difference (ELEV_diff) between the particular HRU and the station is calculated. The mean elevation of each HRU is obtained from the HRU parameter file. The lapse rate is provided as a calibration parameter (LAPSE_rate) in the model. Finally the model calculates the temperature of each HRU (TEMP_hru) using the lapse rate and temperature of the station on a particular day using the following equations:

$$Elev_{diff} = Elev_{station(closest)} - Elev_{HRU} \tag{6.4.8}$$

$$Temp_{hru} = Elev_{differ} \cdot Lapse_{rate} + Temp_{station} \tag{6.4.9}$$

To better understand the existing lapse rate in the study area, the data from two stations, Okhaldhunga (1720 m) and Chialsa (2770 m) for the period between 1988-1995 were used to calculate the existing lapse rate. The lapse rate in Figure (6.3) was calculated per 100 m. The annual average lapse rate is 0.6°C/100 meter. The data indicates that there is temporal variability of the surface temperature lapse rate. The higher lapse rate of about 0.5°C/100 meter was observed during the summer season (June-September) (higher lapse rate indicates a greater-than-normal change of temperature associated with a change in elevation). After September till May, a greater variation in lapse rate was observed between 0.6 to - 0.7°C /100 meter. This suggested that the summer (or monsoon) season has a higher lapse rate than the winter season which is important information for the calculation of snow and glacier melt. Sakai et al. (2004) has also found a lapse rate of 0.5°C/100 meter during the monsoon season in 1996 in the Langtang area in Central Nepal. A similar variation in lapse rate was observed in the

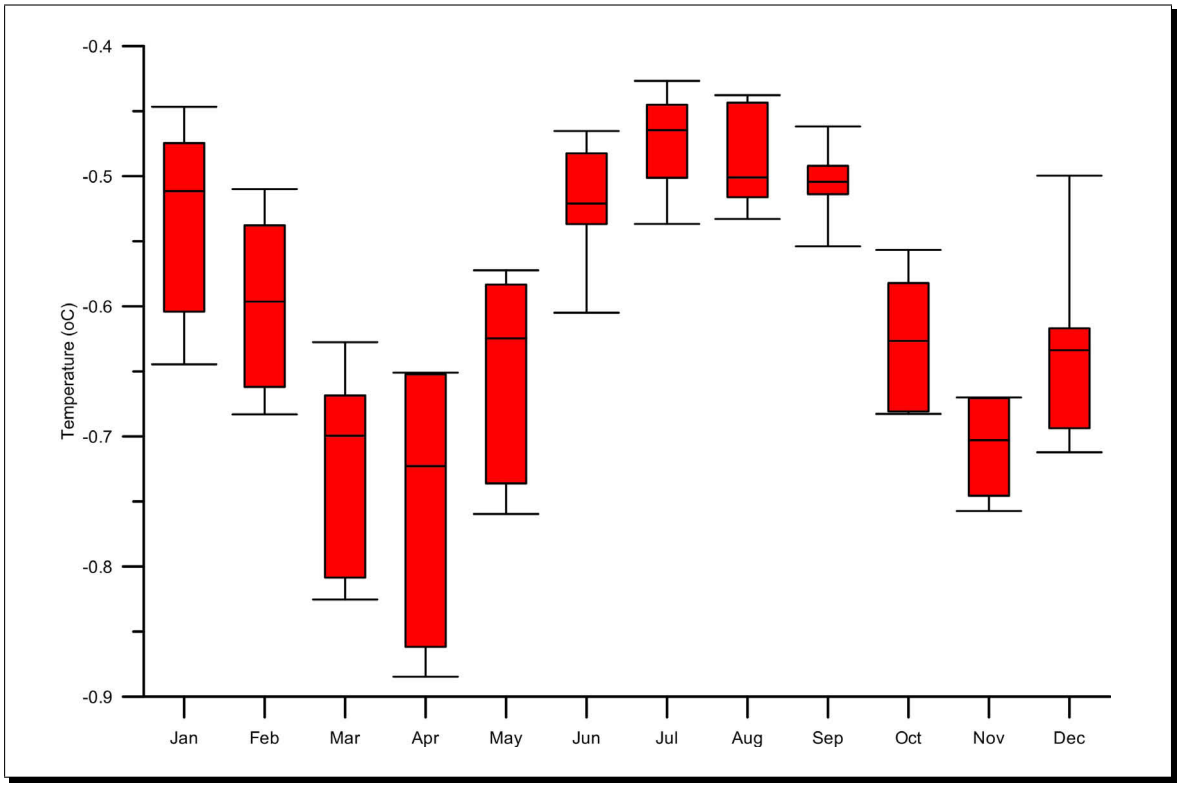

Figure 6.3: A box plot of mean temperature lapse rate between Okhaldhunga (1720 m) and Chialsa (2770 m) station (1988-1995) per 100 meter

Tibetan Plateau (Kawashima et al. 2007) and the mountains of the United States (Minder et al. 2010). The difference in seasonal lapse rate is possibly due to the dry and wet adiabatic rate resulting from moisture content in the air. At wet (or moist) adiabatic rate, the latent heat is released when water condenses, thus decreasing the rate of temperature drop as an increase of elevation. When the air is saturated with water vapor during the summer season (rainy period), a wet (or saturated) adiabatic rate applies which is typically higher compared to other months when the air is relatively dry.

The J2000 modelling system requires daily maximum (Tmax) and minimum (Tmin) temperature. From these values, the mean day temperature (Tmean) is calculated as an average. The regionalisation of the station values (Tmax, Tmean and Tmin) is conducted according to the temperature lapse approach.

6.4.2 Precipitation correction

Measuring precipitation in a mountain region is a challenging task due to accessibility and maintenance. Systematic measurement errors (or bias) occur during the precipitation measurement which have to be corrected. Some of the influencing factors include: deformation of wind field over the precipitation gauge orifice, evaporation (or moistening) and splash losses, interception loss, observation and instrument errors etc (Konz and Devkota 2009). Due to these factors, daily precipitation

values commonly are underestimated.

In Nepal, precipitation data are recorded using a standard 8-inch diameter American type ordinary rain gauge which is manufactured locally. The readings are observed daily at 08:45 Nepal Standard Time (NST). The exposure height is kept at about one meter above ground level.

The correction of the moistening and evaporation errors is conducted according to Richter (1995). In order to offer a constant correction of the error (which results from the moistening and evaporation loss), logarithmic functions were applied through approximate separate functions for the summer half year (May-October) and winter half year (November-April). These functions were applied to the discrete tabulated values in the J2000 modelling system. If the precipitation values are greater than 9 mm per day, the moistening and evaporation errors are set to a constant value.

The moistening and evaporation errors for precipitation heights less than or equal to $\leq$ 9 mm/d are calculated according to the following equations:

$$BV_{summer} = 0.08 \cdot LogPrecip + 0.225[mm] \tag{6.4.10}$$

$$BV_{winter} = 0.05 \cdot LogPrecip + 0.13[mm] \tag{6.4.11}$$

For precipitation values > 9.0 mm, the moistening and evaporation error is:

$$BV_{summer} = 0.47[mm] \tag{6.4.12}$$

$$BV_{winter} = 0.30[mm] \tag{6.4.13}$$

$$Precip_{corr} = Precip + BV_{summer}, BV_{winter}[mm^{-1}] \tag{6.4.14}$$

The quantification of the expected precipitation error is done according to investigations by (Richter 1995) as a function of precipitation depth and station location. It is assumed that the relative wind error (KR_{Wind}) for both rain and snow precipitation is distinctly inversely proportional to the precipitation depths (Pm). The calculation is made according to the following equations:

$$KR_{Wind} = \begin{pmatrix} 0.1349 \cdot P_m^{-0.494} \\ 0.5319 \cdot P_m^{-0.0197} \end{pmatrix} \tag{6.4.15}$$

The calculation of the corrected precipitation depths with regard to evaporation and wind error is carried out as follows:

$$P_{corr} = P_m + P_m \cdot KR_{wind} + BV_{summer}, BV_{Winter}[mmd^{-1}] \tag{6.4.16}$$

There is no systematic study about the precipitation correction in the Nepal Himalaya. The Richter's correction procedure mentioned here was developed for German condition with elevation less than 700 m. In the absence of other alternative approach, this method is applied in this study although it is not fully representative for the Himalayan region,

6.4.3 Calculation of relative humidity

The relative humidity (*rhum*) [%] is the ratio of the actual amount of moisture in the air to the saturated amount. The relative humidity can be measured at a station on a daily basis. A direct regionalisation of the values is not recommended because they depend on two parameters: the absolute moisture content and the maximum possible moisture content of the air for a particular level of temperature. Therefore, the absolute humidity (*ahum*) is calculated from the relative humidity and the temperature. Afterward, it is regionalised and the absolute humidity is converted into the relative humidity. For this purpose, several calculation steps are necessary which are indicated below.

Calculation of the saturation vapor pressure

The saturation vapor pressure (e_s) is calculated for the mean air temperature (T):

$$e_s = 0.6108 \cdot e^{(\frac{17.62 \cdot T}{243.12+T})} \ [kPa] \tag{6.4.17}$$

Calculation of the maximum humidity

The maximum humidity (*mhum*) is calculated against the saturation vapor pressure (e_s) and the mean air temperature (T) according to:

$$mhum = e_s \cdot 10 \cdot \frac{216.7}{T + 273.15} \ [g/m^{-3}] \tag{6.4.18}$$

Calculation of the absolute humidity

The actual water content of the air, the absolute humidity (*ahum*), results from the maximum humidity (*mhum*) and the relative humidity (*rhum*) [in %]:

$$ahum = mhum \cdot \frac{rhum}{100} \ [gm^{-3}] \tag{6.4.19}$$

The calculated station values of the absolute humidity are then regionalised according to the IDW method. Finally, the relative humidity *rhum* is calculated according to:

$$rhum = \frac{ahum}{mhum} \cdot 100 \ [\%] \tag{6.4.20}$$

6.4.4 Calculation of evapotranspiration

Evaporation is a process by which liquid water is transferred from land and water masses of the earth to the atmosphere. Water evaporates from a variety of surfaces, such as lakes, rivers, pavements, soil and wet vegetation. Transpiration is the counterpart of evaporation component attributable to water losses to the atmosphere by plants. It is the process by which soil moisture taken up by vegetation is eventually evaporated. Evaporation and transpiration occur simultaneously and thus there is no easy way of distinguishing between the two processes. Evaporation and transpiration combined **(Evapotranspiration)** generally constitute the largest component of water losses in rainfall-runoff physical processes. Accordingly, good estimates of evaporation are the prerequisite for estimating accurately water balances through hydrological modelling (Viessman and Lewis 2003). Transpiration is a vital component of the water budget within vegetated and agriculture areas. There are many climatic parameters involved in the process of evapotranspiration as there is a continuous exchange of water molecules between an evaporating surface and its overlying atmosphere. Weather parameters, crop characteristics, water management and environmental aspects are factors affecting evapotranspiration. Conversion of snow or ice into water vapor is in reality rather in the form of sublimation than evaporation however, the effects of these two processes are the same.

Energy is required to change the state of the water molecules into vapor. It is a function of solar radiation, air temperature, air humidity, and the difference between the vapor pressure at the evaporating surface and that of the surrounding atmosphere. As evaporation proceeds, the surrounding air becomes gradually saturated and the process will slow down and might stop if the wet air is not transferred to the atmosphere. The replacement of the saturated air with drier air depends greatly on wind speed (Allen et al. 1998, Viessman and Lewis 2003).

The calculation of potential evapotranspiration (PET) is done in the J2000 modelling system according to the Penman-Monteith equation in several steps with regard to numerous parameters. The potential evapotranspiration is the loss expected over a surface with no limitation of water. It is a function of the atmospheric demand, i.e. the rate at which the resulting vapor can be moved away from the surface (Beven 2001a). Because the calculation is very complex and time-consuming, it was outsourced in the preprocessing part of the modeling system. This outsourcing is possible because most of the parameters that are used for the calculation are derived from the input data and are thus considered as independent of the modeled dynamics of water availability. The only parameter that is used in the calculation but can only be defined during the modeling is the current soil moisture. Its declining influence is taken into account using appropriate reduction functions during the modeling process. A detailed description of the calculation of PET and net radiation are provided in Allen et al. (1998) and also documented in Appendix B.

Adaptation to evaporation

Slope and aspect of an HRU (or area) significantly influence the evaporation amount. Therefore, these factors are taken into account by using the following correction factors (Golf 1981):

$$Correc_E TP = (0.01605 \cdot \sin(\delta - 90) - 0.00025) \cdot \alpha + 1 \tag{6.4.21}$$

δ : aspect from north in degree

α : slope in degree

The corrected evaporation considering slope and aspect will be:

$$ETP' = ETP \cdot Correc_{ETP} \; [mmd^{-1}] \tag{6.4.22}$$

In the J2000 modelling system, the actual evapotranspiration (AET) is carried out by using the actual water storage against the potential evapotranspiration. It is assumed that vegetation can only transpire water from soil storage up to the root depth. First the model checks actual water storage within different storages (interception and soil storage). It is then checked against the potential evapotranspiration (ETP). The actual evapotranspiration cannot exceed potential evapotranspiration. Inside the soil storage, if the water storage is zero, a condition of a permanent wilting point is realised and the actual evapotranspiration is set to zero.

The evaporation is also estimated from snow surface from both glacier and non-glacier areas. It is assumed that the evaporation (or sublimation) of water from the seasonal snow pack occurs at a rate equal to the PET rate. The PET of the snow surface is further adapted by a calibration parameter. If the snow storage is zero, no snow-related evaporation occurs.

6.5 Preparation of dataset for Dudh Kosi river basin

The section describes the development of the dataset required for the J2000 model for the Dudh Kosi river basin. The Dudh Kosi river basin is one of the tributary catchment exhibiting the steepest slope within the Kosi river basin as shown in Figure 4.2. The total area of the basin, upstream from the gauging station at Rabuwabazaar (460 m) is 3,712 km^2. The Dudh Kosi river basin along with the hydro-meteorological stations are provided in Figure 6.4. The average slope of the basin is 26 degrees. Nearly 45 percent of the catchment area is located higher than this slope. The highest peak in the world, Mt. Everest (8,848 m) is also located in the basin, including other peaks higher than 7,000 m. About 30 percent of the land is located higher than 5,000 m and 32 percent of land is located between 3,000-5,000 m.

6.5.1 Hydro-meteorological stations in the Dudh Kosi river

There are six meteorological stations in the study area where the daily data is available. One station (Okhaldhunga) which is located very close to the border was also selected because long-term data at this station also was available. The Okhaldhunga station is also a climate station where data for other meteorological variables are available. The detailed list of stations and their other characteristics are given in Table 6.7. The station Chialsa also contains temperature data between 1986-1996 with frequent data gaps: therefore, the Okhaldhunga station was selected for the analysis. The availability

of relative long- time series data also indicates that the station serves as a good data source and has operated for a longer time with relatively few problems. These stations are shown in Figure 6.4

Table 6.7: Hydro-meteorological stations in the Dudh Kosi river basin

Station ID	Station Name	Elevation	Parameters
1206	Okhaldhunga	1720	P, Tmax, Tmin, SH, RH
1203	Pakarnas	1982	P, W
1220	Chialsa	2770	P
1219	Sallery	2378	P
1204	Aisealukhark	2143	P
1202	Chaurikhark	2619	P
670	Rabuwabazaar	460	D

Notes on variables of Table 6.7: **P:** Precipitation, **Tmax:** Maximum temperature, **Tmin:** Minimum temperature, **SH:** Sunshine hour, **W:** wind speed, **RH:** relative humidity, **D:** Discharge

In the case of wind data which commonly have a gap of a few months and no nearby station having data for that particular period of gap, the long-term monthly average was calculated and used for the missing periods. The interpolation of the station values to the area is carried out according to the IDW method - without elevation corrections. Because there are only data available from one station, the same value is applied to the entire catchment. The lack of representative data for the entire catchment and using a data value from a single station might bring some uncertainty in the model output. The wind speed data is used for the calculation of evapotranspiration. The process of removal of water vapor depends to a larger extend on wind and air turbulence. When vaporising water, the air above the evaporating surface becomes gradually saturated. The evaporation rate decreases if the air is saturated and increases if the air is dry. If the saturated air is replaced by drier air by wind speed, the evapotranspiration decreases. As suggested by Allen et al. (1998), the role of wind speeds in evapotranspiration rate in arid conditions (hot and dry) is far greater than humid conditions. In the latter, wind can replace saturated air with slightly less saturated air and remove heat energy whereas small variation in wind speed may result in larger variations in the evaporation rate in the hot and dry condition. Since most of the study area in lower elevation areas represent humid and warm climate, the variation in estimated potential evapotranspiration can be assumed low. The higher elevation areas have less evapotranspiration primarily due to low heat energy associated with low temperature. Therefore, the wind data from the single station might bring rate uncertainty in the estimated potential evapotranspiration.

Because there is only one station in the study area for measurement of relative humidity, the regionalised absolute humidity as described in Section 6.4.3, is the same for the entire catchment. However, the same absolute value for the entire catchment is not realistic as it might differ with elevation, especially in high-altitude areas. The same regionalised value of the *ahum* might bring some level of uncertainty in the estimated *rhum* for the calculation of evapotranspiration. This is specially true in high-altitude areas where the *ahum* might be different due to low temperature.

6.5.2 Digital Elevation Model (DEM)

The Digital Elevation Model (DEM) provides important information about the physiographic characteristics of the study area. DEMs are important for environmental modelling as they incorporate the spatial variation of significant environmental characteristics of a watershed. Any distributed hydrological model (such as J2000) requires detailed information of watershed topographic properties such as basin size, boundary, slope, aspects, channel network and contributing sub-catchments. In recent years, there has been a widespread use of GIS technologies to assist for model parameterisation for operational relief analysis (Flügel et al. 2001, Beven 2001b).

The DEM data with 90-m resolution were collected from the NASA Shuttle Rader Topographical Mission (SRTM) in 2010 and obtained through the CGAIR-CSI Geoportal[3]. A DEM is a raster representation of a continuous surface, usually referring to the surface of the earth. It is a digital model or 3-D representation of a terrain's surface. The accuracy of these data is determined primarily by the resolution (the distance between sample points).

The data were processed in ArcInfo program. The sinks within DEM were filled by using the Landscape based Sink Algorithm (LaSA) method (Pfennig and Wolf 2007). The objective of LaSA is to minimize the interferences in DEM surfaces. Elimination of sinks should be realised by a landscape-based optimum between filling sinks and the carving of flow paths in flow barriers (Pfennig and Wolf 2007). After filling the sinks in DEM, it was further processed to obtain additional drainage parameters of the basin. Figure 6.4 shows the DEM of a delineated watershed boundary of the Dudh Kosi river basin.

6.5.3 Land use and land cover

The land-cover data were derived from a 300-m global land-cover map derived from the ESA GlobCover initiative (Defourny et al. 2006). GlobCover uses MERIS fine resolution (300-m) mode data acquired between mid-May 2005 and mid 2006. The objective of the ESA Globcover project is the generation of a land-cover map of the world using an automated processing "chain" from the 300-m MERIS time series. The resultant GlobCover land-cover product is the first freely available product at a 300-m resolution description level.

The project was conducted by an international consortium in April 2005 and relied on feedback and a number of comments from a larger partnership including end users belonging to international institutions (such as FAO and UNEP) in addition to the ESA internal assessment . The detail about the GlobCover product and validation are described in Bicheron et al. (2008).

The 15 thematic global cover classes were found in the study area which were further reclassified to eight classes. The land-cover classes which have similar effects on hydrological dynamics were combined. For example, irrigated croplands, rainfed croplands and mosaic croplands vegetation were reclassified as agriculture land. In addition, permanent snow and ice layer of GlobCover were combined and designated as bareland because snow accumulation is calculated within the J2000 model.

[3] http://srtm.csi.cgiar.org/

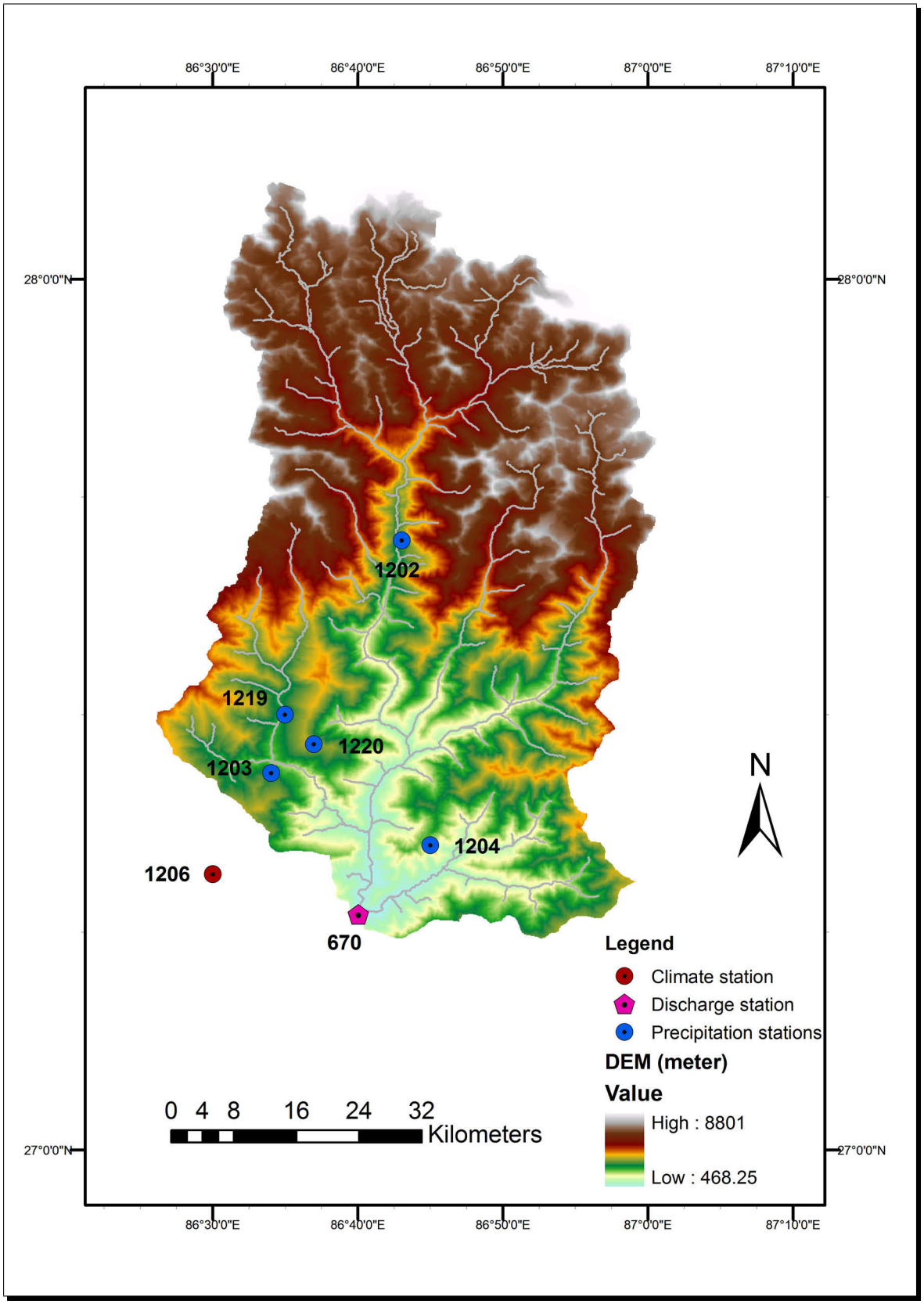

Figure 6.4: DEM of the Dudh Kosi river basin and the reference stations used as an input data for the J2000 model

Table 6.8: Land-use land-cover categories in the Dudh Kosi river basin

S.N.	Land-use land-cover type	Area in %
1	Agriculture	11
2	Mixed forest	10
3	Coniferous forest	24
4	Deciduous forest	7
5	Grassland	4
6	Shrubland	3
7	Bareland	25
8	Water bodies	1
9	Rock	2
10	Glaciers	14

A glacier layer, derived by ICIMOD, was overlayed to the land cover data. It was derived from both satellites, the topographic map, and field-based observation. ICIMOD and its partner institutions carried out a systematic inventory of glaciers and glacial lakes of Nepal and Bhutan in 1999-2001 (Mool et al. 2001b,a) in collaboration with United nations Environment Programme /Regional Resource Centre for Asia and the Pacific (UNEP/RRC-AP).

The GlobCover data were found less reliable especially in high-altitude areas. Therefore, in high-altitude areas, it was reclassified based on subjective judgment, which includes expert knowledge, field-based knowledge and literature (MoFSC 2002). Threshold elevations were assigned for specific land-use types. These included: agriculture land beyond 4,500 m, forest above 4,000 m and grassland above 5,000 m were converted into bare land. The lower elevation area is dominated by deciduous forest. Higher elevation areas between 2,000-4,000 m are dominated by mixed forest and coniferous forest. Deciduous forest higher than 3,300 m is converted into coniferous forest. Similarly, mixed forest higher than 3,600 m is converted into coniferous forest. Higher than 4,000 m have grass and shurbland dominated by bareland. The final land-use and land-cover categories in the Dudh Kosi river basin are provided in Table 6.8.

The Dudh Kosi river basin is one of the most densely glaciated regions of Nepal. About 14 percent of the basin area is covered by glaciers. More than 40% of the basin is covered by forests including deciduous, coniferous and mixed forest types. Information on different land-use and land-cover types is provided in Table (6.8). According to ISRC (2008), the Solukhumbu district comprises about 456 km^2 of total cultivated land. Most of the the Dudh Kosi river basin lies in the Solukhumbu district, except some parts of the lower right areas which are located in another district. The land-cover data in this referenced study have about 422 km^2 of agricultural land which can be considered fairly close with this study which is 410 km^2. Sharma et al. (2000a) compared the land cover of the Middle Mountains and Mahabharat range in the Nepalese part of the Kosi river basin between the years 1965 and 1979. The result suggested that forest cover is nearly 55 percent although the study does not include higher elevation areas. The forest cover of the Dudh Kosi river basin derived from GlobCover which is about 41 percent (summed from S.N. codes 2,3 and 4 in Table 6.8) can be assumed fairly representative. The relatively low value of forest in the GlobCover occurs, because the former information source

does not include higher elevation areas which is dominated by land-cover types other than forest.

In the study area, about 30 percent of the area is located above 5,000 m in elevation and nearly 40 percent is located below 3,000 m. Similarly, 60 percent of the glaciers are located below 5,500 m . As such, these lower-elevation glacier areas are sensitive to recent global warming.

6.5.4 Soil

Soil and Terrain Databases (SOTER), at a scale of 1:1 million, provided by the Department of Survey (DoS), Government of Nepal have been used to derive the soil parameter for the J2000 model. This dataset is generalised from the original Soils and Terrain database of Nepal at a scale of 1:50,000 compiled by FAO and DoS. The FAO-UNESCO Soil Map of the World revised legend has been used as a basis for characterizing the soil component of the SOTER database. Basic-data sources for the construction of SOTER units are topographic, geomorphological, geological data and soil maps at a scale of 1:1 million or larger (FAO 1995).

Eleven distinctive soil classes were identified in the Dudh Kosi river basin. The soil depth and texture information were different within similar classes in different sampling points. In such cases, the average value of the characteristic was determined and was subsequently defined as one soil class. According to the World Reference Base for Soil Resources (WRB), the soil in the areas is dominated by the combination of Cambisol, Umbrisol and Regosol. The soil map of the study area showing the different soil types are provided in Figure 6.5(b). The lower elevation soil is dominated by a combination of Cambisol and Umbrisol which characterizes medium-to fine-textured materials. The soil in these areas is loamy to fine loamy with a relatively thick soil profile. A Cambisol is a soil with a beginning of soil formation which is developed from medium- and fine-textured materials. It is derived from a wide range of rocks mostly in alluvial and colluvial deposits. A Umbrisol is characterized by a surface with an organic top soil layer and a high content of organic matter within the top mineral soil. The higher elevation areas are mostly dominated by a Regosol which are very weakly developed mineral soils in unconsolidated materials characterized by minimal soil profile development as a consequence of young age. This class is also known as forest soils and generally found in upslope locations with fresh soil moisture (FAO 2006, Lundin et al. 2004).

The information about the soil characteristics from the SOTER dataset, mainly soil depth and texture are taken and processed as described in Section 6.3.2, Item 3 in order to obtain needed information about the LPS and MPS in different soil horizons. Generally, the volume of the MPS is five times higher than that of the LPS in lower elevation. In higher elevation areas represented by a Regosol in Figure 6.5(b), the volume of the LPS is nearly equal to the MPS. The high elevation areas (such as mountains) comprise shallow (thin) soil as the soil is not fully developed. The larger LPS, in these areas, is attributed to the presence of rocks, sandy soil and unconsolidated materials.

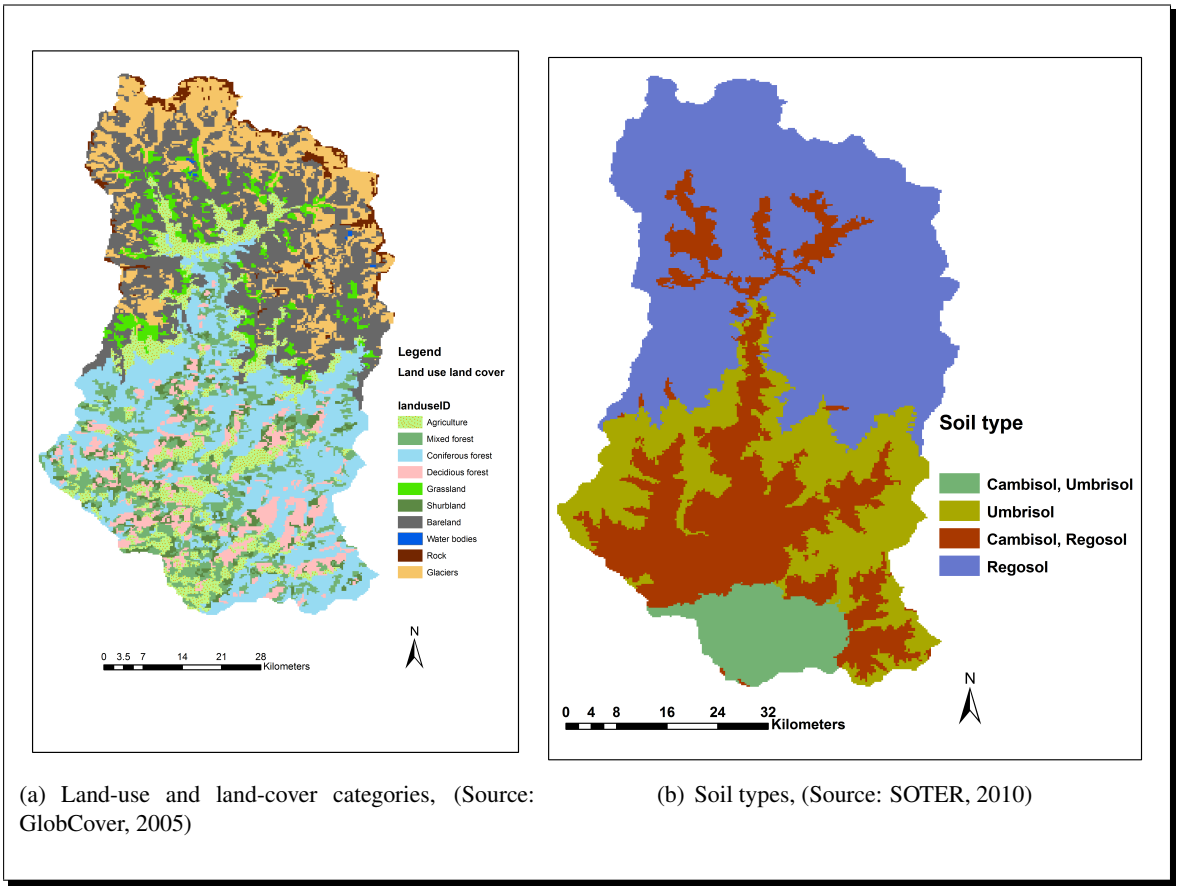

(a) Land-use and land-cover categories, (Source: GlobCover, 2005)

(b) Soil types, (Source: SOTER, 2010)

Figure 6.5: Land-use and land-cover categories and soil types in the Dudh Kosi river basin

6.5.5 Geology

Because of the lack of a good geological dataset, the geological information for the study area was derived from basic geological characters of the region which control the maximum percolation rates and ground-water storages. Three regional areas (classes) of geological information are derived based on the information from soil data and the literature. These include: Glacier, The Higher Himalaya and Lower Himalaya regions. The Higher Himalaya area in general represents the Regosol areas of the basin (Figure 6.5(b)) except for areas of glaciers, and is considered as one geological class. The remaining lower elevation area in the basin is considered as one class. In glacier areas, no infiltration and percolation to the soil occurred, hence it is regarded as no soil area.

The Higher Himalayan region consists of a huge pile of strongly metamorphosed rocks. The main rock types are gneiss, schist, marble and quartzite. Vertical or steep rocky slopes are very common in this zone. Rocks of the Higher Himalaya are intensively folded and faulted (Dahal 2006). As suggested by Beven (2001a) the bedrock in upland catchments is commonly impermeable, however, secondary permeability in the form of joints and fractures may be present which can provide important flow pathways and storages.

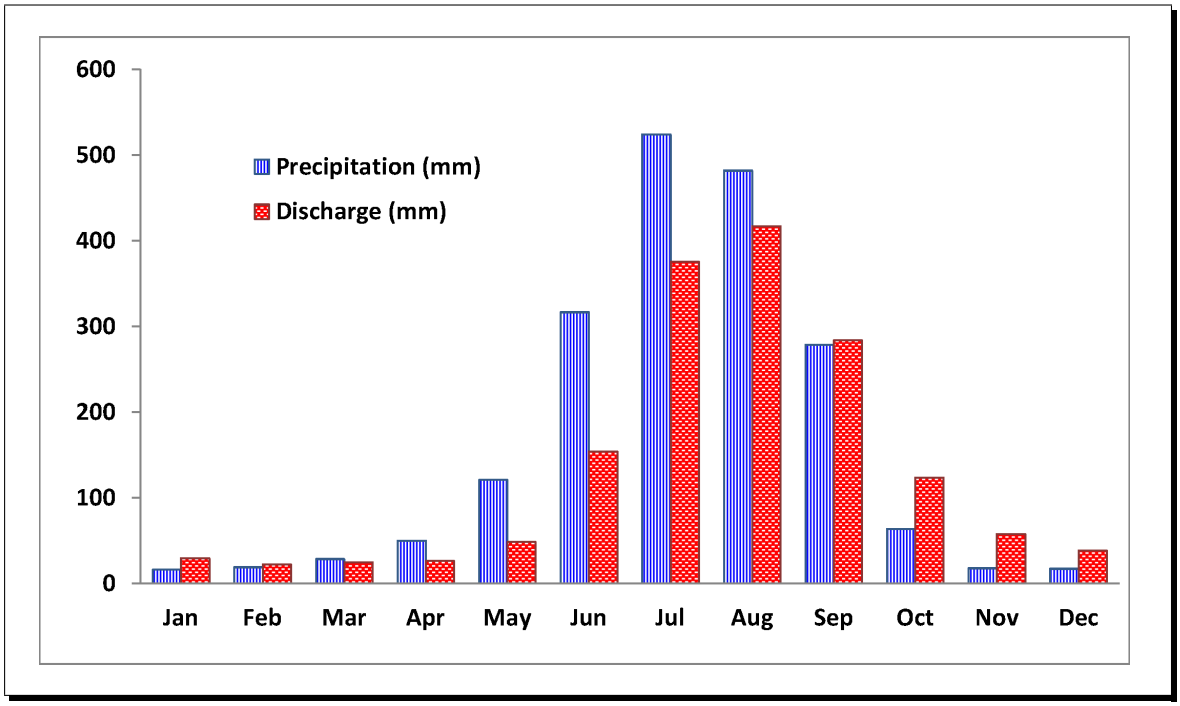

Figure 6.6: Observed monthly precipitation and discharge of the Dudh Kosi basin (1985-1997)

6.6 Hydro-meteorological conditions

The basin has sub-tropical to temperate climate at a lower altitude. The higher altitude areas exhibit sub-alpine and alpine climate associated with low temperature (MoFSC 2002). About 82 percent of the total rainfall occurs during the June-through-September period when the summer monsoon brings moist air from the Bay of Bengal as shown in Figure 6.6. During this period, the region experiences intense rainfall events which causes floods and widespread damage to property and lives. Figure 6.6 indicates the mean monthly observed precipitation and stream discharge of the Dudh Kosi river basin. This time-series plot indicates that most of the precipitation is concentrated during the summer months (June through September). The annual observed precipitation of the six stations in the study area was 1934 mm and the average discharge at Rabuwabazaar station was 1,602 mm during the period of 1985 to 1997. The volume of the discharge starts rising from June and reaches its peak in August. During April and May, the snow and glacier melt also contribute to the streamflow which can be seen by the slight increase in discharge during these months. The melt period coincides with the rainy season when there is relatively high precipitation. The runoff components gets higher during the last two months of the monsoon season producing a higher amount of runoff compared to the initial two months. In September, the discharge is higher than rainfall which indicates the streamflow is contributed also from soil storage and groundwater.

Figure 6.7 shows the monthly temperature at the Okhaldhunga station in the Dudh Kosi river basin. The figure shows that the temperature is low during the winter period (December to February) . After February, the temperature starts rising and reaches its maximum level throughout the monsoon pe-

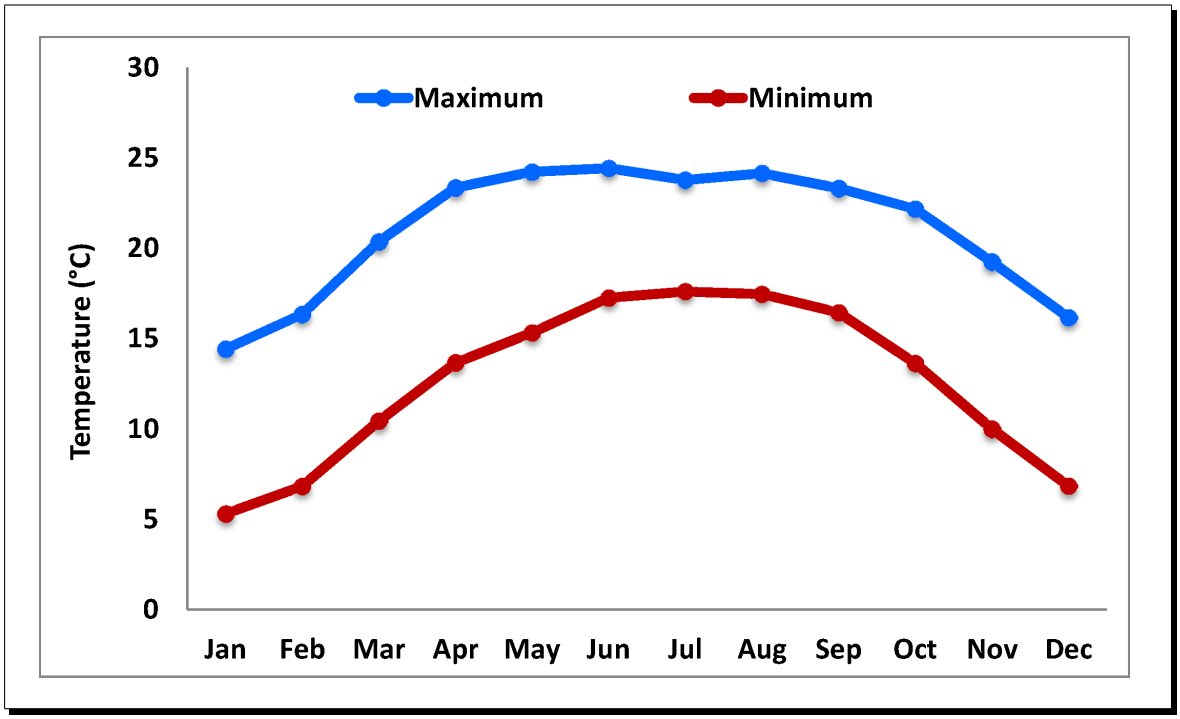

Figure 6.7: Monthly average temperature of the Dudh Kosi river basin at Okhaldhunga station (1720 m) (1985-1997)

riod. The average maximum and minimum temperature is 21 and 12.6 °C at the Okhaldhunga station located at 1720 m. More detailed information about the precipitation dynamics are provided in Chapter 5. Due to high temperature, the maximum snow and glacier melt also occurs during the summer period.

6.7 Modelling entities: Hydrological Response Units (HRUs)

The original approach of HRUs by Leavesley et al. (1983) describes physio-geographic heterogeneity of a catchment area based on physically-derived segments. An HRU can be defined as an area within a catchment that exhibits the same characteristic features in terms of topographic and physiographic attributes and is considered as relatively homogeneous in regard to these properties.

HRUs defined by Flügel (1995) are "spatial model entities which are distributed, heterogeneous structured entities having a common climate, land-use soil and geology controlling their hydrological dynamics". In this distributed approach of the HRU, in contrast to the topographically-based approach by Leavesley et al. (1983), the heterogeneity of the landscape attributes to maintain the process-oriented characteristics which are taken into account.

In the J2000 modelling system, the calculation of hydrological behavior is done for each HRU. HRUs are applied as model entities which have been derived from spatially distributed information about topography, land use, soil type and geology. In this process, the areas which comprise similar proper-

ties such as topography (slope, aspects) land use, soil and geology i.e. which behave similarly in their hydrological response, are merged together to develop an HRU. The variation of the hydrological process dynamics within the HRU should be relatively small compared with the dynamics in a different HRU (Flügel 1995).

The biggest advantage of the HRU concept is the reduction of modelling entities without losing information resulting in a hydrologically sound division of a catchment and thus resultant more efficient (faster) modelling performance. Instead of calculating the hydrological behavior in each modelling entity (raster cells), merging(or combining) areas (or raster cells) with similar properties significantly reduces the number of modelling entities and thereby computation time. The model is run for each HRU and thereby produces the average value for the particular area. The distribution concept of HRUs (Flügel 1995) was further enhanced by a topological routing scheme (Staudenarausch 2001) for the simulation of lateral flow processes between HRUs. In this manner, water from one HRU is passed to the next HRU until it reaches a nearby downstream channel.

6.7.1 Delineating HRUs

The HRUs were delineated by overlaying the data layers of DEM (elevation, slope, aspect), land use and soil type in ArcInfo program using a process developed by Pfennig and Wolf (2007). The DEM, land-use and land-cover and soil datasets were used for delineation. All these maps were reclassified to 250-m resolution. The following major steps were involved in delineating HRUs using this method:

1. A Topographic Wetness Index (TWI) was developed from SRTM-DEM using SAGA GIS program (Olaya 2004). The TWI is a function of natural logarithm of ratio of local upslope contributing area and slope ($ln(\alpha/tan\beta)$. The TWI is commonly used to quantify topographic control on hydrological processes (Soerensen et al. 2006). The TWI is instrumental in deriving relief parameters while also delineating HRUs.

2. The resampled input data (DEM, Land use, Soil and TWI) were provided to the tool developed by Pfennig and Wolf (2007).

3. The minimum number of accumulation cells (in hectares) to generate stream network was provided

4. The minimum number of cells (in hectares) to develop watershed sub-basins was provided

5. While merging cells to generate HRUs, there is an option to set a minimum number of cells (or areas) to develop one HRU. Users can set the threshold number of HRUs (in hectares) which are essential to develop one HRU. Any HRUs fewer than this threshold will again merge with nearby HRUs. This is an important step to control the number of HRUs and eliminate some HRUs that otherwise might be delineated and formed by a relatively small number of cells.

6. The merging of cells can be restricted by some specified land-use type. This helps to keep some key land-use properties intact with other land-use types (such as glaciers).

7. In case the river-channel width is known at the gauging stations, it can be a basis to calculate river width of upstream areas to develop reach parameter file.

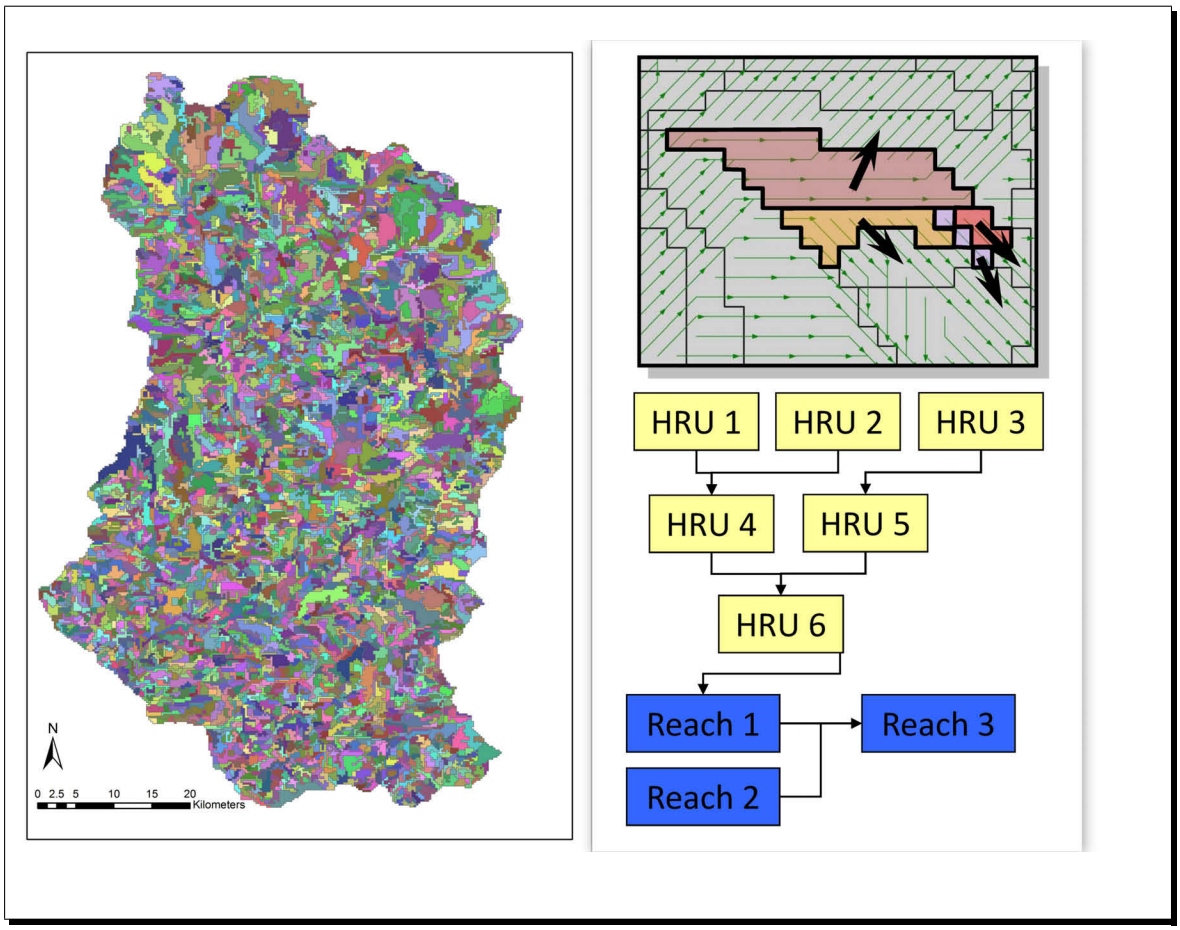

Figure 6.8: HRU map: **Left)** HRU map of the Dudh Kosi river **B)** Schematic diagram of topological linkages between HRUs and reaches

In general, any raster cells can merge with nearby raster cells irrespective of different properties such as land use and soil. However, it is sometimes necessary to keep some land use properties of some class intact from other land-use types as pointed out above in step (6). In this case, the glacier layer inside the land-cover map was kept intact from other land-use types. This means the glacier layer was forced to merge only with a glacier land-cover. This approach was useful to keep the glacier land-cover close to the original glacier layer. Without this approach, it was found that glaciers tend to merge with other land-cover types from adjacent areas which would tend to disrupt the glacier path. The channel width was provided by measuring the river width in Google earth at the gauging station.

At the end, 3,799 HRUs were received with varying sizes between 0.06 and 18 km^2. The HRU map of the Dudh Kosi river basin is provided in Figure 6.8. These HRUs were topologically connected for lateral routing to simulate lateral water-transport processes between an HRU to an HRU and was further connected to a nearby reach for reach routing. The schematic diagram of topological linkages between HRUs and Reach is shown in Figure 6.8, right. The distribution concept of HRUs keeps the

hru.par: HRU-Parameter fuer den Pegel in RabDud (400 Reliefeinheiten)

HRUID	x	y	elevation	area	type	to_poly	to_reach	slope	aspect	flowlengtl	soilID	landuseID	hgeoID
0	0	0	0	0	0	0	0	0	0	0	0	0	0
9999	9999999	9999999	10000	1E+10	3	9999	9999	90	360	999999	9999	9999	9999
n/a	m	m	m	m2	n/a	n/a	n/a	deg	deg	m	n/a	n/a	n/a
1	458216	3109220	5995	1062500	2	0	1	20.1	114.255	0	17	17	2
2	459841	3109079	6012	812500	2	0	1	26.5	284.117	0	17	19	2
3	458966	3107733	5736	6312500	2	0	118	17	115.11	0	17	222	1
4	470091	3108939	7588	687500	2	0	2	47.7	151.76	0	17	19	2
5	473341	3106939	7011	3437500	2	0	2	42	204.108	0	17	19	2
6	468341	3108579	7553	625000	2	0	2	54.6	168.622	0	17	19	2
7	476216	3105798	6374	1.7E+07	3	0	118	18.3	199.087	0	17	222	1
8	470966	3108579	7272	625000	2	0	2	43.9	194.246	0	17	19	2
9	457591	3108548	6017	125000	2	0	1	18.4	129.039	0	17	222	1
10	460591	3108220	6114	937500	2	0	1	31.5	250.735	0	17	19	2
11	466841	3107814	7257	1125000	2	0	2	44.3	115.23	0	17	19	2
12	469466	3108298	7074	62500	2	0	2	18.7	144.075	0	17	19	2
13	467466	3107720	7544	875000	2	0	118	46.5	112.68	0	17	222	1
14	468716	3107500	6577	1750000	2	0	118	22.4	208.4	0	17	222	1
15	469466	3107829	6982	437500	2	0	118	37.3	213.984	0	17	222	1
16	475216	3107281	7506	625000	2	5	0	49	202.703	0	17	19	2
17	457716	3107314	5914	312500	2	0	1	29.9	78.8598	0	17	17	2
18	459216	3107548	6002	750000	2	0	118	38.4	240.098	0	17	222	1
19	460716	3107329	6141	750000	2	0	118	33	338.349	0	17	222	1
20	467216	3106970	7123	750000	2	26	0	46.4	156.925	0	17	19	2
21	469716	3107298	6840	62500	2	0	51	42.3	211.696	0	17	19	2

Figure 6.9: An example of a HRU parameter table of the Dudh Kosi river basin

heterogeneous nature of the catchment by maintaining the high spatial resolution with many small polygons in higher hydrological dynamics (in areas such as steep slopes) whereas regions with lower dynamics (flat land) comprise a smaller number of larger polygons. This allows an efficient simulation of the hydrological dynamics with minimum redundancy.

The topologically connected lateral routing is calculated by a gradient analysis. In general, an HRU passes water to the adjacent HRU which has a lower elevation. However, lateral routing between HRUs has to be checked in case of HRUs representing glaciers ID. In glaciers, water flows within glaciers from the upper area to the lower area and joins the stream network originating from the glacier tongue and considered as overland flow (RD1). Hence, all the HRUs were manually checked if there is water flowing from a glacier-HRU to a non-glacier-HRU (HRU other than glacier area) and vice versa. If any HRU from a non-glacier-HRU is connected to a glacier-HRU through lateral routing, the water conveyed by the non-glacier HRUs (into Interflows (RD2 and RG1) and baseflow (RG2) will be vanished in the glacier HRU. Therefore, all such cases were corrected by changing the lateral routing sequence in the HRU parameter file. At the end, it was made sure that the glacier HRU routes only to glacier HRUs or to a stream reach. Similarly, no routing exchange between glacier and non-glacier HRUs was allowed in the model application to take place.

The HRU parameter file stores the spatial attributes of the catchment area where information about elevation, area, aspect, coordinates, land-use type, hydrogeology and soil is stored for each HRU. The HRU parameter file of the Dudh Kosi river basin is provided in Figure 6.9. For example, as indicated in Figure 6.9, the HRU ID 1 contributes water directly to REACH ID 1 whereas HRU ID 16

contributes water to HRU ID 5 which then contributes to REACH ID 2. The interactions between the parameter files were solved by a relation between the soil, land use and hydrogeological descriptors in the HRU parameter file and respective descriptors in the other parameter files.

6.8 Modelling strategies

6.8.1 Calibration and validation

Calibration is a process in which parameter adjustments are made to obtain a better fit between observed and simulated variables. A desired model accuracy is achieved by changing the model-parameter values until a "satisfactory" agreement between simulated and recorded variables is obtained (Refsgaard and Storm 1996, Gupta and Beven 2005). The objective of the calibration process is to minimize the errors due to non-optimal parameter values (Gupta and Beven 2005) and to obtain best possible results.

Three different methods have been reviewed by Gupta and Beven (2005). They are: i) the manual trial-and-error method, ii) automatic or numerical parameter optimization and iii) a combination of both methods. The trail-and-error method implies a manual parameter assessment through a number of simulation runs. This method has been widely used especially for more complicated models including those of a distributed type. This method is recommended when a good graphical representation of the simulation results is a prerequisite. The automatic method uses a numerical algorithm over a large number of iterations to optimize the objective functions in a systematic approach. The main idea of this method is to search through as many combinations of parameter sets as possible to achieve a set which is the optimum or ‘best’ in terms of satisfying the criterion of accuracy. This process is fast and carried out by computers and is less subjective than the trail-and-error method. The third method involves a combination of the first and second methods, regardless of which comes first. In this study, the third method was used. The advantage of this method is the possibility of defining clear adjustable model-parameter boundaries.

A distributed modelling system such as the J2000 hydrological model involves a relatively large number of calibration parameters to be optimized during model setup. For model calibration, all 36 parameters were used. The calibration parameters associated with different modules are provided in Table 6.9. The calibration was achieved by the combination of trial-and-error and automatic methods as described earlier. At first, the trial-and-error method was applied by varying every single parameters. The calibration strategy was to initially simulate the long-term water balance correctly and then to simulate the distribution of different hydrological dynamics (such as high peaks and baseflow). In this process, reasonable upper and lower limits of adjustable parameters are determined. Sensitivity analysis (Section 6.8.3) was conducted as a part of automatic calibration. From this process, information about higher and moderate sensitive parameters were obtained. After that effort, a finer adjustment of those calibration parameters was made in order to attain the best fit between observed and simulated values. The higher and moderate sensitive parameters were responsible for visible and prominent variation in the model results.

For this study, the model was first applied in the **Dudh Kosi river basin** using input data from 1985 through 1997 on a daily basis. However. the entire time series data for this period was split up into 1986-1991 for the calibration and 1992-1997 for the validation period. The first year is considered as an initialisation period. Model quality was quantified by the data from the validation period which were not used for the model calibration. By using the split-sample-test Klemes (1986), evidence is given that the model calibration parameter set represents the hydrological process dynamics adequately not only during the calibration period but also when using independent data during the validation period. After a successful application in the Dudh Kosi river basin, the parameters were transferred to the other sub-basin of the Kosi river, the **Tamor river basin**, using a proxy-basin test approach. The proxy-basin test should serve as a basic test for geographical transposability of a model, i.e. transposability within this region. This approach is useful for obtaining information for ungauged catchment areas from a gauged one (Klemes 1986, Refsgaard et al. 1995). This approach indicates the robustness of the model which can be applied in other catchments of similar climatological and physiographic conditions.

6.8.2 Evaluation of the model performance

The evaluation of hydrological model behavior and performance is useful to provide a quantitative estimation of the model's ability to reproduce watershed behavior (Krause et al. 2005). In general, the model performance should be assessed on the basis of both visual inspection and numerical evaluation of the model's results. This is because a good statistical agreement might not necessarily mean that the model has predicted the hydrological behavior with sufficient accuracy involving different components such as water balance. The selection and use of specific efficiency criteria can be challenging, because each criterion may place different emphasis on different types of simulated and observed behaviors.

Because a single efficiency criteria often cannot measure the complete and reliable picture of the model performance, a combination of different objective functions is proposed. In this study, three different efficiency criteria are applied: coefficient of determination (r^2), Nash-Sutcliffe (E_{NS}), and Logarithm Nash-Sutcliffe (LNS).

The r^2 is defined as the squared value of the coefficient of correlation. It is defined as:

$$r^2 = \left(\frac{\sum_{i=1}^{n}(O_i - \overline{O})(P_i - \overline{P})}{\sqrt{\sum_{i=1}^{n}(O_i - \overline{O})^2} \cdot \sqrt{\sum_{i=1}^{n}(P_i - \overline{P})^2}} \right)^2 \tag{6.8.1}$$

In this equation, i is the time step, O and P are observed and predicted values. The value of r^2 ranges between 0 and 1. A value of zero indicates no correlation at all and a value of 1 means that the dispersion of the prediction is perfectly equal to that of the observation. The major drawbacks of r^2 is that only the dispersion is quantified. The r^2 could be higher value in the case where a model systematically over- or under-predicts all the time even if the predictions were wrong (Krause et al. 2005).

The limitation of r^2 can be overcome in conjunction with an efficiency criterion known as the Nash-Sutcliffe (E_{NS}) (Nash and Sutcliffe 1970) criterion. This has been widely used in the field of hydrological modelling. E_{NS} is defined as one minus the sum of the absolute squared differences between the predicted and observed values normalized by the variance of the observed values during the period under investigation. It is defined as:

$$E_{NS} = 1 - \frac{\sum_{i=1}^{n}(O_i - P_i)^2}{\sum_{i=1}^{n}(O_i - \overline{O})^2} \tag{6.8.2}$$

The range of E_{NS} lies between 1 (perfect fit) and $-\infty$, with better results close to 1. An efficiency lower than zero indicates that the mean value of the observed time series would have been a better predictor than the model. The greatest disadvantage of this approach is the fact that the differences between the observed and predicted values are calculated as squared values. As a result larger values in a time series are strongly overestimated whereas lower values are neglected (Legates and McCabe 1999). This tendency leads to an over-estimation of the model performance during peak flows and an under-estimation during low flow conditions. Similar to r^2, the E_{NS} is not very sensitive to systematic model over-or under-prediction especially during low-flow periods (Krause et al. 2005).

Krause et al. (2005) suggested that to reduce the problem of the squared differences and resulting sensitivity to extreme values, the E_{NS} should be calculated with logarithmic values of observed and predicted time series known as Logarithm Nash-Sutcliffe (LNS). The resulting LNS flattens the peaks and low flows are kept more or less at the same level. As a result, the influence of the low-flow values is increased in comparison with the flood peaks.

In addition to the statistical evaluation of the model performance, sensitivity and uncertainty analysis are conducted to assess the robustness of the model and discussed in subsequent section.

6.8.3 Sensitivity analysis

Sensitivity analysis is a process to determine how sensitive a model structure and estimated parameter(s) is with regard to its output. It aims to describe how much model output values are affected by changes in model input values. A sensitivity analysis of a model helps to understand the nature of model parameters in term of their influence on the total outputs. Sensitivity analysis is potentially useful in all phases of the modelling process: model formulation, model calibration and verification (McCuen 2005). Therefore, for any model, it is necessary to find out which parameters are sensitive and should be taken into account during an optimization process. The process also reveals the few or no sensitive parameters which can be put to a constant value to make the optimization process simpler (Jansson et al. 2003).

In this study, Regional Sensitivity Analysis (RSA) (Hornberger and Spear 1981, Spear and Hornberger 1980) (also called generalized sensitivity analysis) has been used to analyse the sensitivity of the model parameters. This method estimates the impact of a number of parameters and their interactions in the model output. RSA is a method of assessing the sensitivity of model parameters where sensitivity is defined as the effect of the parameters on the overall model performance as indicated by

objective functions. The general concept of applying RSA is to split the various model samples into good (behavioral) and bad (non-behavioral) populations and to compare their distribution functions in the objective function space. The parameter sets are split into groups based on their likelihood. For each group the likelihoods are normalized dividing by their total, and the cumulative frequency distribution is calculated and plotted. If the model performance is sufficiently sensitive to a particular parameter there will be a large difference between the cumulative frequency distributions, i.e. the parameter has a significant effect on the model output (Wagener et al. 2001).

Sixteen effective model parameters, out of 36, were selected for the sensitivity analysis principally based on a study Baese (2005) and experiences from the 'trial-and-error' method during the calibration process. The same 16 parameter set was used for uncertainty analysis as well which is discussed in Section 6.9.6. The other model parameters were not included because their sensitivity was judged to be quite low during the trail-and-error. The parameter ranges were specified within upper and lower boundaries are provided in Table 6.9. The trial-and-error process during calibration of the parameters was instrumental in defining those boundaries. The range was even reduced for sensitivity analysis to include only behavioural simulations. The parameters in bold letters in Table 6.9 were the 16 effective parameters used for the sensitivity analysis.

The Monte Carlo Analysis (MCA) was conducted using all 16 parameters to produce 1,600 simulations. A random sampling method was used where the values of the parameters were chosen within the range provided. The two objective functions E_{NS} and r^2 were used for the analysis.

The 1,600 simulations were further analysed by using the RSA method. The large difference between the cumulative frequency distributions of the parameters sets indicates the higher sensitivity. An example of the RSA of high and low sensitive parameters are provided in Figure 6.10. Figure 6.10(a) which has higher difference between the parameter set indicates the higher sensitivity of the parameter to the model performance and vice versa for Figure 6.10(b). The RSA of 16 parameters with two objective functions is provided in Appendix E, page 217. Figure 6.11 provides a comprehensive depiction of the sensitivity of the parameters based on RSA with different objective functions. The parameter ranking was done by the normalization of each parameter based upon its sensitivity as suggested by Fischer et al. (2012). The more sensitive parameters get higher stakes in the figure. For example, as shown in Figure 6.11, the *soilLatVertLPS* is the most sensitive parameter based upon the efficiency criteria (E_{NS}) where this parameter explained 23 percent of the variation in model results. The parameters *LatVertDistLPS* and *soilConCRD1* are the most sensitive parameter in both objective functions. With (E_{NS}), parameters *soilConcRD2*, *gwRG2Fact*, *baseTemp*, *soilLinRed* and *soilConcRD1flood* are moderately sensitive. The other parameters are less sensitive. With r^2, *gwRG2Fact*, *soilConcRD2*, *soilLinRed*, *soilConcRD1flood*, and *soilMaxPerc* are moderately sensitive.

6.9 Modelling results

In this section, the modelling results from the Dudh Kosi river basin are described. The model was run on a daily basis with the calibrated parameters as described in the previous section. The model performance during calibration and validation periods is described in Section 6.9.5. The model evalu-

Table 6.9: Calibration parameters of the J2000 hydrological model

Parameters	Descriptions	Actual value	Range
PRECIP DISTRIBUTION			
Trs	base temperature	0	-1 - +1
Interception Module			
a_rain	interception storage for rain	1.0	0 - 5
a_snow	interception storage for snow	1.28	0 - 5
SNOW MODULE			
snowCritDens	critical density of Snow	0.381	0 - 1
snowColdContent	cold content of snow pack	0.0012	0 - 1
baseTemp	**threshold temperature for snowmelt**	0	-5 - +5
t_factor	**melt factor by sensible heat**	2.84	0 - 5
r_factor	melt factor by liquid precipitation	0.21	0 - 5
g_factor	melt factor by soil heat flow	3.73	0 - 5
GLACIER MODULE			
meltFactorIce	**melt factor for ice melt**	2.5	0 - 5
alphaIce	radiation melt factor for ice	0.2	0 - 5
kIce	routing co-efficient for ice melt	10	0 - 50
kSnow	routing co-efficient for snowmelt	5	0 - 50
kRain	routing co-efficient for rain runoff	5	0 - 50
debrisFactor	debris factor for ice melt	3	0 - 10
tbase	**threshold temperature for snowmelt**	-1	-5 - +5
SOIL MODULE			
soilMaxDPS	maximum depression storage	2	0 - 10
soilLinRed	**linear reduction co-efficient for AET**	0.6	0 - 10
soilMaxInfSummer	**maximum infiltration in summer**	60	0 - 200
soilMaxInfWinter	**maximum infiltration in winter**	75	0 - 200
soilMaxInfSnow	maximum infiltration in snow cover areas	40	0 - 200
soilImpLT80	infiltration for areas lesser than 80% sealing	0.5	0 - 1
SoilDistMPSLPS	MPS-LPS distribution coefficient	0.27	0 - 10
SoilDiffMPSLPS	MPS-LPS diffucusion coefficient	0.1	0 - 10
soilOutLPS	outflow coefficient for LPS	0.3	0 - 10
soilLatVertLPS	**lateral vertical distribution coefficient**	0.5	0 - 10
soilMaxPerc	**maximum percolation rate to groundwater**	10	0 - 100
soilConcRD1Flood	**recession coefficient for flood event**	1.3	0 - 10
soilConcRD1Floodthreshold	threshold value for soilConcRD1Flood	300	0 - 500
soilConcRD1	**recession coefficient for overland flow**	2.8	0 - 10
soilConcRD2	**recession coefficient for Interflow**	3	0 - 10
GROUNDWATER MODULE			
gwRG1RG2dist	**RG1-RG2 distribution coefficient**	2.1	0 - 5
gwRG1Fact	**adaptation for RG1 flow**	0.3	0 - 10
gwRG2Fact	**adaptation for RG2 flow**	0.5	0 - 10
gwCapRise	capillary rise coefficient	0.01	0 - 10
REACH ROUTING			
flowRouteTA	**flood routing coefficient**	1.3	0 - 10

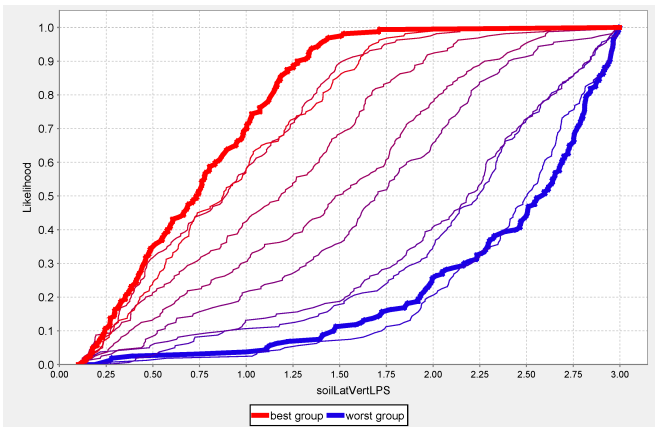

(a) RSA of soilLatVertLPS parameter

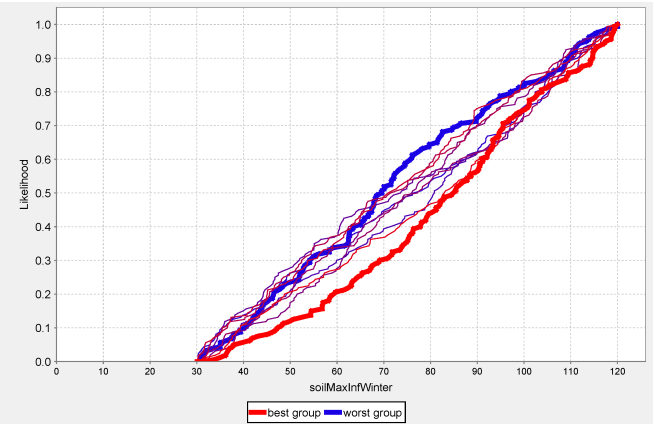

(b) RSA of soilMaxInfWinter parameter

Figure 6.10: Regional Sensitivity Analysis of the parameters with Nash-Sutcliffe efficiency. The red line shows the cumulative distribution function of the behavioral parameter set and blue shows the non-behaviour set

ation was done using a split-sample-test (Klemes 1986) where the time period 1985-1997 was divided into two periods. The first-half period (1986-1991) is considered as a calibration period and second-half (1992-1997) as a validation period. The first year was considered as the model-initialization period. The hydrological systems analysis (such as evapotranspiration, snow and glacier melt and runoff components) based on the model outputs are described by considering outputs from 1986-1997 in subsequent sections.

6.9.1 Simulated precipitation

Inverse Distance Weighting (IDW) was used for the regionalisation of the precipitation data as described in Section 6.4. The elevation-correction factor was not used, because of the fairly low density

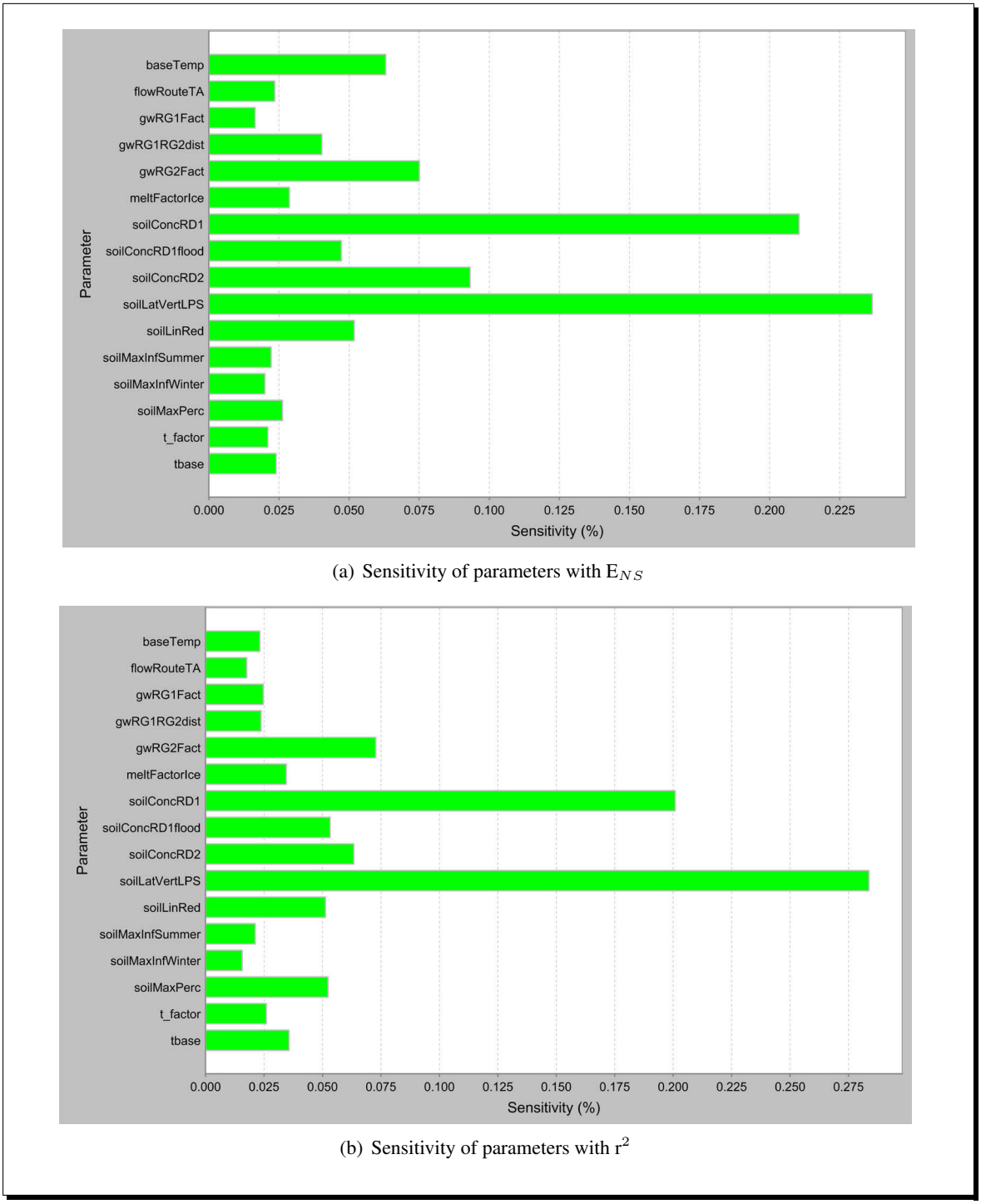

(a) Sensitivity of parameters with E_{NS}

(b) Sensitivity of parameters with r^2

Figure 6.11: Ranking of the selected parameters using different objective functions. The y-axis indicates the 16 model parameters used in this analysis.

Figure 6.12: A typical rainfall station (red circle) located in the Dudh Kosi river basin.

precipitation network in the model-calibration phase of the study. It was found that, by using the elevation correction factor, the simulated precipitation is high in some particular cases. In case there was an increase in precipitation with an elevation in station values, the model simulates a higher amount of precipitation in upstream areas. This is because there are few precipitation stations in the Dudh Kosi river basin. Particularly, the northern part of the basin where most of the high elevation areas are located, does not have any precipitation station (Figure 6.4). The IDW, without elevation correction, is able to reduce such errors. Before the IDW, the precipitation data were corrected by using the Richter approach (Section 6.4.2). This approach has increased the overall precipitation amounts by about 11 percent considering the evaporation and wind errors. The simulated average annual precipitation between the modelling period (1986-1997) is 2,114 mm/year. The regionalisation of the precipitation data is always a challenging task in the mountainous region, especially in the Himalayan region, because of a smaller network of precipitation stations and also due to the variation of the spatial distribution of precipitation in the region. The precipitation is generally underestimated because the stations are located in low elevation areas and valleys as discussed in Section 5.4. The similar result is also indicated by Sharma (1997) in the Tamor sub-basin of the Kosi river basin. Figure 6.12 shows a typical rainfall station in the high elevation areas of the Dudh Kosi river basin. The station is located about 2,600 m and the nearby mountains are about 5,000 to 6,000 m high.

The precipitation pattern in the high-altitude areas of the Dudh Kosi river basin is discussed in Section 5.4.2.2, page 58. The discussion in general suggests that there is variation in precipitation amount in the river valleys and mountains. The mountain and ridges receive nearly four to five times higher precipitation amount than river valleys. At the same time, the precipitation generally decreases to the

Higher Himalayan region as the moisture content of cloud decreases in the high-altitude areas.

6.9.2 Simulated evapotranspiration

First potential evapotranspiration (PET) for the basin is calculated as described previously in Section 6.4.4. The value of actual evapotranspiration (AET) is then calculated depending upon the water availability in different storage components. As indicated in Figure 6.13, it can be seen that the AET is higher in lower elevation areas and gradually decreases to the higher elevation areas. The average annual PET and AET of the entire basin were calculated to be 527 and 428 mm respectively. The highest evapotranspiration zone lies in the range of 500-1,000 m which is the lowest elevation in the area. In the higher elevation areas, the PET is in the range of 200-300 mm. In few HRUs, the AET is found to be high in the range of 2,000 mm because of the cascading effects of HRUs. The HRUs which get water from upper HRUs results the higher AET on that particular HRU. The same HRU when run without cascading (running the model in a single HRU) showed the lower amount of AET.

Figure 6.14 indicates the average monthly PET and AET in the study area. The AET is close to the PET during the monsoon season which indicates that the water availability during this period is quite high. During the winter season (December through February), both PET and AET remain low. The pre-monsoon period (April and May) experiences the highest PET and AET because of higher temperature, more sunshine hours and higher wind speed compared to other months and water availability is maintained through soil-moisture storage. Although, the water availability is high during the monsoon season, the other parameters affecting evapotranspiration such as wind speed and sunshine hours (duration) are relatively low.

The PET calculated by the J2000 model was compared to the observed data from the Okhaldhunga station (1,720 m) measured by using a Class "A" evaporation pan. The model results are from a single HRU with same elevation of the station. Because data were not available for a longer period, the annual value of 1985 which had no data gaps is compared . The measured (station) and simulated (from the J2000 model) annual PET for the year 1985 was 1,180 mm and 1,223 mm. The coefficient of determination (r^2) of monthly values is 0.86. Sharma (1997) has developed an equation for Nepal relating Class A pan evaporation with elevation. According to this equation, the PET value for the elevation similar to the Okhaldhunga is close to the observed values. Therefore, PET values estimated in this study can be assumed representative for the study area.

6.9.3 Soil moisture conditions

The soil-moisture condition in the J2000 model is characterized by the water content in the Large Pore Storage (LPS) and Middle Pore Storage (MPS). As indicated in Figure 6.15, the soil condition of the MPS is fully saturated during the monsoon season because of higher precipitation. The maximum saturated MPS is nearly 86 percent because 14 percent of the study area has glaciers where no soil horizon is assumed in the model (Section 6.5.5). The LPS is filled primarily during the monsoon season when the MPS is fully saturated and the excess water is allocated to the LPS. A gradual decrease

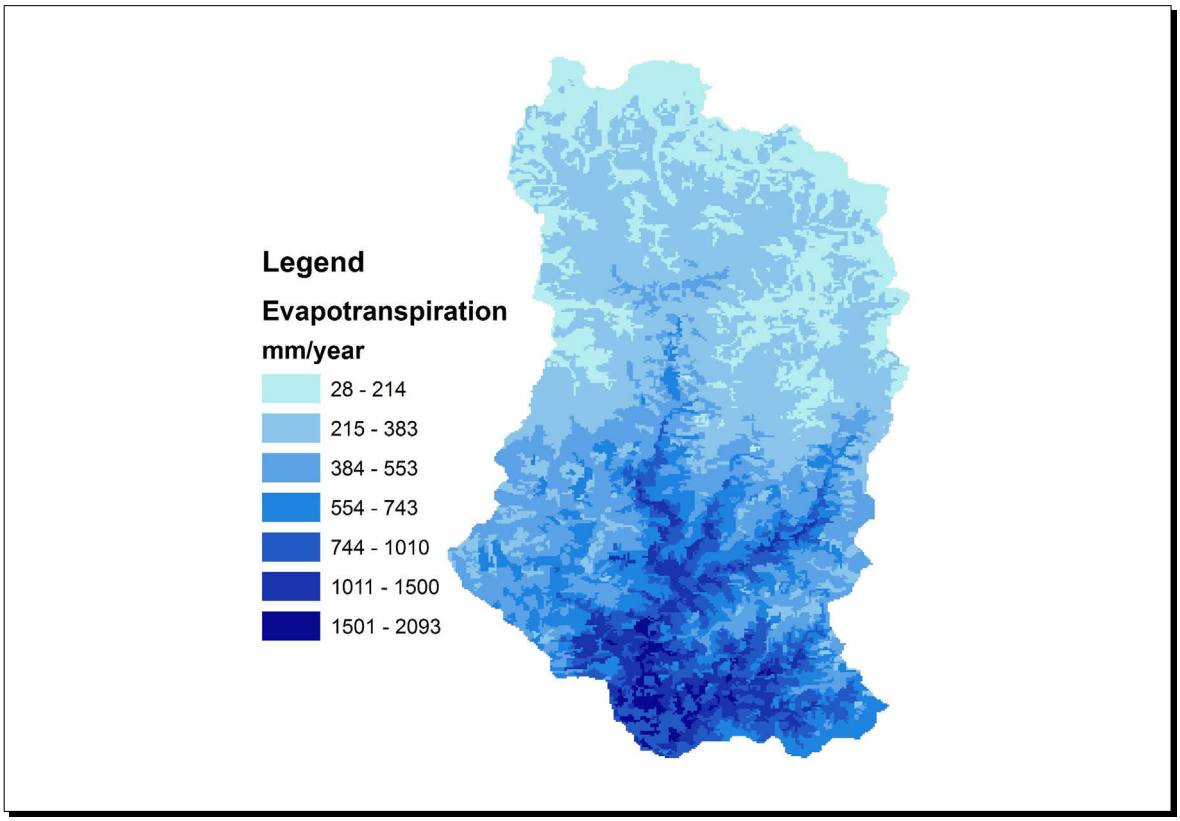

Figure 6.13: Actual evapotranspiration estimated based on potential evapotranspiration derived from Penman-Monteith method

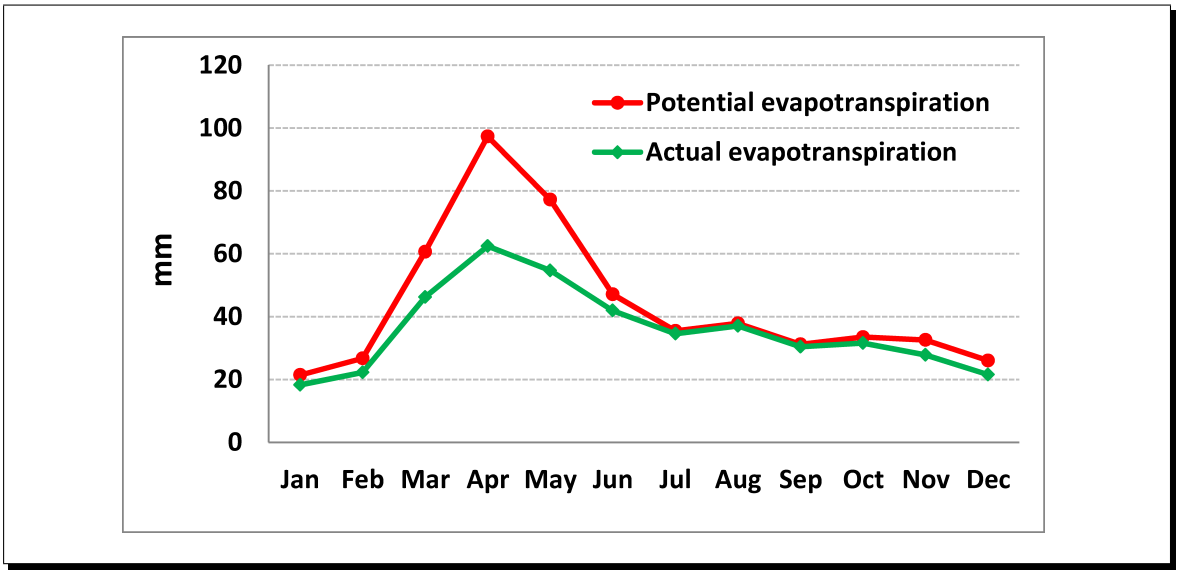

Figure 6.14: Monthly average potential (PET) and actual evapotranspiration (AET) estimated by the model using the Penman-Monteith method (1986-1997)

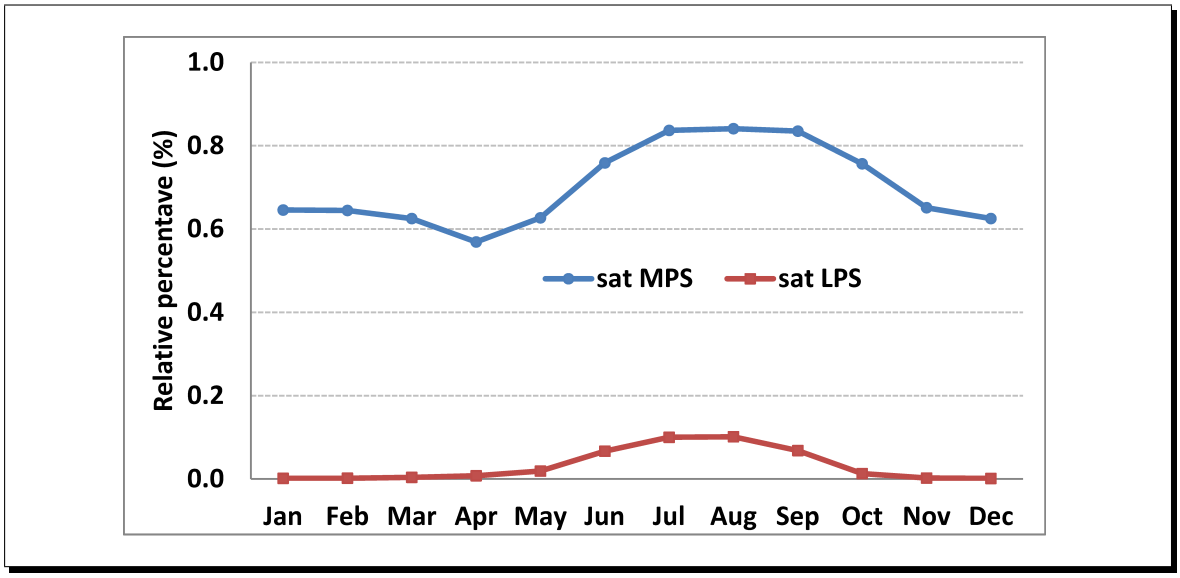

Figure 6.15: Monthly average saturated MPS (sat MPS) and LPS (sat LPS) (1986-1997)

in the MPS during the pre-monsoon period is related to evapotranspiration (Figure 6.14) when the AET is increased during the same time period. A favorable condition of higher evapotranspiration during that period consumes water from the MPS.

6.9.4 Interception

Interception storage is a significant part of the water balance. The most important role of this hydrological component is serving as a rainfall reducer. This causes a significant amount of rainfall to be directly returned back to the atmosphere through evapotranspiration which is not available for infiltration (Gerrits 2010). The average annual interception storage is 186 mm which represents about 9 percent of the total rainfall. The interception has a distinctive seasonal pattern with higher interception of about 64 percent during the monsoon season. Figure 6.16 shows the results of the monthly variation of interception. The maximum daily interception is about 4 mm occurring predominately during the monsoon season. The maximum interception storage is found to be occurred during the months of May to September in the range of 22-33 mm per month.

6.9.5 Hydrograph analysis

The model performance during the calibration (1986-1991) and validation (1992-1997) periods is discussed in this section. Figure 6.17 provides the model results during the calibration period using the calibrated parameters described in previous sections. The global parameter sets derived from the calibration period is also applied for the validation period. The result of the validation period is provided in Figure 6.18. The model performance is validated by using the daily observed data at Rabuwabazaar (Station 670) stations for both periods. In general, the model is able to reproduce the

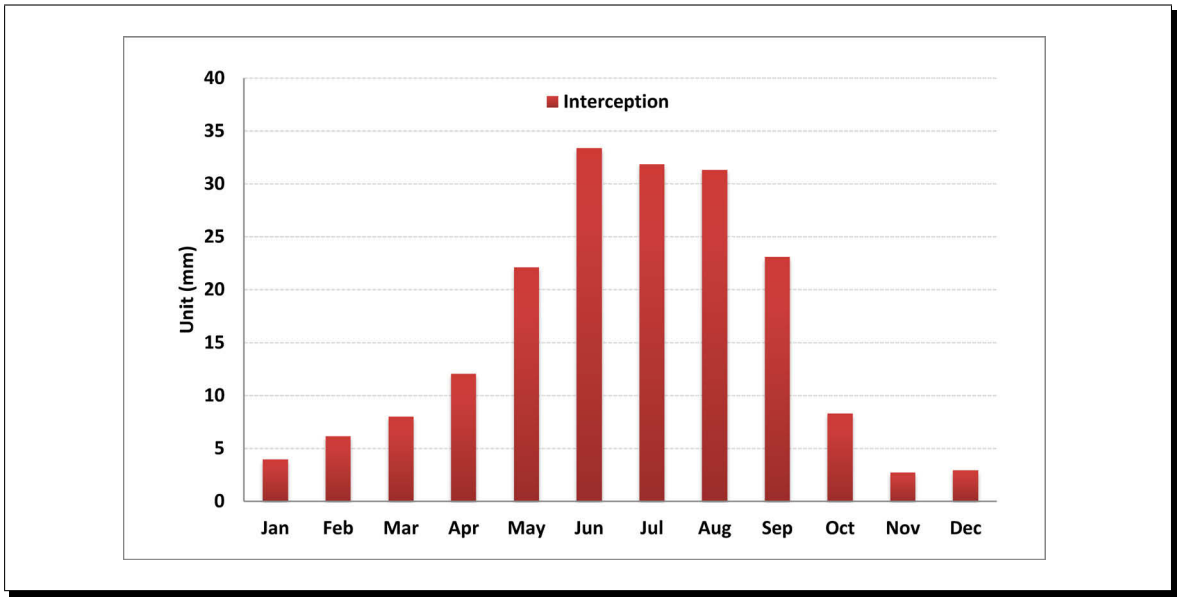

Figure 6.16: Average monthly interception storage (1986-1997)

overall runoff dynamics of the basin fairly well based upon the graphical and statistical evaluation which is discussed in subsequent sections.

6.9.5.1 Representation of low range flows

The baseflow which mostly results from the groundwater contribution is well represented in most of the years, although over-and under-predictions can be seen in the two initial years of the calibration period. The groundwater is recharged during the monsoon period and then gradually released in the form of baseflow. Right after the monsoon period, the contribution from sub-surface flow (or interflow) is high. Interflow is mostly attributed from the unsaturated zone of the soil (also called the vadose zone). When the soil moisture in the unsaturated zone is gradually depleted during the post-monsoon period, the more stable source of groundwater is expected from the saturated zone (or groundwater table). The groundwater reservoirs in two different geological storages and their runoff behaviors in the J2000 modelling system have simulated the recession period fairly well in the monsoon-dominated climate.

Similarly, the rising limbs during the pre-monsoon period (March-May) are reproduced fairly good by the model, although, both under-and over-prediction of daily streamflows are observed in both calibration and validation period. Streamflows during the pre-monsoon period are derived primarily from two sources. The baseflow from the groundwater is supplemented by the contribution from snow and glacier melt. The snow and glacier melt approaches of the model are able to capture the general pattern of increasing streamflow characteristics that occur mostly during the month of May. Starting in June, the melt runoff is mixed up with seasonally high precipitation and therefore difficult to distinguish. Moreover, the snow and glacier melt during the monsoon period are a function of several factors, such as temperature, radiation, albedo, soil fluxes and energy balance etc. In addition,

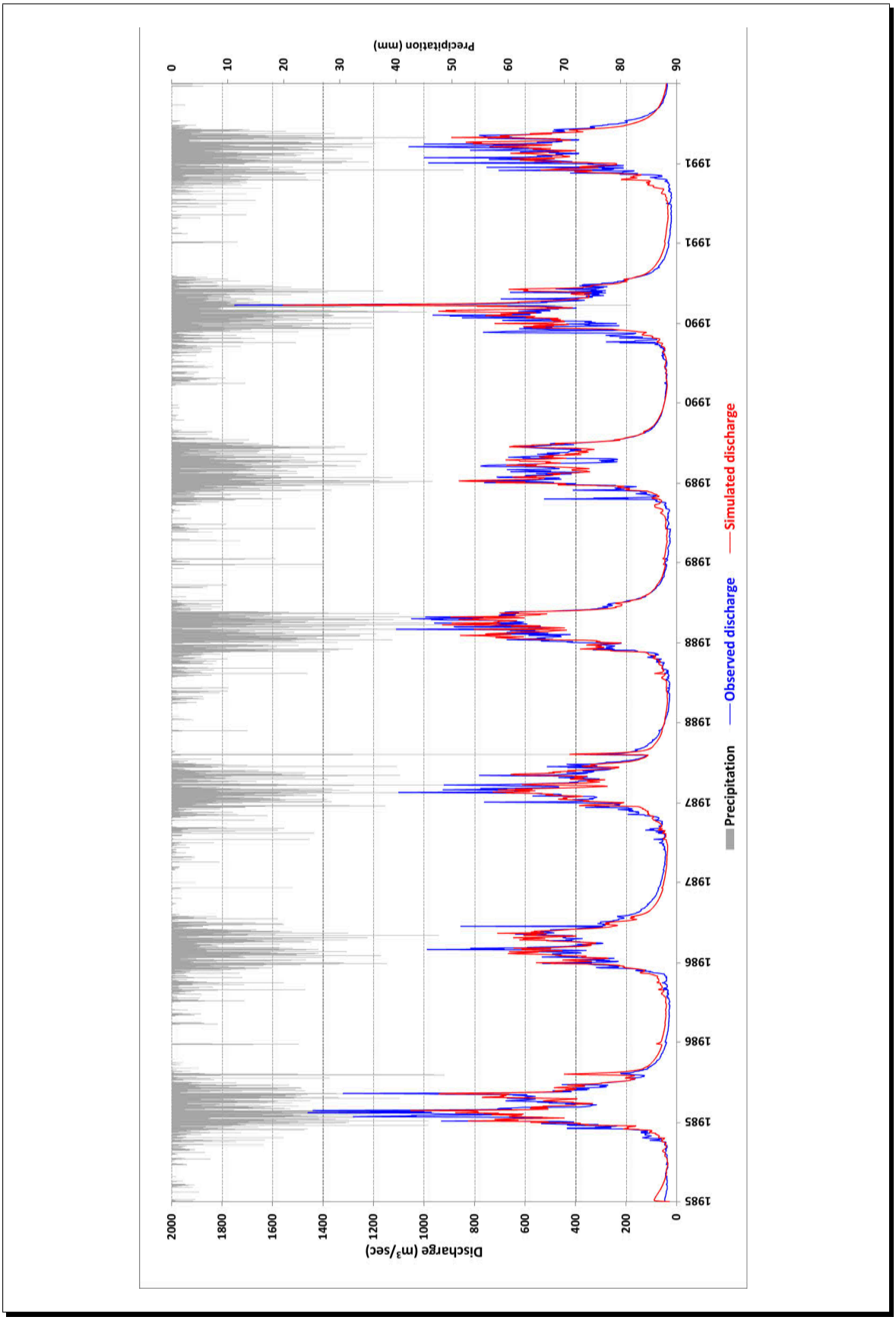

Figure 6.17: Observed and simulated discharge during the calibration period (1986-1991) in the Dudh Kosi river basin. The red and blue lines represent simulated and observed discharge. The daily mean precipitation (grey) is shown in upper panel.

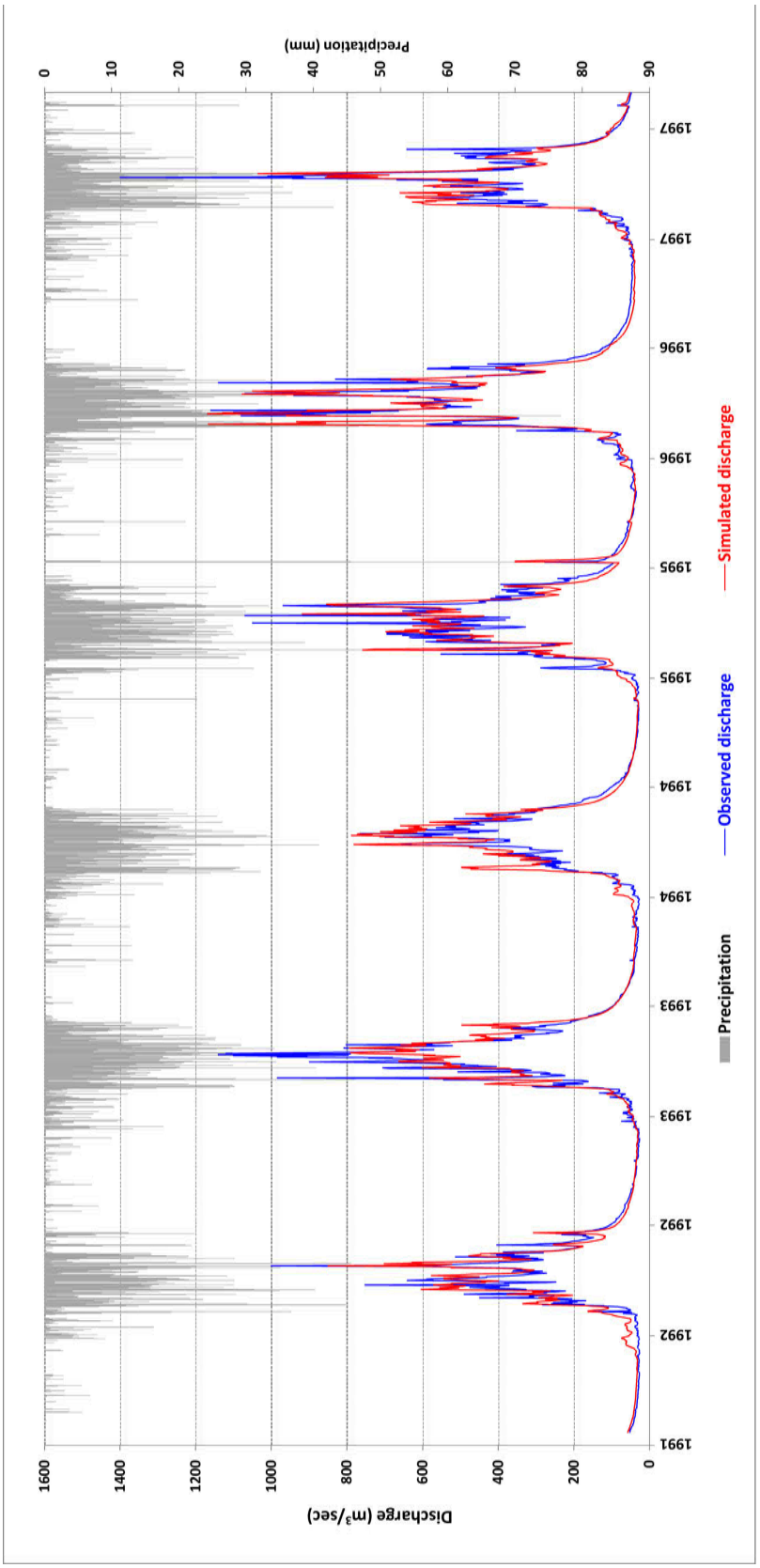

Figure 6.18: Observed and simulated discharge during the validation period (1992-1997) in the Dudh Kosi river basin. The red and blue lines represent simulated and observed discharge. The daily mean precipitation (grey) is shown in upper panel.

the complex phenomenon of glacier melt such as subsurface water storage and flow under the glacier surface is difficult to reproduce because of the complex dataset required for calculation. Such a dataset in the study area was not available . However, the snow module (J2kProcesssnow) and glacier module (improvised degree-day factor) implemented and adapated in this study were able to produce the general increasing pattern of streamflows during the pre-monsoon period.

6.9.5.2 Representation of floods

The flood periods during the monsoon season are also well reproduced by the J2000 model application, although some under- and over-prediction can be seen. During the calibration period, the most visible flood under-prediction occurred in 1990 and 1991, principally during the months of June and July. Similarly, in the validation period, flows for the year 1993 is under-predicted during the monsoon period and 1994 is over-predicted in most of the flood months.

The model has predicted the streamflows during the extreme precipitation event fairly well in October 1987. Normally in this month the precipitation amount is low, however, the relatively higher soil moisture prevails as the monsoon occurs until September. The model also simulates flood peaks fairly good, which mostly occur during the monsoon period, although some variation in the form of over- and under-prediction can be seen. The high peaks in 1990, 1996 and 1997 are well-represented by the model simulation results. However, peaks during 1987, 1991, and 1993 were underestimated. The highest flood peak during the period is on 12 August 1990 where the model simulates the recorded streamflow fairly well. The reason for the well-matching results is the high value of precipitation on that day which was distributed to all precipitation stations.

The introduction of a new parameter (*soilConcnRD1Flood*) into the soil module of the J2000 hydrological model has improved the results in obtaining flood peaks. The original model has a parameter called (*ConcRD1*) which acts as a recession coefficient for overland flow with a single value for the entire year. The new value is activated when the output value of RD1 reaches a threshold set by a model user. The high value of RD1 is expected during the monsoon season when there is continuous rainfall and subsequently the soil is saturated. In such cases, the rainfall-runoff coefficient becomes higher as the infiltration capacity of the soil is reduced and most of the rainfall is drained as a overland flow. The new parameter increases the rainfall-runoff coefficient (compared to *concRD1*) and therefore a greater amount of overland flow is realised. The saturated soil condition is perceived in the model when there are higher or frequent rainfall events and the MPS and LPS are filled with water which leads to the reduction of the infiltration capacity of the soil. The new parameter realises the non-linear behavior of a catchment under specific conditions when fully saturated soil causes higher overland flow. Figure 6.19 shows the comparison of the two hydrographs with versus without the use of the new parameter. Figure 6.19(a) is without the new parameter and uses the same value (recession coefficient for RD1) for the entire period. Figure 6.19(b), on the other hand, is an output with the use of a new parameter. The clear difference can be seen during the high flood peaks period in 1990. Similar favorable results were observed in 1996 and 1997 during high flood peaks.

The efficiency results of the model performance is provided in Table 6.10. It indicates good performance between observed and simulated discharge. This shows that the model is equally good in both

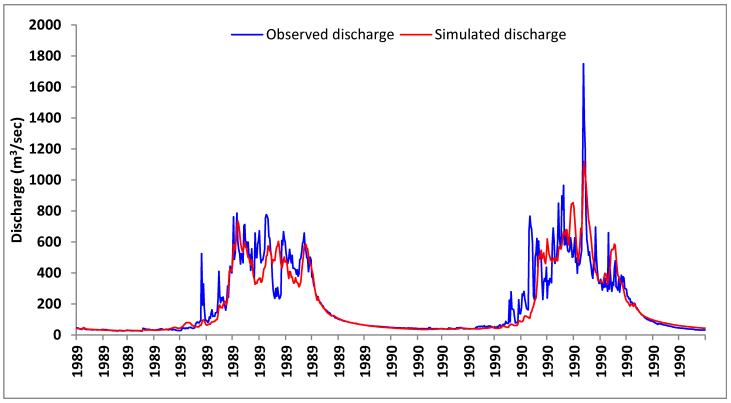

(a) Model results with concRD1 parameter

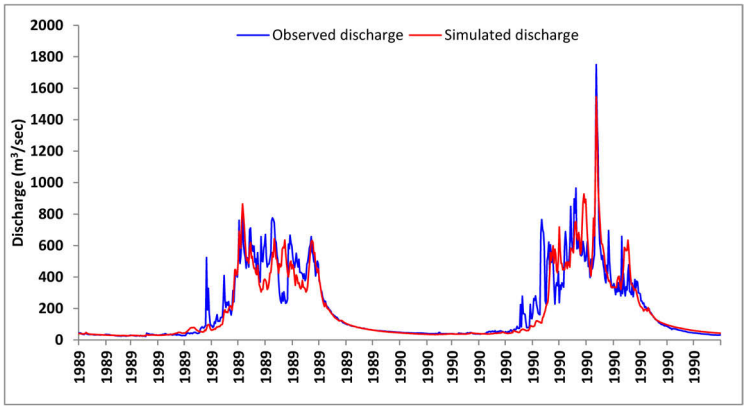

(b) Model results including concRD1Flood parameter

Figure 6.19: Difference in model results when using a new parameter

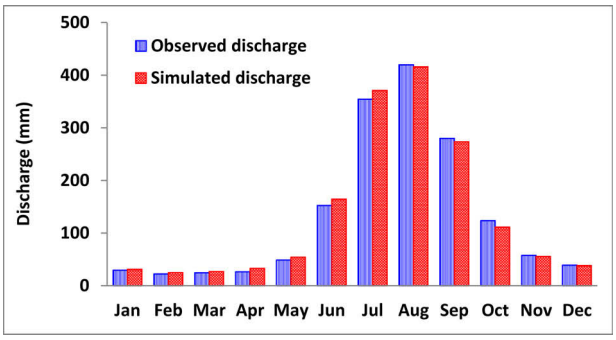

(a) Average monthly observed and simulated discharge

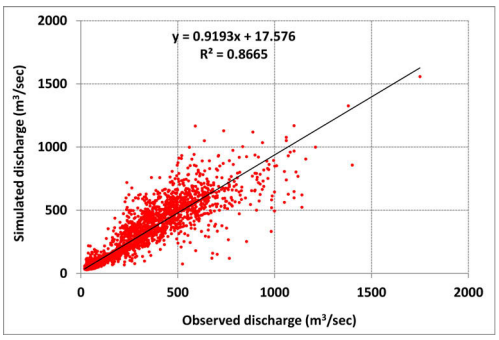

(b) The scatter plot between daily observed and simulated discharge

Figure 6.20: Model results of observed and simulated streamflow (1986-1997)

calibration and validation periods, with a slightly improved result for the validation period.

The comparison of average monthly simulated and observed runoff (Figure 6.20(a)) indicates a reasonably good fit throughout the year for this period of record (1986-1997). The simulation of the low-flow period is quite good and high-flow months are slightly over- and under-estimated. Figure 6.20(b) shows the scatter plot between daily observed and simulated runoff. In general, the agreement looks good except for some more extreme outliers during high-flow period towards the observed runoff side.

Table 6.10: Efficiency results during calibration and validation periods

Objective Functions	Calibration	Validation	Whole period
E_{NS}	0.84	0.87	0.85
LNS	0.90	0.95	0.93
r^2	0.85	0.88	0.86

6.9.6 Uncertainty analyses

Outcomes or events that cannot be predicted with certainty are often called risky or uncertain (Loucks et al. 2005). The results from hydrological models are subject to uncertainties from different sources. The usefulness of any model depends upon the accuracy and reliability of its output. Uncertainty analyses as methodological tools provide a general basis for the evaluation of model performance (Weichel et al. 2007, Crosetto and Tarantola 2001). Therefore, for effective decision-making processes using modelling results, the uncertainty associated with model predictions has to be properly assessed.

The hydrological model incorporates a significant amount of uncertainty which may arise from different sources. Walker et al. (2003), Beven (2001b), Beven and Freer (2001) describe uncertainty based on its location within the whole model complex. The first source of uncertainty is related to the model context i.e. the implemented processes and algorithms in the model structure as it is always a simplified description of the processes as compared to nature. The second source of uncertainty comes from the input data used to operate or run the model which can carry systematic or random errors. The data used to validate the model results also contain significant errors. The third source of uncertainty is model-parameter uncertainty which is associated with the data and method used to calibrate the model parameters. Krause et al. (2009) noted that model approaches which use many calibration parameters imply parameter uncertainties which might significantly affect model results. In addition, "equifinality" is a concept associated with model parameters and structures which suggest that different sets of estimated model parameters may produce similar model results (Beven 2001b, Beven and Freer 2001).

For this study, the General Likelihood Uncertainty Estimation (GLUE) method (Beven and Binley 1992) is applied for the uncertainty estimation. GLUE is a procedure for uncertainty assessment based on Monte Carlo (MC) simulations. It has been widely applied in hydrology and environmental modelling to estimate the uncertainty associated with model outputs and parameter estimates (Beven and Binley 1992, Beven and Freer 2001, Montanari 2005). The advantage of GLUE compared to

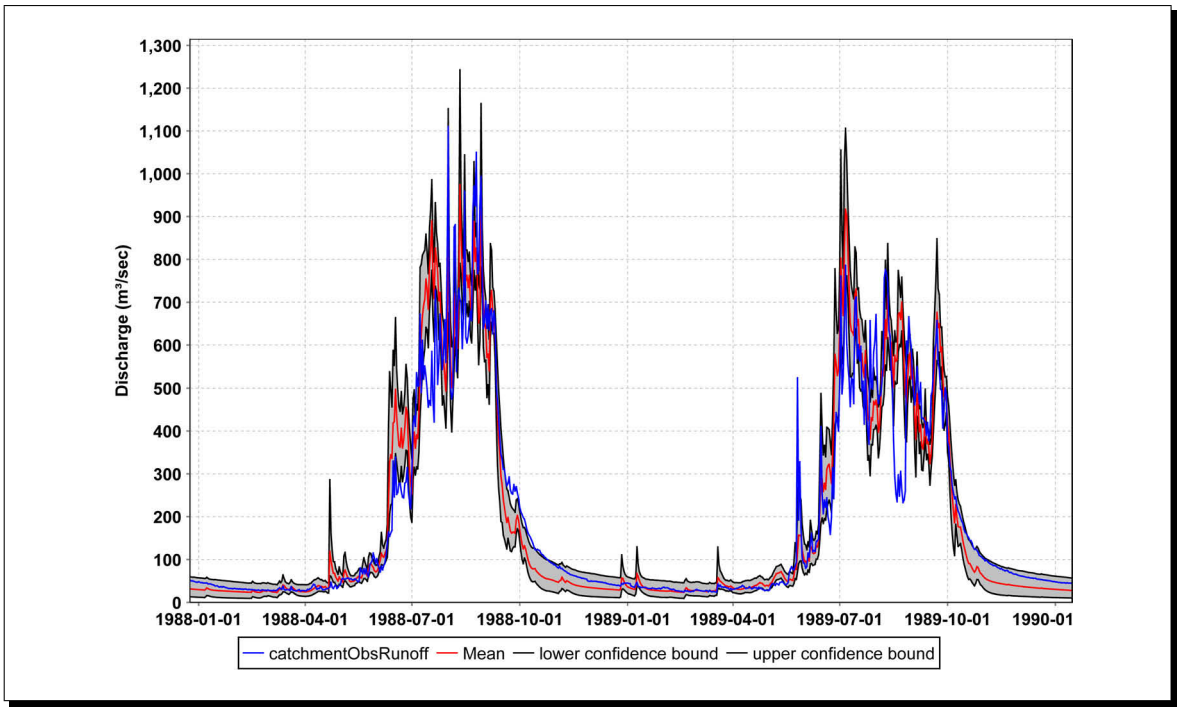

Figure 6.21: Results of the uncertainty analysis using the GLUE method (1988-1989). The grey band represents ensemble values from 1600 simulations. The blue and red lines are observed runoff and the mean of ensemble values.

other models mainly resides in the fact that the uncertainty accounts for all sources of uncertainty, i.e. input uncertainty, structural uncertainty, parameter uncertainty and response uncertainty. This is the case, because 'the likelihood measure value is associated with a given parameter set and reflects all these sources of error and any effects of the covariance of parameter values of model performance implicitly' (Beven and Freer 2001).

The GLUE analysis was applied to the entire period of 1985 to 1997. 1600 simulations were produced by using Monte Carlo simulations considering the selected 16 parameters as described in previous Section 6.8.3. Figure 6.21 shows the uncertainty band during the 1988-1989 sub -period. The uncertainty plot of all the years are provided in Appendix F. The uncertainty band comprises 0.95 percentile using each simulation higher than 0.7 E_{NS}. In this manner, nearly 3 percent of the simulations were omitted from the analysis. The upper and lower ranges of the parameter as shown in Table 6.9 were further reduced to include only behavioral simulations in the analysis based on the experiences from trial-and-error and automatic optimization (Section 6.8.1).

The uncertainty analysis indicates that the observed hydrograph falls within the range of uncertainty bands, mainly during low-flow, rising and recession periods (Figure 6.21). During the flood-peak period, observed streamflows are located towards the lower range of uncertainty bands and in some cases outside the bands. Similarly, some of the flood peaks are also outside the uncertainty band. The uncertainty analysis for the entire period is provided in Appendix F which looks similar to the figure. In addition, there is a fairly good agreement between the observed runoff and the ensemble mean as

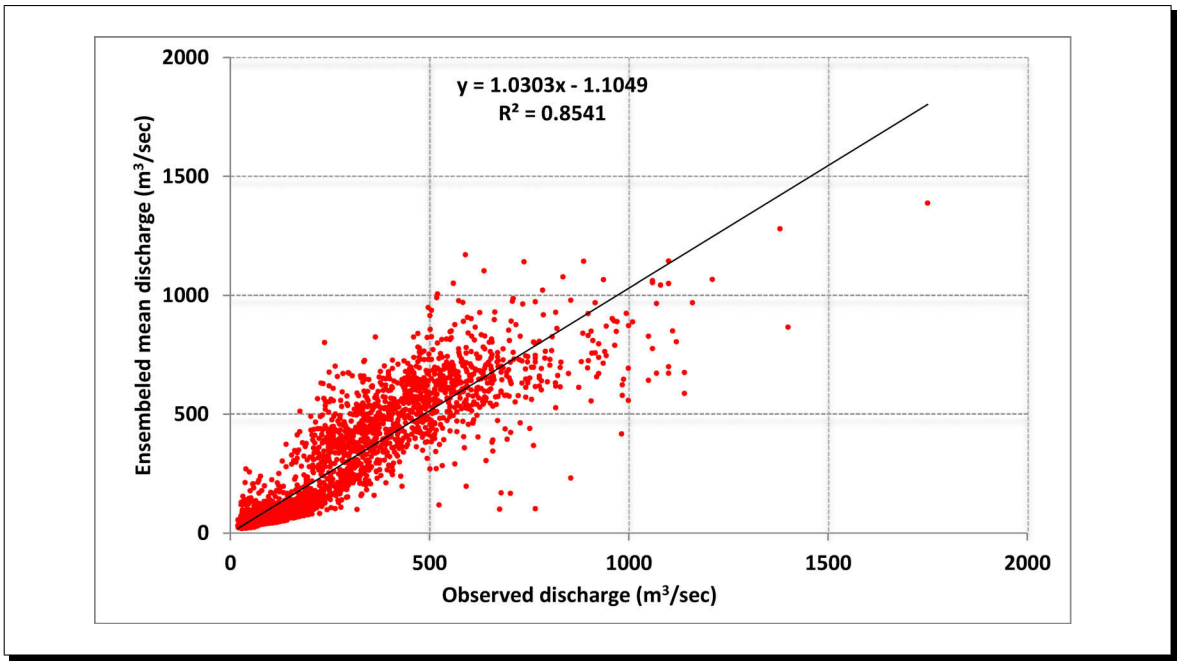

Figure 6.22: The scatter plot between daily ensemble mean and observed runoff

shown in Figure 6.22. The ensemble mean is the average of the 1600 simulations and provided as red line in Figure 6.21. This indicates that the process description within the model J2000 is generally acceptable for purposes of model application. The coefficient of determination r^2 between observed and ensemble mean is 0.85. Because some of the observed values lie below the uncertainty range during the high flood period, considerable uncertainty from a model structure also exist.

The available input data also contains a great deal of uncertainty. Due to the low density network of stations for input data, and especially due to the lack of stations in high-altitude areas, the precipitation input data are also a source of uncertainty. Figure 6.23 shows the runoff variation resulting from the $\pm$ 10 percent variation in precipitation input data. The uncertainty plot for the entire year is provided in Appendix D. The grey band represents the uncertainty due to the variation in precipitation data. The plot suggests that uncertainty is high primarily during the monsoon period. The magnitude of uncertainty increases during the extreme precipitation events. For example, the first major two peaks in 1996 (26 June and 11 July) brings higher uncertainty, mainly due to higher rainfall in those dates. The periods other than the monsoon seasons brings very low level of uncertainty. Overall, the variation of precipitation forms rather narrow uncertainty. The uncertainty of the entire year in Appendix D also shows similar pattern in other years. In some cases, the uncertainty can be attributed to the limited precipitation input data. Especially, due to lack of precipitation stations to the north (that is, high-altitude areas of the river basin), the model relies upon the most northern station (Chaurikhark) to simulate precipitation in the upstream areas. The higher precipitation value on this station likely to result over-prediction of the runoff hydrograph. For example, on 27 June 1996, Chaurikhark station received 82 mm of precipitation and other five stations in average received 20 mm of precipitation. The modelled streamflow is overestimated by about 570 m^3/sec higher than the observed value (an

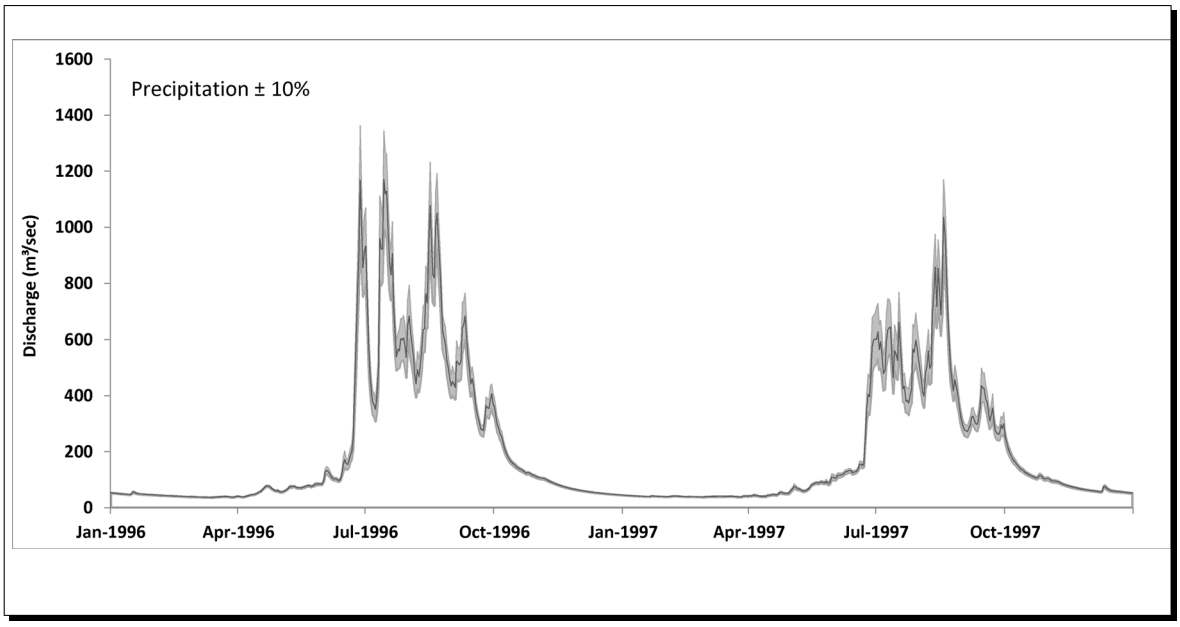

Figure 6.23: Uncertainty in the model result from $\pm$ 10% precipitation change

overestimation by about 100 percent).

As stated by Efstratiadis et al. (2007) uncertainty is inherent, thus unavoidable. Because all models are imperfect representations of the real world conditions, and precise input data are rarely if ever available, all outputs are subject to imprecision. Moreover, as suggested by Beven (2001b), Beven and Freer (2001), there may be many different model structures or parameter sets that could be considered as acceptable in simulations suggesting equifinality. In this study, the uncertainty band in Figure 6.21 can be considered equifinality, primarily coming from parameter uncertainty.

The validation data (discharge) also might be a source of errors especially during high flood time. The discharge volume of flood peaks is estimated using a rating curve. These rating curves are calculated based on a few measurements especially during low flow periods in the range of 30-600 m^3/sec (associated level of river of 1-4 m). The lowest and highest measured values to derive the rating curve is provided in Appendix C. Any values higher than this are normally estimated by the extrapolation of the rating curve. As suggested by Kattelmann (1987), a stage-discharge- rating curve may be based on an inadequate number of measurements in the Himalayan region, hence, it contains a major source of uncertainty. Therefore, there is high confidence in the lower values of discharge and uncertainty is greater for higher values. The rating curve of the Rabuwabazaar gauging station is provided in Appendix C, Figure C.1. The stage-discharge-rating curve indicates that the stage higher than 3 m always consists of the same volume of water (for example: 3.6 m = 671 m^3/sec, 4.3 m = 1040 m^3/sec) (Refer Appendix C, Figure C.2). The exception in the year 1998-2000 is most probably due to the damage caused by the glacial flood in 1998. The DHM Nepal regularly carries out the update of the rating curve, however, they mostly consider variation in the low flow period and high flow periods are not taken into account. During the field visit to the gauging station, I was informed that the river profile has been changed in the past years (personal communication with the person involved in measuring

Figure 6.24: The river profile at Rabuwabazzar gauging station. The gauging station is located at the right hand of the river (not shown in the photo). The dotted line indicates the side of the river before 1998. After the 1998 flood, the side of the river was further extended to the left side providing a larger river width (distance shown by the arrow).

the discharge). After the 1998 glacial lake outburst flood, the river profile has been extended to the left, providing a larger river width compared to earlier as shown in Figure 6.24. Such effects are not taken into account in the rating-curve updates and therefore high flow consists of greater uncertainty. Moreover, the discharge is measured three times a day: 08:00, 12:00 and 16:00 o'clock. However, it is reported that the precipitation events are high during evening and night time.The clouds formed in the day time are condensed in the late evening and night time due to low temperature and this falls as precipitation. Therefore, higher flow was reported during the night and early morning by the person involved in discharge measurement and also by the hydrologist (Dr. K. P. Sharma, DHM, Nepal). Therefore, there is a higher possibility that the observed data of high flow contains sources of errors and thus it brings uncertainty. In addition, the human errors in measurement is also not unlikely. A sudden drop of observed data during the last two weeks of August 1989 (Refer Figure 6.17) is also an example which is possibly due to measurement errors.

The annual volume of rainfall and runoff indicate that the rainfall-runoff coefficient (the ratio of runoff to rainfall volume) has high variation year to year. Figure 6.25 shows the annual value of observed precipitation and discharge and simulated discharge along with the percentage of volume error above the x axis. In 1987, the model streamflow is under predicted by 10 percent. The observed precipitation shows the decreasing value than the previous year while the observed discharge is increased. This inconsistency might have caused the under estimation by the model result. However, in the year 1989 which is one of the wettest years of record, the model predicted the values close to the observed ones, not only on an the annual basis, but also for the daily values.

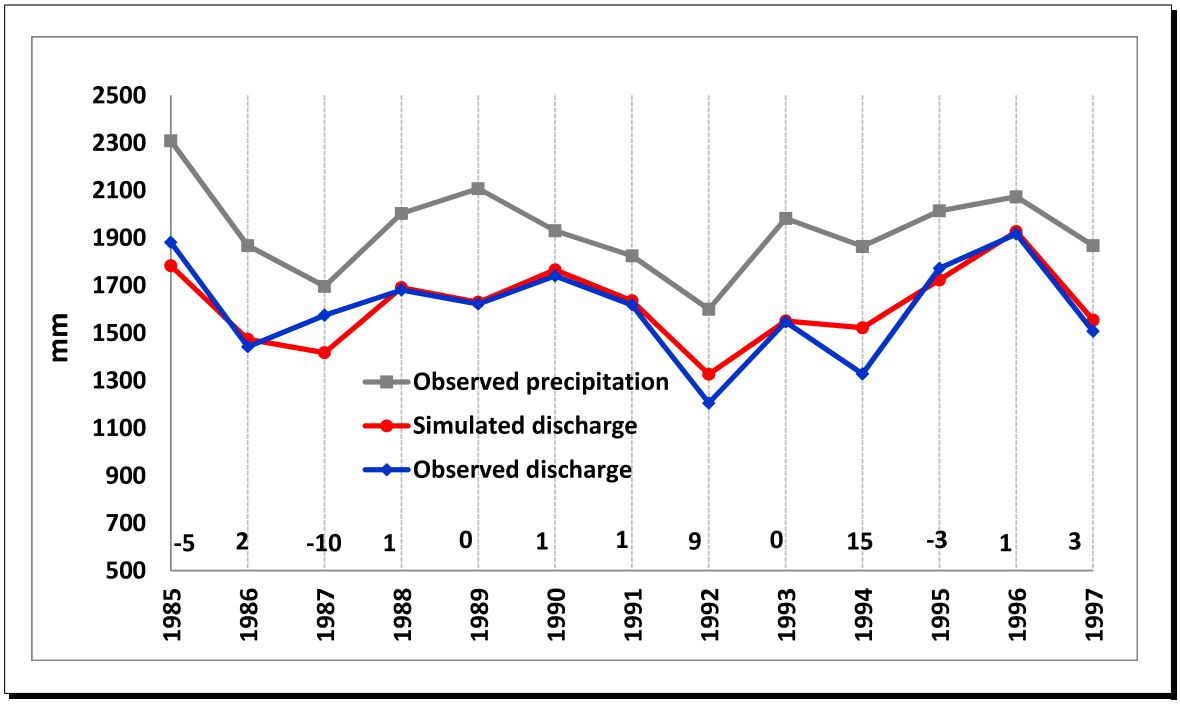

Figure 6.25: Precipitation, observed and simulated discharge (mm) of the Dudh Kosi river basin (1985-1997). The numbers above the x axis (in the red box) indicate the relative discharge volume error (%) (PBAIS) of the respective years.

The J2000 hydrological model for this study used available but limited data. The precipitation stations are judged less representative especially in the upstream areas of the basin. The climate data (such as temperature, wind, sunshine hour, relative humidity) are extrapolated from one station for the entire catchment. The land-cover data was derived from the data of recent years (2005-06) and the data of glacier layers was from 2000 which is different from the model run period. All these datasets are not fully representative for the entire catchment. A constant glacier layer was used throughout the model run period and the feedback mechanism (change in glacier area due to a change in temperature) are not applied in the model. The precipitation is the major source of errors as it is the driving force for the model and takes the major share in discharge output. The other climate data mainly used for the calculation of evapotranspiration has a lower degree of uncertainty compared to precipitation. All these limitations bring in uncertainties at various levels in the model results.

6.9.7 Water balance

The water balance analysis indicates that the average input into the system from precipitation and ice runoff are 2,114 mm and 74 mm per year respectively between 1986 to 1997. Of which nearly 72 percent are used to generate stream flow and 20 percent is estimated to be lost to the system as actual evapotranspiration (AET). Nearly 8 percent of the precipitation are stored in the basin as snow. Snowfall in high-altitude areas is stored as snow. Most of the snow above the mean equilibrium altitude is stored as snow where the mean temperature is below zero through the year as discussed in

Section 6.2.4. The other forms of storages are soil (middle and large pores), groundwater and interception. The primary components of the annual water balance are provide in Table 6.11. The annual AET is increasing at a rate of 5 mm/year which is statistically significant at 0.05 level of significance. The increasing AET trend is mostly due to higher temperature trend in the study area (Refer Figure 5.20, page 77). During the J2000 model run period (1985-1997), the maximum temperature trend was found to be at a rate of 0.188°C/year which is very high compared to the long-term trend (0.053°C/year). On the other hand, the snow storage is found to be decreasing especially after 1991 which is represented by the trend of 11 mm/year; however, the trend is statistically insignificant. The higher temperature trend causes a snow line to shift in higher areas which reduces the snow storage capacity of a catchment. Probably this phenomenon has caused the decreasing snow storage trend.

Table 6.11: Water balance of the Kosi river basin (1986-1997)

Year	**Input (mm)**	**Discharge (mm)**	**AET (mm)**	**Snow storage (mm)**
1986	1,953	1,474	375	146
1987	1,976	1,417	407	182
1988	2,343	1,690	410	256
1989	2,302	1,629	444	207
1990	2,367	1,765	376	246
1991	2,296	1,635	434	252
1992	1,892	1,326	454	115
1993	2,191	1,551	442	175
1994	2,018	1,522	472	50
1995	2,414	1,723	439	192
1996	2,418	1,927	456	64
1997	2,087	1,554	433	80
Average	**2,188**	**1,601 (72%)**	**428 (20%)**	**164 (8%)**

6.9.8 Runoff components analysis

The model generates four different runoff components originating from different sources (Figure 6.1). The overland flow (RD1) and Interflow 1 (RD2) contribute about 50 and 10 percent respectively of the total runoff. The component with the highest temporal dynamics is the fast direct runoff (RD1). It consists of runoff from sealed areas, saturation excess runoff, infiltration excess overland flow and snow and ice melt from glacier areas which directly drain to nearby stream channels. The slow direct runoff (RD2) contribution comes from the unsaturated soil zone when it becomes saturated after the rainfall events and the outflow comes from the LPS. The higher percentage of overland flow (RD1) is due to high intensity of rainfall during the monsoon season. During this period, the soil becomes partly or fully saturated after intense rainfall events and most of the rainfall is drained as overland flow. In addition to this, steep topography, rocky mountains and barelands in higher altitude areas provide favorable conditions for overland flow. The lower amount of RD2 is possibly due to shallow soil conditions in most of the upstream areas. Moreover, joints and fractures are common in the Higher Himalayan region, as discussed in Section 6.5.5, which enable to flow the infiltrated water

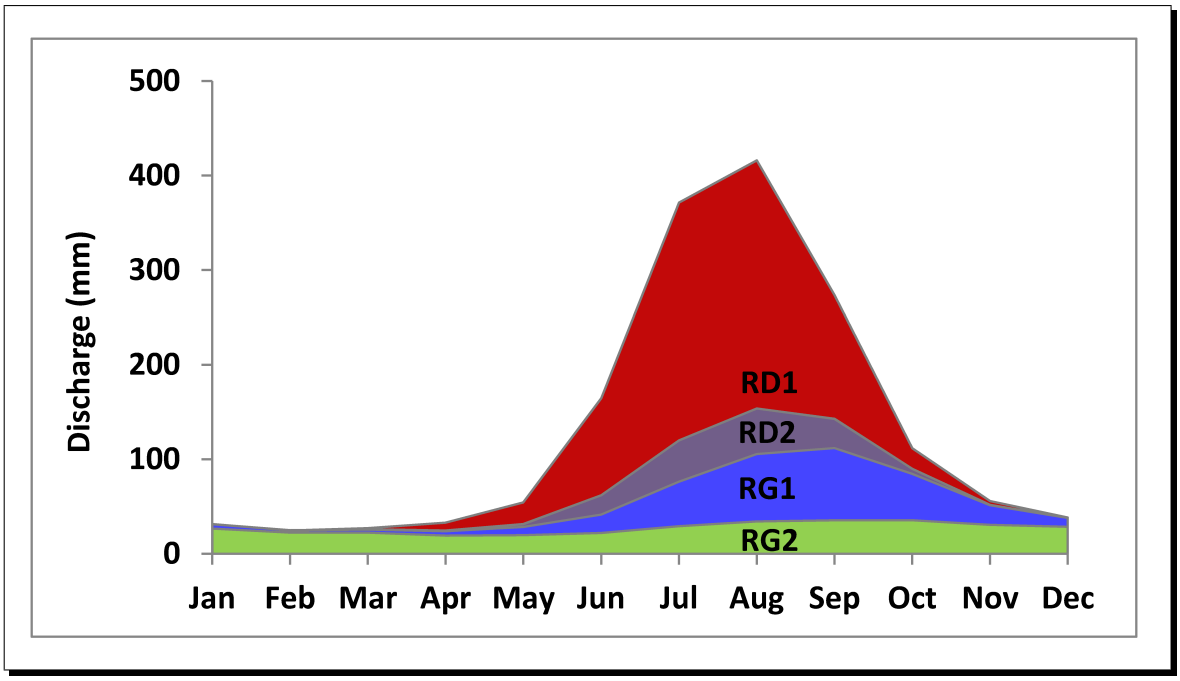

Figure 6.26: Runoff components from simulated runoff: RD1 (Overland flow), RD2 (Interflow 1), RG1 (Interflow 2), and RG2 (baseflow)

for vertical percolation. The contribution of the different runoff components is represented in Figure 6.26. The contribution of RG1 (Interflow 2) and RG2 (baseflow) is 20 and 20 percent respectively. The results from the different runoff component suggests that the overland flow is the most dominating components of the runoff. The intense rainfall during the short period of time primarily caused the high amount of overland flow.

6.9.9 Contribution from snow and glacier melt

The glacier module which has been implemented and adapted into the J2000 hydrological model as a part of this study has provided important knowledge and understanding about the melt runoff from glacier areas. The average contribution from snow and glacier melt to the annual streamflow is estimated to be about 34 percent. The melt from glacier areas alone contribute about 17 percent (including 5 percent from glacier ice melt). Similarly, snowmelt which occurs, apart from glacier areas, contributes nearly 17 percent of which more than 50 percent are contributed from rain coming on snow surface. The meltwater originating from glaciers is about 49 percent. Rain-on-snow is a phenomenon which is high in lower altitude areas and the proportion gets lower in higher altitude area. Figure 6.27 shows the contribution of snow and glacier melt to the stream-flow. The contribution during the monsoon season (June-September period) is about 36 percent, also including the contribution from rain-on-snow. The contribution in April and May is about 69 and 79 percent respectively, which indicates the significance of glacier and snowmelt during the pre-monsoon period. The contribution from melt water during this period is primarily from the melt process associated with higher temperature.

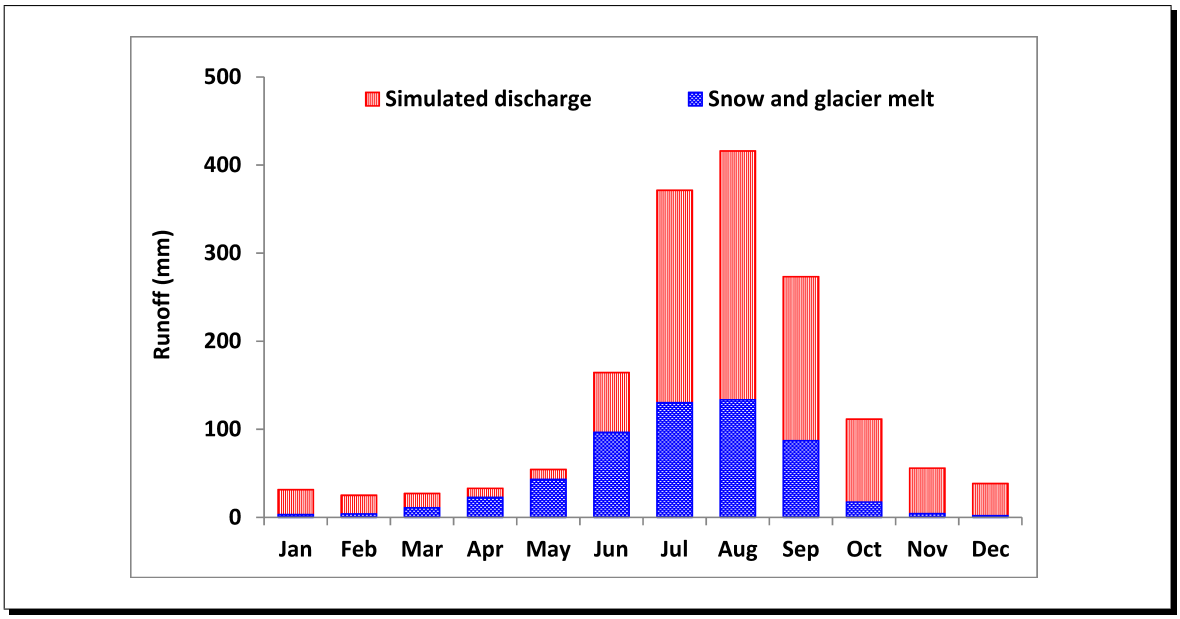

Figure 6.27: Contribution of snow and glacier melt to the stream flow

The winter monsoon period (December to February) brings little precipitation to the area which is stored as snow in the higher altitude areas. The stored snow is melted away as soon as the temperature increases– mostly during the pre-monsoon period. Therefore, the pre-monsoon season brings relatively higher streamflow associated with melt runoff which is visibly apparent during the month May (Figure 6.20(a)). Table 6.12 provides the monthly contribution of the different components of snow and glacier melt. In the table, snowmelt represents the melt coming from areas other than glaciers. Glacier melt includes the total melt (snow, ice and rain runoff) from glacier areas.

The higher streamflow during the monsoon season comes principally from precipitation and melt runoff. The rainy season coincides with higher temperature and therefore the volume of melt water is the highest during this period of the year. The summer season not only brings higher precipitation but also a net gain of snow to the accumulation zone of glaciers. At the same time, most of the snow located in the lower elevation areas is melted away.

The model is able to predict the snow and glacier melt runoff fairly well. The monthly discharge during the pre-monsoon period are judged to compare well with observed versus simulated runoff (Figure 6.20(a)) which indicates that the model prediction of melt behavior is satisfactory. This is because the streamflow during the pre-monsoon period is mostly due to melt runoff and groundwater (baseflow). The contribution from melt runoff during the monsoon season is mixed up with the high precipitation and associated runoff and therefore it cannot be as accurately predicted for that part resulting from rain and melt.

Because the estimated average snow and glacier runoff contribution is relatively high, it is likely that in the context of global climate change, the hydrological regime of the study area is likely to be affected, especially the melt-runoff contribution. The glacier and snowmelt runoff have a higher significance for the downstream areas especially during the the pre-monsoon period. Streamflows during this period

Table 6.12: Monthly snow and glacier melt contributions to total streamflow.

Months	Snowmelt (%)	Glacier melt (%)	Ice melt (%)	Snow and glacier melt (%)
January	10	0	0	10
February	16	0	0	16
March	38	2	1	41
April	47	23	10	69
May	43	36	16	79
June	29	30	8	59
July	16	19	4	35
August	16	17	3	32
September	15	17	5	32
October	6	10	6	16
November	4	4	3	8
December	5	0.4	0.4	5

are important for many beneficial uses such as for agriculture (irrigation) and hydropower.

Immerzeel et al. (2010) estimated that the melt water coming from glaciers in the Ganges River basin is about 40 percent and the contribution of snow and glacier melt to the total streamflow is about 10 percent. The former estimation is close to the result from this study, which is about 49 percent. The latter value in this study is high. The reason is that the estimation by Immerzeel et al. (2010) applied to the entire Ganges basin. The contribution becomes lower if the melt runoff is estimated for the entire basin. In this study, the estimation is based on the study area relatively located in upstream areas where the contribution is normally greater. Alford and Armstrong (2010) estimated the glacier melt to the total streamflow in the Dudh Kosi river basin. They estimated the melt runoff from the relationship between mean specific runoff and mean altitude and energy exchange gradient (or ablation gradient). By this approach, they estimated the contribution of the glacier melt is about 18 percent which is very close to the percentage obtained in this study.

6.10 Modelling Tamor river basin: Proxi-basin approach

To further analyze the model performance and credibility, a proxy-basin validation approach (Klemes 1986) was adopted in this study. The proxy-basin test was designed for validating the capability of the models to represent flow dynamics of ungauged catchments. It has been expected that the physically-based models would produce better results than the conceptual models (Refsgaard et al. 1995). In this research study, the calibrated and validated model in the Dudh Kosi river basin is transferred to the Tamor river basin, using the same values of the calibration parameters. The modelling in the Tamor river basin was conducted using daily data for the 1996-2002 period, which is independent from the model run period in the Dudh Kosi river basin. The first year was considered for the initialization of the model and therefore not included in model results.

The Tamor river basin is a tributary of the Kosi river basin and is located to the west of the Dudh Kosi

river basin. Figure 6.28 shows the location of the Tamor river basin. The total area of the basin is 4,005 km^2. The basin is also one of the steepest basins of the Kosi river basin where the elevation extends from 483 m to 8,438 m. The average slope of the sub-basin is 27 degrees and about 47 percent of the land is located above this slope. About 22 percent of the area is located above 5,000 m elevation and the total area below 3,000 m is around 50 percent. In the glacier part, about 68 percent of the glaciers are located above 5,500 m and only 6 percent are located below 5,000 m. The climate of the basin is similar to the Dudh Kosi river basin.

Table 6.13: Hydro-meteorological stations in the Tamor river sub-basin

Station ID	Station Name	Elevation	Parameters
1403	Lungthung	1,780	P
1404	Taplethok	1,383	P
1405	Taplejung	1,732	P, Tmax, Tmin, SH, RH, WS,
1406	Memenjagat	1,830	P
1420	Dovan	763	P
684	Majhitar	533	D

Notes on variables of Table 6.13: **P:** Precipitation, **Tmax:** maximum temperature, **Tmin:** minimum temperature, **SH:** Sunshine hour, **W:** wind speed, **RH:** relative humidity, **D:** Discharge

6.10.1 Land use, soil and geology

The data source for land-use and land-cover and soil is similar to the Dudh Kosi river basin. The land-use information in the upstream areas was corrected using the same procedure as described in the case of the Dudh Kosi river basin. Figure 6.29 shows the land-use and land-cover of the basin. As shown in the figure, nearly 48 percent of the land is covered by forests. Agriculture and glacier area occupy about 8 percent and 13 percent of the area respectively.

The soil properties of this sub-basin are comparable to those of the Dudh Kosi river basin which is mainly affected by topography and elevation. Soil at lower elevation is dominated by medium to fine texture materials with loamy to fine loamy characteristics. These soils are a combination of Cambisol and Umbrisol. The soil in high-altitude areas are dominated by a Regosol which has a shallow soil profile and weakly developed mineral soils with unconsolidated materials. The geological information for this basin was derived using the same procedure as for the Dudh Kosi river basin.

There are five precipitation stations in the Tamor river basin (Table 6.13) above the gauging station. The location of the Tamor rive basin is provided in Figure 6.28. One climate station comprises all the climate data required to run the model. The discharge data from Majhitar gauging station is used to validate the model results. There is another gauging station (Mulghat) which located about 50 km downstream of Majhitar. The reason for choosing the upstream station (Majhitar) is that the discharge data quality was qualified as ‘good’ by the Department of Hydrology and Meteorology (DHM). On the contrary, the Mulghat station is termed as ‘fair’. In addition, the Mulghat station also failed the test of homogeneity as described previously in Chapter 5.

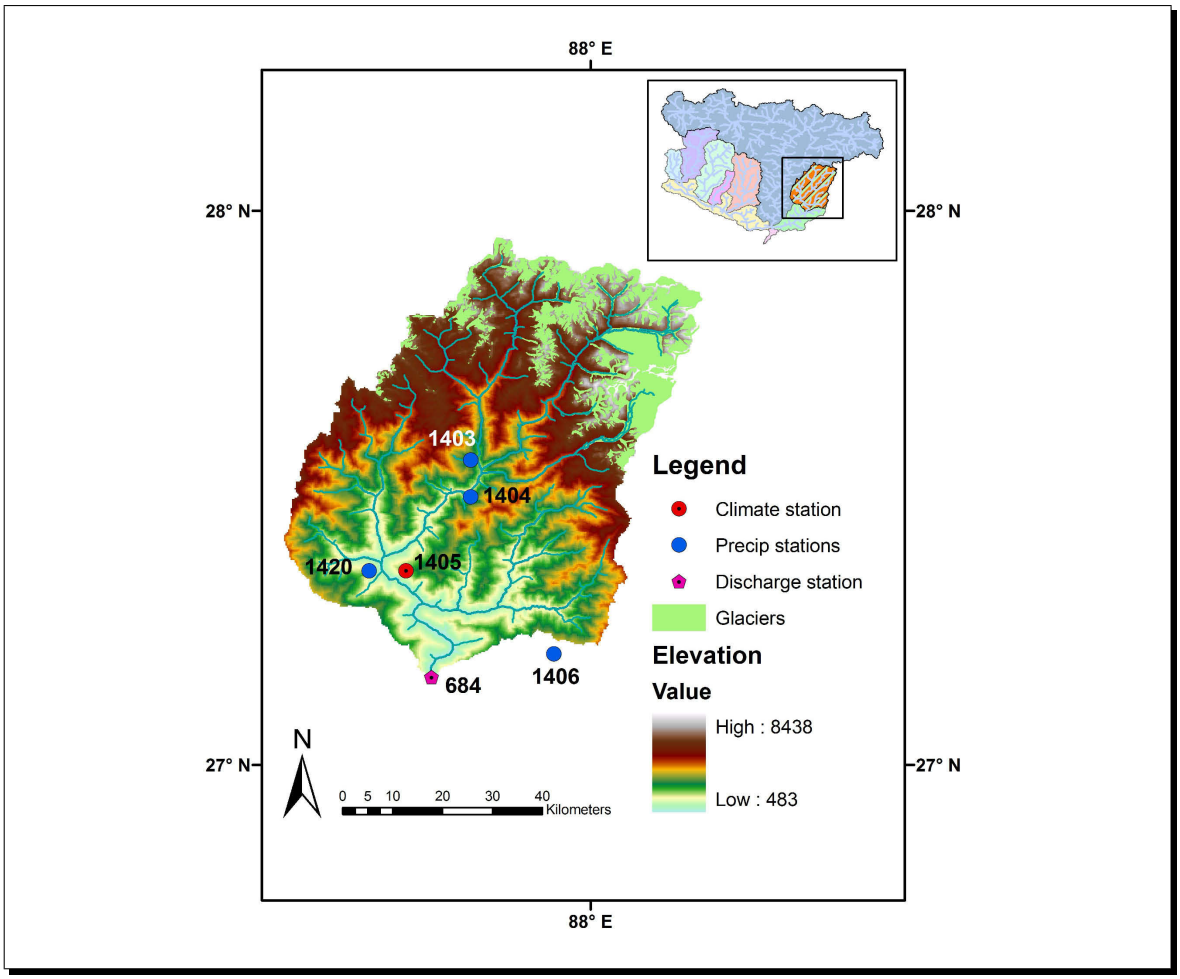

Figure 6.28: Tamor river basin. The Kosi river basin (Inset) indicates the relative location of the Tamor basin. The station numbers are referred in Table 6.13

6.10.2 Hydro-climatic conditions

Detailed information about the general climatic conditions of the Tamor river-corridor area is provided in (Section 5.4.4). Considering the precipitation stations located upstream of the gauging station, approximately 72 percent of the total precipitation occurs during the monsoon season (for the period of 1996-2002), of which nearly 11 percent occurs in the month of May. In contrast the contribution during the monsoon season and in May is about 81 and 6 percent respectively in the Dudh Kosi river basin. The station Taplethok is the station exhibiting greatest amount of precipitation, where the average annual precipitation is 2,815 mm followed by Lungthung with a value of 2,505 mm during the model run period. The lowest precipitation is observed in Dovan with a value of 1,857 mm. The location of the stations are provided in Figure 6.28.

Figure 6.30 indicates the average monthly observed precipitation and discharge of the Tamor river basin. The average observed precipitation and discharge are 2,295 mm and 2,158 mm respectively. It is interesting to compare the observed precipitation and discharge graph of this basin with the Dudh

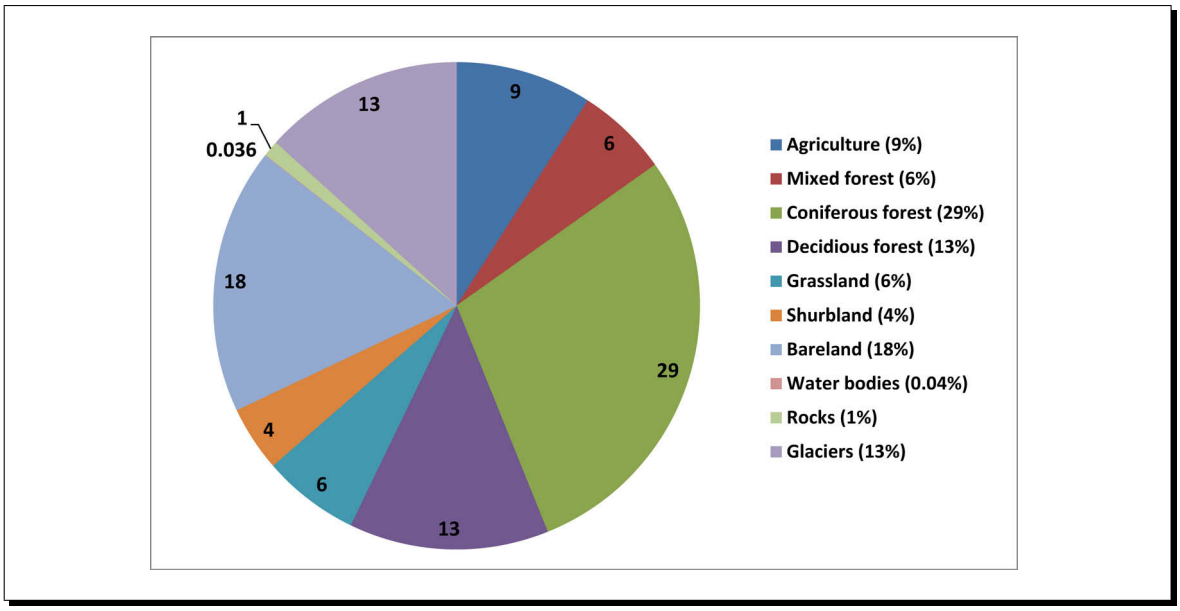

Figure 6.29: Land-use and land-cover data in the Tamor river sub-basin

Kosi river basin which is provided in Figure 6.6, page 117. The average monthly precipitation pattern and magnitude looks similar in both cases, although the magnitude of pre-monsoon precipitation is higher in the Tamor river basin. However, the magnitude of discharge is higher in the Tamor river basin. Especially, in the month of July and August, the rainfall-runoff coefficient is much higher as shown in Figure 6.30. The graphs of monthly precipitation and discharge for individual years are provided in Appendix G. These graphs indicate that the discharge in August is always higher than the precipitation for the entire time period. In the case of July, only in the years 1998 and 1999, the precipitation is higher than discharge. Comparing the graphs of the two river basins, it is concluded that the discharge proportion in the Tamor river is higher than in the Dudh Kosi river during the June-August sub-period.

6.10.3 Modelling results

6.10.3.1 Hydrograph analysis

The observed and simulated discharge from the model is provided in Figure 6.31. The model is able to reproduce overall hydrological dynamics fairly well except for under-prediction during high flow periods. The figure indicates that the J2000 model predicts the baseflow conditions quite well. The rising limbs and recession limbs are also simulated equally well; however slight under-prediction during the pre-monsoon period can be observed in years 1998, 2001 and 2002. However, low flow simulations in 1999 and 2000 are in fairly good agreement. The flood period in 1998 and 2000 are substantially under-predicted. The reason for those differences is judged to be caused primarily to the input data where the discharge is higher than precipitation. When the precipitation is higher than discharge (such as in July 1997 and 2001), the model simulate the streamflow fairly good. The average

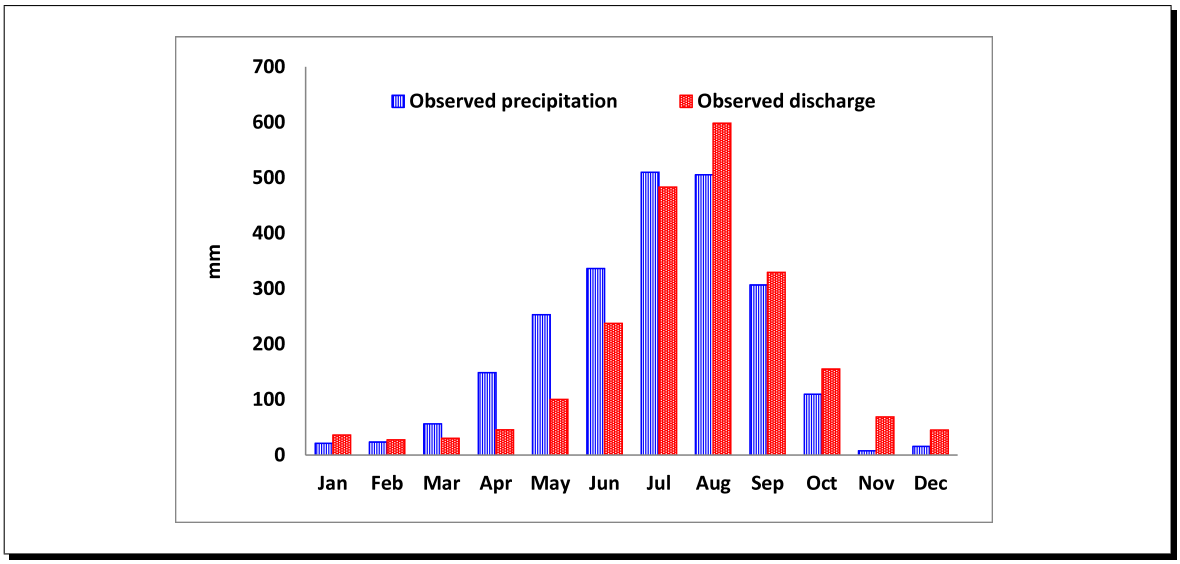

Figure 6.30: Observed precipitation and discharge in the Tamor river sub-basin

monthly discharges simulated by the model and observed values (Figure 6.32(a)) also indicates good agreement during low and medium range flows. However, flows during the months of July and August are under-predicted as discussed earlier primarily due to the inconsistency in rainfall-runoff ration. The efficiency results of the model evaluation with different objective functions is provided in Table 6.14. The results suggests that the model result is good during the lowflow period suggested by the higher LNS efficiency. The efficiency results for both the river basins indicate that the model results are satisfactory.

The under-prediction is clearly due to a lower amount of precipitation inputs assumed for the entire sub-basin. Possibly, the source of errors is related to the locations of the precipitation stations (low elevation areas and valleys) which are unable to capture the precipitation dynamics of the basin due. The second source of bias could be the reported discharge data. The measurement of discharge during high flood time has inherent higher uncertainty probably due to the stage-discharge rating curve which is not robust enough to measure the high flow magnitude during the flood period. (Kattelmann 1987) also suggested that the rating curve of Himalayan rivers are based on an inadequate number of measurements in the Himalayan river.

The highest flood peak in the period occurred on 02-08-2000 when the daily hydrograph increased from 1,500 to 2,740 m^3/sec from the previous day. The average precipitation on that day is 49 mm which is among the highest in the monsoon season. A similar range of precipitation (42 mm) was also observed on 21 July, however, the observed discharge is only 860 m^3/sec on that day. On the contrary, the streamflow at the downstream station Mulghat reported a decrease of about 500 m^3/sec from the previous day. This implies that the uncertainty associated with the data is possibly more subject to the validation data (discharge) than to precipitation input.

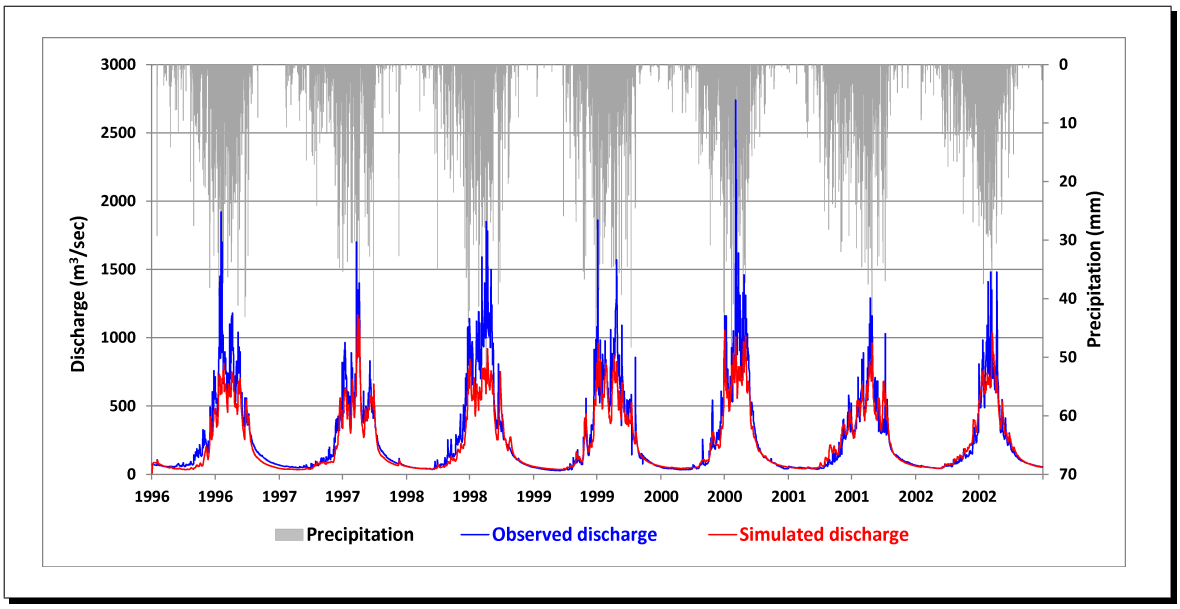

Figure 6.31: Observed and simulated discharge in the Tamor river basin

Table 6.14: Efficiency results of model evaluation

Objective Functions	Tamor river	Dudh Kosi
E_{NS}	0.81	0.85
LNS	0.94	0.93
r^2	0.86	0.86

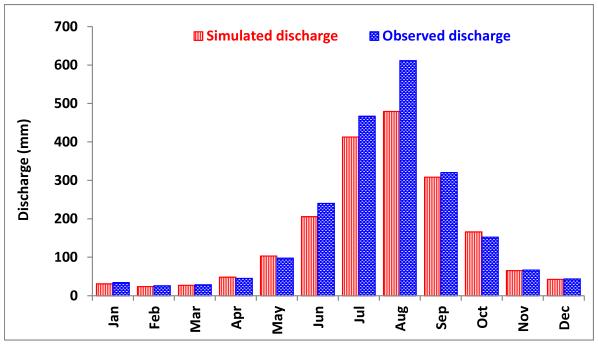

(a) Average monthly observed and simulated discharge

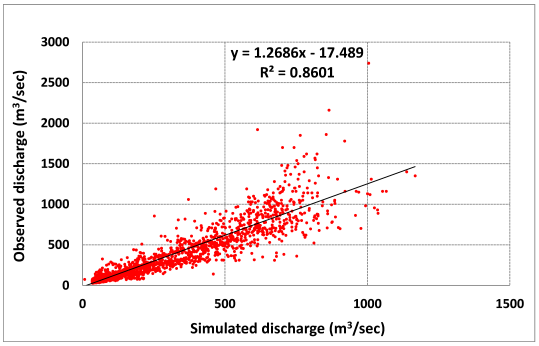

(b) A scatter plot between observed and simulated discharge

Figure 6.32: Agreement between observed and simulated discharge of the Tamor river basin

6.10.3.2 Hydrological system analysis

The simulated precipitation of the Tamor river sub-basin averages 2,559 mm annually. About 70 percent of the input (precipitation and ice melt) is used to produce streamflow. Similarly, about 18 percent (472 mm) is estimated as a loss through evapotranspiration and about 8 percent of the precipitation is stored as snow in the sub-basin. The contribution of runoff components are: RD1 (44 percent), RD2 (12 percent), RG1 (24 percent) and RG2 (20 percent). The contribution from glacier runoff to the total streamflow is about 14 percent of which 3 percent is from ice melt. The snowmelt other than glacier areas contributes about 13 percent.

6.11 Comparison of hydrologic conditions between the Dudh Kosi and Tamor river basins

The Tamor river basin is wetter than the Dudh Kosi river basin. The modelling periods of both basins used different time periods. However, using the precipitation analysis of the same time period (Table 5.5) in Chapter 5, also indicates higher "wetness" (precipitation) in the Tamor basin. The higher AET in the Tamor river sub-basin is attributed to higher temperatures exhibited in a time-trend during the model run period compared to the Dudh Kosi river sub-basin (Figure 5.20(b)). The overland flow (RD1) component in the Tamor river sub-basin is about 6 percent less than that of the Dudh Kosi river basin. This is probably due to higher intensity rainfall during the monsoon season which is about 82 percent in the Dudh Kosi river basin compared to 72 percent in the Tamor river sub-basin. A higher intensity of rainfall leads to a higher rainfall-runoff coefficient due to saturation and infiltration access rainfall.

The contribution from snow and glacier melt is lower in the Tamor river -basin than in the Dudh Kosi river basin. One possible reason is that in the Tamor river basin, the area of glacier located below 5,500 m is nearly 179 km^2 (about 31 percent of the total glacier area) whereas in the Dudh Kosi river sub-basin, this is about 300 km^2 (about 60 percent of the total glacier area). The higher glacier area below 5,500 m where the effective melting process occurs has resulted in a higher melt contribution. In addition, the land area in between 5,000 - 6,000 is about 200 km^2 larger in the Dudh Kosi river sub-basin. This land area thus is primarily responsible for the snow and ice storage occurring during the monsoon season.

6.12 Summary of this chapter

The J2000 hydrological model was applied to monsoon-dominated two sub-basins of the of the Kosi river basin. These watersheds constitute a great heterogeneity and complex terrain dominated by glaciers in high-altitude areas. The modelling application is conducted in the region where the data coverage is poor and heterogeneity is very high. The model parameters were calibrated and validated in the Dudh Kosi river basin and were further transferred to another basin (Tamor river) to assess

the robustness of the model parameters. The detailed analysis answered many questions related to hydrological systems based on the model output. The following are the key points from the chapter.

1. The study provides a basis that the process oriented J2000 hydrological model, applying HRUs as modelling entities, is able to simulate daily streamflows of the monsoon-dominated watersheds of Kosi river basin. The adaptation of high flood peaks using the new calibration parameter has provided better results to simulate high flood peaks by considering the non-linear behavior of the catchment.

2. The result of the proxy-basin validation approach indicates that the calibrated model is satisfactory for simulating streamflows via model transfer to other catchments of the Himalayan region however, systematic under-prediction occured during the monsoon season. The approach further suggested that the model performs better if the two prerequisites in the form of input data (precipitation) and validation data (discharge) are in a systematic order.

3. The application of glacier module has simulated the melt runoff from glacier areas and provided important knowledge about the snow and glacier melt process of the region.The contribution of meltwater to streamflow suggests that the significance of snow and glacier melt is relatively high. The contribution during April and May when the melting process accelerate, is about (69 and 79 percent) respectively in the Dudh Kosi river basin (with about 50 percent contribution from rain-on-snow). The glacier melt contribution to the annual total streamflow is about 17 percent including 5 percent from the glacier ice melt. The meltwater during this period is vital to downstream communities for different activities such as agriculture and hydropower.

4. The overland flow dominates the streamflow in the region which is about 50 percent (Dudh Kosi) and 44 percent (Tamor). During the monsoon season when about 70-80 percent of the rainfall comes during the four months, the soil gets saturated most of the time and thereby increases the rainfall-runoff coefficient and associated overland flow. The critical role of intense rainfall in overland flow is also suggested by the difference in the amount of overland flow in the two river sub-basins.

5. The model runs were made with limited climatological data and therefore uncertainties in model-simulation results undoubtedly occur due to several factors. The most prominent one is judged to be the poor representation of input data especially in high-altitude areas. The validation data and associated quality constitute another source of uncertainty in the model results especially the values during high flood time. The extrapolation of rating curves to estimate the high flows is a possible source of uncertainty because it is found that high flow values were reported to remain the same in longer periods of time. On the contrary, the river profiles are continuously changing due to the force of the river flows during the flood time.

7 Upstream-downstream linkages

This chapter addresses the forth study objective and describes the upstream-downstream linkages based upon the results of the hydrological modelling in the study area. This study topic includes mainly the impact of land-use and climate change on hydrology in the Dudh Kosi river basin and how these changes influence the availability of water to downstream areas. In addition, other aspects of upstream-downstream linkages are also discussed.

7.1 Impacts of land-use changes

The different aspects of the impacts of land-use changes on hydrology have been discussed in the relevant scientific literature (Section 2.2.1). The methods for analysing the impact of land-use change on hydrology based on modelling are still very much at an early stage. The prediction of effects of future changes (and the validation of those predictions) has hardly even started (Beven 2001a). Because land-use change is a dynamic process, the spatial and temporal changes in a hydrological model are considered a challenging task. In most modelling studies, the information about the land-use and land-cover is considered as a static model component which does not change over time periods. Nonetheless, the availability of detailed spatial databases in GIS systems along with distributed modelling systems have made it possible to deal with such issues in recent years. Beven (2001a) suggested that the effect of land-use change on streamflow involves interacting processes associated with deforestation and afforestation. The condition of land surface after the deforestation and particularly an infiltration process determines the shape of the hydrograph.

The distributed process-oriented modelling of the runoff generation makes the J2000 hydrological model a suitable tool to assess the impact of land-use changes on the water balance of a large catchment. In addition, the evapotranspiration is calculated according to Penman-Monteith which takes into account the vegetation parameters and soil-water storage components. This process reflects the influence of different vegetation classes in a scientifically sound manner (Krause 2002). Moreover, by using the distribution concept of Hydrological Response Units (HRUs), the specific condition of the HRUs (such as different land-cover classes) can be changed into hypothetical classes (e.g. deforestation) in order to better predict and understand the influence of different land-use changes.

7.1.1 Land-use change scenarios

Two scenarios (Scenarios 1 and 2) have been formulated to quantify the impact of land-use change on the hydrological dynamics in the Dudh Kosi river basin. The forest in Nepal in general is managed

by the Government (government-managed forest) and communities (a community forestry program). Deforestation (cutting forests and trees) in general has been discouraged by the government unless it has been specified by an expert to cut down a few trees to maintain the forest ecosystem. Therefore, mass deforestation is unlikely to happen in the study area. Moreover, population and livelihood activities are mostly concentrated up to 2,500 m elevation, with most of the nation's population living at about 1,500 m in the middle mountain region. At higher than the middle mountain region, a few sparse settlements, permanent or seasonal, can be observed. Therefore, regions higher than 2,500 m are unlikely to be influenced by anthropogenic activities, due to their relative remoteness and inaccessibility. Few exceptions are possible regarding these assumptions. The land-use change scenarios are compared with the model results from 1985-1997 (Refer Chapter 6) which has been defined as the baseline period for change detection in the Dudh Kosi river basin.

7.1.2 Scenario 1

A more realistic scenario is depicted in Scenario 1. In this case, the forests (deciduous, coniferous and mixed) up to an elevation of 3,000 m are converted into shrubland (bushes) where anthropogenic activities are likely to impact land cover (vegetation). Shrubland is a plant community characterized by vegetation dominated by shrubs and including native grasses and herbs. They are shorter than forest trees and have relatively shallow root depth. It is assumed that if deforestation takes place, the land cover will be replaced by shrubland. A similar transformation from forest to shrubland has been noted throughout Nepal (DFRS 1999). In regions higher than 3,000 m elevation, human influence is very low. In this scenario, 28 percent of forests (decidious, mixed and coniferous) land is assumed to be converted into shrubland (increasing the shurbland area from 3 to 31 percent). In the HRU parameter file, the land-use classes with the corresponding elevations are converted into a single class of shrubland. The detailed information of the two scenarios are also presented in Table 7.1. The land-use information of forests, shurbland and bare land is provided because the other land use types are not changed in the scenarios.

Table 7.1: Land-use change scenarios (change in percentage)

Land-use type	Baseline	Scenario 1	Scenario 2
Forests	41	13	0
Bushes	3	31	3
Bare land	25	25	66

7.1.3 Scenario 2

In Scenario 2, an extreme situation is realised which may be less realistic. All the forests are converted into bare land resulting in a total deforestation of 41 percent as shown in Table 7.1. Bare land, in this scenario, means a land with no vegetation rather only bare soil.

In this process of assumed changes in the land-use pattern, the J2000 model application also considers

the change in the whole land-system dynamics. This is realised by a change in the capacities of soil-water storage for different land covers. The forested land will have a larger MPS due to greater root depth. Therefore, the land-use change scenario in the modelling system indicates that the complete land system is changed. It does not mean that the effect is analysed just on the next day of the deforestation when the soil conditions remain the same. The transpiration through the effective root depth of vegetation occurs in the vegetative area. In this scenario, due to a change of forest to bare land, affecting model parameters such as albedo, LAI, RSCO(1-12) and effective height (Table 6.2) also change which influence both PET and AET.

The infiltration capacity of the land varies with different vegetation types. Soil infiltration capability is greatly affected by soil physical and chemical characteristics and root system. The bare land has poorer soil infiltration capacity compared to land covered by vegetation surface such as forest (Liu et al. 2007). The decrease in infiltration tends to increase overland (surface) flow. The forested areas have higher evapotranspiration compared to bare land due to greater root depth. The higher evapotranspiration rates in vegetative areas compared to bare land are suggested in Chen et al. (2011, 2005). The infiltration process in different land-use types is similar in most cases in the J2000 model unless specified in the land use parameter file. A simple empirical approach of infiltration rate based on the land cover is realised using the parameters *SoilImpGT80* and *SoilImpLT80* in the J2000 model. The former parameter is more representative of impervious areas (such as urban areas with roof tops and buildings and concrete structures such as roads and walkways/sidewalks) where the infiltration opportunities are low and most of the rainfall results in overland flow. In the study area, there is no impervious areas and therefore only the latter parameter is adjusted to be effective in the case of bare land. Therefore, infiltration will be decreased by reducing the value of the parameter *SoilImpLT80*. Ensemble runoff was generated using a Monte-Carlo analysis with the parameter value in between 0.5 and 0.1 (the low value represents less infiltration). The value less than 0.1 is suitable for impervious areas and the value 0 means no infiltration from the land area. The change in infiltration depends upon how the land system is used after deforestation. As suggested by Bruijnzeel and Bremmer (1989), Beven (2001a), the use of heavy machines and construction activities leads to compact soil and reduce the infiltration capacity.

7.1.4 Results of Scenarios 1 and 2

In Scenario 1, streamflow is increased by only 1 percent and AET is decreased by 4 percent (19 mm/year). This can be explained by the fact that shrubland evaporates at a lower rate, due to shorter root depths of vegetation than the forest trees. As shown in Figure 7.1, there is slight decrease in AET compared to the baseline condition. In addition, during the monsoon season, water availability is relatively high for enhancing evapotranspiration. The decreased evapotranspiration is eventually available for streamflow. This overall assessment indicates that there will be very minimal impact on hydrology by converting forest to shrubland (to the degree assumed in the scenario), and the effect can be assumed to be negligible. The change in infiltration is not realised in Scenario 1, because vegetative cover has in general similar infiltration to soil. The effect of change in infiltration is realised in Scenario 2 in the case of bare land and is explained in next paragraph.

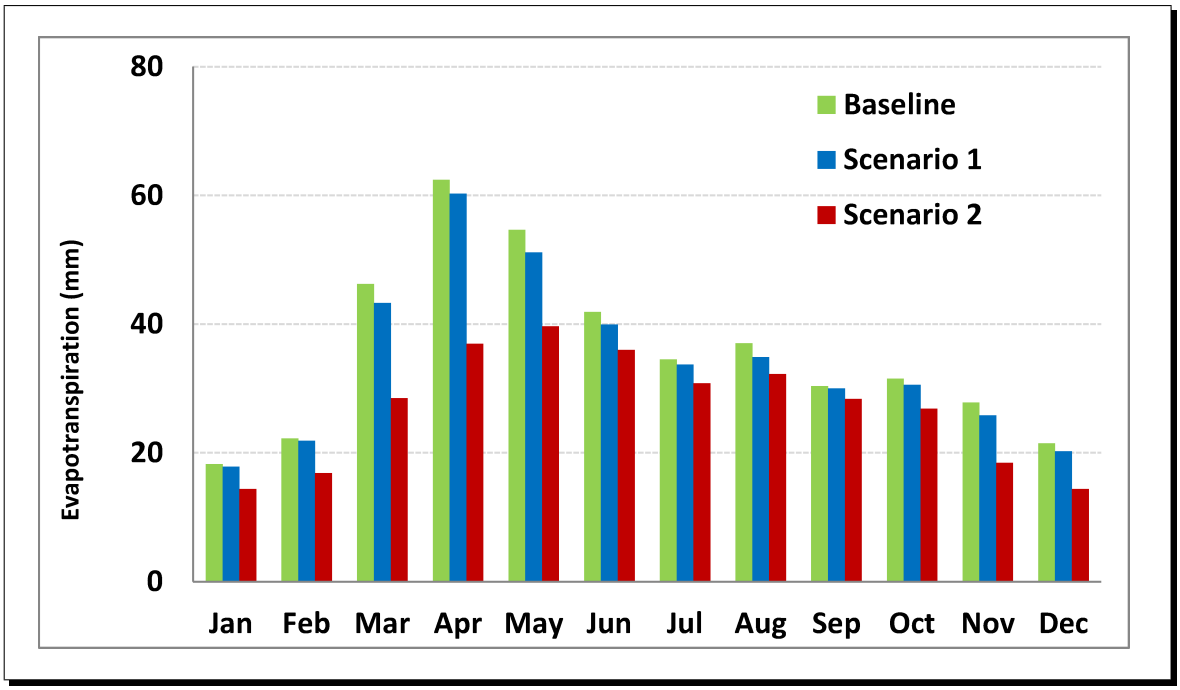

Figure 7.1: Change in monthly evapotranspiration in different land-use change scenarios

Scenario 2 is less realistic in terms of a high probability of occurrence. However it can be seen as a hypothetical demonstration exercise of the impact of deforestation in the study area. In this scenario, the AET is decreased by 24 percent (105 mm/year). Figure 7.1 indicates the changes in average monthly evapotranspiration. In this scenario, the AET is reduced by a larger amount compared to Scenario 1, because of lack of root depth in bare land areas. The difference is most visible during the pre-monsoon period (March-May) when the soil is partly saturated. In addition, there are more favorable conditions for higher AET in this period, such as higher temperature, sunshine-hour duration and wind speed. All these factors result in the soil more readily losing water content through evapotranspiration. The differences of AET in Scenarios 1 and 2 during the monsoon period are low, because the soil-moisture content is close to field capacity and enough water is available for evapotranspiration. The role of vegetation in transpiration during the monsoon season is partly overshadowed by intense rainfall during this period and prevailing saturated conditions of the soil. Due to a sufficient water content in the soil, the AET is close to PET as indicated in Figure 6.14 also. In such conditions, a higher amount of AET is expected even if there were no vegetation.

In Scenario 2, the streamflow is increased by about 7 percent compared to the baseline condition. The average value of whole period (1985-1997) does not differ much with the parameter value (0.5 and 0.1) although the streamflow is slightly (6 mm) increased towards the parameter value 0.1. The magnitude of increase in streamflow for the years 1996 and 1997 is provided in Figure 7.2(a). The grey band represents the ensemble runoff while changing the *SoilImpLT80* parameter value in between 0.5 and 0.1. The model results suggest that the streamflow will be increased during the pre-monsoon period and beginning of the monsoon period (June through July) when the soil is partly saturated. It can be assumed that the flood events (related to overland flow) will be increased during this period.

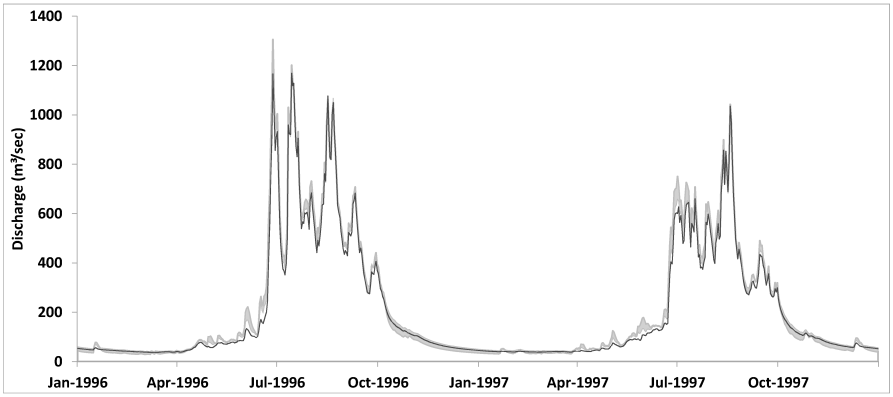

(a) Impact of land-use change on daily hydrograph

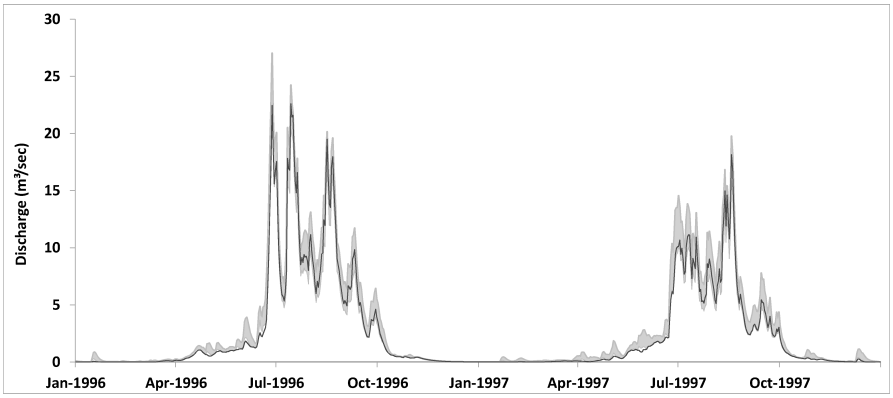

(b) Impact of land-use change on overland flow (RD1) component

Figure 7.2: Impact of land-use change on hydrological regime in Scenario 2. The grey band represents the ensemble runoff by changing the parameter *SoilImpLT80* to reduce the infiltration. The black lines indicate the simulated runoff (upper) and simulated overland flow RD1 (below) during the baseline period.

From the mid-monsoon (normally, the month of August) period when the soil gets saturated due to heavy precipitation from earlier months, the streamflows increase to a lower degree because there will be less infiltration in saturated soil. During the recession and baseflow periods, the streamflow might decrease compared to the baseline period as indicated in Figure 7.2(a).

The deforestation scenario has more influence on different runoff components. Due to less infiltration in bare land areas, the precipitation quickly drains the ground surface as overland flow. Figure 7.2(b) shows the change in overland runoff component in Scenario 2. The overland flow is increased during the pre-monsoon and beginning of the monsoon periods (June through July), compared to the baseline. Similarly, the overland flow does not change much during the high floods and the last two months of the monsoon season, due to saturated soil condition. The scenario exercise indicated that the overland flow could be increased up to 32 percent compared to the baseline period. The maximum increase was

observed to the value close to 0.1 because of decrease in infiltration. On the contrary, the baseflow is decreased up to 20 percent. This is because of the less infiltration in this scenario, which causes less groundwater storage and associated flow.

In both cases, the J2000 modelling system is able to replicate the land-use change scenarios fairly well. The primary effect of deforestation is the change in evapotranspiration which the model is able to capture the physical hydrologic processes in both scenarios well. Regarding the effect of deforestation on hydrograph, under assumption of decrease in infiltration, the model results can be considered fairly representative. Moreover, the effect of deforestation during the later period of the monsoon season is also accurate and convincing. The saturated soil conditions after the continuous rainfall events during the monsoon season reduce the infiltration and thereby behaves similar to surfaceflow in the condition with or without vegetation.

7.1.5 Impact on downstream area

In both of the scenarios, the volume of streamflow will be increased. Particularly, with Scenario 2 (deforestation), the model results suggest that the hydrograph will be increased due to higher amount of overland flow compared to baseline. The bare land will produce higher overlandflow than the forest areas. This will indicate the the magnitude of flood events during the monsoon season might increase in the absence of vegetation. The increase in overland flow is mainly dominated during the pre-monsoon and first-two months (July and July) of the monsoon season. After this period, the soil becomes saturated due to intense monsoon rainfall and the role of vegetation is overshaowed. The infiltration will be decreased due to the saturated soil conditions. Nonetheless, most of the increase in streamflow is concentrated during the monsoon season when there is already too much water due to intense rainfall. The pre-monsoon period might have slightly higher streamflow compared to the baseline condition. On the contrary, due to less infiltration, the volume of water during the recession and baseflow are likely to decrease. In addition, there will be minimum change in downstream water availability due to change in vegetation type (such as forest to shrubland in Scenario 1) primarily because there is minimum change in evapotranspiration. In this case, the critical assumption is that the infiltration rate will not differ much.

The role of vegetation in hydrological dynamics is manyfold. In terms of streamflow, the state of deforestation increases the total volume of the streamflow which is supported by the literature as well (Section 2.2.1). In this study, the deforestation scenario has lead to an increase in total streamflow as a result of a decrease in AET. The effect of vegetation on soil erosion is another important aspect. The vegetative cover always reduces the erosion by providing better protection against soil erosion (such as contributing dead leaves and litter) and also by retaining soil particles with roots. In the monsoon-dominated Himalayan region, the role of vegetation is partly influenced by intense rainfall. Especially, during the monsoon period, the soil becomes saturated and the role of plant roots to hold soil particles gradually declines resulting in soil loss on the land surface. However, in this study, the effect of vegetation surface on erosion is not considered.

The role of vegetation in streamflow is most visible in micro-catchments (<100 km^2) due to relatively rapid response of the watershed. In macro-catchments, the effect is overshadowed by the complexity

of the catchment such as lag time and channel storage. As suggested in the literature review, the impact of land-use change on streamflow depends upon the condition of infiltration after the change. There is some uncertainty in the modelling results due to complexity of the process and the parameter values adopted for the change in infiltration. As suggested by Beven (2001a), the prediction of the impact of forest deforestation or reforestation are likely to be associated with some uncertainty. Therefore, the results shows the possible change in hydrological regime after the deforestation and should be taken as indicative only.

7.2 Impact of global climate change

The impact of global climate change on the hydrological regime of the Himalayan region has been a topic of discussion in recent years and the related studies are described in Section 2.2.3. Especially, the warming trends observed in recent decades and rapid glaciers shrinkage in the high altitude areas of the region have caught the attention of wider communities. Therefore, it is important to better understand the role of glaciers in the hydrological regime and the impacts associated with climate change. The past climatic trends in the study area are discussed in Chapter 5.

A hydrological model can be applied by using the output from General Circulation Models (GCMs) however, the spatial resolution of GCMs (about 250 km) might be too coarse to represent critical features such as topography, elevation and land-use. This brings considerable challenges for the impact assessment of climate change on hydrological dynamics in a river basin (Watson et al. 1996, Akhtar et al. 2008, Tisseuil et al. 2010). Therefore, considerable effort has been put forward to bridge the gap between the large- versus local-scale climate data through statistical downscaling (Wilby et al. 1999) and dynamical downscaling (Hay et al. 2002). In the latter, Regional Climate Models (RCMs) use GCM outputs in the regional area of interest. The high resolution of RCMs (10 to 50 km) provides a better spatial variability of climate-related model-input data (such as precipitation). As suggested by Akhtar et al. (2009), hydrological simulation in data-sparse regions like the Himalayan region using RCM output includes considerable problems such as uncertainties in inputs, model structure and parameters. The most critical uncertainties are related to the GCM with additional uncertainties linked to the local-scale patterns in downscaling of temperature, precipitation and evapotranspiration.

7.2.1 Climate projection data

In this study, climate projection data from PRECIS (Providing REgional Climates for Impact Studies) between 1961-2096 have been used for the analysis. PRECIS is a regional climate modelling system at the of the Hadley Centre, UK, which was run at the Indian Institute of Tropical Meteorology (IITM), Pune, India at 50 km x 50 km horizontal resolution over the South Asian domain. The PRECIS data were provided by IITM upon request. PRECIS is based on the atmospheric component of the Hadley Centre Coupled Model (HadCM3) GCM (Gordon et al. 2000) and is well described in Jones et al. (2004). PRECIS is one of the very few RCMs available in the monsoon dominated Himalayan region. Kripalani et al. (2007) compared the output of the coupled climate models in South Asian

summer monsoon precipitation variability. Out of the 22 models examined, 19 are able to capture the maximum rainfall during the summer monsoon period with varying amplitude. Out of the 19 models, seven models are considered to simulate the inter-annual summer monsoon mean and variability well, including the HadCM3. Therefore, output from PRECIS has been chosen for this study, as HadCM3 is a driving GCM for PRECIS.

In PRECIS, originally, three simulations from a 17-member Perturbed Physics Ensemble were generated using HadCM3 for quantifying the uncertainty in the Model Predictions (QUMP) project and were used to drive PRECIS (Kumar et al. 2011). Therefore, the output from PRECIS comprises three simulations. Among the three, the data with standard parameter settings (Q0) were used for this study. The other simulations (Q1 and Q14) were run with different parameter settings to quantify model uncertainties. The comparison of these three sets of data with the observed data in the Indian sub-continent was made by Kumar et al. (2011) which suggested that the standard parameter settings (Q0) simulations have shown better results regarding its ability to simulate the seasonal monsoon rainfall. The PRECIS simulations correspond to the IPCC SRES A1B emission scenario. The A1 storyline and scenario family describe a future world of very rapid economic growth, global population that peaks in mid-21st century and declines thereafter, and the rapid introduction of new and more efficient technologies. The three A1 groups are distinguished by their technological emphasis: fossil intensive (A1FI), non-fossil energy sources (A1T), or a balance across all sources (A1B)[1]) (IPCC 2000). The PRECIS has been used to simulate the monsoon dynamics and the future impact on hydrology in the region (Akhtar et al. 2008, Kumar et al. 2006, Akhtar et al. 2009).

The climate models are not a perfect representation of the complex system of nature and therefore uncertainties exist in the model output data. In this study, the impact of climate change on the hydrological regime of the Dudh Kosi river basin is conducted by using PRECIS RCM data without bias correction. It can be assumed that the bias behavior of the climate model data is consistent in the past and future (for example, if pre-monsoon is overestimated, the overestimation holds for the whole time period). In addition, as suggested by Hagemann et al. (2011) bias correction has an impact on the climate change signal for specific locations and months and thereby creating another level of uncertainty in the model. Kay et al. (2006) have demonstrated the good ability of dynamically downscaled data (without bias correction) to reproduce the flood frequency estimation. In this study, it is intended to compare the hydrological model results in the future with the baseline data which uses the same input data from PRECIS. In this way, comparison of the same dataset is done for baseline and future conditions.

While predicting the impact of climate change on hydrology, it has to be considered that the outputs of the GCMs and RCMs as best estimates of future conditions, while remembering the limitations of the model that produced the estimates. The output results can be accepted as possible scenarios for changed monthly or seasonal average precipitation and temperatures, but they may be subject to considerable uncertainty (Beven 2001a).

[1]Balanced is defined as not relying too heavily on one particular energy source, on the assumption that similar improvement rates apply to all energy supply and end use technologies

7.2.2 Future projection of precipitation and temperature

The 50 km x 50 km resolution data from the entire Kosi river basin has been used for this study. Altogether 54 PRECIS data cells were overlaid in the basin as shown in Figure 7.3. The variability of the PRECIS data was compared with the measured dataset in Nepal (the western part of the basin) where the spatial coverage of the station data is good compared to the northern part of the Kosi river basin. The purpose of this was to compare the variation of the PRECIS data in relation to the measured data. Data from the cells and closest stations were compared to get the monthly and annual variability for some years.

Because not every grid cell have one or more observed stations, the grid cells (14, 15, 20, 21, 26, 27, 32 and 33) from the Dudh Kosi, Arun and Tamor river basins were chosen for comparison. These grid cells included 29 precipitation stations, the location of which are indicated on Figure 7.3(a). For temperature, Okhaldhunga station (the top station in grid 14) was chosen. The monthly average precipitation of these 29 stations were taken from 1985-1997 which was the similar time period for the analysis of precipitation dynamics (Chapter 5). From the analysis of precipitation variability for this period of record, it was found that between 73 to 81 percent of precipitation occurs during the monsoon season. It is important to understand how the PRECIS represents the monthly distribution of precipitation, especially during the monsoon period. Comparing the grid values with the observation station(s) is not easy because the grid value represents the entire 50 km of grid cells, whereas the station value is only representative for the point. The complexity increases in the mountainous region, similar to the study area, because within the grid, the elevation differences could be very high. For example, in grid 21, the difference between the lowest and the highest elevation is nearly 6,000 m.

Figures 7.3(b) and 7.3(c) indicate the monthly precipitation and temperature values between observed stations and grid data (projected). These monthly plots suggest that the projected precipitation values are higher than measured station data both in the pre-monsoon and post monsoon periods, however the seasonal trends are captured fairly well. During the monsoon season, both over and underestimation in compared values can be noted, however, the difference between the total volumes is less than 100 mm (5 percent of the grid data). About 58 percent of the precipitation occurs during the monsoon season, in comparison to the average of 75 percent of the observed data. In the case of the monthly temperature data (Figure 7.3(c)), the observed station (Okhaldhunga) and the value from grid 14 were compared. The monthly comparison suggested that the PRECIS data is close to the observed data and follows the seasonal trend fairly well. Nonetheless, the grid data are underestimated compared to station data during the winter period, and the comparison is quite closer during the summer period. This inconsistency is due to the minimum temperature. The maximum temperature shows a consistent trend with the observed data, but the minimum temperature is lower than the station data values during the winter period. This overall condition suggests that the uncertainties in precipitation projections using grid data are greater than those in temperature. Therefore, the PRECIS data is less representative for precipitation distribution in the mountainous regions of Nepal whereas the temperature data are fairly close to the observed station data. The PRECIS was originally run for the Indian sub-continent and is more representative of lowland areas compared to the mountains (Prof. L. Devkota, Tribhuvan University, Nepal, personal communication). As suggested by Randall et al. (2007) climate models

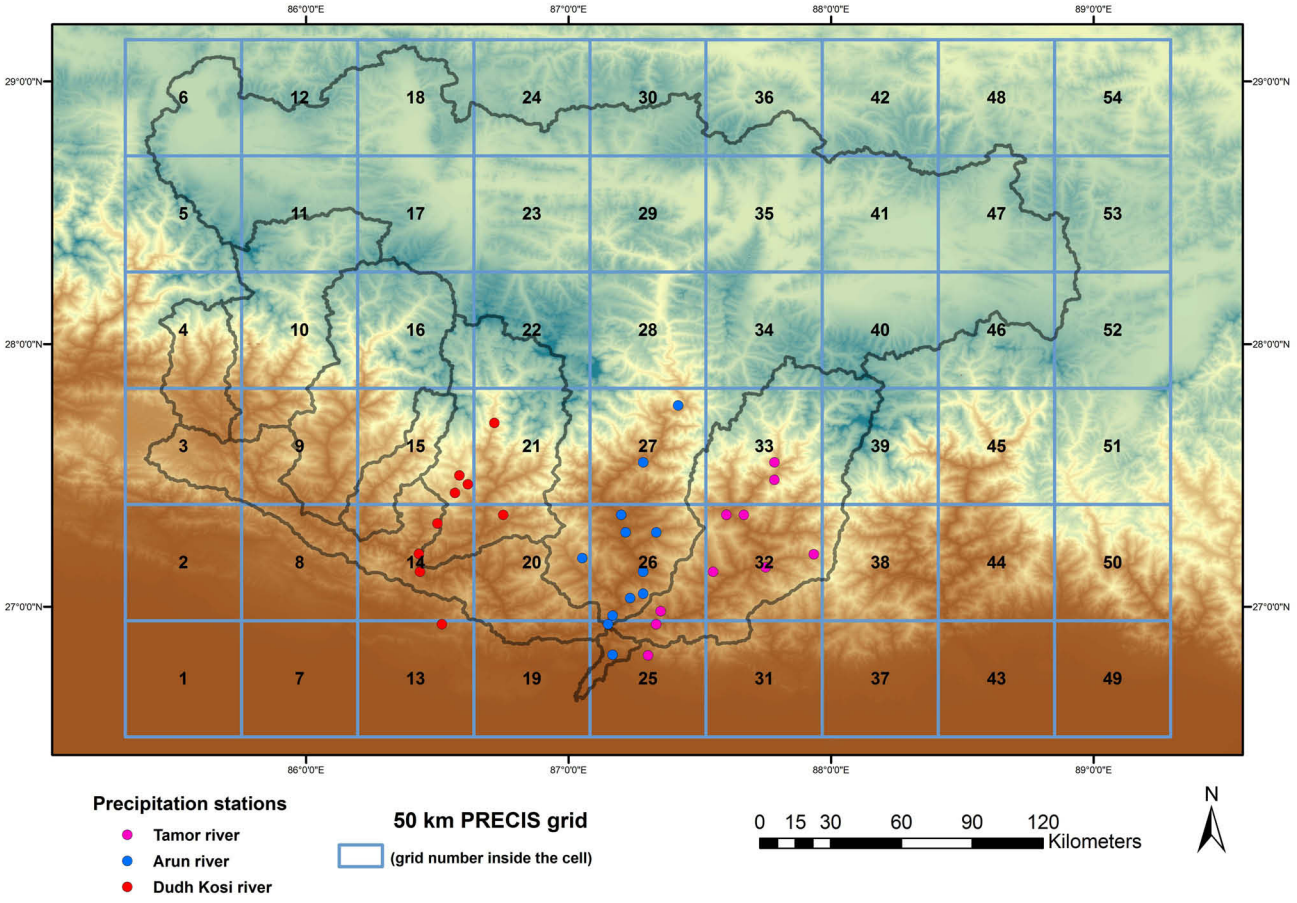

(a) Overlay of PRECIS grid for the Kosi river basin. The numbers in the cells represents grid numbers

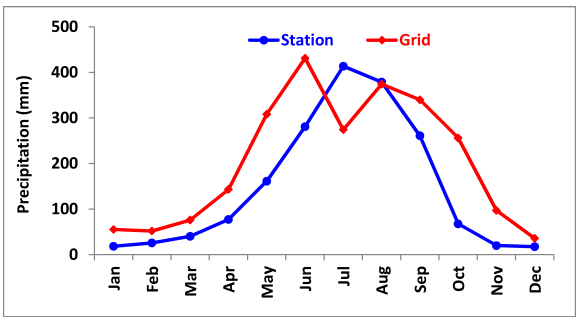

(b) Comparison of monthly PRECIS and observed precipitation data (1985-1997)

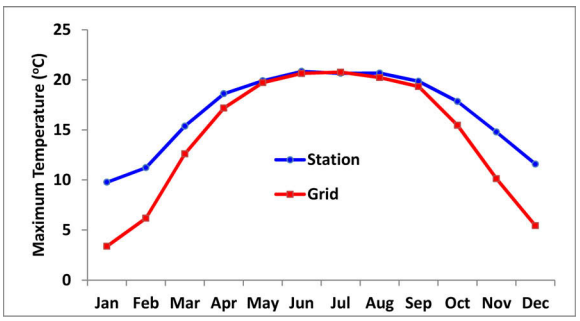

(c) Comparision of monthly PRECIS and observed mean temperature data (1985-1997)

Figure 7.3: Comparison of PRECIS and observed station data

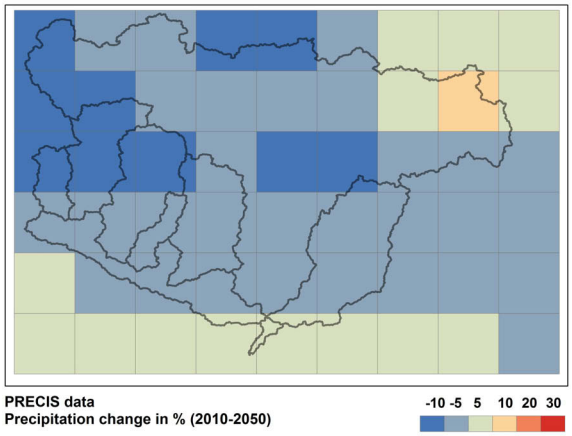

(a) Change in annual precipitation (2010-2050)

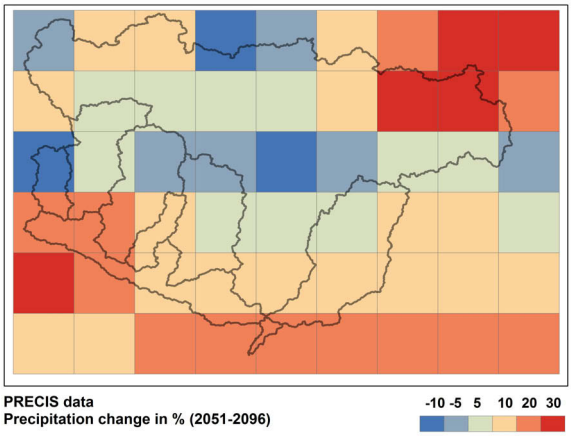

(b) Change in annual precipitation (2051-2096)

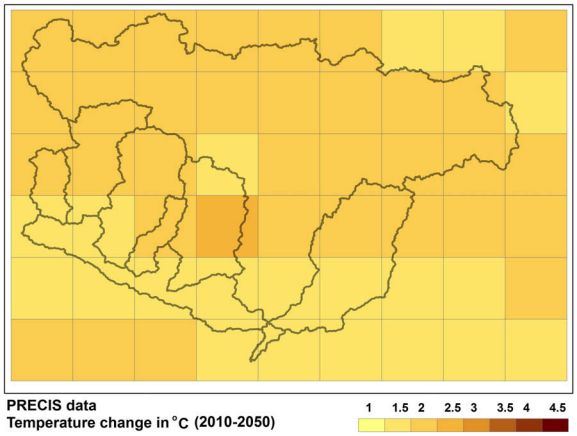

(c) Change in mean annual temperature (2010-2050)

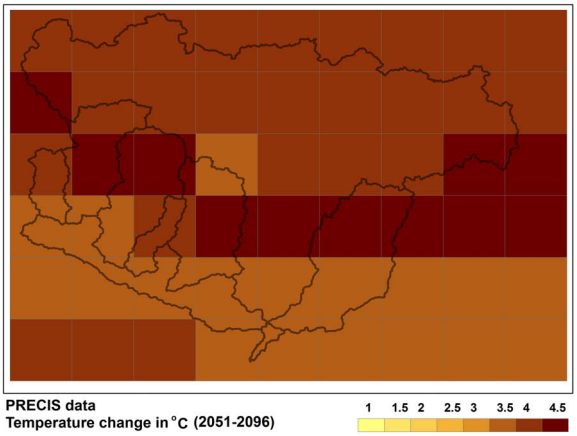

(d) Change in mean annual temperature (2051-2096)

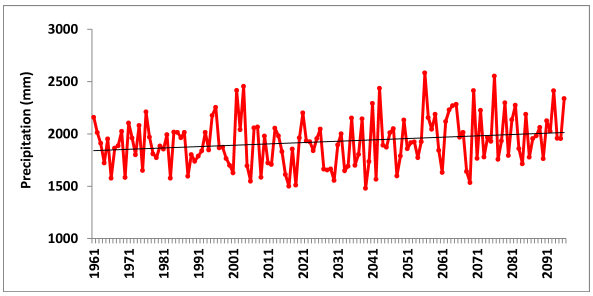

(e) Change in annual precipitation in the Kosi river basin (1961-2096). The black line indicates the annual trend

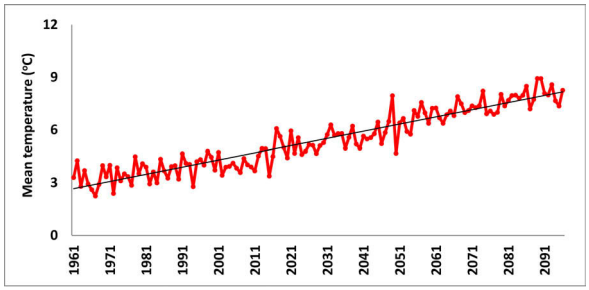

(f) Change in mean annual temperature in the Kosi river basin (1961-2096). The black line indicates the annual trend

Figure 7.4: Figure a, b, c, d: Projected change in precipitation and temperature in two future scenarios with respect to the baseline period (1961-2009). One grid represents 50 km x 50 km spatial resolution of data from PRECIS RCM. Figure e, f: Projected precipitation and temperature trend in the Kosi river basin from 1961 to 2096 respectively

are based on well-established physical principles and have been demonstrated to reproduce recent climate and past climate changes. There is considerable confidence that Atmosphere-Ocean General Circulation Models (AOGCMs) provide credible quantitative estimates of future climate change, particularly at continental and larger scales. However, confidence in these estimates is higher for some climate variables (eg. temperature) than for others (eg. precipitation).

Figure 7.4 shows the projected changes in mean annual precipitation and temperature in the Kosi river basin. The two future scenarios 2010 to 2050 (hereafter, referred to as Future 1) and 2051 to 2096 (hereafter, referred to as Future 2) were compared to the baseline period (1961-2009). Figures (7.4(a) and 7.4(b)) suggest that the precipitation in the Kosi river basin in general will decrease in Future 1, although the lower elevation areas indicate an increase in amount of precipitation. In Future 2, the precipitation will in general increase more in the southern part with higher magnitude in the lower elevation areas. Few grid cells in the northern part (upper corner of the right hand side) indicate increases in precipitation. Figure 7.4(e) suggests that the precipitation is likely to increase by 14 percent (32 mm/decade) in by the end of the century. Most of the precipitation change and associated trend is attributed to the seasonal precipitation occurring during the monsoon season. The other seasons indicate a relatively lower increasing trend which accounts for 4 percent (post-monsoon) and 2 percent (winter and pre-monsoon).

In temperature projection, Figures 7.4(c) and 7.4(d) indicate the warming trend prevailing all over the Kosi river basin in both future scenarios, with a relatively higher magnitude of change in Future 2. A gradual increase in temperature is predicted in the cases of both future scenarios at the rate of 0.46 ^{o}C /decade as shown in Figure 7.4(f). The mean temperature is likely to be increased by about 4 ^{o}C by the end of the 21st century based upon the PRECIS RCM data. In contrast to the precipitation trend, the mean temperature change is likely to be higher in the higher elevation areas. The southern low land areas will warm at a lower rate.

The climate projection data of grids 14, 15, 16, 20, 21 and 22 (Figure 7.3(a)) are considered as an input for the hydrological model in the Dudh Kosi river basin for future scenarios. In Future 1, the precipitation will be decreased. However, the model data suggest that precipitation will be increased in Future 2 primarily in the lower elevation areas of the basin. The two grids in the higher elevation areas (16 and 22) showed a decreasing trend in Future 2 as well. The precipitation is estimated to increase by 12 percent (Figure 7.4(b)) between the years 2010 and 2096. There is a more consistent warming trend in both future scenarios, with a higher trend in Future 2. The mean temperature will rise by nearly 4^{o}C by the end of the century.

7.2.3 Impact of climate change on hydrological regime

The impact of climate change on hydrological dynamics in the Himalayan region has been a topic of discussion in recent years (Eriksson et al. 2009, Bates et al. 2008, Immerzeel et al. 2010, 2012). The hydrological systems are closely connected to the climate system and influenced by climate change and variability. In general, specifically in the study area, the increasing precipitation and temperature trends will influence the hydrological regime in several ways. On the one hand, the positive temperature trend will result in higher AET and on the other hand, in an increase in snow and glacier melt. In

addition, it will cause the snow line to shift upwards in elevation and thereby will tend to decrease the snow occurrence and snow-storage capacity of a basin.

7.2.3.1 Modelling strategies

In this study, the calibrated and validated J2000 model for the study period 1985-1997 (Chapter 6) has been used for the analysis of baseline and future scenarios. The baseline condition is generated between 1975-2009 for change detection by using the PRECIS data. Two future conditions have been simulated between 2010 to 2050 (hereafter Future 1) and 2051 to 2096 (hereafter Future 2). Both baseline and future scenarios were simulated by using the J2000 hydrological model. The baseline conditions will be compared to the future conditions to understand the change in hydrological regime.

For this purpose in the analysis, the center of a grid is considered as a station. The elevation of the station is derived from the average elevation of the grids. In the calibrated and validated model, the temperature regionalisation was conducted using a lapse rate, since there were only a few temperature stations in the study area. However, in the case of climate-projection data, six stations are available and therefore the IDW with elevation correction (Section 6.4) is applied for temperature regionalisation. The precipitation, wind speed and relative humidity are also provided by the PRECIS model on a daily basis. Unfortunately, the PRECIS model does not produce future sunshine-hour data. Therefore, a monthly sunshine-hour is calculated by using the observed data for the period between 1985 to1997 and then applied to the entire time period. The same land-cover information was used for the two future scenarios.

The analysis using the climate projection data is considered without the glacier ice melt and only snow melt from glacier areas is included. The glacier areas and ice storage do not change with time in the J2000 modelling system. The contribution from ice melt will increase if the air temperature rises and vice versa because the ice melt is a function of the degree-day factor. However, in reality the glacier areas might change due to change in temperature. Therefore, the hydrograph (Figure 7.5(a)) is considered without the glacier ice melt.

7.2.3.2 Impact on monthly hydrograph

Figure 7.5(a) indicates the monthly pattern of streamflow in the Dudh Kosi river basin for two future scenarios. The streamflow is increased mainly during the monsoon season in both Future 1 and 2 scenarios compared to the baseline period as shown in Figure 7.5(a). During the monsoon season, the discharge is increased by 4 percent and 8 percent in Future 1 and 2 respectively. In Future 2, there is a decrease in streamflow in August which is due to a decrease in precipitation during that period. As discussed in previous chapters, the increasing trend in precipitation data occurs mostly during the monsoon season, the most visible increase in monthly hydrography is also reflected in the monsoon period. The increase in average annual discharge by 2 percent and 6 percent in Future 1 and 2 scenarios respectively can be attributed to an increase in annual precipitation of approximately 14 percent (32 mm/decade). In addition, due to assumed trend of increasing air temperature in future, the snowline will shift to high altitude areas and thereby more snow storage will be exposed for

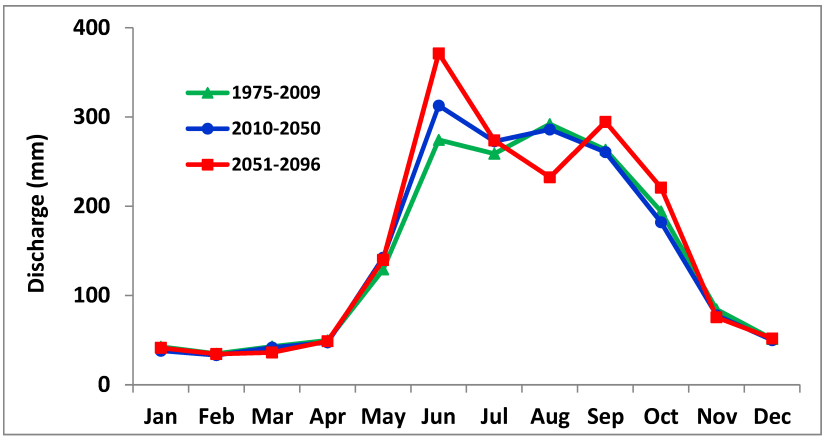

(a) Impact of climate change on monthly discharge cycle. Period 1975-2009: Baseline period, 2010-2050: Future 1 and 2051-2096: Future 2

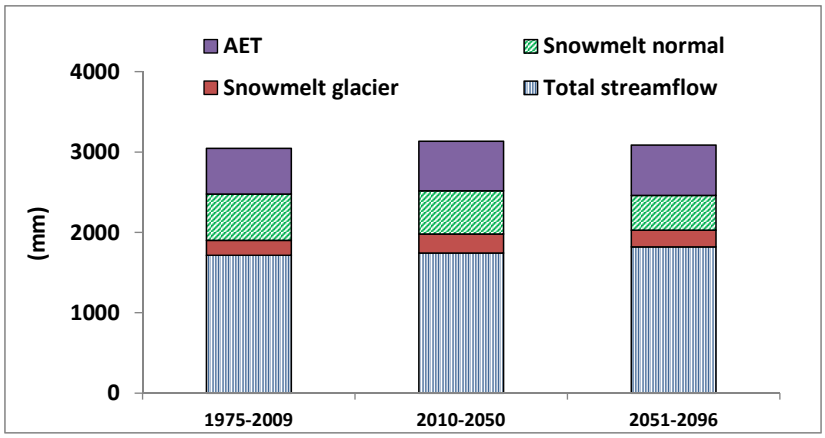

(b) Impact of climate change on different water balance components

Figure 7.5: Impact of climate change on hydrological regime

melt. Part of the increased precipitation is estimated to be lost through higher AET associated with a increaseing temperature trend. The AET in Futures 1 and 2 is increased by 9 percent and 11 percent (Figure 7.5(b)) respectively compared to the baseline period. The snowmelt outside of the glacier area (*snowmelt normal*) is decreased by 7% in Future 1 and to 25% in Future 2 whereas snowmelt from glacier area (*snowmelt glacier*) is increased by 28% in Future 1 and then decreases to 12% in Future 2. In both scenarios, the positive increase in temperature will shift the snowline towards higher altitude areas. This will decrease the snow storage capacity of the basin. Other than the glacier area, the precipitation is stored as snow in lower elevation areas especially during the winter and pre-monsoon periods when the temperature is relatively low. These areas will be greatly affected in terms of snow storage by the anticipated increase in temperature, therefore, snowmelt from these areas (*snowmelt normal*) will decrease in both Future 1 and Future 2 scenarios. On the contrary, snowmelt from glacier area (*snowmelt glacier*) will increase in Future 1. As the temperature increases, more snow

will be available for melt as the snow is stored above the snowline from previous years. In higher temperature scenarios, the stored snow will be melted away in Future 1. In Future 2, the snowmelt is gradually decreased because the storage is consumed (melted away over time) and less snow storage is available for melt in subsequent years of Future 2. The snowmelt scenarios (in glacier and non-glacier areas) indicated that the total snowmelt contribution of the basin will decrease in these future scenarios. It can be assumed that this will gradually change the basin streamflow from a 'melt' river to 'rain' river type of stream. As the melt season coincides with the rainy season, no shift in hydrograph is anticipated to occur in this study.

The impact of projected climate change on different runoff components is also analysed. The most visible impact can be seen in the change in overland flow (RD1) which has been increased by 8 percent and 18 percent in the two future scenarios respectively. This may be because of two reasons: (a) The increasing trend in precipitation results mostly during the monsoon season as described in the previous section. The higher precipitation during the monsoon season increases the rainfall-runoff coefficient due to saturated soil condition. (b) Secondly, there may be more extreme precipitation events in the future which may cause the higher overland flow. Any additional precipitation during the monsoon season is likely to produce overland flow due to the saturated condition of soil during this period. The snowmelt contribution from glacier areas (which directly goes to the stream and is considered as overland flow) decreases in Future 2. In spite of the decrease in snowmelt, an increase in overland flow indicates that extreme precipitation events may occur more frequently in future.

The understanding of fluctuations of glacier area and melt runoff from glacier ice storage in the context of climate change is limited. Under the assumption of warming temperature due to climate change, it is likely that the glacier areas on the lower elevation areas might decrease. At the same time, due to rise in temperature, more glacier area will be exposed for melt and thereby increasing streamflow caused by larger glacier melt rates (Jansson et al. 2003, Hock et al. 2005). This will lead to the increase in runoff which will last for a few decades, and then decreases as the glacier disappear. In the area with large glaciers and storage, the extra runoff may persist for a century or more (Gitay et al. 1998). All these processes primarily depend upon how much ice is stored under glaciers. The fluctuations of glaciers discharge under warming climate is complex and to replicate the response in a modeling system is a challenging task (Hock et al. 2005, Singh and Kumar 1997). As suggested by Hock et al. (2005), the response of glacier runoff to climate warming is a matter of timescale.

Only two studies have been found in literature suggesting the future response of glacier icemelt runoff under climate change scenarios in the Himalayan region (Immerzeel et al. 2012, Prasch 2010). Immerzeel et al. (2012) suggested that assuming a warming climate trend (0.6^{o}C/decade), between 2000-2100, the glacier area will decrease by 32 percent in 2035, by 50 percent in 2055 and by 75 percent in 2088 in the central Himalaya of Nepal. The total ice volume also shows a similar decreasing trend but the decrease is slightly faster than the area. Prasch (2010) studied the glacial melt pattern in Lhasa catchment in Tibet under different SRES scenarios. In A1B scenario, the study suggested that the glacier area is decreased by 37 percent in between 2011-2040 and by 77 percent in between 2051-2080. Similarly, the ice water reservoir is decreased by 26 percent and 73 percent in between 2011-2040 and in between 2051-2080 respectively. The icemelt from glacier areas is decreased by 10 percent in between 2011-2040 and by 17 percent in between 2051-2080. These two studies indicate

that under the warming temperature trend, the glacier areas will be decreased. This will subsequently also affect the glacier ice-storage and thereby the ice-melt runoff will also decrease.

From this analysis, it is found that snowmelt runoff and AET are sensitive to climate change. The change in these two components towards the end of the century could be high. The temporal change estimated in this study is the average of a certain period and therefore represents a moderate value. In the case of actual increase in temperature by 4^{o}C towards the end of the century as suggested by the PRECIS RCM, the change in AET and snowmelt pattern could be higher than the average value presented here. The glacier icemelt contribution to the total streamflow during the baseline period is only 5 percent. The possible change in the glacier icemelt contribution due to climate change (both increase or decrease) can be considered low in the overall hydrology.

7.2.3.3 Impact to downstream areas

The impact of global climate change i.e. increases in temperature and precipitation, as suggested by the climate model data, indicate that the total streamflow will be increased in future. The model results further suggest that the river will be gradually shifted from a melt river to a rain river. The downstream areas might face more serious flooding events as the precipitation is increased mainly during the monsoon season. This is also suggested by the increase in an overland flow component in future with PRECIS data. In addition, due to higher temperature in future, more precipitation will occur as rain rather than stored in the watershed as snow. The scenario does not indicate a significant shift in the monthly hydrograph because the melt season coincides with the rainy season.

Although, the contribution of the glacier icemelt is low compared to that of the total streamflow for a meso-scale basin (similar to the Dudh Kosi river basin), the role in the upstream areas can not be neglected. Although small in volume, it may be an important source for local livelihoods (such as irrigation) during the pre-monsoon season when the discharge is relatively low. As the glacier ice contribution during the April through May period is 13 percent (Table 6.12), a decrease in glacier ice volume and related melt (due to global climate change) will most likely influence the streamflow during these months.

7.3 Multi-dimension of upstream-downstream linkages

In this study, the discussion on the upstream-downstream linkages is driven primarily by the analysis of the change in land-use and climate. Because the upstream-downstream linkages are multi-faceted and integrated in nature, the other water management aspects are also discussed. Overall, the purpose is to discuss other aspects of upstream-downstream linkages so that potential benefits can be achieved between upstream and downstream communities by reducing the risks (eg. floods) and enhancing the benefits (eg. better management of watershed). In this section, a multi-purpose dam project in the Kosi river basin has been discussed with focus on upstream-downstream linkages .

Many issues in upstream-downstream linkages are scale-dependent. As suggested by Walling (1999,

2001), there is clear evidence of the sensitivity to land-use change related to human activity in a small-scale watershed. For example, the change from natural vegetation to cultivation can increase soil erosion. However, the impact of land-use change on sediment yields of bigger watershed (such as 1,000 km^2) is less clear. Much of the eroded soil would be deposited before reaching the stream network. In case of deforestation and streamflow, the impact of deforestation is more relevant where the immediate impact can be seen in the form of higher overland flow. When the scale increases (bigger watershed), the effects are unclear and overshadowed by other components.

7.3.1 A multi-purpose dam project

The Government of Nepal (GON) and the Government of India (GOI) have agreed to conduct a joint investigation for the preparation of a Detailed Project Report (DPR) of the Sapta Kosi High Dam Multipurpose Project and Sun Kosi Diversion Schemes[2]. The main objective of the project is to develop hydropower, irrigation, navigation and flood control and management for the mutual benefits of both countries. The 1981 feasibility report, prepared by India, envisages a flood moderation of up to one-third of the live storage of the reservoir to be created by the 269 m high dam with a flood cushion capacity of 2.4 billion m^3. The high dam project is expected to provide water for irrigation (68,500 ha in Nepal and 1.5 million ha in India) and includes a hydropower plan with a proposed capacity of 3,489 MW (Bhattarai 2009). The dam is proposed at the confluence of Sun Kosi and Arun river, about 1.6 km upstream of Chatara, and covers the entire Sun Kosi river systems (Figure 4.2) (Mr. S. Bajracharya, Project Manager, The Sapta Kosi high dam project, personal communication, 2012). These estimates are based upon a very preliminary assessment and are likely to be changed after more detailed assessment and evaluation of the proposed project.

In case of this dam scenario, the hydrological dynamics of the upstream-downstream linkages are linked with aspects of land and water management. The human role in the land and water resources of the upstream areas directly influences life of the reservoir. Better watershed management protects the soil erosion and thereby reduces the sedimentation in the proposed dam. On the contrary, the higher soil erosion from upstream areas will make the bottom of the reservoir rise and thereby reduces the overall life of the dam.

Secondly, the reservoir will affect the overall hydrology of the Kosi river basin. The 269 m high dam will submerge the immediate areas upstream of the reservoir which will include settlements, agricultural lands and forest areas. The resettlement of those communities will be a challenging task which will be associated with socio-economic and cultural impacts to the communities concerned. At the same time, the hydrological system of the downstream areas will be influenced as the water is

[2]The **Sapta Kosi High Dam Multipurpose Project** is in a very preliminary planning stage. A lot of discussions are on-going between the Governments and civil societies whether to build the high dam project or not. The discussions also indicate the impacts and risk associated with the high dam project both in upstream areas (submerged and relocation) and downstream (possible risk of disaster) because the proposed area is in a highly geologically unstable and earth quake-prone area. The concept of the project is still in a infancy stage and subject to a political decision between the Governments. The sole objective of mentioning the scenario in this study is to indicate the possible upstream-downstream linkages of the proposed dam and to indicate what can be done for the sustainable dam management for the benefits of the larger community. In any case, the assessment in this study, should not be taken as an indication to build or not build the project.

stored in the reservoir and downstream flow will be controlled. The use of downstream water consists irrigation, drinking water and aquatic ecosystem. Minimum flows for maintaining aquatic habitat has to be released from the dam regularly. Similarly, the existing water use for irrigation and drinking water should also be maintained. With the storage concept, more irrigation lands will be developed in a systematic way. The pool of water in the reservoir will lose water through evaporation which will be an amount far higher than that of evapotranspiration of the existing condition. It also influence the groundwater flow and recharge pattern. The Kosi river brings large amounts of sediments during the monsoon season. When the dam traps the sediments, the water storage capacity of the dam may be decreased. As reported in Aswan dam in Egypt, the river bed level downstream of the dam has dropped as the result of erosion caused by the flow of sediment-free water (as the sediment is trapped in the dam) (Biswas 1992). In addition, the deposited sediment serves as a fertilizer in agriculture activities. The construction of the dam might change the pattern of sediment distribution and soil fertility to downstream. In Aswan dam, the reduction in soil fertility due to loss of the nitrogenous component of the silt now has to be compensated by the annual addition of 13,000 tonnes of lime nitrate fertiliser (Biswas 1992).To understand the magnitude, extent and duration of specific issues of the foreseen project, a detailed integrated study is required in relation to the specific detail of the proposed project.

It is important that the concept of Payment for Environmental Services (PES) is also implemented in this scenario. The PES has been implemented and practiced very recently as a market-based instrument for the management of natural resources (Kosoy et al. 2007). As suggested by Butle et al. (2008), PES is a concept of paying for the provision of environmental services to obtain more efficient environmental outcomes for the benefits of the larger community. The PES approach should also be implemented in the Kosi river basin, especially in the case of the proposed dam project, where the upstream communities are supported by the benefits of the project so that they can better manage their watershed. For example, the part of the benefits from the reservoir such as electricity, recreation, boating and fishing could be provided to upstream communities as an incentive for better and sustainable watershed management. Such a sharing mechanism and instrument could be different under specific conditions. Nonetheless, the existing mechanism of PES of the Kulekhani watershed in Central Nepal can be taken as a learning example (Adhikaree 2010). The Kulekhani hydropower project (92 MW) receives the water from the Kulekhani watershed area and sedimentation is a major issue regarding for the reservoir's construction and operation. When using the PES mechanism, the benefits of reservoir and hydropower production have been shared among the upstream communities for watershed management under the Rewarding Upland Poor for Environmental Services (RUPES) program since 2003 (Adhikaree 2010). Adhikaree (2010) did a research study in the Kulekhani watershed area and suggested that the PES mechanism in the area is in the beginning stage and that a more robust mechanism for channelizing resources to the right community responsible for the conservation of the watershed is needed. A study by Nepal and Adiga (2006) indicated that the forest-user group and immediate irrigation-user group in the middle hills of Nepal are willing to cooperate for better watershed management. Especially the lowland community users indicated their willingness to support the forest-user group for implementing forest-conservation activities. Pant et al. (2005) also suggested that forest- and irrigation-user groups could learn from each other's experiences and an integrated management approach would provide better natural resources management. As this concept

is still new to Nepal, a more specific policy and awareness is required (Adhikaree 2010).

7.3.2 Kosi river basin management strategic plan (2011-2021)

The Government of Nepal has recently prepared the Kosi River Basin Management Strategic Plan (KRBMSP) (2011-2021) to operationalise the National Water Plan 2005 (WECS 2011). The plan emphasises that IWRM is implemented at the Kosi river basin. It aims to utilise the water and related resources and at the same time uses IWRM as an effective tool to mitigate the impacts of climate change in the river basin. For this, it plans to use lessons and experiences from the implementation of IWRM at the Dudh Kosi river basin (WECS 2011). For the implementation of the KRBMSP, this study has provided very important information about the upstream-downstream dimensions of the river basin. The hydrological system and scenarios analysis could provide a basis for the better implementation of the KRBMSP.

7.3.3 Summary of this chapter

In this chapter, the land-use and climate change scenarios have been assessed using the J2000 hydrological model. The following are the major findings of the chapter.

1. The use of the distributed J2000 hydrological model for analysing the land-use change scenarios was examined. The results show that the model has been able to replicate the behavior of land-use change fairly well in the region of a monsoon-dominated climate. Evapotranspiration is a major driving factor of deforestation which effects the hydrological regime. The model has depicted the dynamics of change in evaporation in the context of land-use change. It has also realised the effect on different runoff components and total streamflow. The model results suggest that the change of vegetation (forest to shrub or grassland) has minor impact on the streamflow. However, in the case of change of deforestation (forest to bare land), the streamflow would increase due to reduction in infiltration in the bare land areas.

2. The RCM data were used for the modelling of future scenarios. PRECIS RCM is one of very few RCMs run in the monsoon-dominated Himalayan region. The study has provided a basis which allows to use RCM output data in the J2000 hydrological model to evaluate the impacts of climate change on hydrology. Although PRECIS data replicated the seasonal pattern of precipitation and temperature fairly well, over-prediction during pre-and post-monsoon is frequent. In the A1B climate scenario, the temperature and precipitation of the Kosi river basin is presumed to be increased by 4^{o}C and 14 percent by the end of the 21st century respectively. From the modelling results, the basin's discharges will increase mostly during the monsoon season. Although interflows and baseflow do not change substantially, the overland flows are expected to increase which might cause more flooding in downstream areas. Due to an increase in temperature, evapotranspiration will be increased. Similarly, the snowline will shift to higher altitude areas which will decrease the snowmelt contribution. This will reduce the snow-storage capacity of the basin, and the stream is likely to be shifted in type from a 'melt-dominated river' to a 'rain-dominated river'.

8 Conclusions and future outlook

This chapter provides the summary of and conclusions based upon the principal study results discussed in previous chapters. In addition, a brief outlook on future research is given.

8.1 Summary and conclusions

The study was conducted in the Himalayan region to understand the upstream-downstream linkages of hydrological dynamics. Data and information of the region is sparse and not readily available. Primarily, very few data are available in the high-altitude areas due to geographical settings and remoteness. The primary objective of the study is to evaluate the upstream-downstream linkages of hydrological dynamics in the Himalayan region. The study attempted to understand the hydrological system dynamics of the Kosi river basin using the J2000 hydrological model and the model application enables assessment of changes in climate and land use. The understanding of process characteristics of precipitation and runoff generation derived from the modelling was instrumental in recognising the upstream-downstream relationship. The results and findings are discussed below:

The following are the major findings from the results related to the first and second objective as mentioned in Chapter 3.

The spatial distribution of precipitation in different mountain systems of the study area was analysed. The annual and monthly distribution of precipitation between 1985 to 1997 were analysed in four different river corridors of the western part of the Kosi river basin. In addition, the hydro-climatic trend based on the available data of the last 23 to 56 years period was also analysed using non-parametric trend analysis to understand the past climate change situation. The following are the main results and findings:

- The spatial distribution of precipitation is controlled by the underlying geology of the mountain systems. Due to this effect, the high mountains and windward side receive relatively higher precipitation than the leeward and valley areas.
- There is a high confidence in recent temperature warming, and most of the stations indicate positive increasing temperature trends which are statistically significant. All the stations indicate a gradual increase in average annual temperature after the 1980s. The magnitude of the trend is higher in maximum temperature than in the minimum. The three temperature stations which have relatively data available for last 40-50 years show an increasing trend of maximum temperature at the rate of 0.57^{o}C/decade. The observation in this study supports similar observations in other parts of the Himalayan region (Shrestha et al. 1999, Liu and Chen 2000). On the

contrary, the precipitation data does not indicate any clear trend; however, some localised trends both increasing and decreasing, were observed. The discharge data of the gauging stations also indicate both increasing and decreasing trends.

- About 77 percent of the precipitation occurs during the monsoon season on the southern part of the Kosi river basin. Some precipitation stations with a high annual precipitation value indicated that the pre-monsoon rainfall (especially during the month of May) is very high compared to other stations. This indicates that convective rainfall dominates in those areas. However, more research studies and field observations are required to detect the real cause of this seasonal occurrence of high precipitation.

The results from the hydro-climatic data analysis suggest that the Kosi river basin indicates a warming trend prevailing all over the area; however, the precipitation does not show any significant trend. This suggests that the hydrological regime of the region might be altered in the context of climate change.

The following are the major findings from the results related to the third objective as mentioned in Chapter 3.

The application and adaptation of the process-oriented and distributed J2000 hydrological model in the Dudh Kosi and Tamor river basins were conducted. The glacier module is integrated into the J2000 hydrological model to simulated the melt runoff from glacier areas. The model entities were developed using the distributed concept of HRUs by considering input from physiographic properties of the basin (such as digital elevation model, land use, and soil types). A total of 3,799 HRUs were delineated, which represented the spatial heterogeneity of the basin. The model was calibrated and validated within the period of 1985 to 1997 in the Dudh Kosi river basin. In addition, the model parameters were transferred from the Dudh Kosi river basin to the Tamor river basin using a proxy-basin approach. The model output provides information about the precipitation-runoff characteristics of the basin and were used to understand how the catchment responds to precipitation.

- The model is able to reproduce the hydrological dynamics of the basin satisfactorily based upon the graphical and statistical evaluations. During the validation period in the Dudh Kosi river basin, the efficiency results are E_{NS}: 0.87, LNS: 0.95 and r^2: 0.88, which can be considered good from a statistical evaluation. The low flow, including rising and recession limbs, is fairly representative. However in the case of high flow periods, both over- and under-predictions were observed. The proxy-basin approach applied in the Tamor river basin indicates satisfactory results for low- and mid-range flows. However, during the flood periods, the model results are underestimated in most of the years. This can be explained by the fact that the measured discharges in August are always higher than measured precipitation. This has caused the model to underestimate the streamflow in this period. The consistent higher value of observed discharges than precipitation in August has two possible explanations. First, the observed precipitation is underestimated due to the specific locations of rainfall stations in the valley areas. Secondly, the estimated discharge using the existing rating curve is not sufficient for the high flow periods. Since, the rainfall-runoff ratio of the Dudh Kosi river basin is fairly representative (discharge is lower than precipitation), there is a higher possibility that the rating curve is less representative for the Tamor river basin. Therefore, the model performance is better if there is a consistency

in the rainfall-runoff ratio.

- The adaptation of the parameter in the soil module to represent the high flood peaks works fairly good. The parameter has adapted the non-linear behavior of the catchment during the monsoon season and is suitable for simulating high flood periods.
- The glacier module, implemented in the J2000 hydrological model, simulates the snow and glacier melt runoff fairly good. The glacier melt contributes about 17 percent to the total streamflow including 5 percent from the glacier ice melt. The adaptation of different factors (such as radiation, slope, aspect and debris covered) in the glacier module has produced good results for simulating melt runoff. The role of melt runoff (snow and glacier) in streamflow is significant during the pre-monsoon season as streamflow is relatively low during this period. During the monsoon season, the melt runoff is mixed with streamflow generated by monsoon precipitation and and thus is difficult to distinguish.
- The model application represents different discharge components which has improved insight into the hydrological dynamics of the region. The model results suggest that the hydrograph of the basin is dominated by overland flow with about 50 percent contribution to the streamflow. The high contribution of overland flow is attributed to intense rainfall during the monsoon season which causes the saturation of soil. This provides more opportunities for saturation and infiltration access overland flow and most of the precipitation is drained as overland flow. About 72 percent of the precipitation is consumed to generate streamflow and 20 percent is for evapotranspiration, which suggest that evapotranspiration is one of the primary components of the water balance.

The application of the model results suggests that the J2000 hydrological model represents the processes of the monsoon dominated Himalayan river basins with glaciers in the high altitude areas. The proxy-basin approach indicates that the J2000 model can be used in other watersheds with similar geographic and climatic conditions. However, the input (precipitation) and output (discharge) data should be in a systematic order for reliable model performance. The results also suggested that distributed and process oriented models are useful to understand the hydrological response of a mountain watershed and that they provide important information about the watershed behavior. These information and results are very crucial for the implementation of sustainable IWRM in the region.

The following are the major findings from the results related to fourth objective as mentioned in Chapter 3.

The calibrated and validated model in the Dudh Kosi river basin is further examined to address upstream-downstream linkages. For this purpose, the impact of land-use change on hydrological regime and water availability to downstream are discussed. Two hypothetical land-use change scenarios and their impacts are discussed. Similarly, the impact of climate change on future precipitation and temperature is analysed using the climate projection data from a Regional Climate Model (RCM). The climate projection data were applied in the model to run two future scenarios and their impacts on future water availability.

- The primary effect of land-use change on hydrology is change in evapotranspiration. The model

has replicated this process quite satisfactorily. In Scenario 1 (change from forest to shrubland) the evapotranspiration is decreased at a low rate because the shrubland evaporates at a lower rate than forest due to short root depth. In Scenario 2 (change from forest to bare land), the evaporation decreased at a higher rate than Scenario 1 due to the lack of root depth in bare land.

- The deforestation might increase floods as infiltration on bare land areas decreases due to the lack of vegetation cover. The decrease in infiltration causes higher overland flow which might increase flood risk. The downstream communities will be more vulnerable by increasing flood levels. Nonetheless, the hydrological response after deforestation depends upon the infiltration from the land surface and therefore the response contains some level of uncertainty.

- The effect of climate change has higher uncertainty in terms of future water availability for downstream areas. Under the conditions suggested by the RCM, the temperature and precipitation of the region will be increased by about 4°C and 14 percent respectively by the end of century. In such a scenario, the streamflow will be increased primarily during the monsoon season. Because, the water level in the river is already high during the monsoon period, the additional increase in streamflow means increase in flood levels, with subsequent impacts to downstream communities.

- The rise in temperature is likely to affect many hydrological components. The glacier ice contribution, which is 5 percent, might be altered; however, the understanding of glacier fluctuations and related melt under climate change scenarios are very limited in the region. The overall contribution of glacier ice melt to the total streamflow can be considered small at the basin scale. Nonetheless, the role of glacier ice melt in the upstream areas during the pre-monsoon period can be significant relative to water availability for local use. Similarly, the snowline will be shifted to higher areas due to a rise in temperature. Subsequently, the snowmelt pattern will be changed as the basin will lose its snow-storage capacity. Therefore, it is likely that the river will shift from a 'melt-dominated river' to a 'rain-dominated river' in future under the assumed climate change scenario. Similarly, due to rise temperature, the increase in the value of evapotranspiration might affect the overall hydrology of the basin. Therefore, based on the analysis from this study, the evapotranspiration and snowmelt pattern are found to be more sensitive than glacier ice melt to change in temperature.

This research study suggested that the tools from geoinformatics are supportive in addressing upstream-downstream linkages within the framework of integrated systems analysis. The J2000 hydrological model, in conjunction with other tools, is able to address the processes in upstream areas and their effects on downstream areas. The study provides a process-based understanding of the watershed using a modelling approach where the hydrological modelling, including snow and glacier melt, and impact of land-use and climate change are studied together within the framework of integrated systems analysis. In addition, the study also provides a basis for the understanding of 'what-if' scenarios and the potential future response of hydrology under a climate projection scenario in the region. This study enables a better understanding of the relationship between upstream and downstream areas by using the proposed methodological approach. Therefore, it is concluded that the methodology is suitable for evaluating upstream-downstream linkages in the Himalayan region and it could be a basis for further

assessment of other linkages to understand the broader picture of the upstream-downstream linkages.

The study suggested that there are some limitations and uncertainties in the results primarily due to: i) input data set, ii) understanding of the system and iii) future climate change. First, the modelling of a river system is challenged by a lack of a representative dataset for the entire basin. One of the principal limitations is the lack of precipitation stations located in the high-altitude areas. Similarly, the validation data (river discharge) is another source of uncertainty, since the river discharge during the flood periods is less representative. Second, the understanding of the system behavior and converting that knowledge into modelling systems (model codes) bring another level of uncertainty. For example, the response of glacier fluctuations and associated melt runoff under temperature change is limited. The third level of uncertainty arises from the climate projection data which is too coarse in resolution to represent the complexity of the Himalayan region.

The complex processes between upstream and downstream areas indicate that the downstream areas have larger impacts than the upstream areas. Therefore, the downstream communities are more vulnerable to the activities and processes which occur on upstream areas. Due to monsoon dominated climatic system of the Himalayan region, the change in climatic variables such as precipitation is likely to concentrate during the monsoon period. As there is already too much water during the period, any increase in precipitation and associated runoff will pose more threat to downstream communities in terms of floods.

Because the downstream communities are more vulnerable due to upstream activities, more attention is needed to enhance their adaptation practices to cope with the flooding. Adaption practices are required, as there is higher uncertainty for results related to 'what-if' scenarios of both climate and land-use change. For better and sustainable watershed management, the payment for environmental services (PES) approach might provide a framework for cooperation which would help to pool resources of both upstream and downstream areas.

Implementing adaptive IWRM options requires a better understanding of watershed and its hydrological behavior (Flügel 2011). In this study, the tools and methodological approach provide many important spatial and temporal characteristics of a river basin which are required for the implementation of IWRM approach. Information such as the role of snow and glacier melt, overland flow, baseflow and water balance are required for sustainable water management and planning. Therefore, the study with its methodological approach also provides a basis to support the implementation of adaptive IWRM options in the Himalayan region in the context of climate change.

8.2 Future outlook

Given the scope and limitation of the study, the following suggestions for further research are provided.

- This study was conducted in the area where the scarcity of hydro-meteorological data is high. The additional data of higher resolution (such as more stations at higher elevations and high-resolution climate data) will help to enhance the understanding derived from this study. One of the prominent issues involves the precipitation pattern in the high altitude areas of the Hima-

layan region. At present, the understanding is not very clear which is a great challenge for hydrological modelling. A comparative study of the spatial distribution of precipitation in other corridors of the region (where the data are available) and an integration of data derived from various sources (such as remote sensing, and weather generators) can provide a basis for a better understanding in this field.

- Similar studies need to be carried out in other parts of region which represent different climate systems within the Himalayan region. For example, the eastern and western parts of the Himalayan region have different climate systems, due to a variation in dynamics of the monsoon system. A comparative study of the hydrological regime will provide a basis of how the system responds to different spatial and temporal distributions of the monsoon system. In addition, such studies will provide important and useful information about the sensitivity of the Himalayan rivers to global climate change.

- Soil erosion and sedimentation processes are important issues in the upstream-downstream linkages, but the analysis in this field was outside the scope of this study. Future studies on soil erosion, sedimentation and their role in water quality and quantity might provide a broader overview of upstream-downstream linkages. In the Himalayan region, the soil erosion and sedimentation are complex but important processes, due to intense rainfall during the monsoon season. The data availability and quality for such a study constitutes a major challenge at the moment. Therefore, understanding the causes and process of soil erosion at small scale (test plot) might be helpful.

- The model structure needs to be further adapted according to the specific characteristics and requirements of the region. One of the major improvements is required in the glacier module which needs to consider the glacier ice storage. This will provide a further basis to understand the glacier response under different climate change scenarios. For this purpose, studies carried out by Immerzeel et al. (2012) and Prasch (2010) could be helpful. Immerzeel et al. (2012) used historic climate data for a simulation and spatial distribution of glaciers and their response to climate change. On the other hand, Prasch (2010) used glacier layer and depth information to derive the glacier ice storage. The similar approach to derive the glacier ice storage in the J2000 modelling system might better represent the glacier feedback mechanism under temperature change scenarios.

- Data scarcity and their quality are the major sources of uncertainty in the region. In this study, the comparative study of two sub-basins of the Kosi river basin also indicated that the method of deriving discharge data might need more attention and higher priority in the future. Especially, the discharge data during the high flow periods have inherently a greater uncertainty as the approach of deriving the discharge value using a stage-discharge rating curve is not sufficient in the region as suggested by Kattelmann (1987). The extrapolation of the rating curve based on the few measurements done during the low flow periods might not be sufficient to capture the complexity of higher flow discharge during the monsoon season. Therefore, the data collecting agency, Department of Hydrology and Meteorology (DHM), needs to update the existing method of rating curve analysis to make the discharge data more representative.

Bibliography

Acharya, K. P., Dangi, R. B., 2009. Case studies on measuring and assessing forest degradation, Forest degradation in Nepal, review of data and methods, Forest Resources Assessment Working Paper 163. Tech. rep., FAO, Italy.

Adhikaree, K., 2010. Socio-technical assessment of payment for environmental services (PES) scheme: A case study of Kulekhani watershed, Nepal. Master's thesis, School of Environment, Resources and Development, Asian Institue of Techonology (AIT), Thailand.

Ageta, Y., 1976. Characteristics of precipitation during monsoon season in Khumbu Himal. Seppyo, 38 (Special Issue), 84–88.

Akhtar, M., Ahmad, N., Booij, M. J., 2008. The impact of climate change on the water resources of Hindukush-Karakorum-Himalaya region under different glacier coverage scenarios. Journal of Hydrology 355 (1-4), 148–163.

Akhtar, M., Ahmad, N., Booij, M. J., 2009. Use of reginal climate model simulations as input for hydrological models for the Hindukush-Karakorum-Himalaya region. Hydrological Earth System Sciences 13, 1075–1089.

Alcamo, J., 1994. Integrated modeling of global climate change. Kluwer Academic Press, Dordrecht, Boston.

Alford, D., 1992. Hydrological aspects of the Himalaya region. International Centre for Integrated Mountain Development (ICIMOD), Kathmandu Nepal.

Alford, D., Armstrong, R., 2010. The role of glaciers in stream flow from the Nepal Himalaya. The Cryosphere Discussions 4 (2), 469–494.

Allamano, P., Claps, P., 2010. Precipitation measurement errors at high-elevation sites in the Italian Alps. EGU General Assembly 2010, held 2-7 May, 2010 in Vienna, Austria, p. 11287, p. 11287.

Allen, R. G., Pereira, L., Raes, D., Smith, M., 1998. Crop evapotranspiration: Guidelines for computing crop water requirements. FAO Irrigation and Drainage Paper 56, FAO, Rome.

Anderson, M. G., Burt, T. P., 1985. Modelling strategies. In: Anderson, M. G. and Burt, T. P. (Eds.) Hydrological Forecasting, John Wiley & Sons, Chichester.

Andreaassian, V., 2004. Waters and forests: from historical controversy to scientific debate. Journal of Hydrology 291, 1–27.

Armstrong, R. L., 2011. The glaciers of the Hindu Kush Himalaya region, a summary of the science regarding glacier melt/retreat in the Himalayan, Hindu Kush, Karakoram, Pamir, and Tien Shan mountain ranges. International Centre for Integrated Mountain Development (ICIMOD). Kathmandu, Nepal.

Arnell, N. W., 1999a. Climate change and global water resources. Global Environmental Change 9, S31–S49.

Arnell, N. W., 1999b. The effect of climate change on hydrological regimes in Europe: a continental perspective. Global Environmental Change 9, 5–23.

Arnold, J. G., Allen, P. M., Bernhardt, G., 1993. A comprehensive Surface-groundwater Flow Model. Journal of hydrology 142, 47–69.

Awasthi, K. D., Sitaula, B. K., Singh, B. R., Bajacharaya, R. M., 2002. Land-use change in two Nepalese watersheds: GIS and geomorphometric analysis. Land Degradation & Development 13 (6), 495–513.

Aziz, O. I. A., Burn, D. H., 2006. Trends and variability in the hydrological regime of the Mackenzie River Basin. Journal of Hydrology 319 (1-4), 282–294.

Baese, F., 2005. Beurteilung der Parametersensitivität und der Vorhersageunsicherheit am Beispiel des hydrologischen Modells J2000. Master's thesis, Friedrich-Schiller-Universität Jena.

Bajracharya, S. R., Mool, P., 2009. Glaciers, glacial lakes and glacial lake outburst floods in the Mount Everest region. Annals of Glaciology 50 (53), 81–86.

Bajracharya, S. R., Mool, P., Shrestha, B., 2007. Impact of Climate Change on Himalayan Glaciers and Glacial Lakes: Case Studies on GLOF and Associated Hazards in Nepal and Bhutan. International Centre for Integrated Mountain Development (ICIMOD), Kathmandu.

Bandara, C., Kuruppuarachchi, T., 1988. Land-use change and hydrological trends in the upper Mahaweli basin. In: Workshop on Hydrology of Natural and Man-made forests in the Hill-Country of Sri Lanka.

Bandyopadhyay, J., Gyawali, D., 1994. Himalayan Water Resources: Ecological and Political Aspects of Management. Mountain Research and Development 14 (1), 1–24.

Barnett, T. P., Adam, J. C., Lettenmaier, D. P., 2005. Potential impacts of a warming climate on water availability in snow-dominated regions. Nature 438, 303–309.

Barros, A. P., Lettenmaier, D. P., 1994. Dynamic modeling of orographically induced precipitation. Reviews of Geophysics 32, 265–284.

Bates, B. C., Kundzewicz, Z. W., Wu, S., Palutikof, J. P. E., 2008. Climate Change and Water. Technical Paper of the Intergovernmental Panel on Climate Change. Tech. rep., IPCC Secretariat, Geneva, 210 pp.

Baumgartner, A., Liebscher, H. J., 1990. Allgemeine Hydrologie - Quantitative Hydrologie. Lehrbuch der Hydrologie, Band 1. Gebrüder Bornträger Verlag. Stuttgart.

Bende-Michl, U., Krause, P., Kralisch, S., Fink, M., Flügel, W.-A., 2006. Current development and application of the modular Java based model JAMS to meet the targets of the EU-WFD in Germany. In: Voinov, A. and Jakeman, A. and Rizzoli, A. (Eds). Proceedings of the iEMSs Third Biennial Meeting: 'Summit on Environmental Modelling and Software'. International Environmental Modelling and Software Society, Burlington, USA, 2006.

Bergstroem, S., 1976. Development and Application of a conceptual runoff model fro Scandinavian catchment. Report Rho 7. Tech. rep., Swedish Meteorological and Hydrological Institute, Norrkoping, Sweden.

Bergstroem, S., Carlsson, B., Gardelin, M., Lindstrom, G., Pettersson, A., Rummukainen, M., 2001. Climate change impacts on runoff in Sweden - assessments by global climate models, dynamical downscaling and hydrological modeling. Climate Research 16 (2), 101–112.

Bertle, F. A., 1966. Effects of Snow compaction on runoff from rain and snow. Bureau of Reclamation, Engineering Monograph No. 35, Washington.

Beven, K., 2001a. Rainfall-Runoff Modelling: The Primer. John Wiley & Sons, Chicester.

Beven, K., Binley, A. M., 1992. The future of distributed models: model calibration and uncertainty prediction. Hydrological Processes 6, 279– 298.

Beven, K., Freer, J., 2001. Equifinality, data assimilation, and data uncertainty estimation in mechanistic modelling of complex environmental systems using the GLUE methodology. Journal of Hydrology 249, 11–29.

Beven, K. J., 2001b. How far can we go in distributed hydrological modelling? Hydrology and Earth System Sciences 5(1), 1–12.

Bhattarai, D., 2009. Multi-purpose projects. In Pun, S. B. and Dhungel, D. N. (Eds). The Nepal-India water relationship: challenges. Springer, Netherland.

Bicheron, P., Defourny, P., Brockmann, C., Schouten, L., Vancutsem, C., Huc, M., Bontemps, S., Leroy, M., Achard, F., Herold, M., Ranera, F., Arino, O., 2008. GLOBCOVER: Products Description and Validation. Tech. rep., European Space Agency (ESA).

Bicknell, B. R., Imhoff, J. C., Donigian, A. S., Johanson, R. C., 1997. Hydrological Simulation Program-FORTRAN (HSPF), User's Manual For Release 11. EPA-600/R-97/080. Tech. rep., U.S. Environmental Protection Agency, Athens, GA.

Biswas, A. K., 1992. The Aswan High Dam revisited. Ecodecision, 67–69.

Blaikie, P. M., Muldavin, J. S. S., 2004. Upstream, Downstream, China, India: The Politics of Environment in the Himalayan Region. Annals of the Association of American Geographer 94 (3), 520–548.

Bongartz, K., 2003. Applying different spatial distribution and modelling concept in three nested mesoscale catchments of Germany. Physics and Chemistry of the Earth 28, 1343–1349.

Bosch, J. M., Hewlett, J. D., 1982. A review of catchment experiments to determine the effect of vegetation changes on water yield and evapotranspiration. Journal of Hydrology 55, 3–23.

Braun, L. N., July 1986. Simulation of snowmelt runoff in lowland and lower Alpine regions of Switzerland. In: Modelling Snowmlet-Induced processes. Proceedings of the Budapest Symposium. pp. 125–140.

Bronstert, A., Niehoff, D., Bürger, G., 2002. Effects of climate and land-use change on storm runoff generation: present knowledge and modelling capabilities. Hydrological Processes 16, 509–529.

Brooks, K. N., Folliott, P. F., Gregersen, H. M., Thames, J. L., 1991. Hydrology and the management of watersheds. Iowa State University Press, Iowa.

Bruijnzeel, L. A., 1990. Hydrology of moist tropical forests and effects of conversion: A state-of-knowledge review. UNESCO International Hydrological Programme., Paris.

Bruijnzeel, L. A., 2004. Hydrological functions of tropical forests: not seeing the soil for the trees? Agriculture, Ecosystems and Environment 104, 185–228.

Bruijnzeel, L. A., Bremmer, C. N., 1989. Highland Lowland Interaction in the Ganges Brahmaputra River Basin - A Review of Published Literature. International Centre for Integrated Mountain Development, Kathmandu, (ICIMOD), Kathmandu.

Butle, E., Lipper, L., Stringer, R., Zilberman, D., 2008. Payments for ecosystem services and poverty reduction: concepts, issues, and empirical perspectives. Economic and Development Economics 13, 245–254.

Calder, I., Hall, R., Bastable, H., Gunston, H., Shela, O., Chirwa, A., Kafundu, R., 1995. The impact of land use change on water resources in sub-Saharan Africa: a modelling study of Lake Malawi. Journal of Hydrology 170 (1-4), 123–135.

Carson, B., 1985. Erosion and Sedimentation Processes in the Nepalese Himalaya. International Centre for Integrated Mountain Development, Occasional Paper No. 1., Kathmandu.

CBS, 2001. National Population Census 2001 - Nepal, Tenth Census. Central Bureau of Statistics, Government of Nepal, Kathmandu, Nepal.

Chang, H., 2004. Water Quality Impacts of Climate Change and Land-Use Changes in Southeastern Pennsylvania. The Professional Geographer 56, 240–257.

Chang, H., Franczyk, J., 2008. Climate Change, Land-Use Change, and Floods: Toward an Integrated Assessment. Geography Compass 2 (5), 1549–1579.

Chapra, S. C., Pelletier, G. J., 2003. Qual2k: A modeling framework for simulating river and stream water quality (beta version): Documentation and users manual. Tech. rep., Civil and Environmental Engineering Dept., Tufts University.

Chen, H., Shao, M., Wang, K., 2005. Water cycling characteristics of grassland and bare land soils on Loess Plateau. Chinese. Journal of applied ecology 16(10), 1853–1857.

Chen, J., Y, Z., Zhu, Y., Yang, C., 2011. Relationship between land use and evapotranspiration- A case study of the Wudaogou Area in Huaihe River basin. Procedia Environmental Sciences 10, 491–498.

Chiew, F. H. S., McMahon, T. A., 2002. Modelling the impacts of climate change on Australian streamflow. Hydrological processes 16, 1235–1245.

Chiew, F. H. S., Whetton, P. H., McMahon, T. A., Pittock, A. B., 1995. Simulation of the impacts of climate change on runoff and soil moisture in Australian Catchments. Journal of Hydrology 167, 121–147.

Christensen, N. S., Wood, A. W., Lettenmaier, D. P., Palmer, R. N., 2004. Effects of Climate Change on the Hydrology and Water Resources of the Colorado River Basin. Climate Change 62, 337–363.

Costa, M. H., Botta, A., Cardile, J. A., 2003. Effects of large-scale changes in land cover on the discharge of the Tocantins River, Southeasterne Amazonia. Journal of Hydrology 283, 206–217.

Crosetto, M., Tarantola, S., 2001. Uncertainty and sensitivity analysis: tools for GIS-based model implementation. International Journal of Geographica l Information Science 15 (5), 415–437.

Cruz, R. V., Harasawa, H., Lal, M., Wu, S., Anokhin, Y., Punsalmaa, B., Honda, Y., Jafari, M., Li, C., N., H., 2007. Asia. Climate Change 2007: Impacts, Adaptation and Vulnerability. Contribution of Working Group II to the Fourth Assessment Report of the Intergovernmental Panel on Climate Change, M.L. Parry, O.F. Canziani, J.P. Palutikof, P.J. van der Linden and C.E. Hanson, Eds. Cambridge University Press, , Cambridge, UK.

Cunderlik, J. M., Simonovic, S. P., 2003. Assessment of water resources risk and vulnerability to changing climatic conditions: Hydrologic model selection for the cfcas project. Report No. I. Tech. rep., The University of Western Ontario, London, Ontario, Canada.

Dahal, R. K., 2006. Geology for Technical Students. Bhrikuti Academic Publications, Kathmandu, Nepal.

Dahal, R. K., Hasegawa, S., 2008. Representative rainfall thresholds for landslides in the Nepal Himalaya. Geomorphology 100 (3-4), 429–443.

Daniel, E. B., Camp, J. V., LeBoeuf, E. J., Penrod, J. R., Dobbins, J. P., Abkowitz, M. D., 2011. Watershed Modeling and its Applications: A State-of-the-Art Review. Open Hydrology Journal 5, 26–50.

DeCoursey, D. G., Shaake, J. J. C., Seely, E. H., 1982. Stochastic models in hydrology. In: Haan, C. T. Johnson, H. P. and Brakensiek, D. L. Hydrologic modeling of small watersheds. American Society of Agricultural Engineers: St Joseph, Michigan, pp. 19–78.

Defourny, P., Vancutsem, C., Bicheron, C., Brockmann, C., Nino, F., Schouten, L., Leroy, M., 2006. GLOBCOVER : A 300 M Global Land Cover Product For 2005 Using ENVISAT MERIS Time Series. ISPRS Commission VII Mid-term Symposium "Remote Sensing: From Pixels to Processes", Enschede, the Netherlands, 8-11 May 2006.

DeFries, R., Eshleman, K. N., 2004. Land-use change and hydrologic processes: a major focus for the future. Hydrological Processes 18 (11), 2183–2186.

DFRS, 1999. Forest Resources of Nepal (1978-1998), Publication No. 74. Tech. rep., Department of Forest Research and Survey, Ministry of Forest and Soil Conservation, Government of Nepal,.

Dhar, O. . N., Rakhecha, P. R., 1981. The effect of elevation on monsoon rainfall distribution in the Central Himalayas. In: International Symposium on Monsoon Dynamics, Cambridge University Press, pp. 253-260.

Dhungel, D. N., 2009. Historical Eye view. In Pun, S. B. and Dhungel, D. N. (Eds) The Nepal-India water relationship: challenges. Springer, Netherland.

Dickinson, R. E., 1984. Modelling evapotranspiration for three-dimensional global climate models. In: Climate Processes and Climate Sensitivity Geophysical Monograph, Hansen, J. E. Takahasi, T. (Eds.), Series 29, Washington.

Dixit, A., 2009. Kosi Embankment Breach in Nepal: Need for a paradigm shift in responding to floods. Economic & Political weekly 44 (6), 70–78.

Douglass, J. E., Swank, W. T., 1975. Effects of management practices on water quality and quantity: Coweeta Hydrologic Laboratory, North Carolina. In: Municipal Watershed Management Symposium, USDA Forest Service Technical Repport. NE-13, Upper Darby, pp. 1-13, Upper Darby PA, USA.

Dyck, S., Peschke, G., 1995. Grundlagen der Hydrologie. Verlag für Bauwesen. Berlin.

Dyurgerov, M. B., Meier, M. F., 2000. Twentieth century climate change: evidence from small glaciers. In: Proceedings of the National Academy of Sciences of the United States of America. Vol. 97 (4). pp. pp 1406–1411.

Dyurgerov, M. D., Meier, M. F., 2005. Glaciers and Changing Earth System: A 2004 Snapshot, Boulder (Colorado). Tech. rep., Institute of Arctic and Alpine Research, University of Colorado.

Eckholm, E., 1976. Losing Ground: Environmental Stress and World Food Prospects. W.W. Norton & Co., New York.

Efstratiadis, A., Nalbantis, I., Koukouvinos, A., Rozos, E., Koutsoyiannis, D., 2007. HYDROGEIOS: A semi distributed GIS-based hydrological model for disturbed river basins. Hydrol Earth Syst. Sci. Discuss 4, 1947–1998.

Eriksson, M., Jianchu, X., Shrestha, A. B., Vaidya, R. A., Nepal, S., Sandström, K., 2009. The Changing Himalayas Impact of climate change on water resources and livelihoods in the greater Himalaya. International Centre for Integrated Mountain Development (ICIMOD). Kathmandu.

Eschner, A. R., Satterlund, D. R., 1966. Forest protection and streamflow from an Adirondack watershed. Water Resources Research 24, 765–783.

Falkenmark, M., Lundqvist, J., 1999. Towards upstream/downstream hydrosolidarity. In: Towards upstream/downstream hydrosolidarity. Stockholm International Water Institute (SIWI).

FAO, 1995. Global and Natiional Soils and Terrain Digital Databases (SOTER). Tech. rep., Food and Agriculture Organization of the United Nations.

FAO, 2006. World reference base for soil resources 2006. A framework for international classification, correlation and communication. Tech. rep., Food and Agriculture organization of the United Nations, Rome.

FAO, CIFOR, 2005. Forests and Floods: Drowning in Fiction or Thriving in Facts? UN Food and Agriculture Organization and Center for International Forestry Research, Bangkok, Thailand.

Fink, M., Krause, P., Kralisch, S., Bende-Michl, U., , Flügel, W.-A., 2007. Development and Application of the Modelling System J2000-S for the EU-Water Framework directive. Advances in Geosciences 11, 123–130.

Fischer, C., Kralisch, S., Flügel, W.-A., 2012. An integrated, fast and easily useable software toolbox which allows comparative and complementary application of various parameter sensitivity analysis methods. In: Managing Resources of a Limited Planet, Sixth Biennial Meeting, Leipzig, Germany R. Seppelt, A. A. Voinov, S. Lange, D. Bankamp (Eds.). International Congress on Environmental Modelling and Software, 2012.

Fish, I. L., Lawrence, P., Atkinson, E., 1986. Sedimentation in the Chatara Canal, Nepal. Tech. rep., Hydraulics Research Wallingford.

FISRG, 1998. Stream corridor restoration: principles, processes, and practices. Vol. 2. Federal Interagency Stream Restoration Working Group (FISRG).

Flügel, W.-A., 1995. Delineating Hydrological Units (HRU's) by GIS analysis for regional hydrological modelling using PRMS/MMS in the drainage basin of the River Broel, Germany. Hydrological Processes 9, 423–436.

Flügel, W.-A., 2007. The Adaptive Integrated Data Information System (AIDIS) for Global Water Research. Water Resources Management 21(1), 199–210.

Flügel, W.-A., 2009. Applied Geoinformatics for sustainable IWRM and climate change impact analysis. Technology, Resource Management and Development 6, 57–85.

Flügel, W.-A., 2011. Development of adaptive IWRM options for climate change mitigation and adaptation. Advances in Science and Research 7, 91–100.

Flügel, W.-A., Müchen, B., Hochschild, V., Steinocher, K., 2001. ARSGISIP, A European Project on the application of remote sensing techniques for the parameterization of Hydrological, Erosion and Solute Transport Models. IAHS-Publication, Remote Sensing and Hydrology 267, 563–568.

Fox, A. M., 2003. A distributed, physically based snow melt and runoff model for alpine glaciers. Ph.D. thesis, St Catherine's College, Cambridge University.

Fujji, Y., Higuchu, K., 1977. Statistical analysis of the forms of glaciers in Khumbu region. Journal of Japanese Society of Snow Ice (Seppyo) 39, 7–14.

Gardner, R., Gerrard, A. J., 2003. Runoff and soil erosion on cultivated rainfed terraces in the Middle Hills of Nepal. Applied Geography 23 (1), 23–45.

Gautam, A. P., Webb, E. L., Shivakoti, G. P., Zoebisch, M. A., 2003. Land use dynamics and landscape change pattern in a mountain watershed in Nepal. Agriculture, Ecosystems and Environment 99, 83–96.

Gemmer, M., Becker, S., Jiang, T., 2004. Observed monthly precipitation trends in China 1951-2002. Theoretical and Applied Climatology 77 (1-2), 39–45.

Gerrits, M., 2010. The role of interception in the hydrological cycle. Ph.D. thesis, Delft University of Technology, Netherland.

Gilmour, D. A., 1977. Effect of logging and clearing on water yield and water quality in a high rainfall zone of north-east Queensland. In: The Hydrology of Northern Australia. Institution of Engineers, Australia, National Conference Publ. No. 77/5: 156-160.

Gilmour, D. A., Bonell, M., Cassells, D. S., 1987. The effects of forestation on soil hydraulic properties in the Middle Hills of Nepal: a preliminary assessment. Mountain Research and Development 7, 239–249.

Gitay, H., Noble, I. R., Pilifosova, O., Alijani, B., Safriel, U. N., 1998. The Regional Impacts of Climate Change: An Assessment of Vulnerabilityy. Watson R.T., Zinyowera M.C., Moss R.H. and Intergovernmental Panel on Climate Change. Working Group II (Eds.). Cambridge University Pressy, Cambridge, UK, Ch. Middle East and Arid Asia, pp. 233–250.

Gleick, P. H., 1989. Climate change and hydrology and water resources. Review of Geophysics 27, 329–344.

Gole, C. V., Chitale, S. V., 1966. Inland delta building activity of Kosi river. Journal of Hydraulic division, ASCE 91, 111–126.

Golf, W., 1981. Ermittlung der Wasserressource im Mittelgebirge. Wasserwirtschaft-Wassertechnik 31, 93–95.

Gordon, C., Cooper, C., Senior, C. A., Banks, H., Gregory, J. M., Johns, T. C., Mitchell, J., Wood, R. A., 2000. The simulation of SST, sea ice extents and ocean heat transports in a version of the Hadley Centre coupled model without fux adjustments. Climate Dynamics 16, 147–168.

Gosain, A. K., Sandhya, R., Debajit, B., 2006. Climate change impact assessment on hydrology of Indian river basins Special Section: Climate Change and India. Current Science 90(3), 346–353.

Gupta, H., Beven, K. J. Wagener, T., 2005. Model Calibration and Uncertainty Estimation. In M. G. Anderson, Encyclopedia of Hydrological Sciences. John Wiley & Sons, Ltd, New York.

Gurtz, J., Baltensweiler, A., Lang, H., 1999. Spatially distributed hydrotope-based modelling of evapotranspiration and runoff in mountainous basins. Hydrological Processes 13, 2751–2768.

GWP, 2000. Integrated Water Resources Management, Technical Advisory Committee (TEC) 4. Global Water Partership (GWP).

GWP, IBNO, 2009. A Handbook for Intetrated Water Resources Management in Basins. Tech. rep., Global Water Partnership (GWP) and International Network of Basin Organizations (INBO), 104 p.

Gyawali, D., Dixit, A., 1999. Rethinking the Mosaic, Investigations into Local Water Management. Nepal Water Conservation Foundation, Kathmandu, Ch. Fractured Institutions and Physical Interdependence Challenges to Local Water Management in the Tinau River Basin, Nepal, pp. 371–33.

Hagemann, S., Chen, C., Haerter, J. O., 2011. Impact of a Statistical Bias Correction on the Projected Hydrological Changes Obtained from Three GCMs and Two Hydrology Models. Journal of Hydrometeorology 12, 556–578.

Hamed, K. H., 2008. Trend detection in hydrologic data: The Mann-Kendall trend test under the scaling hypothesis. Journal of Hydrology 349 (3-4), 350–363.

Hamilton, L. S., King, P. N., 1983. Tropical forested watersheds: hydrologic and soils response to major uses or conversions. Westview Press, Colorado.

Hamilton, L. S., Pearce, A. J., 1987. What are the Soil and Water Benefits of Planting Trees in Developing Country Watershed? In: Sotygate, D.D. ad Sisinger, J. (Ed.), Sustainable Development of Natural Resources in the Third World.). Westview Press, Boulder CO, USA, pp. pp. 39–58.

Hamlet, A. F., Lettenmaier, D. P., 1999. Effects of climate change on hydrology and water resources in the Columbia River Basin. Journal of the American water resources association 35 (6), 1597–1623.

Hauer, F. R., Baron, J. S., Campbell, D. H., Fausch, K. D., Hostetler, S. W., Leavesley, G. H., Leavitt, R. R., McKnight, D. M., Stanford, J. A., 1997. Assessment of climate change and freshwater ecosystems of the Rocky Mountains, US and Canada. Hydrological Processes 11, 903–924.

Hay, L. E., Clark, M. P., Wilby, R. L., Gutowski, W. J., Leavesley, G. H., Pan, Z., Arritt, R. W., Takle, E. S., 2002. Use of regional climate model output for hydrological simulations. Journal of Hydrometeorology 3, 571–590.

Helmschrot, J., 2006. An integrated, landscape-based approach to model the formation and hydrological functioning of wetlands in headwater catchments of the Umzimvubu River, South Africa. Ph.D. thesis, Friedrich-Schiller-Universität Jena.

Helsel, D. R., Hirsch, R. M., 1992. Statistical Methods in Water Resources. Elsevier, New York.

Helsel, D. R., Hirsch, R. M., 2002. Statistical methods in water resources. Tech. rep., U. S. Geological Survey.

Herrmann, A., 1976. Einfluss des Alpensüdföhns auf die Schneedeckenentwicklung und das nival gesteuerte Abflussgeschehen. Polarforschung 46(2), 83–94.

Herron, N., R., D., R., J., 2002. The effects of large-scale afforestation and climate change on water allocation in the Macquarie River catchment, NSW, Australia. Journal of Environmental Management 65 (4), 369–382.

Hewitt, K., 2005. The Karakoram anomaly? Glacier expansion and the 'elevation effects' Karakoram Himalaya. Mountain Research and Development 25(4), 332–340.

Hibbert, A. R., 1967. Forest treatment effects on water yield. Pergamon, Oxford.

Higuchi, K., Ageta, Y., Yasunari, T., Inoue, J., 1982. Characteristics of precipitation during the monsoon season in high-mountain areas of the Nepal Himalaya, Hydrological aspects of Alpine and High mountain Areas. In: Proceedings of the Exeter Symposium. IAHS Publication.

HMG, 2000. State of the Environment Nepal. Tech. rep., Ministry of Population and Environment, His Majesty's Government, Kathmandu, Nepal.

Hock, R., 1999. A distributed temperature index ice and snowmelt model including potential direct solar radiation. Journal of Glaciology 45 (149), 101–112.

Hock, R., 2003. Temperature index melt modelling in mountain areas. Journal of Hydrology 282 (1-4), 104–115.

Hock, R., 2005. Glacier melt: a review of processes and their modelling. Progress in Physical Geography 29(3), 362–391.

Hock, R., Jansson, P., Braun, L. N., 2005. Global Change and Mountain Regions (A State of Knowledge Overview),. Springer, Dordrecht, Ch. Modelling the Response of Mountain Glacier Discharge to Climate Warming, pp. 243–252.

Hornberger, G. M., Spear, R. C., 1981. An approach to the preliminary analysis of environmental systems. Journal of Environmental Management 12, 7–18.

Immerzeel, W. M., Beek, L. P. H., Bierkens, M. F. P., 2010. Climate Change Will Affect the Asian Water Towers. Journal of Hydrology 328 (5984), 1382–1385.

Immerzeel, W. M., Beek, L. P. H., Konz, M., Shrestha, A. B., Bierkens, M. F. P., 2012. Hydrological response to climate change in a glacierized catchment in the Himalayas. Climate change 110, 721–736.

Impat, P., 1981. Hydrometeorology and sediment data for Phewa Watershed: 1979 data. Phewa Tal Tech. Rep. No. 15. Integrated watershed management project, Dept. of Soil Conservation and Watershed Management, Ministry of Forests, Kathmandu.

IPCC, 1996. Climate Change 1995. The Science of Climate Change Cambridge University Press, Cambridge.

IPCC, 2000. IPCC Special Report on Emission Scenario: Summary for policy makers. Intergovernmental Panel on Climate Change.

IPCC, 2007. Climate Change 2007: Impacts, Adaptation and Vulnerability. Contribution of Working Group II to the Fourth Assessment Report of the Intergovernmental Panel on Climate Change. Cambridge University Press, Cambridge, UK, 976pp.

ISRC, 2008. Village Development Committee Profile of Nepal. Intensive Study and Research Centre, Kathmandu.

Ives, J. D., 1989. Deforestation in the Himalayas the cause of increased Flooding in Bangladesh and Northern India? Land Use Policy 6, 187–193.

Ives, J. D., 2004. The Himalayan Perception: Environmental Change and well being of the mountain people. Routledge, London.

Ives, J. D., Misserli, B., 1989. The Himalayan Dilemma: Reconciling Development and Conservation. The United Nations University, Routledg, London.

Jansson, P., Hock, R., Schneider, T., 2003. The concept of glacier storage: a review. Journal of Hydrology 282, 116–129.

Jayatilaka, C. J., Storm, B., Mudgway, L. B., 1998. Simulation of flow on irrigation bay scale with MIKE-SHE. Journal of Hydrology 208, 108–130.

Jodha, N. S., 1995. The Nepal middle mountains. In: Regions at Risk: Comparisons of Threatened Environments. United Nations University Press, Tokyo, Japan.

Jodha, N. S., 1997. Highland - Lowland Linkages. Issues in Mountain Development 97/8. ICIMOD.

Jodha, N. S., 2000. Poverty Alleviation and Sustainable Development in Mountain Areas: Role of Highland-Lowland Links in the Context of Rapid Globalisation. International Centre for Integrated Mountain Development (ICIMOD).

Jodha, N. S., 2002. Highland Lowland Linkages in the Globalised World. In: Jodha, N. S., Bhadra, B., Khanal, N. R., Richter, J. (Eds.), Poverty Alleviation in Mountain Areas of China Proceedings of the International Conference held from 11-15 November, 2002, in Chengdu, China.

Jones, G., Noguer, M., Hassell, D., Hudson, D., Wilson, S., Jenkins, G., Mitchell, J., 2004. Generating High Resolution Climate Change Scenarios Using PRECIS. Tech. rep., Met Office Hadley Centre, Exeter, UK, 40pp.

Karssenberg, D., Burrough, P., 2002. The PCRaster Software and Course Materials for Teaching Numerical Modelling in the Environmental Sciences. Transactions in GIS 5 (2), 99–110.

Kasperson, J. X., Kasperson, R. E., Turner, B. L. I. e., 1995. Regions at Risk: Comparisons of Threatened Environments. United Nations University Press, Tokyo.

Kattelmann, R., 1987. Uncertainty in assessing Himalayan water resources. Mountain Research and Development 7 (3), 279–286.

Kattelmann, R., 1990. Hydrology and development of the Arun River, Nepal, Hydrology in Mountainous Regions. I - Hydrological Measurements; the Water Cycle. In: Proceedings of two Lausanne Symposia, August 1990. IAHS Publ. no. 193.

Kattelmann, R., 2003. Glacial lake outburst floods in the Nepal Himalaya: a manageable hazard? Natural Hazards 28, 145–154.

Kawashima, D. M., Yonemura, S., Yamada, T., Zhang, X., Liu, J., Li, Y., Gu, S., Tang, Y., 2007. Temperature distribution in the high mountain regions on the Tibetan Plateau - Measurement and simulation. In: MODSIM 2007 Land, Water and Environmental Management: Integrated Systems for Sustainability. pp. 2146–2152.

Kay, A., Jones, R. G., Reynard, N. S., 2006. RCM rainfall for UK flood frequency estimation, I. Method and validation. Journal of Hydrology 318, 151–162.

Kayastha, R. B., Takeuchi, Y., Nakawo, M., Ageta, Y., 2000. Practical prediction of ice melting beneath various thickness of debris cover on Khumbu Glacier, Nepal, using a positive degree-day factor. IAHS Publication 264, 71–82.

Kendall, M. G., 1975. Rank Correlation Methods. Charles Griffin.

Kiersch, B., 2000. Land use impacts on water resources: a literature review, Discussion paper 1, FAO land and water bulletin 9. In: Proceedings of the electronic workshop 'Land-water linkages in rural watersheds'. FAO Land and Water Development Division 18 September-27 October 2000.

Klemes, V., 1986. Operational testing of hydrological simulation models. Hydrological Sciences Journal 31, 13–24.

Knauf, D., 1980. Die Berechnung des Abflüsses aus einer Schneedecke. Analyse und Berechnung oberirdischer Abflusse DVWK- Schriften, Bonn, Heft 46.

Kochanowski, A., 2009. Reliefbestimmte Analyse der Niederschlagsdynamik im Monsungebiet von Nepal, Himalaya. Master's thesis, Institutue of Geography, Friedrich-Schiller-University Jena, Germany.

Konz, M., Devkota, L., 2009. Manual on Snow and Glacier Melt Runoff Modelling in the Himalayas. Tech. rep., ICIMOD, Kathmandu, Nepal.

Kosoy, N., Tuna, M. M., Muradian, R., Alier, J. M., 2007. Payments for environmental services in watersheds: Insights from a comparative study of three cases in Central America. Ecological economics 61(2–3), 446–455.

Kozak, J. A., Ahuja, L. R., Gree, T. R., Ma, L., 2007. Modelling crop canopy and residue rainfall interception effects on soil hydrological components for semi-arid agriculture. Hydrological Processes 21, 229–241.

Kralisch, S., Krause, P., 2006. JAMS A Framework for Natural Resource Model Development and Application. In: Proceedings of the International Environmental Software Society (IEMSS), Vermont, USA.

Kralisch, S., Krause, P., Fink, M., Fischer, C., Flügel, W.-A., 2007. Component based environmental modelling using the JAMS framework. In: MODSIM 2007 International Congress on Modelling and Simulation. pp. 812–818, peer reviewed.

Kralisch, S., Zander, F., Krause, P., 2009. Coupling the RBIS Environmental Information System and

the JAMS Modelling Framework. In: 18th World IMACS / MODSIM Congress, Cairns, Australia 13-17 July 2009.

Krause, P., 2001. Das hydrologische Modellsystem J2000: Beschreibung und Anwendung in groen Flueinzugsgebieten, Schriften des Forschungszentrum Jülich. Reihe Umwelt/Environment; Band 29.

Krause, P., 2002. Quantifying the Impact of Land Use Changes on the Water Balance of Large Catchments using the J2000 Model. Physics and Chemistry of the Earth 27, 663–673.

Krause, P., 2010. Technical documentation of J2000 modelling system, Internal document. Tech. rep., Friedrich Schiller University Jena.

Krause, P., Bende-Michl, U., Bäse, F., Fink, M., Flügel, W.-A., Pfennig, B., 2006. Multiscale Investigations in a Mesoscale Catchment Hydrological Modelling in the Gera Catchment. Advances in Geosciences 9, 53–61.

Krause, P., Bende-Michl, U., Fink, M., Helmschrot, J., Kralisch, S., Kuenne, A., 2009. Parameter sensitivity analysis of the JAMS/J2000-S model to improve water and nutrient transport process simulation - a case study for the Duck catchment in Tasmania, 18th World IMACS / MODSIM Congress, Cairns, Australia 13-17 July 2009. pp. 1727–1732.

Krause, P., Biskop, S., Helmschrot, J., Flügel, W.-A., Kang, S., Gao, T., 2010. Hydrological system analysis and modelling of the Nam Co basin in Tibet. Advance Geoscience 27, 29–36.

Krause, P., Boyle, D. P., Bäse, F., 2005. Comparison of different efficiency criteria for hydrological model assessment. Advances in Geosciences 31, 89–97.

Krause, P., Hanisch, S., 2004. Prognostic simulation and analysis of the impact of climate change on the hydrological dynamics in Thuringia, Germany. Hydrology and Earth System Sciences Discussions 4 (6), 4037–4067.

Kripalani, R. H., Oh, J. H., Kulkarni, A., Sabade, S. S., Chaudhari, H. S., 2007. South Asian summer monsoon precipitation variability: Coupled climate model simulations and projections under IPCC AR4. Theoritical Applied Climatology 90, 113–159.

Krol, M., Jaeger, A., Bronstert, A., Güntner, A., 2006. Integrated modeling of climate, water, soil, agricultural and socio-economic processes: a general introduction of the methodology and some exemplary results from the semi-arid north-east of Brazil. Journal of Hydrology 328, 417–431.

Kuchment, L. S., Demidov, V. N., Motovolov, Y. G., 1983. Formirovanie rechnogo stok (fiziko-matematichestde modeli) (River runoff formation/physically based models) (in Russian). Nauka. Moscow.

Kumar, K. K., Patwardhan, S. K., Kulkarni, A., Kamala, K., Rao, K. K., Jones, R., 2011. Simulated projections for summer monsoon climate over India by a high-resolution regional climate model (PRECIS). Current Science 101 (3), 312–326.

Kumar, K. R., Sahai, A. K., Kumar, K. K. Patwardhan, S. K., Mishra, P. K., Revadekar, J. V., Kamala,

K., Pant, G. B., 2006. High-resolution climate change scenarios for India for the 21st century. Current Science 90 (3), 334–345.

Kundewicz, Z. W., Robson, A. J., 2004. Change detection in hydrological records – a review of the methodology. Hydrological sciences 49(1), 1–19.

Kundzewicz, Z. W., Mata, L. J., Arnell, N. W., Döll, P., Kabat, P., Jiménez, B., Miller, K. A., Oki, T., Sen, Z., Shiklomanov, I. A., 2007. Freshwater resources and their management. Climate Change 2007: Impacts, Adaptation and Vulnerability. Contribution of Working Group II to the Fourth Assessment Report of the Intergovernmental Panel on Climate Change. Cambridge University Press, Cambridge, UK.

Lang, H., 2005. Hydrometeorologische Ergebnisse aus Abflussmessungen im Bereich des Hintereisferners (Ötztaler Alpen) in den Jahren 1957 bis 1959. Archiv für Meteorologie Series B, Band 14, 280–302.

Leavesley, G. H., Lichty, R. W., Troutman, B. M., Saindon, L. G., 1983. Precipitation-Runoff-Modeling-System, User's Manual. Tech. rep., Water Resource Investigations Report 83–4238, US Geological Survey.

Legates, D. R., McCabe, G. J., 1999. Evaluating the use of "goodness-of-fit" Measures in hydrologic and hydroclimatic model validation. Water Resources Research 35 (1), 233–241.

Legesse, D., Vallet-Coulomb, C., Gasse, F., 2003. Hydrological response of a catchment to climate and land use changes in tropical Africa: case study south central Ethiopia. Journal of Hydrology 275, 67–85.

Liu, D. P., Chen, S. X., Zhang, J. C., Xie, L., Jiang, J., 2007. Soil infiltration characteristics under main vegetation types in Anji County of Zhejiang Province. Chinese. Journal of applied ecology 18 (3), 493–498.

Liu, X., Chen, B., 2000. Climatic warming in the Tibetan Plateau during recent decades. International Journal of Climatology 20:, 1729–1742.

Loerup, J. K., Refsgaard, J. C, M. D., 1998. Assessing the effect of land use change on catchment runoff by combined use of statistical tests and hydrological modelling: case studies from Zimbabwe. Journal of Hydrology 205, 147–163.

Loucks, D. P., Van Beek, E., Stedinger, J. R., Dijkman, J. P. M., Villars, M. T., 2005. Water resources systems planning and management: an introduction to methods, models and applications. Paris: UNESCO.

Lundin, L., Lode, E., Stendahl, J., Melkerud, P., Bjoerkvald, L., Thorstensson, A., 2004. Soils and site types in the Forsmark area. Tech. rep., SLU, Department of Forest Soils.

Maniak, U., 1997. Hydrologie und Wasserwirtschaft. Springer Verlag. Berlin.

Mann, H. B., 1945. Non-parametric tests for against trend. Econometrica 12, 245–249.

Mattson, L. E., Gardner, J. S., Young, G. J., 1993. Ablation on debris covered glaciers: an example from the Rakhiot glacier, Punjab Himalaya, Snow and glacier hydrology. In: Proceedings of the Kathmandu Symposium, November, 1992.

McCuen, R., 2005. The role of sensitivity analysis in hydrologic modelling. Journal of Hydrology 18, 37–53.

Medina, S.and Houze, R. A., Kumar, A., Niyogi, D., 2010. Summer Monsoon convection in the Himalaya region: Terrain and land cover effects. Quarterly Journal of the Royal Meteorological Society 136, 593–616.

Menzel, L., 1996. Modellierung der Evapotranspiration im System Boden-Pflanzen-Atmosphäre. Ph.D. thesis, ETH Zürich.

Middelkoop, H., Daamen, K., Gellens, D., Grabs, W.and Kwadijk, J. C. J., Lang, H., Parmet, B. W. A. H., Schädler, B., Schulla, J., Wike, K., 2001. Impact of climate change on hydrological regimes and water resources management in the Rhine basin. Climate Change 49,, 105–128.

Miller, J. T., Spoolman, S., 2009. Living in the Environment: Principles, Connections, and Solutions. Brooks/Cole Pub Co, Canada.

Milliman, J. D., Meade, R. H., 1983. World-wide delivery of river sediment to the oceans. The Journal of Geology 91, 1–21.

Minder, J. R., Mote, P. W., Lundquist, J. D., 2010. Surface temperature lapse rates over complex terrain: Lessons from the Cascade Mountains. Journal of Geophysical Research 115, 1–13.

Moench, M., 2010. Responding to climate and other change processes in complex contexts: Challenges facing development of adaptive policy frameworks in the Ganga Basin. Technological Forecasting and Social Change 77 (6), 975–986.

MoFSC, 2002. Forest and Vegetation types of Nepal. Ministry of Forest and Soil Conservation, Government of Nepal and Natural Resource Management Sector Assistance Programme (NARMSAP), TISC Document Series, No. 105.

Montanari, A., 2005. Large sample behaviors of the Generalized Likelihood Uncertainty Estimation (GLUE) in assessing the uncertainty of rainfall-runoff simulations. Water Resources Research 41, 1–13.

Mool, P. K., Bajracharya, S. R., Joshi, S. P., 2001a. Inventory of Glaciers, Glacial Lakes, and Glacial Lake Outburst Flood Monitoring and Early Warning Systems in the Hindu Kush-Himalayan Region - Bhutan. ICIMOD, Kathmandu.

Mool, P. K., Bajracharya, S. R., Joshi, S. P., 2001b. Inventory of Glaciers, Glacial Lakes, and Glacial Lake Outburst Flood Monitoring and Early Warning Systems in the Hindu Kush-Himalayan Region - Nepal. International Centre for Integrated Mountain Development (ICIMOD), Kathmandu Nepal.

Morgan, R., Morgan, D., Finney, H., 1984. A predictive model for the assessment of soil erosion risk. Journal of Agricultural Engineering Research 30, 245–253.

Morris, E. M., 1985. Snow and ice. In: Anderson, M. G. and Burt, T. P. (Eds) Hydrological Forecasting, John Wiley & Sons, Chichester.

Narayana, V. V. D., 1987. Downstream Impats of Soil conservation in the Himalaya region. Mountain Research Development 7 (3), 287–298.

Nash, J. E., Sutcliffe, J. V., 1970. River flow forecasting through conceptual models, Part I - A discussion of principles. Journal of Hydrology 10, 282–290.

Nepal, S., Adiga, P. B., 2006. Linkages between watershed and irrigation, a case study on management practices of Farmer Managed Irrigation System (FMIS), Argali, Palpa, Nepal. In: Proceedings of the Fourth International Seminar on Irrigation in Transition: Interacting with Internal and External Factors and Setting the Strategic Actions, Kathmandu, Nepal.

Nepal, S., Krause, P., Flügel, W.-A., Fink, M., Pfennig, 2011. Understanding the impact of climate change in the glaciated alpine catchment of the Himalaya Region using the J2000 hydrological model. In: Proceedings of the Second International Symposium on Building Knowledge Bridges for a Sustainable Water Future, Panama, 2011. pp. 55–60.

Niehoff, D., Fritsch, U., Bronstert, A., 2002. Land-use impacts on storm-runoff generation: scenarios of land-use change and simulation of hydrological response in a meso-scale catchment in SW-Germany. Journal of Hydrology 267 (1-2), 80–93.

Nijssen, B., O'Donnell, G. M., Hamlet, A. F., Lettenmaier, D. P., 2001. Hydrologic Sensitivities of Global Rivers to Climate Change. Climate Change 50, 143–175.

Oestrem, G., 1959. Ice Melting under a Thin Layer of Moraine, and the Existence of Ice Cores in Moraine Ridges. Geografiska Annaler 41, 228–230.

Olaya, V., 2004. A gentle introduction to SAGA GIS. Tech. rep.

Overpeck, J., Anderson, D., Trumbore, S., Prell, W., 1996. The southwest Indian Monsoon over the last 18000 years. Climate Dynamics, 12, 213–225.

Pant, D., Thapa, B., Singh, A., Bhattarai, M., Molden, D., 2005. Integrated management of water, forest and land resources in Nepal: Opportunities for improved livelihood. CA Discussion Paper 2. Tech. rep., Colombo, Sri Lanka: Comprehensive Assessment Secretariat.

Paul, F., Kääb, A., Maisch, M., Kellenberger, T., Haeberli, W., 2004. Rapid disintegration of Alpine glaciers observed with satellite data. Geophysical Research Letters 31, L21402.

Pauleit, S., Ennos, R., Golding, Y., 2005. Modeling the environmental impacts of urban land use and land cover change-a study in Merseyside, UK. Landscape and Urban Planning 71(2–4), 295–310.

Pfennig, B., Wolf, M., 2007. Extraction of process-based topographic model units using SRTM elevation data for Prediction in Ungauged Basins (PUB) in different landscapes. MODSIM07 : International Congress on Modelling and Simulation, December 10-13, 2007.

Prasch, M., 2010. Distributed Process Oriented Modelling of the Future Impact of Glacier MeltWater

on Runoff in the Lhasa River Basin in Tibet,. Ph.D. thesis, Dissertation der Fakultät für Geowissenschaften der LMU München,.

Raghunath, H. M., 2006. Hydrology, Principles, Analysis and Design. New Age International (P) Limited, New Delhi, India.

Rai, S. C., Sharma, E., 1998. Comparative assessment of runoff characteristics under different land use patterns within a Himalayan watershed. Hydrological processes 12,, 2235–2248.

Ramsay, W. J. H., 1987. Deforestation and erosion in the Nepalese Himalaya - is the link myth or reality? In: Forest Hydrology and watershed management - Proceedings of the Vancouver Symposium, August 1987: IAHS Publication no 167. IAHS.

Randall, D. A., Wood, R. A., Bony, S., Colman, R., Fichefet, T., Fyfe, J., Kattsov, V., Pitman, A., Shukla, J., Srinivasan, J., Stouffer, R. J., Sumi, A., Taylor, K. E., 2007. Climate Models and their Evaluation. In: Climate Change 2007: The Physical Science Basis. Contribution of Working Group I to the Fourth Assessment Report of the Intergovernmental Panel on Climate Change [Solomon, S., D. Qin, M. Manning, Z. Chen, M. Marquis, K.B. Averyt, M.Tignor and H.L. Miller (eds.)]. Cambridge University Press, Cambridge, United Kingdom and New York, NY, USA.

Refsgaard, J., 2007. Hydrological Modeling and River Basin Management. Phd thesis, Geological Survey of Denmark and Greenland, 90.

Refsgaard, J. C., 1996. Terminology, modelling protocol and classification of hydrological model codes. In: Abbott, M. B. and Refsgaard, J. C. (Eds): Distributed Hydrological Modelling. Kluwer Academic Publishers.

Refsgaard, J. C., Storm, B., 1996. Construction, calibration and validation of hydrological models. In: M. B. Abbott and J. C. Refsgaard (Eds), Distributed Hydrological Modelling. Kluwer Academic Publisher, Dordrecht, 41–54.

Refsgaard, J. C., Storm, B., Refsgaard, A., 1995. Validation and applicability of distributed hydrological models. In: Modelling and Management of Sustainable Basin-scale Water Resource Systems (Proceedings of a Boulder Symposium, July 1995). IAHS Publ. no. 231. pp. 387–397.

Regmee, S. B., 2004. Water induced disasters in nepal: Recent trends and measures. In: International Symposium on Utilization of Disaster Information, Organizing and Sharing Disaster Information in Asian Country, JSECE, Publication No. 44. The Japan Society of Erosion Control Engineering.

Richter, D., 1995. Ergebnisse methodischer Untersuchungen zur Korrektur des systematischen Messfehlers des Hellmann-Niederschlagsmessers. Berichte des Deutschen Wetterdienstes Nr. 194, Offenback am Main.

Ring, P. J., Fisher, I. H., 1985. The effects of changes in land use on runoff from large catchments in the upper Macintyre Valley, NSW. In: Hydrology and Water Resources Symposium, Sydney, 14 -16 May, 1985. The Institution of Engineers, Australia, National Conference Publication 85/2:153-158. pp. 153–158.

Sakai, A., Fujita, K., Kubota, J., 2004. Evaporation and percolation effect on melting at debris-covered Lirung Glacier, Nepal Himalayas, 1996. Bulletin of Glacier Research 21, 9–15.

Sakai, A., Takeuchi, N., Fujita, K., Nakawo, M., 2000. Role of supraglacial ponds in the ablation process of a debris-covered glaciers in the Nepal Himalayas. In: Debris Covered Glaciers (Proceedings of a workshop held at Seattle, Washington, USA, September 2000). IAHS Publ. no. 265, 2000.

Sangjun, I., Hyeonjun, K., Chulgyum, K., Cheolhee, J., 2009. Assessing the impacts of land use changes on watershed hydrology using MIKE SHE. Environmental Geology 57, 231–239.

Scheffer, F., Schachtschabel, P., 1984. Lehrbuch der Bodenkunde. Enke Verlag. Stuttgart.

Schelling, D., 1992. The tectonostratigraphy and structure of the Eastern Nepal Himalaya. Tectonics 11, 925–943.

Schindler, D. W., 1997. Widespread effects of climatic warming on freshwater ecosystems in North America. Hydroloigical Processes 11, 1043–1067.

Schneeberger, C., Blatter, H., Ayako, A., Wild, M., 2003. Modelling changes in the mass balance of glaciers of the northern hemisphere for a transient 2 X CO2 scenario. Journal of Hydrology 282, 145–163.

Schulla, J., 1997. Hydrologische Modellierung von Flussgebieten zur Abschätzung der Folgen von Klimaänderungen. Ph.D. thesis, Geographisches Institut der ETH, Zürich.

Searcy, J. K., 2002. Flow duration curves - Manual of hydrology, Part 2. Low flow techniques. USGS, Water Supply Paper 1542-A.

Sen, P. K., 1968. Estimates of the Regression Coefficient based on Kendall's Tau. Journal of American Statistical Association 63(324), 1379–1389.

Sevruk, B., 1986. Correction of precipitation measurements, summary report. In: Sevruk, B. (Ed.), Correction Of Precipitation Measurements. ETH/IASH/WMO Workshop on the Correction of Precipitation Measurements, Zürich, April 1–3, 1985. Züricher Geographische Schriften 23, ETH, Geographisches Institut, Zürich, pp. 13–23.

Sharma, K. P., 1993. Role of meltwater in major river systems of Nepal. In: Young, GJ (ed) International Symposium on Snow and Glacier Hydrology, Kathmandu, International Association of Hydrological Sciences, Publication No. 218, pp 113 - 122. Wallingford (UK): IAHS.

Sharma, K. P., 1997. Impact of land-use and climatic chagnes on hydrology of the Himalayan Basin: A case study of the Kosi Basin. Ph.D. thesis, University of New Hampshire.

Sharma, K. P., Moore III, B., Vorosmarty, C. J., 2000a. Anthropogenic, Climatic and hydrological trends in the Kosi basin, Himalaya. Climate Change 47, 141–165.

Sharma, K. P., Vorosmarty, C. J., Moore, B., 2000b. Sensitivity of the Himalayan Hydrology to Land-use and Climatic Changes. Climate Change 47, 117–139.

Shiga Declaration, 2002. Shiga Declaration on Forests and Water. Tech. rep., International Expert Meeting on Forests and Water 20-22 November 2002, Shiga, Japan.

Shiklomanov, A. I., Yakovleva, T. I., Lammers, R. B., Karasev, I. P., Vörösmarty, C. J., Linder, E., Jul. 2006. Cold region river discharge uncertainty-estimates from large Russian rivers. Journal of Hydrology 326, 231–256.

Shiraiwa, T., Ueno, K., Yamada, T., 1992. Distribution of mass input on glaciers in the Langtang Valley Nepal Himalayas. Bulletin of Glacier Research 10, 21–30.

Shrestha, A. B., Eriksson, M., Mool, P., Ghimire, P., Mishra, B., Khanal, N. R., 2010. Glacial lake outburst flood risk assessment of Sun Koshi basin, Nepal. Geomatics, Natural Hazards and Risk 1(2), 157–169.

Shrestha, A. B., Wake, C. P., Dibb, J. E., Mayewski, P. A., 2000. Precipitation fluctuations in the Nepal Himalaya and its vicinity and relationship with some large-scale climatology parameters. International journal of Climatology 20, 317–327.

Shrestha, A. B., Wake, C. P., Mayewski, P. A., Dibb, J. E., 1999. Maximum Temperature Trends in the Himalaya and Its Vicinity: An Analysis Based on Temperature Records from Nepal for the Period 1971-94. International journal of Climatology 12, 2775–2787.

Shrestha, D. P., 1997. Assessment of soil erosion in the Nepalese Himalaya, a case study in Likhu Khola Valley, Middle Mountain region. . Land Husbandary, 94 (3), 2:59–80.

Shrestha, T. B., 1989. Development of Ecology of the Arun River Basin in Nepal. International Centre for Integrated Mountain Development (ICIMOD), Kathmandu, Nepal.

Silveira, L., 1997. Multivariate analysis in hydrology: the factor correspondence analysis method applied to annual rainfall data. Hydrological Sciences-Journal-des Sciences Hydrologiques 42(2), 215–224.

Singh, M. P., Singh, J. K., Mohanka, R., 2000. Forest Environment and Biodiversity. Daya Publishing House, New Delhi.

Singh, P., Bengtsson, L., 2004. Hydrological sensitivity of a large Himalayan basin to climate change. Hydrological Processes 18 (13), 2363–2385.

Singh, P., Jain, S. K., 2006. Snow and glacier melt in the Satluj river at Bhakra Dam in the western Himalayan region. Journal of Hydrology 326, 199–214.

Singh, P., Kumar, N., 1997. Impact assessment of climate change on the hydrological response of a snow and glacier melt runoff dominated Himalayan river. Journal of Hydrology 193 (1-4), 316–350.

Singh, P., Ramasastri, K. S., Kumar, N., 1995. Topographical Influence on precipitation distribution in different ranges of Western Himalaya. Nordic Hydrology 26, 259–284.

Singh, P., Singh, V. P., 2001. Snow and Glacier Hydrology. Kluwer Academic Publishers, Boston.

Singh, V. P., Frevert, D. K. E., 2002. Mathematical models of small watershed hydrology and applications. Water Resources Publications, Highlands Ranch, Colorado.

Siriwardena, L., Finlayson, B. L., McMahon, T. A., 2006. The impact of land use change on catchment hydrology in large catchments: The Comet River, Central Queensland, Australia. Journal of Hydrology 326, 199–214.

Smith, R. B., 1979. The influence of mountains on the atmosphere. Advances in Geophysics 21, 87–230.

Soerensen, R., Zinko, U., Seibert, J., 2006. On the calculation of the topographic wetness index: evaluation of different methods based on field observations. Hydrology and Earth System Sciences 10, ,, 101–112.

Souvignet, M., 2011. Climate Change Impacts on Water Resources in Mountainous Arid Zones: A case study in the Central Andeas, Chile. Ph.D. thesis, University of Leipzig.

Spear, R. C., Hornberger, G. M., 1980. Eutrophication in Peel Inlet, II, Identification of critical uncertainties via generalized sensitivity analysis. Water Resources Research 14, 43–49.

Staudenarausch, H., 2001. Untersuchungen zur hydrologischen Topolo-gie von Landschaftsobjekten fuer die distributive Flussgebi-etsmodellierung. Tech. rep., Friedrich-Schiller-Universität Jena.

Stocking, M. A., 1984. Rates of erosion and sediment yield in the African environment. Challenges in African Hydrology and Water Resources. In: Walling, D. E., Foster, S. S. D., Wurzel, P. (Eds.), Proceedings of the Harare Symposium. International Association of Scientific Hydrology (IASH-AIHS), pp. 285–295.

Tartari, G., Verza, G., Bertolami, L., 1998. Meteorological data at the Pyramid Observatory Laboratory (Khumbu Valley, Sagarmatha National Park, Nepal). In: A. Lami & G. Giussani (Eds), Limnology of high altitude lakes in the Mt. Everest Region (Nepal). Mem. Ist. ital. Idrobiol., 57: 23-40.

Tessema, S. M., 2011. Hydrological modeling as a tool for sustainable water resources management: a case study of the Awash River basin. Tech. rep., TRITA LWR.LIC 2056.

Thakur, P. K., Tamrakar, N. K., 2001. Geomorphology, sedimentology, and hazard assessment of the Sapta Kosi alluvial fan in eastern Nepal. Journal of Nepal Geological Society, 24 (Special Issue), 29–30.

Thanapakpawin, P., Richey, P. J., Thomas, D., Rodda, S., Campbell, B., Logsdon, M., 2007. Effects of land use change on the hydrologic regime of the Mae Chaem river basin, NW Thailand. Journal of Hydrology 334, 215–230.

Thomson, M., Warburton, M., 1985. Uncertainty on a Himalayan Scale. Mountain Research Development 5 (2), 115–135.

Thomson, M., Warburton, M., Haltey, T., 2006. Uncertainty on a Himalayan Scale. Himal Books, Kathmandu.

Tisseuil, C., Vrac, M., Lek, S., Wade, A. J., 2010. Statistical downscaling of river flows. Journal of hydrology 385, 279–291.

Tiwari, P. C., 2000. Land-use changes in Himalaya and their impact on the plains ecosystem: need for sustainable land use. Land Use Policy 17, 101–111.

Ueno, K., Toyotsu, K., Bertolani, L., Tartari, G., 2008. Stepwise onset of monsoon weather observed in the nepal himalaya. Monthly Weather Review 136 (7), 2507–2522.

Uhlenbrook, S., 1999. Untersuchung und Modellierung der Abflussbildung in einem mesoskaligen Einzugsgebiet. Ph.D. thesis, Freiburger Schriften zur Hydrologie, Institut für Hydrologie, Univerität Freiburg.

Upreti, B. N., 1999. An overview of the stratigraphy and tectonics of the Nepal Himalaya. Journal of Asian Earth Sciences 17, 577–606.

Vehvilaeinen, B., 1992. Snow cover models in operational watershed forecasting. Yhteenveto: Lumimallit vesistöjen ennustemalleissa. Publications of the Water and Environment Research Institute 11. National Board of Waters and the Environment. Finland, Helsinki.

Viessman, W., Lewis, G. L., 2003. Introduction to hydrology. New York, Intext Educational Publishers.

Virgo, K. J., Subba, K. J., 1994. Land use change between 1978 and 1990 in Dhankuta District, Koshi Hills, Eastern Nepal. Mountain Research Development 14 (2), 159–170.

Vogel, R. M., Fennessey, N. M., 1995. Flow duration curves II: A review of applications in water resources planning. Journal of the American Water Resources Association 31(6), 1029–1039.

Wagener, T., Lees, M. J., Wheater, H. S., 2001. Monte-Carlo Analysis Toolbox User Manual. Tech. rep., Civil and Environmental Engineering Department, Imperial College of Science Technology and Medicine.

Walder, J. S., Costa, J. E., 1996. Outburst floods from glacier-dammed lakes: the effect of mode of lake drainage on flood magnitude. Earth Surface Processes and Landforms 21(8), 701–723.

Walder, J. S., Fountain, A. G., 1997. Glacier generated floods. In: Proceedings of the Conference held at Anaheim, California, June 1996). IAHS Publ. no. 239, 1997.

Walker, W. E., Harremoees, P., Rotmans, J., Van Der Sluijs, J. P., Van, Asselt, M. B. A., Janssen, P., , Krayer von Krauss, M. P., 2003. Defining uncertainty: A conceptual basis for uncertainty management in model-based decision support. Integrated Assessment 4(1), 5–17.

Walling, D. E., 1999. Linking land use, erosion and sediments yields in river basins. Hydrobiologia 410, 223–240.

Walling, D. E., 2001. The Impact of Global Change on Erosion and Sediment Transport by Rivers: Current Progress and Future Challenges. Tech. rep., United Nations Educational, Scientific and Cultural Organization (UNESCO).

Wasson, R. J., 2003. A sediment budget for the Ganga Brahmaputra catchment. Current Science 84 (8) PART 8, 1041–1047.

Wasson, R. J., Juyal, N., Jaiswal, M., McCullochd, M., Sarinb, M. M., Jaine, V., Srivastavac, P., Singhvi, A. K., 2008. The mountain-lowland debate: Deforestation and sediment transport in the upper Ganga catchment. Journal of Environmental Management 88, 53–61.

Watson, R. T., Verardo, D. J., 2000. Land Use, Land Use Changes and Forestry. Cambridge University Press, Cambridge.

Watson, R. T., Zinyowera, M. C., Moss, R. H., 1996. Climate Change 1995: Impacts, adaptations, and mitigation of climate change. Cambridge University Press, Cambridge.

WECS, 2011. Koshi River Basin Management Strategic Plan (2011-2021). Tech. rep., Water and Energy Commission Secretariat, Government of Nepal.

Weichel, T., Pappenberger, F., Schulz, K., 2007. Sensitivity and uncertainty in flood inundation modelling – concept of an analysis framework. Advance Geoscience 11, 31–36.

Wessolek, G., 1993. Erarbeitung eines Schlüssels zur Abschätzung von Versickerung und Oberflächenabfluss versiegelter Flächen Berlins. Tech. rep., Unveröffentlicher Bericht im Auftrag der Bundesanstalt für Gewässerkunde. Berlin.

Whetton, P. H., Fowler, A. M., Haylock, M. R., Pittock, A. B., 1993. Implications of climate change due to the enhanced greenhouse effect on floods and droughts in Australia. Climate Change 25, 289–317.

Wilby, R. L., Hay, L. E., Leavesley, G. H., 1999. A comparison of downscaled and raw GCM output: implications for climate change scenarios in the San Juan River Basin, Colorado. Journal of Hydrology 225, 67–91.

Wilk, J., 2002. Simulating the impacts of land-use and climate change on water resource a availability for a large south Indian catchment. Hydrological Sciences 47(1), 19–30.

Wilk, J., Andersson, L., Plemkamon, V., 2001. Hydrological impacts of forest conversion to agriculture in a large river basin in northeast Thailand. Hydrological process Processes 15, 2729–2748.

WMO, 1988. Analyzing long time series of hydrological data with respect to climate variability, Project description, WCAP -3. Tech. rep., World Meteorological Organisation.

Yasunari, T., 1976. Seasonal weather variations in Khumbu Himal. Seppyo, 38, Special Issue., 74–83.

Yasunari, T., Inoue, J., 1978. Characteristics of monsoonal precipitation around peaks and ridges in Shorong and Khumbu Himal. Seppyo 40 special issue, 26–14.

Zhang, L., Dawes, W. R., Walker, G. R., 1999. Predicting the Effect of Vegetation Changes on Catchment Average Water Balance. Technical report 99/12, 35pp., Cooperative Research Centre for Catchment Hydrology.

A Hydro-meteorological stations

The list of hydro-meteorological stations used for this study. Note for station types. P: precipitation, C: climate, D: discharge

Table A.1: List of Hydro-meteorological stations

S.N.	Station ID (DHM)	Type	Name	Lat	Log	Elevation
1	1115	P	Nepalthok	27.27	85.49	1098
2	1028	P	Pachuwarghat	27.34	85.45	633
3	1023	P	Dolalghat	27.38	85.43	710
4	1062	P	Sangachok	27.42	85.43	1327
5	1020	P	Mandan	27.7	85.65	1365
6	1009	P	Chautara	27.47	85.43	1660
7	1018	P	Baunepati	27.47	85.34	845
8	1008	P	Nawalpur	27.48	85.37	1592
9	1017	P	Dubachuar	27.52	85.34	1550
10	1025	P	Dhap (1025)	27.55	85.38	1205
11	1016	P	Sarmanthang	27.57	85.36	2625
12	1058	P	Tarke Ghyang	28.00	85.33	2480
13	1213	P	Udayapur Gadhi	26.56	86.31	1175
14	1210	P	Kuruleghat	27.08	86.26	497
15	1207	P	Mane Bhanjyang	27.29	86.25	1576
16	1206	C	Okhaldhunga	27.19	86.3	1720
17	1204	P	Aisealukhark	27.21	86.45	2417
18	1203	P	Pakarnas	27.26	86.34	1982
19	1220	C	Chialsa	27.46	86..61	2770
20	1219	P	Sallery	27.3	86.35	2378
21	1202	P	Chaurikhark	27.42	86.43	2660
22	1316	P	Chatara	26.49	87.10	183
23	1309	P	Tribeni	26.56	87.09	143
24	1322	P	Machuwa Ghat	26.58	87.10	158
25	1306	P	Munga	27.02	87.14	1317
26	1304	P	Pakhribas	27.03	87.17	1680
27	1305	P	Laghuwa Ghat	27.08	87.17	410
28	1324	P	Bhojpur	27.37	87.15	1595

Continued on next page

Table A.1 – continued from previous page

S.N.	Station ID (DHM)	Station type	Name	Lat	Log	Elevation
29	1321	P	Tumlingtar	27.17	87.13	303
30	1303	P	Chainpur East	27.17	87.2	1329
31	1325	P	Dingla	27.22	87.09	1190
32	1301	P	Num	27.33	87.17	1497
33	1311	P	Dharan	26.81	87.28	444
34	1308	P	Mulghat	26.56	87.2	365
35	1307	C	Dhankuta	26.59	87.21	1210
36	1314	P	Terhathum	27.08	87.33	1633
37	1419	P	Phidim (Panchther)	27.09	87.45	1205
38	1406	P	Memen Jagat	27.12	87.56	1830
39	1420	P	Dovan	27.21	87.36	763
40	1405	C	Taplejung	27.21	87.4	1732
41	1404	P	Taplethok	27.29	87.47	1383
42	1403	P	Lungthung	27.33	87.47	1780
43	1103	C	Jiri	27.38	86.14	2003
44	1030	C	Kathmandu airport	27.7	85.37	1336
45	670	D	Rabuwabazaar	27.26	86.65	460
46	630	D	Pachuwarghat	27.55	85.75	602
47	600.1	D	Uwagaon	27.6	87.33	1294
48	604.5	D	Turkeghat	27.32	87.19	414
49	695	D	Chatara	26.89	87.17	140

B Calculation of potential evapotranspiration

The following method was used to calculated the evapotranspiration (PET) using Penmann-monteith approach Allen et al. (1998).

$$PET = \frac{1}{L} \cdot \frac{S \cdot (R_N - G) + \rho \cdot C_p \cdot \frac{e_s - e_d}{r_a}}{S + \gamma \cdot (1 + \frac{r_s}{r_\alpha})} \tag{B.0.1}$$

with:

L = latent heat of evaporation [MJ/kg]

s = slope of the vapor pressure curve [kPa/^{o}C]

R_N = net radiation [MJ m^{-2} d^{-1}]

G = soil heat flux [MJ m^{-2} d^{-1}]

c_p = specific heat capacity of the air for constant pressure [Jkg^{-1}K^{-1}]

e_s = saturation vapor pressure [hPa]

e_d = vapor pressure [hPa]

r_a = aerodynamic resistance of the land cover [sm^{-1}]

γ = psychrometer constant [hPaK^{-1}]

r_s = surface resistance of the land cover [sm^{-1}]

The **latent heath of evaporation (L)** is calculated approximately according to:

$$L = \frac{2501 - (2.361 \cdot T_a vg)}{1000} [MJ/kg] \tag{B.0.2}$$

The **saturation vapor pressure (e_s(T))** of the air for the temperature (T) is calculated according to Equation 6.4.17 given above.

The **current vapor pressure (ea)** then is calculated from the saturation vapor pressure and the relative air humidity (U in [%]) as follows:

$$e_a = e_s(T)_d \cdot \frac{U}{100} \ [hPa] \tag{B.0.3}$$

The **slope of the saturation vapor pressure curve (s)** is calculated using the saturation vapor pressure (es(T)) and the air temperature (T_{avg}):

$$s = e_s \cdot \left(\frac{4098}{(T_a vg + 237.3)^2} \right) \ \left[kPa/^oC \right] \tag{B.0.4}$$

The **air pressure (p)** at the height (z) is calculated from the adapted barometric formula as follows:

$$p_z = 101.3 \cdot e^{-\left(\frac{9.811}{8314.3 \cdot T_a bs} \cdot z\right)} \ \left[kPa \right] \tag{B.0.5}$$

p_0 = air pressure at sea level (= 101.3) [kPa]

g = gravitational acceleration (= 9.811) [ms^{-1}]

R = gas constant (= 8314.3) [$Jkmol^{-1}$ K^{-1}]

$T_a bs$ = absolute air temperature [K]

The **psychrometer constant** (γ) results from the specific heat capacity of the air (= (1.013 x $10^{-}3$), air pressure P_z, the relation of mol weights of dry air and water vapor (=0.622) and the latent evaporation heat (L) according to::

$$\gamma = \frac{1.013 \cdot 10^{-3} \cdot P_z}{0.622 \cdot L} [kPa/^oC] \tag{B.0.6}$$

The soil heat flux (G) is then calculated according to a simplified relation where the calculation is carried out for day and night.

$$G_d = 0.1 \cdot Rn \cdot \frac{N}{24} \ [MJm^{-2}d^{-1}] \tag{B.0.7}$$

$$G_n = 0.5 \cdot Rn \cdot (\frac{24 - N}{24} \ [MJm^{-2}d^{-1}] \tag{B.0.8}$$

R_n is daily net radiation and calculated according to Equation B.0.17.

$$G = G_d + G_n \ [MJm^{-2}d^{-1}] \tag{B.0.9}$$

The influence of various vegetation forms on the evaporation is considered in the Penman-Monteith approach using two different resistances, the surface resistance (rs) and the aerodynamic resistance (ra). In order to calculate, the resistance land-use specific parameters are required. Those are in detail: the Leaf Area Index (LIA), the effective growth height (effHeight) and surface resistances at

water saturation (RSC0_1...12). Their values for different land cover classes at different time steps are provided in the land use parameter file (Table 6.2).

Moreover, stand-specific Albedo values are included which are used for the calculation of the radiation balance. The LIA and effective growth height are represented in the form of a different time step (d1...d4) of the year. The points represent the beginning of the vegetation phase (d1), reaching the maximum or full maturity (d2), the phase of full maturity to point d3 and finally the decline until the end of the vegetation period (d4). The separate points are represented by the daily Julian values (d1 = 110, d2 = 150, d3 = 250, d4 = 280) for areas at about 400 m height. For other heights (z) points are approximated according to the following empirical relation:

$$d1...4(z) = d1...4(400) + 0.025 \cdot (z - 400) \tag{B.0.10}$$

The values between the individual points are linearly interpolated. The aerodynamics resistance (ra) for the vegetation with an effective growth height of less than 10 m of the specific land use class is calculated according to the following formula:

$$ra = \frac{9.5}{v2} \cdot (log\frac{2}{z0})^2 [s/m] \tag{B.0.11}$$

with z0 = aerodynamic roughness length (0.1 x effective growth height) [m]

v2 = wind speed at a height of 2 m [ms^{-1}]

For effective growth heights greater or equal to 10 m, the aerodynamic resistance is calculated in a simplified way according to:

$$ra = \frac{20}{0.41^2 \cdot v2} [s/m] \tag{B.0.12}$$

The **surface resistance** of the specific land use is calculated according to:

$$rs = \left(\frac{1 - A}{rsc} + \frac{A}{rss}\right) [s/m] \tag{B.0.13}$$

with: rsc = surface resistance [ms^{-1}]

A = 0.7 ^{LAI} [-] rss = surface resistance of uncovered soil [ms^{-1}]

The model also calculates a hypothetical reference evapotranspiration (refET) by considering standard land cover. A hypothetical reference crop with an assumed height of 0.12 m, a fixed canopy resistance of 70s/m and an albedo of 0.23 is considered for the calculation of refET (Allen et al. 1998).

Calculation of the net radiation balance

The energy that is necessary for the evaporation is provided by radiation. The net radiation balance for each day needs to be defined for the calculation of the amount of energy that results from the energy

balance segments. A detailed description of the process is provided in Allen et al. (1998).

The **global solar radiation ($\mathbf{R}_G$)** is the amount of radiation arriving on the earth surface. It is calculated by taking the extraterrestrial radiation and subtracting the amount which is reflected or absorbed when passing through the atmosphere. In order to calculate the solar radiation the following individual calculations are carried out in the module according to (Allen et al. 1998).

By using the Angstrom formula, the solar radiation (R_G) is calculated using the parameters a and b, the relation between current (sunh) and maximum possible (S_0) sunshine hours and the extraterrestrial radiation (actExtRad).

$$R_G = actExtraRad \cdot \left(a + b \cdot \frac{S}{S_0}\right) \ [MJ \cdot m^{-2} d^{-1}] \tag{B.0.14}$$

The net radiation serves as a source of energy for the calculation of evapotranspiration. It results from extraterrestrial radiation which is reduced to global radiation when transmitted in the atmosphere. By subtracting the longwave radiation from the global radiation, the result is called the net radiation. The following steps are required for the calculation.

The **saturation vapor pressure ($\mathbf{e}_s$)** of the air temperature is calculated according to the equation (6.4.17). The **current vapor pressure ($\mathbf{e}_a$)** results from the (e_s) and the relative humidity (U) in % according to:

$$e_a = e_s \cdot \frac{U}{100} [kPa] \tag{B.0.15}$$

Using the extraterrestrial radiation (extRad) and the elevation (h) of the model entity indicate the global radiation with cloudless, clear sky (R_{cs}):

$$R_{cs} = (0.75 + 2 \cdot 10^{-5} \cdot h) \cdot extRad [MJm^{-2} d^{-1}] \tag{B.0.16}$$

The global solar radiation (R_G) and the albedo (α) of the specific land cover gives the shortwave net radiation (swRad). The longwave net radiation (lwRad) is calculated using the absolute mean temperature, current vapor pressure, global solar radiation, global solar radiation with a cloudless sky and the Boltzmann constant as described by Allen et al. (1998).

The difference of shortwave net radiation and longwave net radiation gives the net radiation according to:

$$netRad = swRad - lwRad \ [MJm^{-2} d^{-1}] \tag{B.0.17}$$

If the longwave radiation is greater than the shortwave radiation, the net radiation is set to zero in the model.

C Rating curve of the Dudh Kosi river basin

Rating curve Type	Period	Water Level (meter)							
		1	1.2	1.6	2	3.6	4	4.3	6
		Discharge of corresponding water level (m3/sec)							
Type11	Jul-1983 to Jul-1986	33	41	95	160	671	870	1040	2470
Type 10	Aug-1986 to Aug-1988	26	42	90	158	672	870	1040	2470
Type 12	Aug-1988 to Aug-1990	54	69	111	175	671	870	1040	
Type 10	Aug-1990 to Aug-1993	26	42	90	158	672	870	1040	2470
Type 6	Aug-1994 to Aug-1996	41	59	108	170	671	870	1040	
Type 9	Aug-1996 to Aug-1997	48	65	111	175	671	870	1040	2470
Type 12	Aug-1997 to Sept-1998	54	69	111	175	671	870	1040	
Type 13	Sept-1998 to Aug-1999					170	310	450	1850
Type 14	Aug-1999 to Sept-2000			23	51	300	420	520	1850
Type 15	Sept-2000 to Aug-2002	18	27	57.3	106	615	857	1040	2470
Type 15	Jul-2003 to Jul-2004	18	27	57.3	106	615	857	1040	2470
Type 16	Jul-2004 to Aug-2005		16	42.8	101	615	857	1040	2470
Type 14	Aug-2005 to Dec-2008			23	51	300	420	520	1850

Figure C.1: The rating curve of the Rabuwabazaar gauging station (Dudh Kosi river basin) showing the relationship between water level and related amount of discharge. Data source: DHM, 2011

.

	Highest value		Lowest value	
Year	Water Level (m)	Discharge (m3/sec)	Water level (m)	Discharge (m3/sec)
1979	0.82	34.6		
1983	1.47	65.3	0.98	27.3
1984	3.58	285	0.91	30.7
1985	2.19	242		
1986	3.27	576	0.98	35.4
1987	1.51	72	1.24	42.8
1988	2.1	191	1.03	79
1989	3.32	388	0.73	38
1990	2.85	351	0.88	45
1991	3.75	692	0.92	20.2
1992	3.1	511	1.08	30.6
1993	3.7	708	1.11	27.9
1994	2.08	171	1.03	35.3
1995	1.43	62.6	1.43	62.6
1996	3.85	606	1.11	51.9
1997	4.06	489	1.09	50.1
1998	4.73	671	0.7	39.4
1999	3.9	255	3.08	72.2
2000	2.71	153	1.97	45.9
2001	3.08	398	1.34	43.7
2004	1.45	43	1.39	41.8
2005	1.67	49.9		
2006	2.04	53.7	2.04	51.9
2007	2.27	85.1	1.9	48.8
2008	2.74	118	1.98	57.1
2009	2.27	55.7	1.99	28.8
2010	2.04	32.2		

Figure C.2: The measured values of water level (m) and corresponding discharge (m^3/sec) to derive the rating curve of the Rabuwabazaar gauging station. Among the few measurements, the lowest and the highest value of the particular year is provided. Data source: DHM, 2011

D Uncertainty analysis of precipitation input data

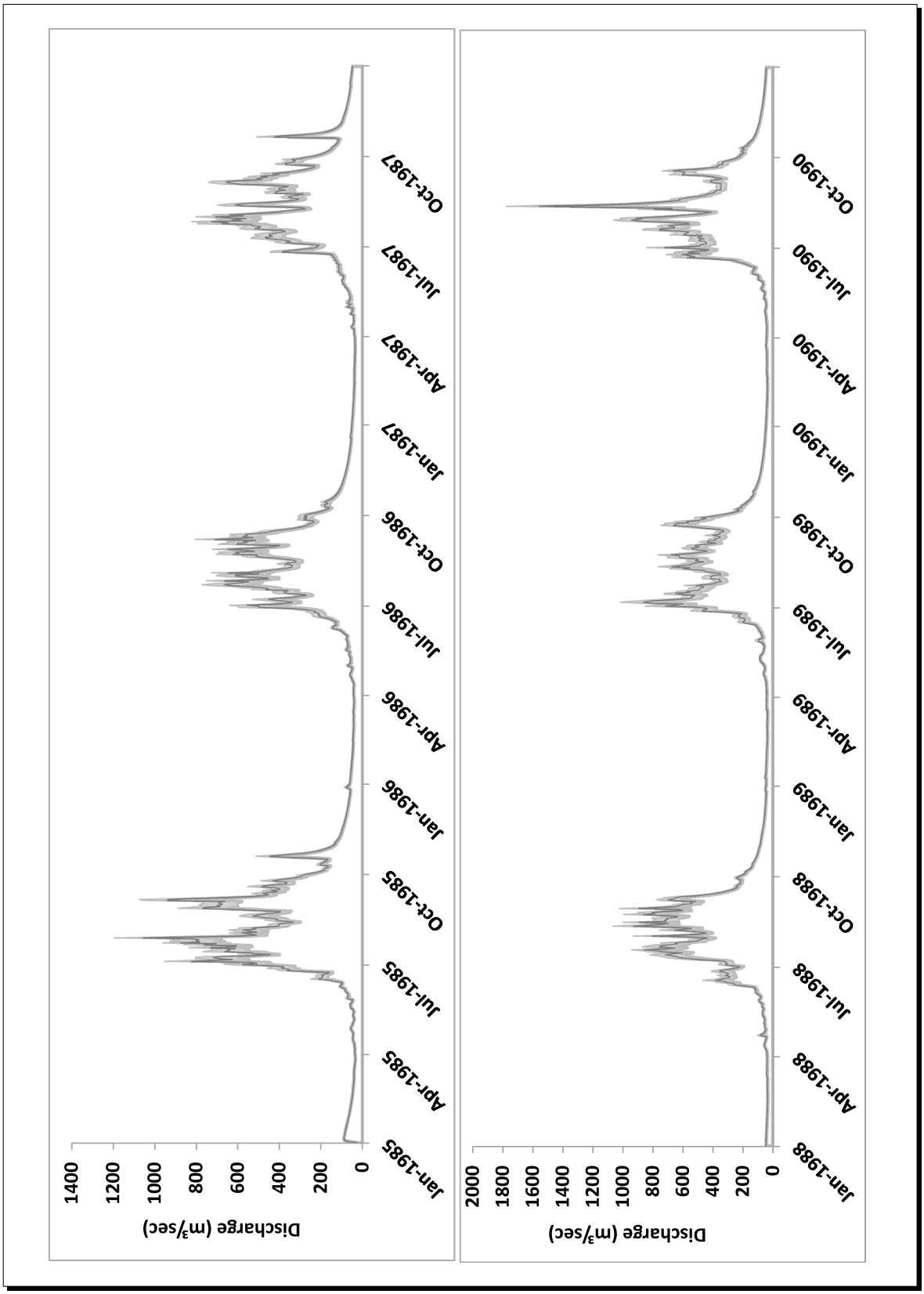

Figure D.1: Uncertainty in the model result from ± 10 % precipitation change (1985-1990).

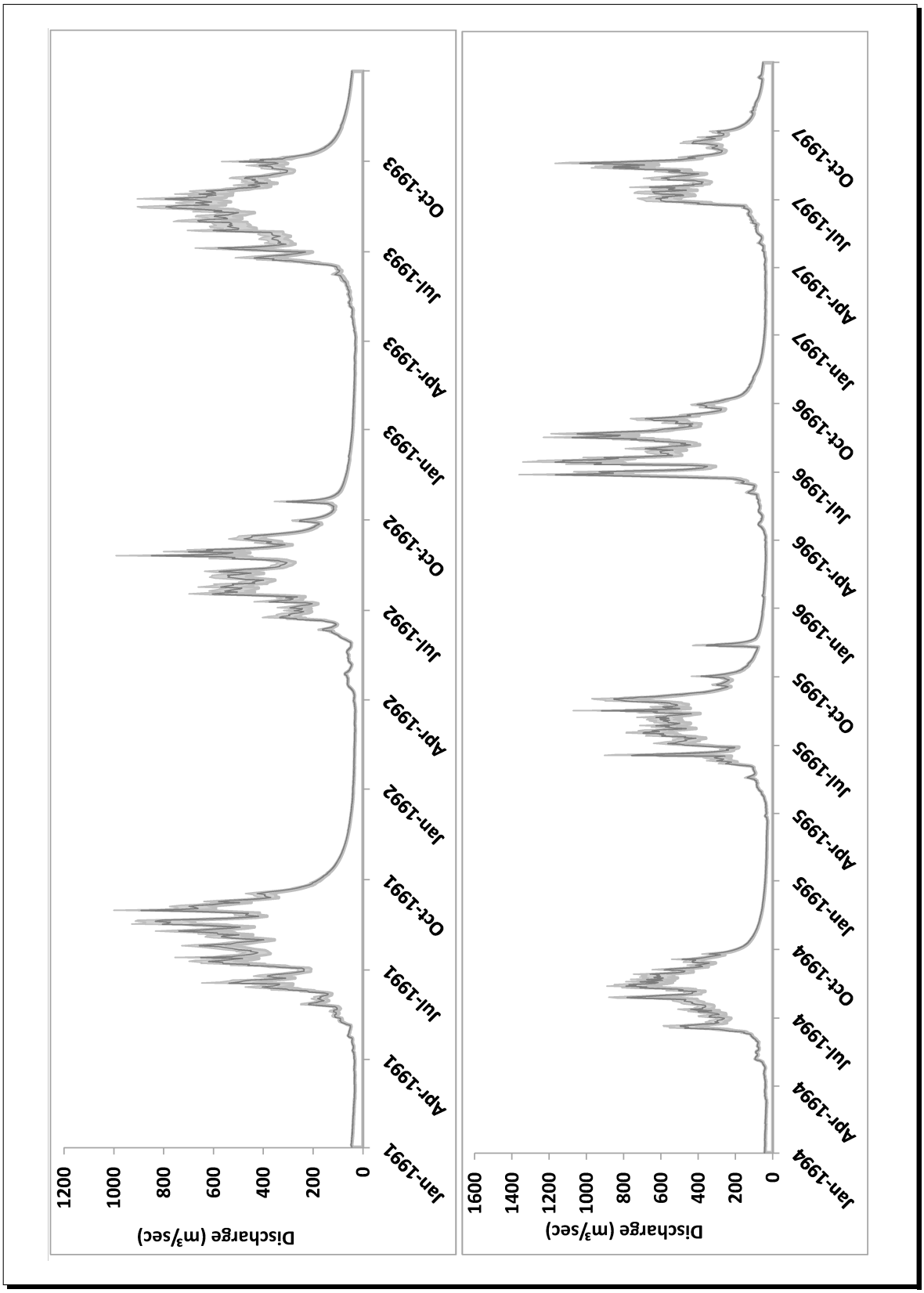

Figure D.2: Uncertainty in the model result from $\pm$ 10 % precipitation change (1991-1997).

E Regional sensitivity analysis

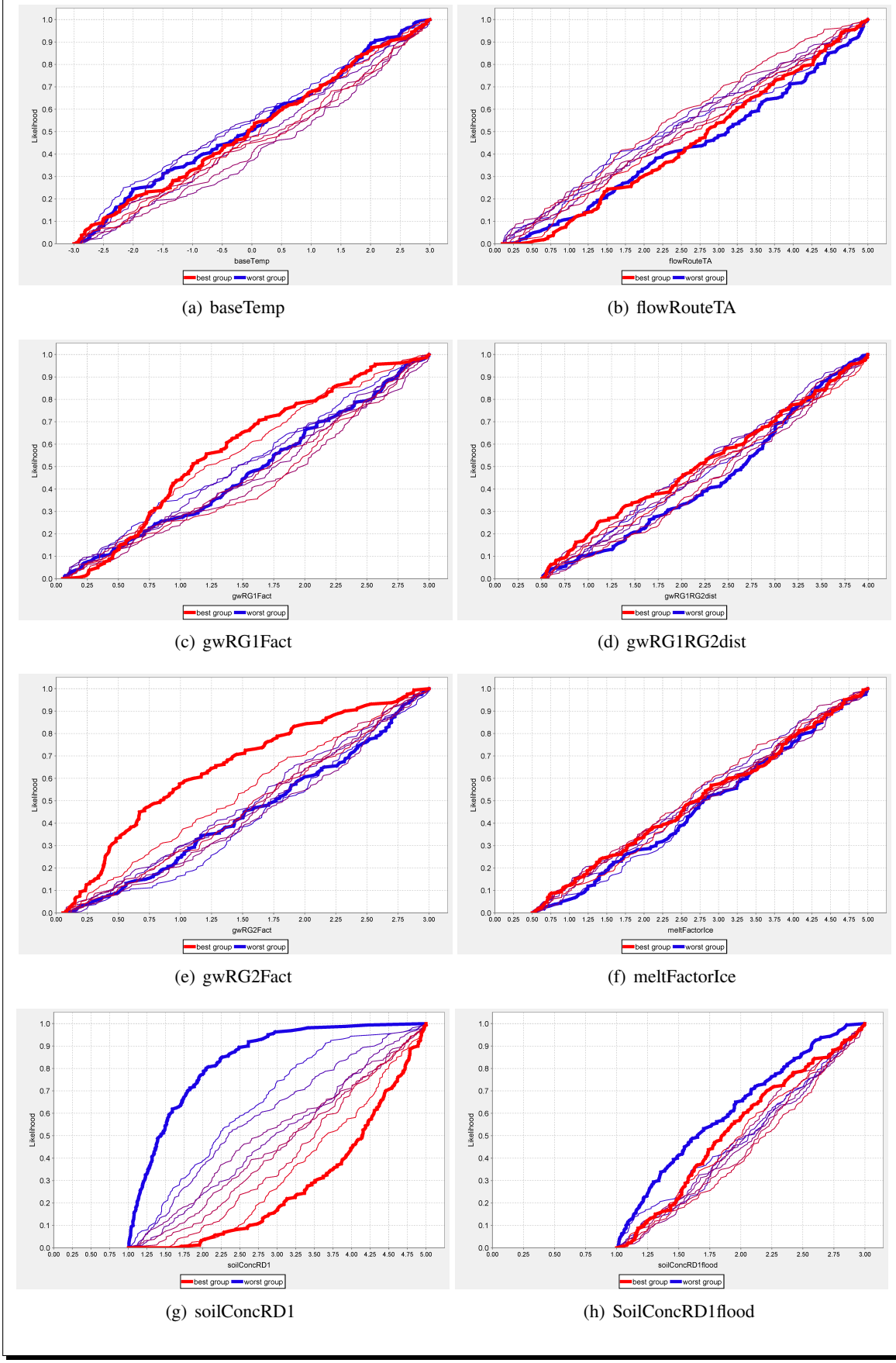

(a) baseTemp (b) flowRouteTA

(c) gwRG1Fact (d) gwRG1RG2dist

(e) gwRG2Fact (f) meltFactorIce

(g) soilConcRD1 (h) SoilConcRD1flood

Figure E.1: Sensitivity of parameters with E_{NS}-A

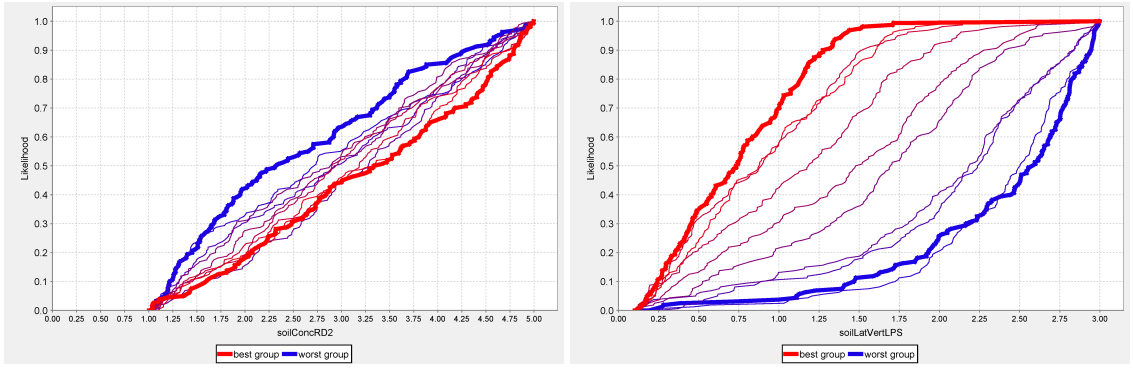

(a) soilConcRD2

(b) soilLatVertLPS

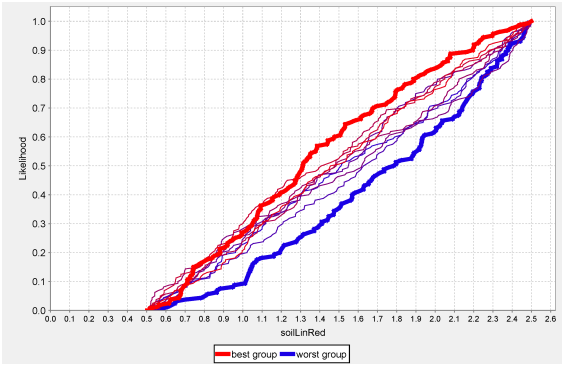

(c) soilLinRed

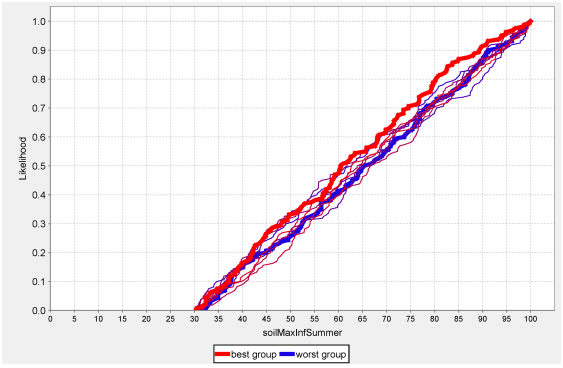

(d) soilMaxInfSummer

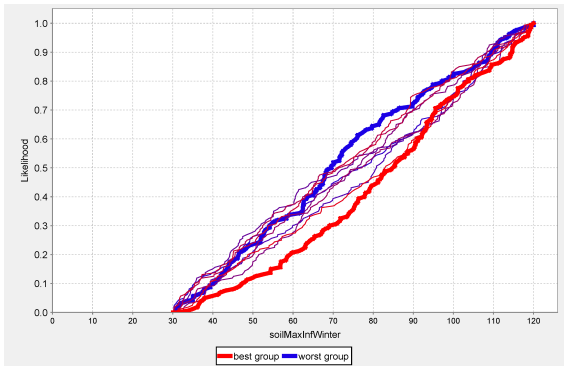

(e) soilMaxInfWinter

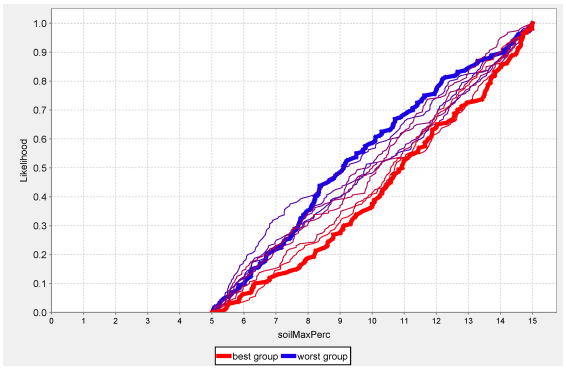

(f) soilMaxPerc

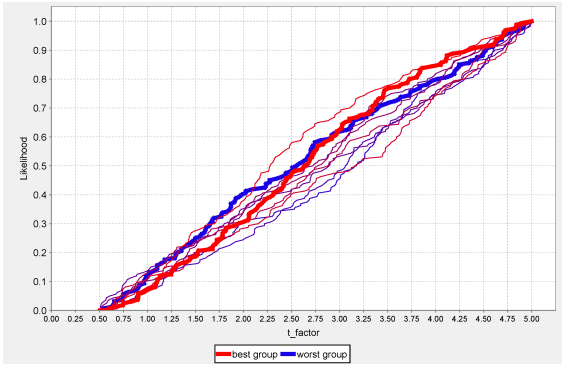

(g) t_factor

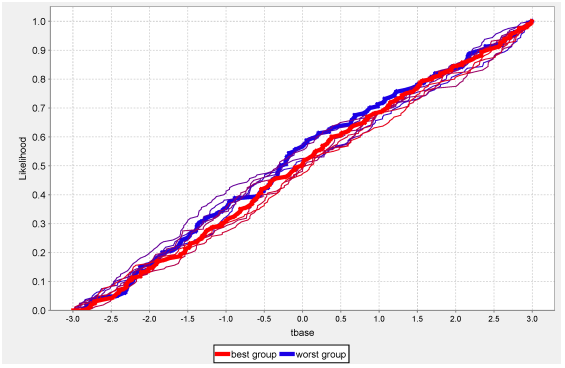

(h) tbase

Figure E.2: Sensitivity of parameters with E_{NS}-B

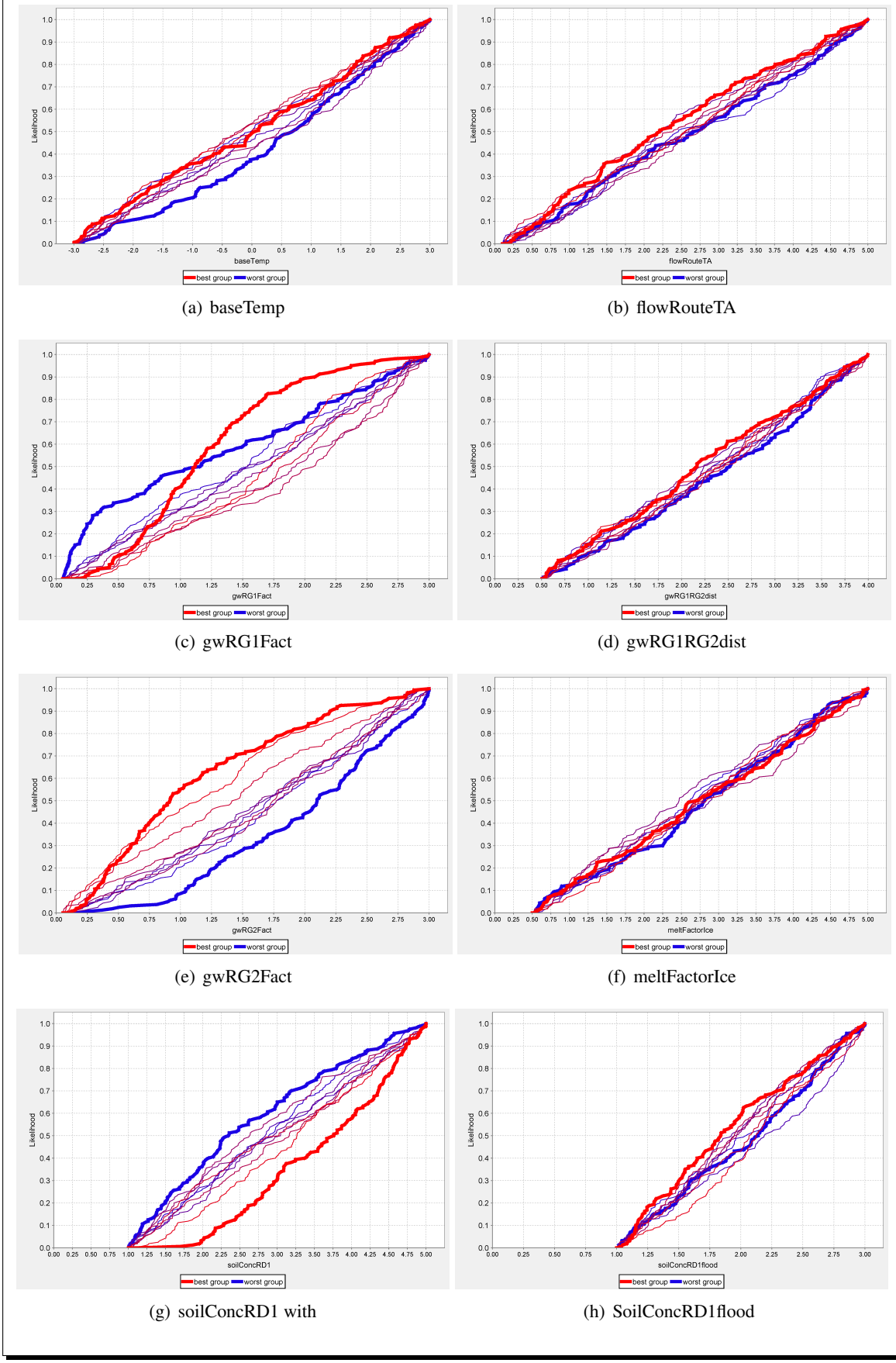

(a) baseTemp (b) flowRouteTA

(c) gwRG1Fact (d) gwRG1RG2dist

(e) gwRG2Fact (f) meltFactorIce

(g) soilConcRD1 with (h) SoilConcRD1flood

Figure E.3: Sensitivity of parameters with LNS-A

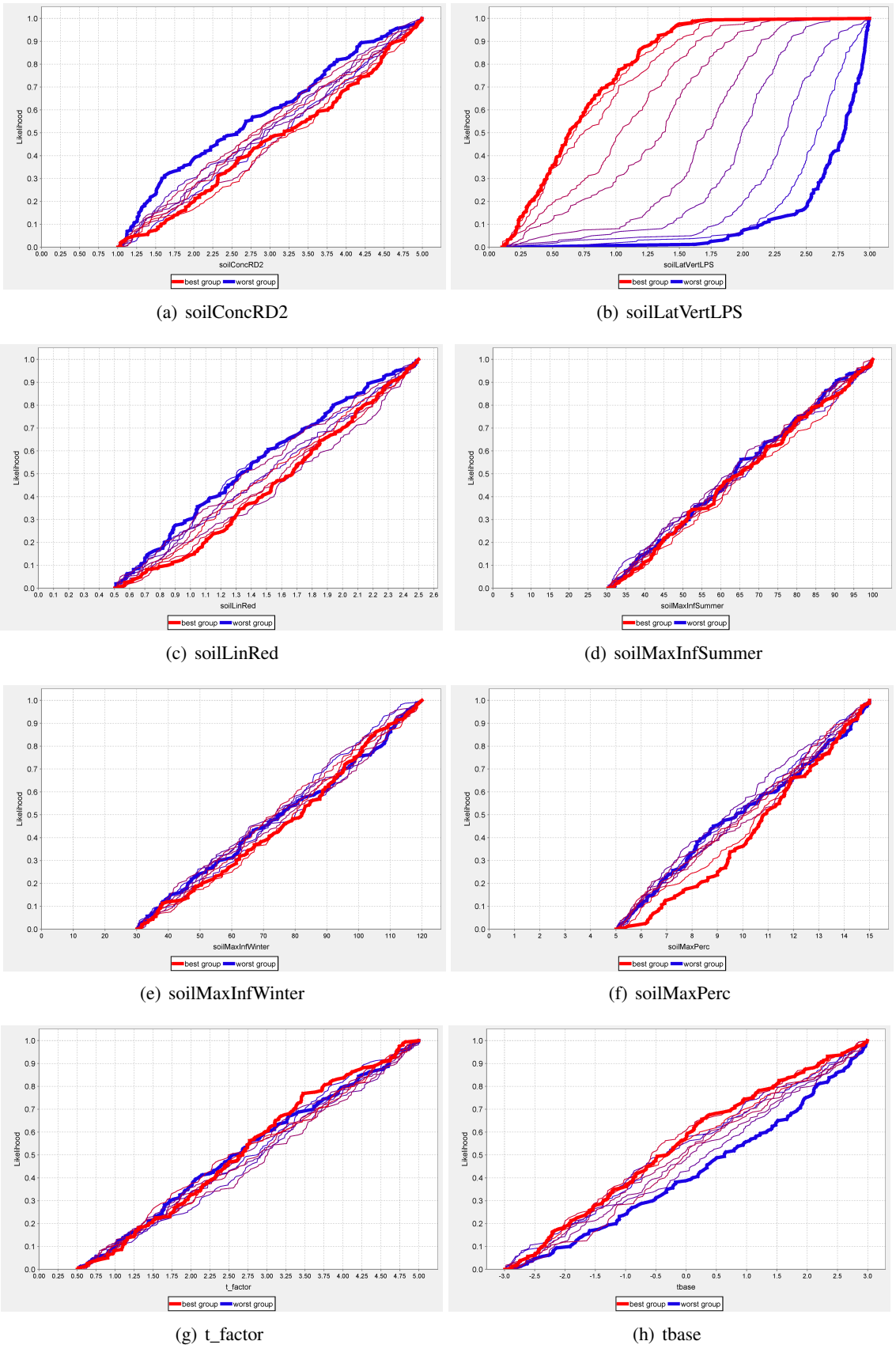

(a) soilConcRD2

(b) soilLatVertLPS

(c) soilLinRed

(d) soilMaxInfSummer

(e) soilMaxInfWinter

(f) soilMaxPerc

(g) t_factor

(h) tbase

Figure E.4: Sensitivity of parameters with LNS-B

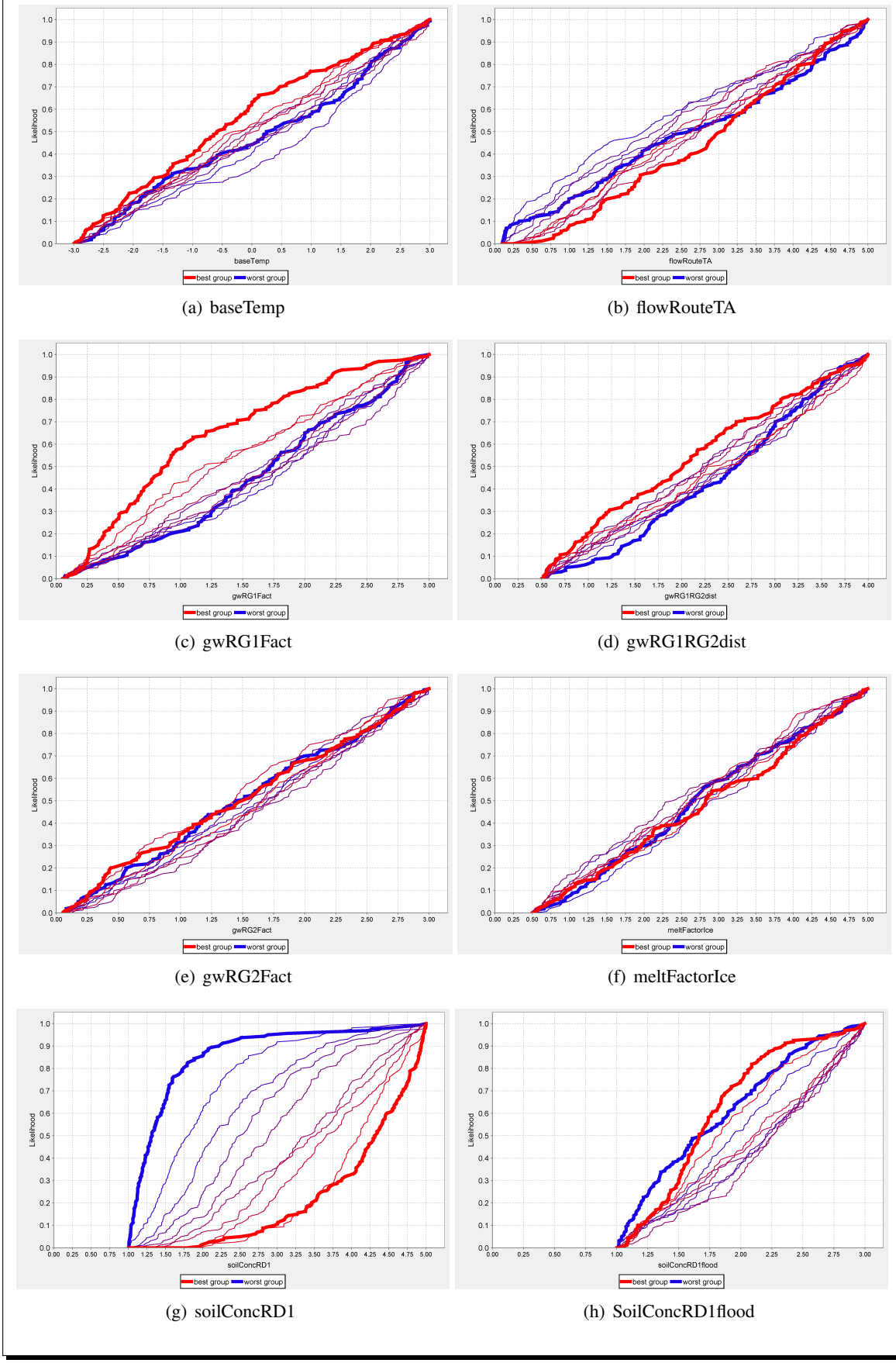

(a) baseTemp (b) flowRouteTA

(c) gwRG1Fact (d) gwRG1RG2dist

(e) gwRG2Fact (f) meltFactorIce

(g) soilConcRD1 (h) SoilConcRD1flood

Figure E.5: Sensitivity of parameters with r^2-A

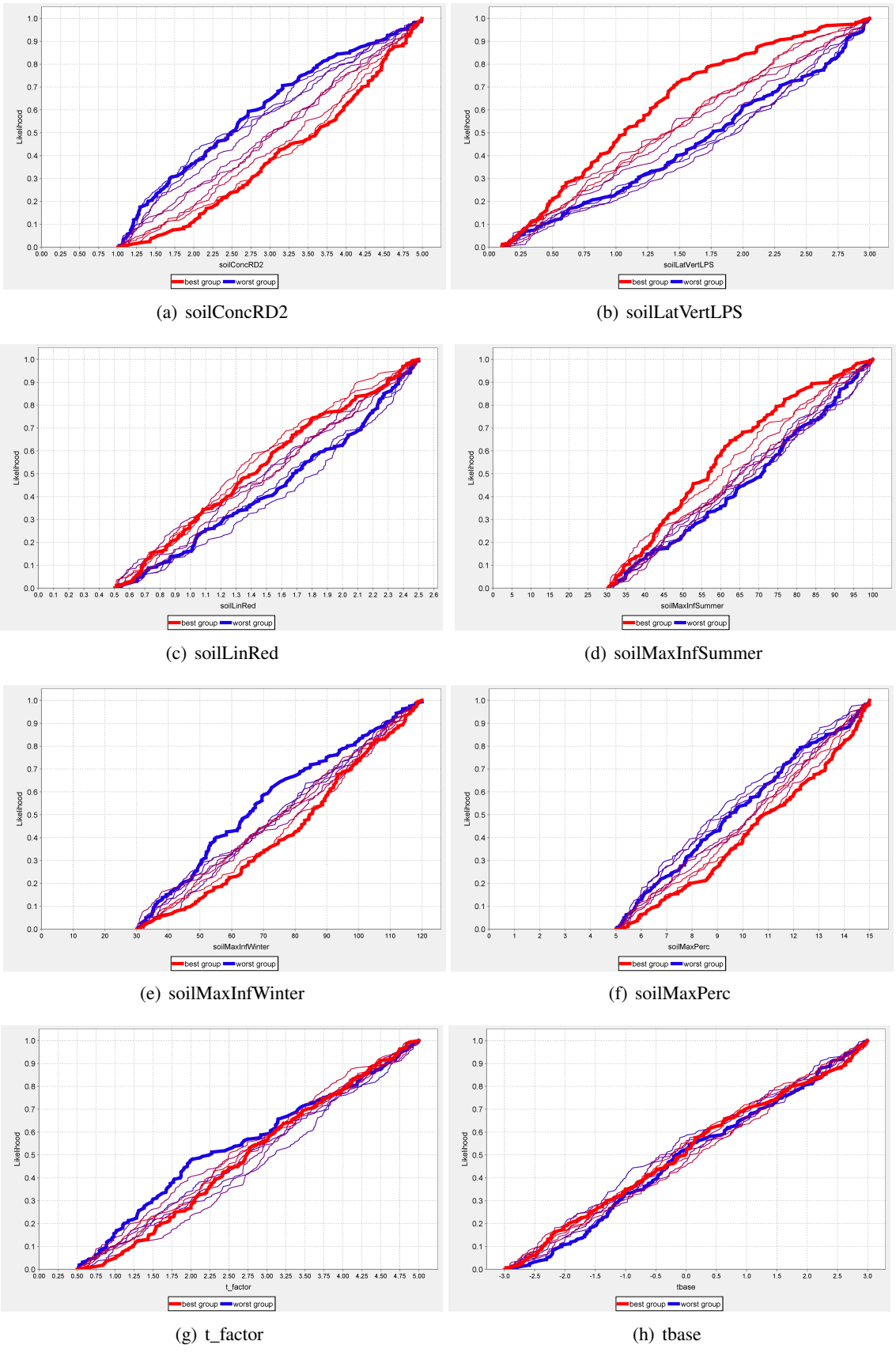

(a) soilConcRD2 (b) soilLatVertLPS

(c) soilLinRed (d) soilMaxInfSummer

(e) soilMaxInfWinter (f) soilMaxPerc

(g) t_factor (h) tbase

Figure E.6: Sensitivity of parameters with r^2-B

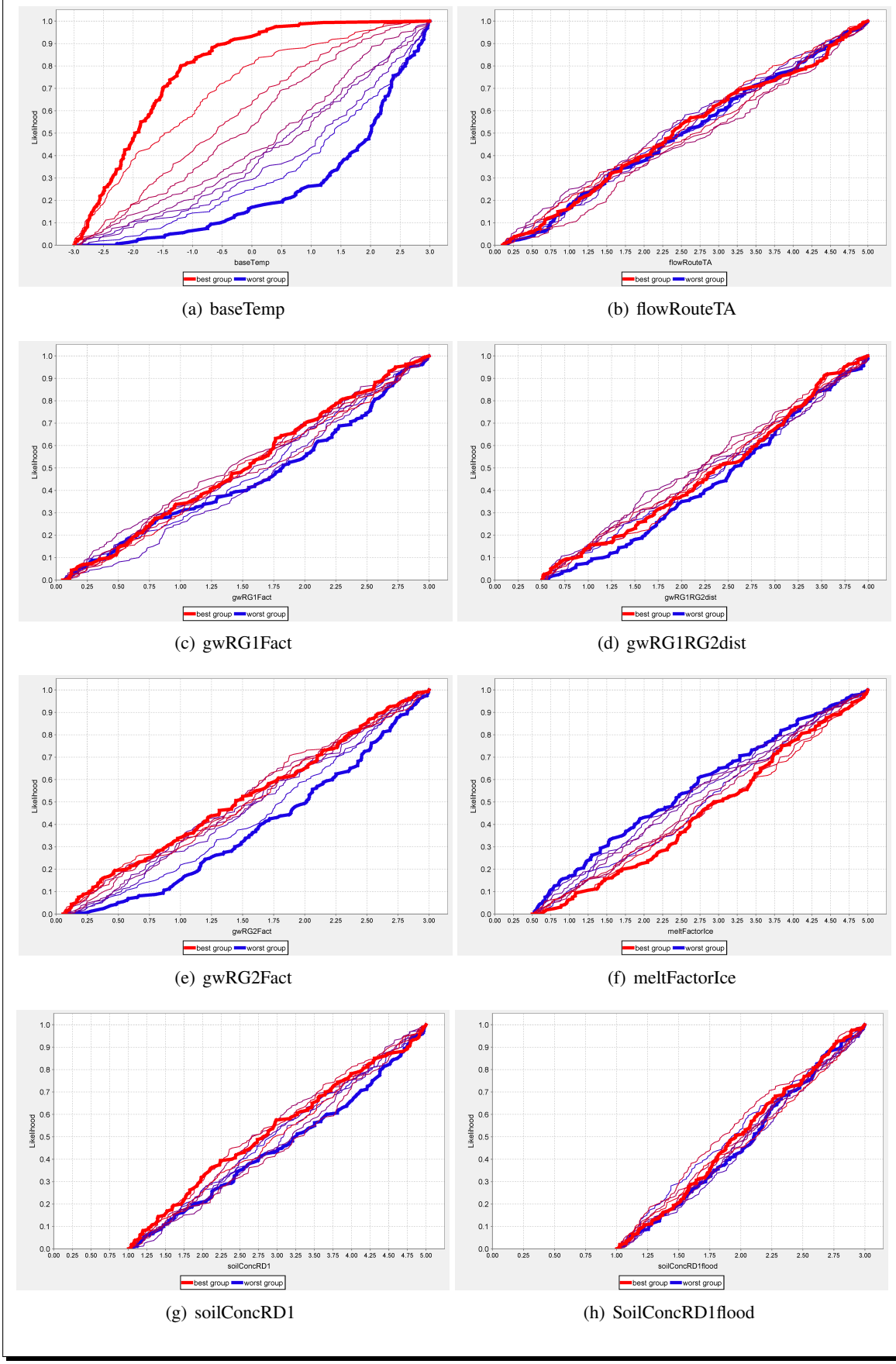

(a) baseTemp (b) flowRouteTA

(c) gwRG1Fact (d) gwRG1RG2dist

(e) gwRG2Fact (f) meltFactorIce

(g) soilConcRD1 (h) SoilConcRD1flood

Figure E.7: Sensitivity of parameters with PBAIS-A

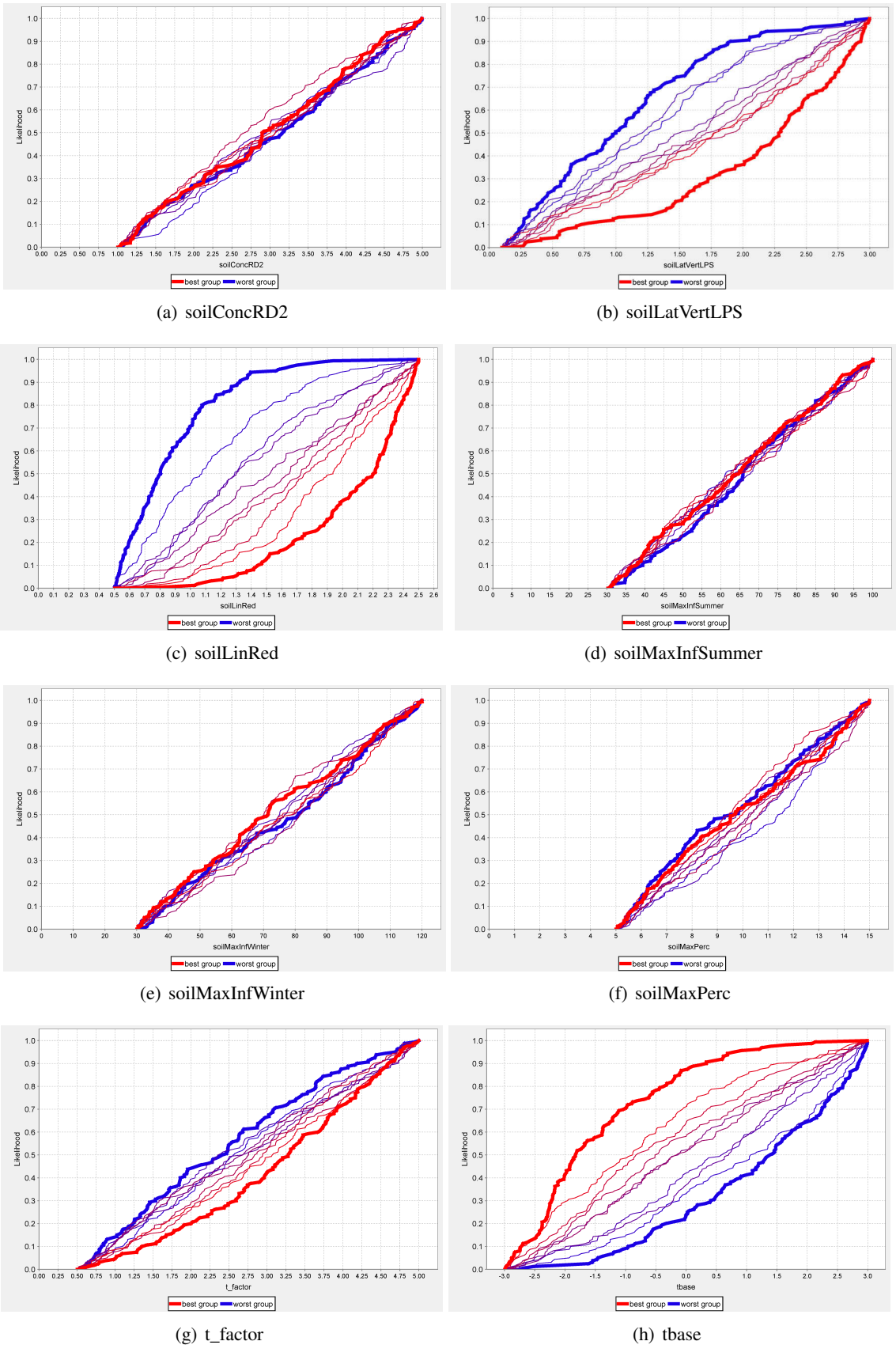

(a) soilConcRD2

(b) soilLatVertLPS

(c) soilLinRed

(d) soilMaxInfSummer

(e) soilMaxInfWinter

(f) soilMaxPerc

(g) t_factor

(h) tbase

Figure E.8: Sensitivity of parameters with PBAIS-B

F Uncertainty analysis

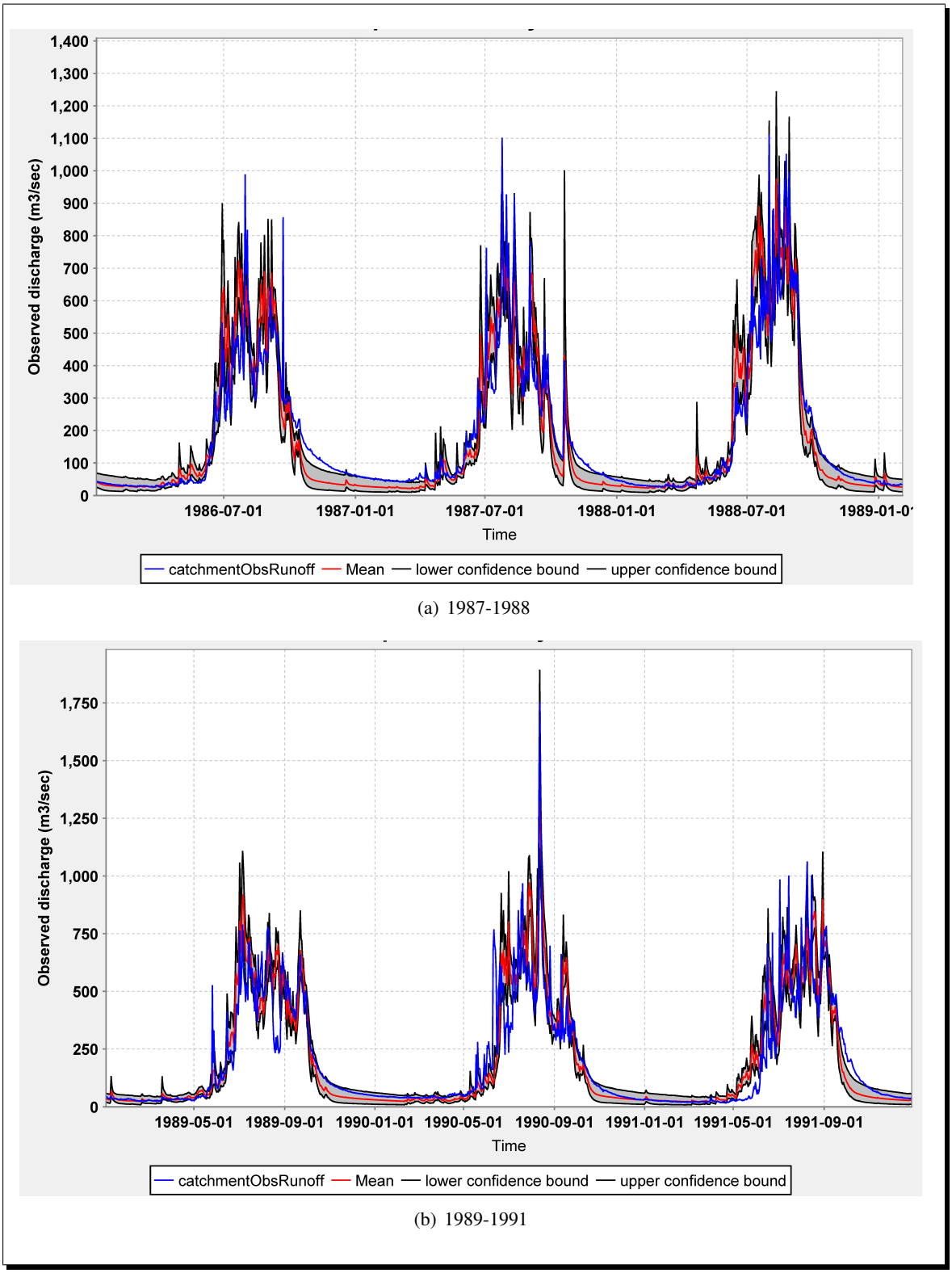

(a) 1987-1988

(b) 1989-1991

Figure F.1: Uncertainty analysis using the GLUE method (1987-1991)

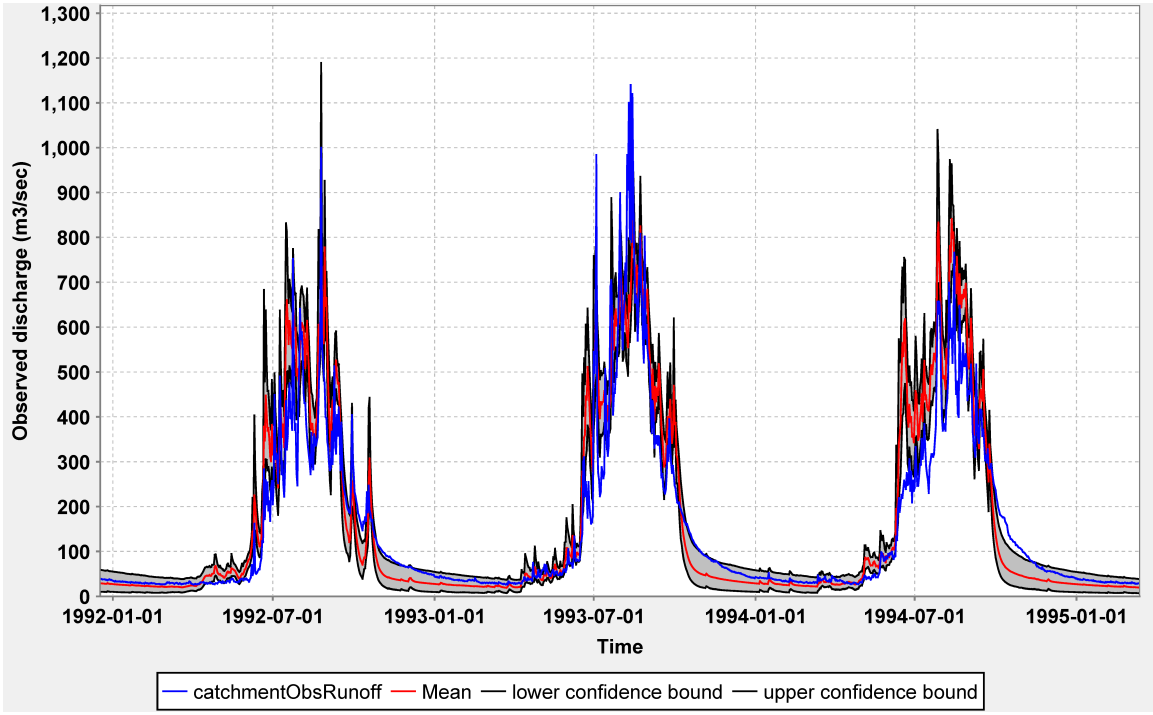

(a) 1992-1994

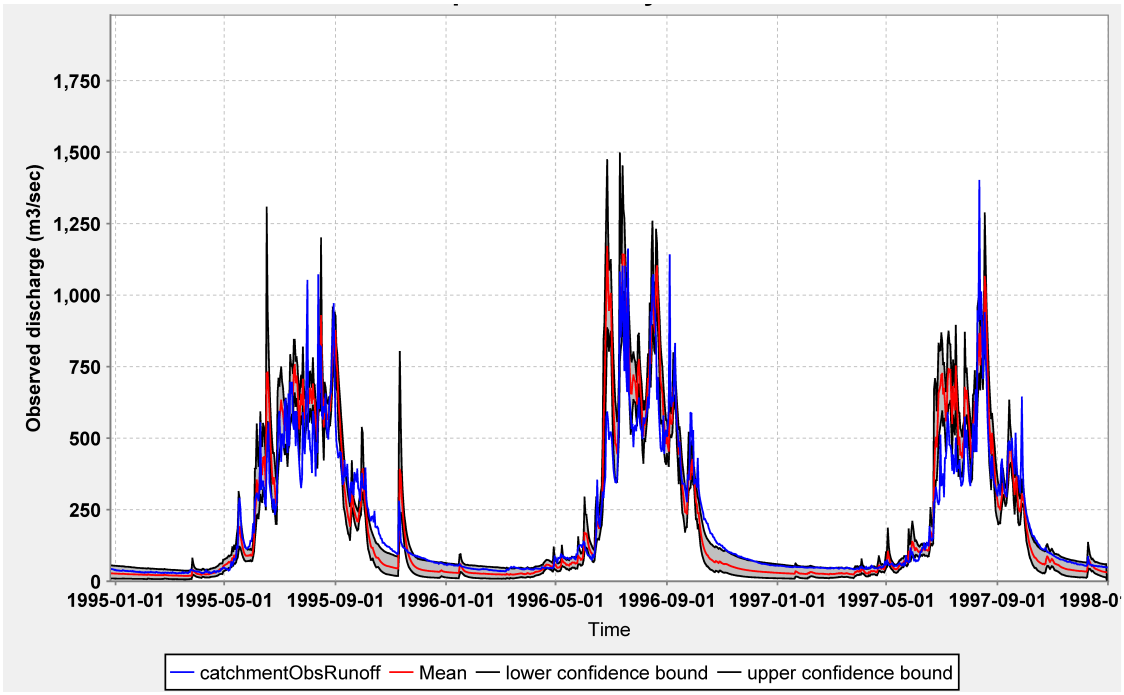

(b) 1995-1997

Figure F.2: Uncertainty analysis using the GLUE method (1992-1997)

G Observed precipitation and discharge of the Tamor river basin

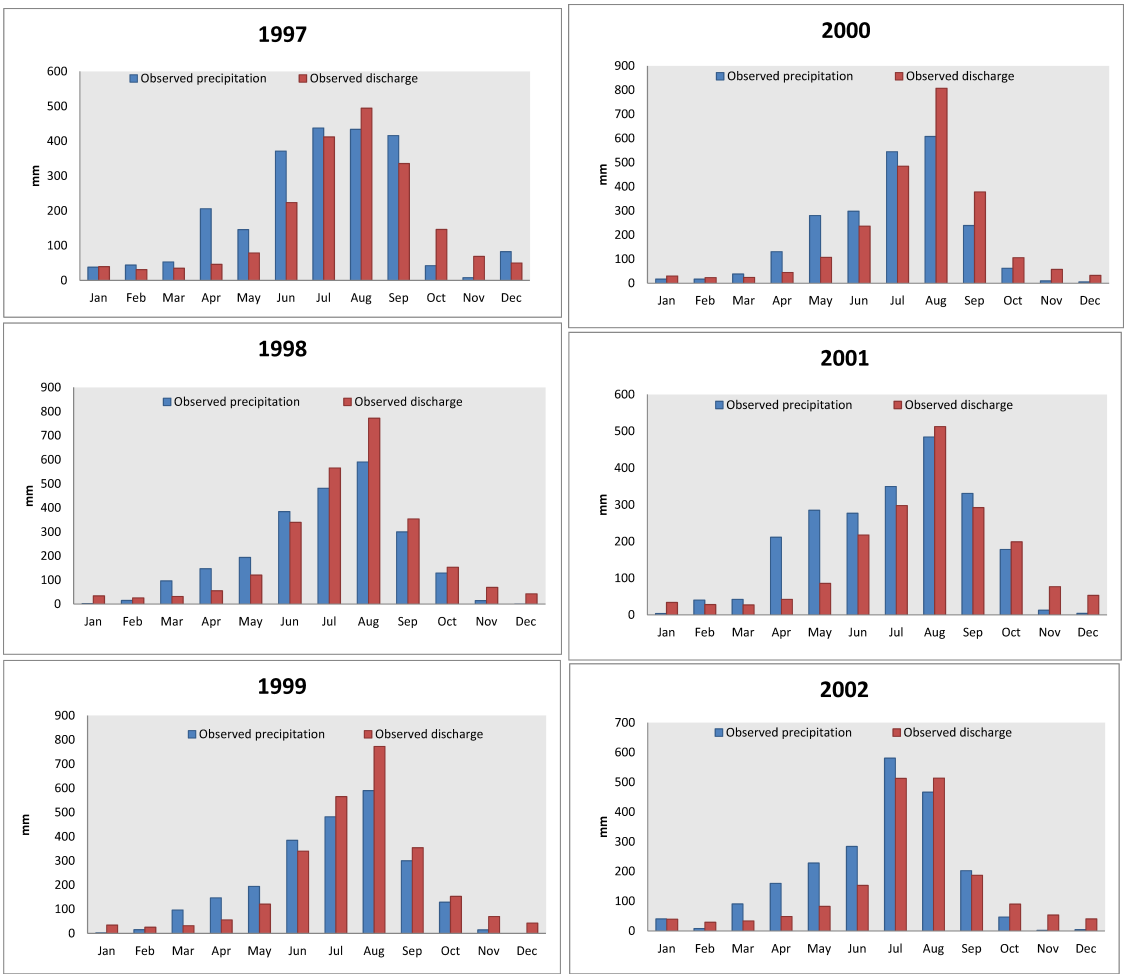

(a) Average monthly observed precipitation and discharge (1997-1999)

(b) Average monthly observed precipitation and discharge (2000-2002)

Figure G.1: Observed precipitation and discharge of the Tamor river basin (1997-2002)

Selbstständigkeitserklärung

Ich erkläre, dass ich die vorliegende Arbeitselbstständig und unter Verwendung der angegebenen Hilfsmittel, persönlichen Mitteilungen und Quellen angefertigt habe.

Jena, 21. May 2012

Curriculum Vitae

Personal information

Name	Santosh Nepal
Date of birth	25.05.1980
Birth place	Palpa, Nepal
Nationality	Nepali
Marital status	Married

Short biography

1985-1996	Bhairab Janta Higher Secondary School, Palpa, Nepal
1997-1998	Intermediate of Science, Biology, Tribhuvan University
1998-2001	Bachelor of Science, Environment Science, Tribhuvan University
2001-2003	Masters of Science, Environmental Management, Pokhara University
2003-2005	Masters of Arts, Sociology and Anthropology, Tribhuvan University
2005-2007	Environmental officer, Butwal Power Company Ltd., Nepal
2007-2009	Research associate, International Centre for Integrated Mountain Development (ICIMOD), Nepal
2007-2009	Faculty member, College of Applied Sciences, Tribhuvan University
2009-2012	Research associate, Department of Geoinformatics, Hydrology and Modelling, Friedrich Schiller University of Jena

Jena, May 2012